Universidad Politécnica de Madrid

Escuela Técnica Superior de ingeniería Agronómica, Alimentaria y de Biosistemas

HYDROLOGICAL MODELLING IMPROVEMENTS IN THE ASSESSEMNT OF WATER RESOURCES OF AGRARIAN SUBBASINS IN SEMIARID REGIONS

Tesis Doctoral

David Andrés Rivas Tabares

Ingeniero Agrícola

Directora:

Ana María Tarquis Alfonso

Dra. Ingeniero agrónomo (Universidad Politécnica de Madrid)

2020

Tribunal nombrado por el Sr. Rector Magfco. de la Universidad politécnica de Madrid, el día …….. de ……. de 2020

Presidente:……..

Vocal:…….

Vocal:…….

Vocal:…….

Secretario:……..

Suplente:……

Suplente:……

Realizado el acto de defensa y lectura de la Tesis el día …… de …….. de 2020 en la E.T.S.I./ Facultad……

Calificación:…….

EL PRESIDENTE LOS VOCALES

EL SECRETARIO

For Esperanza, Diego y Miguel

For Andrea

Aknowledgements

Thanks to my family that although they experienced indelible marks in my absence, they have also lived to believe in the family union. Thanks for allowing me a flight to other horizons to look for questions, for answers, for exploring the world and to come back home to seed, tilling and harvest in my land. This was a long way in which some of my family left this world to grow in our spirit; this is dedicated to all of them.

These lines are also dedicated to my supervisor Prof. Ana María Tarquis Alfonso, a person that changed my thoughts and the way to internalize the maths from nature as never I felt and saw it. She has been more than a supervisor; she's a brilliant philanthropist. Thanks for answering all that I've never request but was answered in this way. I'll never forget all the things that she made for me to pursue this dream, that finally, it came real. Deeply thanks for every minute that she dedicated to this research, thanks for each discussion and every comment that allowed improving every single word of this work. She supported me the beginning of this scientific way, she taught to me how to keep in this race, enjoying the way, passing over the obstacles in science but every moment feeling and living in the human heart, thanks for this. Also, thanks for introducing me to fractals, something amazingly simple but astonishing complex for thinking again the world.

Thanks to Dr Barbara Willaarts for her patience, for her example in research life. Thanks to Dr Ángel de Miguel for being the first person who gave me the opportunity to work on this research project from the IMDEA Water Institute and his support and guidance. To the TALE project team, from whom I received the best disposition and unconditional help. Thanks to CEIGRAM colleagues, great researchers of whom I have deep respect and admiration.

I would like to thank God for opening the doors to a better future full of opportunities. Thank to my parents María Esperanza and Víctor Hugo† who will give their lives for providing the opportunity to educate their children with the best example, being the greatest life teachers. Thanks to my brothers Diego Felipe and Miguel Ángel, who have always shared love, dedication for family unity and for guardians of my mother during difficult moments of health in my absence.

To my fiance Andrea, whom I met during this journey to build a future together, thank you for your patience and always listen to my mess ideas. Love was greater than distance; you will always be the main source of motivation and example of life. For you I always have to "keep going".

Last but not least, my thanks to Technical University of Madrid and the T.A.P.A.S. program, for providing the necessary tools and knowledge in doctoral training. So that the letters consigned in this document are reason for further research and contribution to social responsibility with sustainable agriculture by all and for all.

David A. Rivas Tabares

Agradecimientos

Gracias a mi familia que aunque vivieron marcas imborrables en mi ausencia, también han vivido para creer en la unión familiar. Gracias por permitirme volar a otros horizontes para buscar preguntas, y sus respuestas, explorar el mundo y volver a casa para sembrar, labrar y cosechar en mi tierra. Este fue un largo camino en el que algunos de mi familia dejaron este mundo para crecer en nuestro espíritu; esto está dedicado a todos ellos.

Estas líneas también están dedicadas a mi supervisora la Prof. Ana María Tarquis Alfonso, una persona que cambió mis pensamientos y la forma de interiorizar las matemáticas de la naturaleza como nunca la sentí y vi. Ella ha sido más que una supervisora; ella es una filántropa brillante. Gracias por responder a todo lo que nunca solicité, pero fue respondido de alguna manera. Nunca olvidaré todas las cosas que hizo por mí, para perseguir este sueño, que finalmente se hizo realidad. Muchas gracias por cada minuto que dedicó a esta investigación, gracias por cada discusión y cada comentario que permitió mejorar cada palabra de este trabajo. Ella fue quien me apoyó en el inicio de este camino científico, me enseñó a seguir en esta carrera, disfrutando el camino, superando los obstáculos de la ciencia pero sintiendo y viviendo en cada momento en el corazón humano, gracias por esto. Además, gracias por introducirme al mundo de los fractales, algo asombrosamente simple pero sorprendentemente complejo para pensar de nuevo el mundo.

Gracias a la Dra. Barbara Willaarts por su paciencia, por su ejemplo en la vida investigadora. Gracias al Dr. Ángel de Miguel por ser la primera persona que me brindó la oportunidad de trabajar en este proyecto de investigación del Instituto IMDEA del Agua y su apoyo y orientación. Al equipo del proyecto TALE, de quien recibí la mejor disposición y ayuda incondicional. Gracias a los compañeros de CEIGRAM, grandes investigadores a los que tengo un profundo respeto y admiración.

Me gustaría agradecer a Dios por abrirme las puertas a un futuro mejor y lleno de oportunidades. Gracias a mis padres María Esperanza y Víctor Hugo † quienes dieron su vida por brindar la oportunidad de educar a sus hijos con el mejor ejemplo, siendo los mejores maestros de la vida. Gracias a mis hermanos Diego Felipe y Miguel Ángel, quienes siempre han compartido cariño, dedicación por la unidad familiar y por los tutores de mi madre en los momentos difíciles de salud en mi ausencia.

A mi prometida Andrea, a quien conocí durante este viaje para construir un futuro juntos, gracias por tu paciencia y siempre escucha mis ideas confusas. El amor era más grande que la distancia; siempre serás la principal fuente de motivación y un ejemplo de vida. Para ti siempre tengo que "seguir adelante".

Por último, pero no menos importante, mi agradecimiento a la Universidad Politécnica de Madrid y al T.A.P.A.S. programa, para dotar de las herramientas y conocimientos necesarios en la formación doctoral. De modo que las letras consignadas en este documento sean motivo de mayor investigación y contribución a la responsabilidad social con agricultura sostenible de todos y para todos.

Summary

Hydrological modelling is nowadays an essential step for sustainable management of water and land resources. Despite the fact that most of the hydrological processes are well known and equations performance is accurate, most of the challenge in hydrological modelling focusing on whether the model can, in some close way, represent the real world. Most hydrological models are generally biased during modelling exercises, including setting up and interpreting the results. The correct representation depends on the input data, which also depend on two practices: i) the correct harmonization of the data and the available scales, before the configuration of the model and ii) the use of adequate tools and complementary for data pre-processing. The absence of these practices leads to a reduction in the quality of the data and therefore a decrease in the precision of the results.

The focus of this thesis is in the improvements about hydrological modelling in agrarian sub-basins in the semiarid. These environments are especially sensitive to biophysical aspects as climate, soils, vegetation and land management. This work offers a complementary approach to hydrological modelling of agrarian watersheds in Spain, through using the Soil Water and Assessment Tool (SWAT).

In Spain, when regional modelling and long-term modelling is required, model inputs data are scarce and scales are not usually compatible. One of the main, untreated inputs, to run models over these characteristics is the soil data. In this work, the Self-Organizing maps (SOM) are presented as an alternative method to improve digital soil mapping for hydrological modelling getting promising improvements in comparison to taxonomic classic approach. There is not previous evidence in literature using this method for soil mapping in hydrology modelling.

Other sensitive data is the land use land cover (LULC), as a spatial dynamic array that influences water flows. Using Earth Observation (EO) and surveys allow including a large dataset of crop rotations schemas and crop practices to model more realistic agrarian effect at subbasin scale. Once that model is calibrated and validated, LULC scenarios can be assessed to determine the influence of future land policy making in water resources.

The former model improvements were developed in one of the most recurrent drought alerted watershed in last decades in Duero River basin, the Cega-Eresma-Adaja (CEA) exploitation system. An exploitation system is referred as a management system grouping watersheds with similar characteristics (i.e. biophysical parameters, climate and land management) but this grouping is done to facilitate management and decision making by the River Basin Authority. However, there are important differences from technical point of view referred to hydrology and

land and water dynamics for each River implies different water balance flows as demonstrated in this work.

In this work, was studied the influence of different soil maps and resolutions on the main hydrological components of a sub-arid watershed. The Soil Water and Assessment Tool (SWAT) was parameterized with three different soil maps. A first one was based on Harmonized World Soil database from FAO, at scale 1:1,000,000 (HWSD). The other two were based on a Kriging interpolation at 100x100 m from soil samples. To obtain soil properties map from it, two strategies were applied: one was to average the soil properties following the official taxonomic soil units at 1:400,000 scale (Agricultural Technological Institute of Castilla and Leon - ITACyL) and the other was to applied Self-organizing map (SOM) to create the soil units (SOMM). The results suggest that scale and soil properties mapping influence HRU definition, which in turn affects water flow through the soils. Statistical metrics of model performance were improved from R^2 =0.62 and NSE=0.46 with HWSD soil map to R^2 =0.86 and NSE=0.84 with SOM and similar values were achieved during validation.

The CEA watershed for the period 2004-2014 was calibrated and validated analysing hydrological year types to provide more details of low-flows during spring-summer periods. The study reveals that aspects such as crop rotation, soil management and their associated measures in Mediterranean basins are key factors for water resource management facing climate change. These results are expected to serve stakeholders and River Basin Authorities in conducting better-integrated water management practices in the watershed.

Cereals in CEA midlands are a predominant crop choice because of climate and soil factors. These crops represent most of the agricultural water demand in the midlands. Crop rotations of wheat, fallow and barley are major choices within cereal crop sequences. Characterizing agricultural land processes coupling weather and soils are challenging because of multeity of factors affecting vegetation growth of cereals. One of these growth factors in semiarid is especially the rainfall on agricultural fields, in which soil properties and climate are strongly correlated with crop yield. These relationships are commonly analysed using vegetation indices such as the normalized difference vegetation index (NDVI).

NDVI series from two zones, belonging to different agroclimatic zones from CEA, were examined decomposing them into the overall average pattern, the residual series, and anomalies series. All of them studied by applying the concept of the generalized Hurst exponent (GHE). This is derived from the generalised structure function (GSF), which characterizes the series' scaling properties.

The overall pattern of the NDVI original series, NVDI residual and NDVI anomalies were examined from both zones. These presenting differences explained from climate-soil characteristics. The significant differences found in the soil reflectance bands confirm the differences in these two zones. Original NDVI series are persistent and multiscaling as other works reports. With respect to the scaling properties of the NDVI residual series, these presented Hurst exponents significantly lower than 0.5 indicating the structure of the signals. A stronger anti-persistent character was obtained in NDVI residual series with significant differences between zones. Similar is the case of NDVI anomalies with minor scaling properties.

These findings reveal the influences of soil-climate interactions in the dynamic of the NDVI series for rainfed cereal crops in a semiarid climate.

The assessment of land use and land cover (LULC) scenarios is a relevant field of study to anticipate future environmental impacts at the basin scale. Often the LULC scenarios and transition rules for hydrological modelling are based on expert criteria and disregard a participatory approach for its definition. In this work was analyzed the potential implications of three stakeholder informed LULC scenarios, and its implications in the water balance components of a sub-arid catchment of CEA. The LULC scenarios were defined through a participatory scenario process, involving a wide range of stakeholders and experts, and reflect three contrasting local land use developments: Land Sharing (LSH), Land sparing (LSP) and Land balance (LBA). The SWAT model was used to quantify the water resources implications linked to the LULC baseline scenario and the alternative LULC futures. The three scenario narratives underpinning the modelling scenarios highlight differences among reforestation transitions, landscape fragmentation, cropping patterns, and agricultural specialization.

Resumen

La modelización hidrológica es hoy en día un paso fundamental para la gestión sostenible de los recursos hídricos y de suelo. A pesar de que la mayoría de los procesos hidrológicos son bien conocidos y el funcionamiento de las ecuaciones es preciso, la mayor parte del desafío en la modelización hidrológica se centra en que el modelo pueda, de algún modo cercano, representar el mundo real. La mayoría de modelos hidrológicos generalmente se sesgan durante los ejercicios de modelización, incluida la configuración y la interpretación de los resultados. Una representación adecuada depende en gran parte de los datos de entrada, los cuales también dependen de dos prácticas: i) la correcta de armonización de los datos y de las escalas disponibles, antes de la configuración del modelo y ii) el uso de herramientas adecuadas y complementarias para el pre-procesamiento de datos. La ausencia de estas prácticas conlleva una reducción en la calidad de los datos y por lo tanto una disminución en la precisión de los resultados.

Esta tesis se centra en las mejoras realizadas sobre la modelización hidrológica en subcuencas agrarias en el semiárido. Estos entornos son especialmente sensibles a aspectos biofísicos como el clima, los suelos, la vegetación y la gestión del territorio. Este trabajo ofrece un enfoque complementario a la modelización hidrológica de cuencas hidrográficas agrarias en España, mediante el uso de la herramienta de Evaluación de Agua y Suelo (SWAT), por sus siglas en inglés.

En España, cuando se requiere un modelo regional y un modelo a largo plazo, los datos de entrada del modelo son escasos y las escalas no suelen ser compatibles. Una de las principales entradas, no tratadas, para ejecutar modelos sobre estas características son los datos del suelo. En este trabajo, los mapas Autoorganizados (SOM) por sus siglas en inglés, se presentan como un método alternativo para mejorar el mapeo digital de los suelos para la modelización hidrológica, obteniendo mejoras prometedoras en comparación con el enfoque taxonómico clásico. No existe evidencia previa en la literatura sobre el uso de este método para el mapeo de suelos en modelos hidrológicos.

Otro dato sensible en el modelo, es la cobertura y uso del suelo (LULC) por sus siglas en inglés, como una matriz dinámica espacial que influye en los flujos de agua. El uso de la observación de la Tierra (EO) y de encuestas, permite incluir un gran conjunto de datos de esquemas de rotación de cultivos y prácticas de cultivos para capturar con el modelo el efecto agrario, más realista, a escala de subcuenca. Una vez que ese modelo está calibrado y validado, los escenarios LULC pueden evaluarse para determinar la influencia de la futura formulación de políticas territoriales y de los recursos hídricos.

Las mejoras del modelo se desarrollaron en una de las cuencas hidrográficas con alerta de sequía más recurrentes de las últimas décadas en la cuenca del río Duero, el sistema de explotación Cega-Eresma-Adaja (CEA). Un sistema de explotación se define como un sistema de gestión que agrupa cuencas hidrográficas con características similares (es decir, parámetros biofísicos, clima y gestión de la tierra), esta agrupación se realiza para facilitar la gestión y la toma de decisiones por parte de la autoridad de cuenca. Sin embargo, en la aplicación de este concepto originan importantes diferencias desde el punto de vista técnico referido a la hidrología, la dinámica del uso y cobertura del suelo. El caudal resultante para cada Río es el resultado de diferentes flujos del balance hídrico como se demuestra en este trabajo.

En este trabajo se estudia la influencia sobre los principales componentes hidrológicos de una cuenca sub-árida, usando diferentes mapas de suelos y varias resoluciones. Se parametrizó el modelo SWAT con tres mapas de suelos diferentes. El primero se basó en la base de datos armonizada de suelos mundiales de la FAO, a escala 1: 1.000.000 (HWSD). Los otros dos se basaron en una interpolación de Kriging a 100x100 m de muestras de suelo. Para la obtención del mapa de propiedades del suelo se aplicaron dos estrategias: una fue promediar las propiedades del suelo siguiendo las unidades taxonómicas oficiales de suelo a escala 1: 400.000 (Instituto Tecnológico Agrario de Castilla y León - ITACyL) y la otra fue aplicar el método (SOM) para crear las unidades de suelo (SOMM). Los resultados sugieren que el mapeo de propiedades del suelo y la escala influyen en la definición de las unidades de respuesta hidrológica (HRUs), lo que a su vez afecta el flujo de agua a través de los suelos. Las métricas estadísticas del rendimiento del modelo se mejoraron de $R^2 = 0.62$ y NSE = 0.46 con el mapa de suelos HWSD a $R^2 = 0.86$ y NSE = 0.84 con SOM y se lograron valores similares durante la validación.

La cuenca del CEA para el período 2004-2014 se calibró y validó analizando los tipos de años hidrológicos para proporcionar más detalles de los caudales bajos durante los períodos primavera-verano. El estudio reveló que aspectos como la rotación de cultivos, la gestión del suelo y sus medidas asociadas en las cuencas mediterráneas son factores clave para la gestión de los recursos hídricos frente al cambio climático. Se espera que estos resultados sirvan a los actores y a las autoridades de las cuencas hidrográficas para llevar a cabo mejores prácticas integradas de gestión del agua en la cuenca.

Los cereales en las tierras centrales de CEA son una opción de cultivo predominante debido a factores climáticos y del suelo. Estos cultivos representan la mayor parte de la demanda de agua para la agricultura en la región central. Las rotaciones de cultivos de trigo, barbecho y cebada son opciones muy importantes dentro de las secuencias de cultivos de cereales. Caracterizar los procesos de tierras agrícolas que combinan el clima y los suelos, es un desafío debido a la

multiplicidad de factores que afectan el crecimiento de la vegetación de los cereales. Uno de estos factores de crecimiento en el semiárido, es especialmente la lluvia en los campos agrícolas, en los cuales las propiedades del suelo y el clima están fuertemente correlacionados con el rendimiento de los cultivos. Estas relaciones se analizan comúnmente utilizando índices de vegetación como el índice de vegetación de diferencia normalizada (NDVI).

Se examinaron series de NDVI de dos zonas, pertenecientes a diferentes zonas agroclimáticas del CEA, descomponiéndolas en el patrón promedio general, la serie residual y la serie de anomalías. Estas se estudiaron aplicando el concepto de exponente de Hurst generalizado (GHE). Esto se deriva de la función de estructura generalizada (GSF), que caracteriza las propiedades de escala de la serie.

El patrón general de la serie NDVI de ambas zonas presentó diferencias que podrían explicarse por las características de precipitación y suelo de cada una. Las diferencias significativas encontradas en las bandas de reflectancia del suelo confirmaron las diferencias en entre las zonas. Se encontró que las series originales de NDVI son persistentes y multiescala, tal como lo han reportado otros trabajos. Con respecto a las propiedades de escalamiento de las series residuales del NDVI, estas presentaron exponentes de Hurst significativamente menores a 0.5 indicando una estructura de ruido. Resultados similares se encontraron para las series de anomalías del NDVI, pero con menores propiedades de escalado.

Estos hallazgos revelan las influencias de las interacciones suelo-clima en la dinámica de la serie NDVI para cultivos de cereales de secano en un clima semiárido.

La evaluación de escenarios de uso y cobertura del suelo (LULC) es un campo de estudio relevante para anticipar impactos ambientales futuros a escala de cuenca. A menudo, los escenarios LULC y las reglas de transición para la modelización hidrológica se basan en criterios de expertos y no tienen en cuenta un enfoque participativo para su definición. En este trabajo se analizaron las implicaciones potenciales de tres escenarios LULC informados por diversos actores, y sus implicaciones en los componentes del balance hídrico de una cuenca subárida de CEA. Los escenarios LULC se definieron a través de un proceso de escenario participativo, que involucró a una amplia gama de actores y expertos de la zona de estudio, obteniendo tres escenarios locales de usos del suelo contrastantes: “buscando la multifuncionalidad de los espacios rurales” (LSH), “Hacia la especialización del territorio” (LSP) y “Continuidad de los modelos territoriales vigentes” (LBA). El modelo SWAT se utilizó para cuantificar las implicaciones de los recursos hídricos vinculadas al escenario de línea de base LULC y los futuros LULC alternativos. Las tres narrativas de escenarios que sustentan los escenarios de modelización destacan las diferencias entre las transiciones de reforestación, la fragmentación del paisaje, los patrones de cultivo y la especialización agrícola.

Table of Contents

List of Tables

List of Figures

List of Abreviations

95PPU: 95% prediction uncertainty
AEMET: Agencia Estatal de Meteorología
ANOVA: Analysis of variance
ArcSWAT: ArcGIS-ArcView extension and interface for SWAT
BSL: Bare soil line
CAP: Common Agricultural Policy
CEA: Cega-Eresma-Adaja
CHD: Confederación Hidrográfica del Duero
CN: Curve number
CyL: Castilla y León
DB: Davies Bouldin Index
DEM: Digital elevation model
DRBA: Duero River Basin Authority
DURERO: Project "Duero River Basin: water resources, water accounts and target sustainability indices"
EA: Eresma-Adaja
EC: European Community
EGU: European Geosciences Union
EO: Earth Observations
ET: Evapotranspiration
EU: European Union
FAO: Food and Agriculture Organization
GSF: generalized Structure Function
GHE: Generalized Hurst Exponent
H: Hurst exponent
HRUs: Hydrologic response units
HWSD: Harmonized world soil database
IGME: Instituto Geológico y Minero de España
INFORIEGO: Herramienta de Servicio de Asesoramiento al Regante
ITACyL: Instituto Tecnológico Agrario de Castilla y León
JCyL: Junta de Castilla y León
KGE: Kling-Gupta Efficiency
LCA: Life Analysis Cycle
LCFG: Lastras de Cuellar flow gauge
LULC: land use and land change
MASL: meters above sea level
MDT25: Modelo digital de terreno 25m
MIR: Medium-Infrared
MODIS: Moderate Resolution Imaging Spectroradiometer
NDVI: Normalized difference vegetation index
NIR: Near-Infrared
NSE: Nash-Sutcliffe efficiency coefficient
PBIAS: Percent bias
PNOA: Plan Nacional de Ortofotografía Aérea
PoMs: Program of measures
PTF: pedotransfer functions
R: R programming language
R^2: coefficient of determination
RBA: River basin authority
RBMP: River Basin Management Plan

RBMPs: River Basin Management Plans
SCS: Soil Conservation Service
SD: Standard deviation
SL: Soil line
SOM: Self-organizing maps
SOMM: Self-organizing soil maps
SUFI-2: Uncertainty in Sequential Uncertainty Fitting
SWAT: Soil Water and Assessment Tool
SWAT-CUP: SWAT Calibration and Uncertainty Procedures
TALE: Project “Towards multifunctional Agricultural Landscapes in Europe”
TOPMODEL: TOPography based hydrological MODEL
TPM: Thiessen polygon method
TSU: Taxonomic Soil Units
USA: United States of America
VFG: Valdestillas flow gauge
VIs: vegetation indices
WFD: Water Framework Directive.

1 Introduction

1.1 The hydrological modelling of agrarian semiarid regions

1.1.1 Research context

The hydrologic cycle is one of the continuous mass cycles in the Earth-atmosphere system. Water that is a substance composed by hydrogen and oxygen, circulates in different physical states through the hydrosphere given certain energy potentials (Kleidon et al., 2009). In the hydrological cycle, the energy and mass flows are correlated. Such interaction adds a degree of complexity (physical-chemical) that is difficult to measure in time and space (Mook and Custodio, 2002; Tian et al., 2016). Moreover, due to the different temporal space scales in which the events of the cycle occur, the understanding of continuous process is challenging (Fatichi et al., 2016). For this reason, the study of water dynamics in the hydrological cycle is fundamental in the hydro-meteorological analysis of the terrestrial landscape. The definition of the scale at which scientists and experts want to study the phenomenon is fundamental, since its definition allows attributing different water relations: continental, regional or local over time.

The study of the hydrological cycle, although being a macro cycle at the terrestrial level, focuses on most cases in the continental section (Clark et al., 2015). In this context, it is defined as the fraction between the hydrosphere and the surface-underground advance of the water towards the recharge of seawater, in order to continue a new cycle from the oceans as a universally adopted reference point.

The hydrological cycle at a continental scale, aims to deliver information on water flows in large continental platforms. Which in turn are associated with the response of hydrographic units of large rivers (Vörösmarty et al., 2000). Regional studies of water flows are of greater interest in a country or of a transnational nature when a hydrographic unit is shared by several countries. In Spain, an example of this situation are, *Miño* river, *Lima* river, *Guadiana* river, *Tagus* river and *Duero* river that shares the river basin with Portugal (Caballero, 2019). In addition, the regional scale is mostly used in the evaluation of the hydrological cycle, since there are conflicts over the flows and demands within the same region. Within this scale it is necessary to further detail the processes of the tributary rivers. But only the most concrete situations need evaluation at the local level, a situation that has received much attention over the last decades (Hrachowitz et al., 2016). The local level is aimed at the study of events or effects on very specific water bodies within a tributary river margin or aquifer.

The water quality and quantity for the ecosystems are an essential characteristic and its understanding plays a transversal role in natural sciences, economics, culture, among others (Grizzetti et al., 2016). This relationship has been the subject of multiple studies since the 18th century (Duffy, 2017), since anthropic actions have been modifying and impacting this important relationship. Man activities have been generating continental scale changes related to water resources from the surface, like land-use change for terrestrial part and emissions (gases and energy) for the atmospheric phase (Ramanathan et al., 2001). Thus, producing within the hydrological cycle significant variations that motivate scientist and researchers their understanding and possible control at different scales. The study of the impact of water resources management is related to land use dynamics and emissions which are the expression of social, economic and cultural aspects of society at different scales (i Canals and de Baan, 2015; Newbold et al., 2016).

In the last century, studies of the hydrological cycle at regional and local level have advanced in great detail in developed countries, since the economic and social importance at this scale is evident (Gober et al., 2017; Karabulut et al., 2016; Singh et al., 2018). For this reason, countries and governments have seen the essential need for integrated water resources management at a level of detail that strikes the positive impact of the policies generated (Rubiano et al., 2006). To this end, they have created institutions responsible for managing the water resource in the territory; For example, in Spain there are institutions such as River Basin Authorities (RBA), created by the Royal Legislative Decree of July 20, 2001 and by which the consolidated text of the water act in Spain was approved. The RBA are the institutions that comply with the community policies of the water law, the WFD (Water Framework Directive) 2000/60 / EC.

Although the water resources management at country level through the RBA has been facilitated, the understanding of the relationships of water flows with human activity it's very diverse when scale increases and decisions become more complex and difficult to manage. In Spain, it has been in a learning period (1st and 2nd hydrologic planning cycle). The challenges in terms of management by the authorities are diverse and difficult to address (Giorgi et al., 2015) and land use dynamics include a complex component in time and space given by specific water pressures, such as: complying with supply guarantees (Muñoz et al., 2010), economic viability in circular economy markets (Brears, 2015), environmental responsibility of ecological flows (Willaarts et al., 2014), and the demands of activities such as agriculture and industry (de Miguel et al., 2015). Multiple studies related to the water footprint and LCA (Life Analysis Cycle) (Muñoz et al., 2010) reveal this for different economic sectors.

The imbalance between supply and demand is the common denominator in most Spanish basins (Del Tánago et al., 2012; Duque et al., 2018; Fernández and Selma, 2004). Even in some cases,

such as in agricultural activity, rebound effects have been achieved due to irrigation, increasing pressures on the water resources. The modernization of agriculture water use, being this more efficient, motivates the expansion of the total irrigated area (Berbel et al., 2015; Khadra and Sagardoy, 2019). Irrigated agriculture in Spain, has the tendency to stand out for the concentration of much of the water demand in a small area compared to extensive dryland agriculture, in part motivated by a management model and water use efficiency (Expósito and Berbel, 2017) and motivated by cash crops (Custodio et al., 2016). To cope face this small-scale irrigation supply pressure, a group of legal organizations have been established to manage water supply to farms, called irrigation communities. From these organizations, the water supply pressures were reordered resulting into a water supply net increase, due to the maximization of the water efficiency use of the irrigation systems. However, this increase on water supply have been attempted to shovel with a tariff scheme during the 1st hydrological cycle, without achieving the expected results in terms of guarantee and resource quality (Berbel et al., 2019; Pérez-Blanco et al., 2015). But the situation is accentuating the environmental problem of water resources availability. Since the agricultural activity involves not only water supply but also generates diffusive pollutant loads that the environment is not capable of degrading. The regulation of agricultural practices associated with the CAP (Common Agricultural Policy) must be aligned with the WFD, since the change in land use and the practices associated with these hedges in a consensual manner provide environmental benefits for water allocation and mitigation of water pollution (Salmoral et al., 2017).

1.1.2 Modelling and water resources assessment

Starting from the premise that the hydrological cycle is a complex system, which has been altered by man, its study requires the use of different tools for its calculation in detail. These should allow to chain threads considering lot of variables to establish a balance with a high accuracy level. This chain of variables represents different biophysical processes, allows evaluating the anthropic changes within the hydrological cycle at basin scale. The most important flows within the hydrological cycle (Figure 1) are required to describe system dynamics by decomposing its by inputs (precipitation), storage (soil profile and reservoirs) and exits (ET, river flow and aquifers recharge), among the main hydrological processes involved for any catchment evaluation.

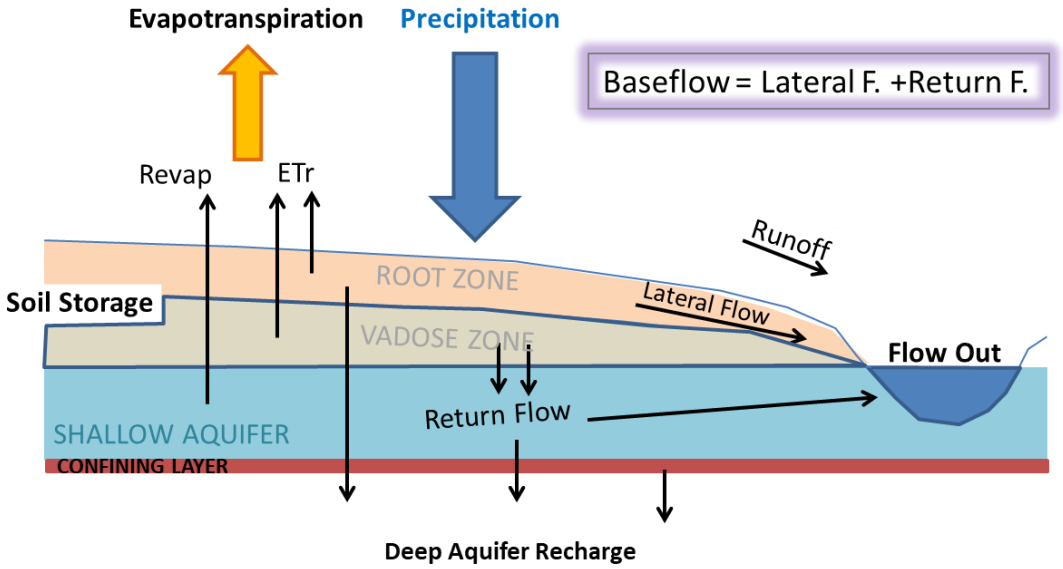

Figure 1. Main water balance parameters of the hydrologic cycle in the continental section.

Water resources assessment and its accuracy depend on data quality, time scale, spatial resolution and the purpose of the analysis. The former characteristics are essential for any water assessment analysis and its simulation. Hydrological modelling is one of the most frequent tools used by scientists and planners for water and land management (Rekolainen et al., 2003). The utility of models implies the river routing of hydrological components for water flow, sediments, nutrients, pollutants and bacteria along the river network, providing outputs for every sub-basin outlet (Krysanova and White, 2015). However, the purpose of the analysis should be the key driver to use models for specific contexts although these have not been developed for that purpose. This situation forces to assign different weights to the input data involved in simulation. Thus, modellers have to use simplifications procedures or schemas to all non-relevant processes related with the purpose of the analysis to get a complete simulation of hydrological cycle.

As in any modelling exercise, hydrological models assume simplifications of a real-basin system and some degree of uncertainty is thus unavoidable. Therefore, the assumed simplifications should be considered cautiously, as they could affect the results. For example, if water demand by land use is expected, as a result, simplifications of this subject must be fully described by the model.

Towards accurate models there is a need of very precise data, every improvement in data input should be translated into model improvements. Hydrological models require accurate data related to input water into the systems, regulations and management data, among others. However, there is a portion of water cycle in which water is very dynamic in time and space, this is the soil. One of the most common simplifications founded in hydrological modelling.

1.1.3 Water management of Agricultural Subbasin in Semiarid regions

The agriculture water consumption is one of the main demands on the global water systems. In semiarid regions usually agricultural land location depends on water availability and vested to climate and soil agrarian aptitudes. These characteristics in turn follow a behavioral spatial order, coupled to sub-basin characteristics. The 3rd order of sub-basins offer a spatial unit in which hydrological processes can be analyzed from a local perspective and any plausible measure can be generalized for it due to global hydrologically homogeneous characteristics (Vieux, 2001). Nevertheless, soil properties, slope and land use serve as sub-clustering tool inside each subbasin (Teshager et al., 2016).

An agricultural sub-basin is defined when the main land cover/use is devoted to agrarian production, usually when more than 50% of the total area is cultivated. In semiarid regions, as Mediterranean zone the 3rd order of sub-basins presents a wide range of possibilities to use land under agricultural schemas. However, only two conditions related to water consumption of agricultural land use can be present, rainfed and irrigated condition. Rainfed is the most common and extensive condition of agriculture in semiarid regions, especially in Mediterranean zone. The dry land agriculture water management is mainly for food production of individual farmers or village sized landholdings. A water source commonly used for annual agriculture exploitation is the groundwater, but usually its renewable rate is higher than one year, making its use very limited (Pulido-Velazquez et al., 2015; Stigter et al., 2014). The soil conservation in dry lands is the primary strategy to follow in agricultural exploitations, since it's the main determining factor of water dynamics for sustainable agriculture schemas. Some strategies have been followed to avoid water losses; one of the most effective and applied in dry lands worldwide is the fallow land stage, in which the land is uncultivated for a period of time to store water into soil and to mineralize some nutrients. However, fallow management is very site specific due to climate, soils, crop rotation schema and tillage machinery manage (Fernandez et al., 2008). Several hydrological process such runoff (Ries et al., 2004), soil evaporation (Bennie and Hensley, 2001), soil porosity (Nyamadzawo et al., 2008), soil water storage (Lampurlanes et al., 2002), among others, are susceptible to vary in time with fallow practice (Moreno et al., 2010).

Water availability in the Mediterranean zone has been a subject of research in recent decades, and its assessment on a basin scale is a priority to secure water availability for different users, including fresh water, industry, agriculture and hydropower in southern Europe (Calbó, 2010; Giorgi et al., 2015; Giorgi and Lionello, 2008; Rafael et al., 2010). Agriculture is the major water user in Europe, accounting on average for 32% of total freshwater abstractions (EUROSTAT, 2017). In southern Europe, agricultural abstractions are greater, accounting for an average of 52% of total freshwater abstractions (EUROSTAT, 2017). In sub-arid climates,

agricultural water extractions can reach 80%, and often become a source of disputes amount water users (European Comission, 2012). The usual implementation of flow regulation strategies in these areas to meet increasing water demands, through reservoirs and artificial recharge of aquifers, captures the majority of the surface flow of rivers and results in a low flow system affecting riverine ecosystems and water availability (Tharme, 2003).

In Mediterranean watersheds of southern Europe, irrigated agriculture is a common strategy to ensure crop production and is considered a key driver in water scarcity (Psomas et al., 2016). Because of this, agricultural water demand must be reformulated, based on an integrated land use management approach, considering both irrigated and rainfed crops. Specific mitigation and adaptation measures for water resources management are needed to reconcile water demands from multiple users, as outlined in the River Basin Management Plans (RBMPs) (European Comission, 2012; European Environment Agency, 2015). The EU 2020 strategy and the Water Framework Directive (WFD) have been promoting several policies for water savings and its protection. Additionally, the Program of Measures – PoMs, aims to achieve a satisfactory status for surface and groundwater bodies. Several tools, such as remote sensing, are used to identify land uses and the application of hydrological models to quantify real and potential water demand for agriculture.

Consequently, a sustainable management vision of water resources at watershed scale requires the inclusion of some measures at plot scale. Hence, through modelling, the cumulative effect of detailed land operations could be assessed for the watershed water fluxes. Hydrology models that include water fluxes related to land use can help decision makers formulate strategies in the water-energy-land-food nexus (Dodds and Bartram, 2016; Hoff et al., 2012). Furthermore, the water balance model alone is not enough; the environmental situation, the inclusion of hydrological dynamics in changing environments (Wang et al., 2016), climate change (Narsimlu et al., 2013), land use (Zhao et al., 2016), crop practices (Ullrich and Volk, 2009) and reservoir operation schedules (Kalogeropoulos et al., 2011) are also required to achieve an integrated water management scheme.

RBA use water management models as a tool to assess and guarantee water demands. Those models serve to manage water fluxes based on predefined and estimated water demands (e.g. water supply, irrigation and industry) and the associated regulatory infrastructure. Nevertheless, water balance is dynamic in time and space. Hence, to improve water management, more variables must be included to achieve a more accurate water balance. The water balance must include land use dynamics and cropland practices. The sensitivity of water availability in the catchment could be modified due to land use change for future water demands. This is why detailed hydrological models can be very useful tools for planning purposes.

1.2 Soils and hydrology relationships

1.2.1 Digital soil maps and data sources

Soil is one of the main characteristics of a landscape, containing physical, biological, chemical, morphological, and mineralogical attributes with 3-D variability (Sigua and Hudnall, 2008). Soil is a key element in the water balance, and its properties have a direct impact on the discharges of many rivers around the world (Devia et al., 2015). The spatial variation of soils depends on soil properties and depth, which are less variable at deeper profiles (Santra et al., 2008). Nonetheless, in regard to hydrological modelling, the simplification of soil variability into soil patterns is a priority to allow the calculation processes at sub-basin scale (Muttiah and Wurbs, 2002). However, soil variability is a complex physical process, and its simplification can lead to severe misrepresentation of the hydrological behaviour through the soil profile (Baveye and Laba, 2015). Soil hydraulic properties are also considered dynamic because they are affected by land management practices (Bünemann et al., 2018). Soil moisture controls the exchange of water and heat energy in the soil-plant-atmosphere system and its variability influences the physical, chemical, and biological spatiotemporal characteristics of soil (Bai et al., 2019). All of this could affect the accuracy of hydrological modelling.

The most common method for the development of detailed soil mapping is based on taxonomic group classifications (TSU), which is an expensive and time-consuming approach. Traditionally, soil maps for hydrological modelling are based on the TSU approach. In general, those maps were developed using the interpretation of aerial photos, available geology maps, soil samples from fieldwork and performing laboratory analytics (Tissari et al., 2007). However, the inter-spatial variation of properties in the same soil unit was not (Lee Ficklin et al., 2014) considered, and in larger units and regional scales, this introduces error forcing modellers to make assumptions (Kamali et al., 2017; Neitsch et al., 2005). For this reason, multidimensional methods applied for soil clustering could facilitate the model set-up of hydrological models (GESSLER et al., 1995).

Soil datasets for hydrological modelling are usually selected and arranged using different geostatistical methods, such as kriging (Matheron, 1962) and self-organizing maps (SOM)(Kohonen, 1982). Kriging represents one of the most commonly used tools since the late 1970s for representing soil properties in maps and predicting attribute values for non-sampled locations (Asa, 2012; Baveye and Laba, 2015; Goovaerts, 1999). Additionally, SOM is an artificial neural network that can be used for clustering datasets and extracting the dimensional values (Vesanto and Alhoniemi, 2000). The SOM, alone or with other techniques (Rivera et al., 2015), is also an ideal tool for visualizing multidimensional datasets in maps in the exploratory phase (Merdun, 2011).

1.2.2 Hydrologic soil properties

At global scale, little attention has been given to soil properties for hydrological modelling. Especially due to high costs for mapping exhaustively the soil properties at precise scales to get maps at resolution higher than 1:100.000. This is especially true when harmonizing soil maps for hydrology modelling at 1st to 3rd basin order.

Among a pull of soil properties that interact at the same time to develop water fluxes over basins, there are some of them too sensitive and attributable to hydrological processes. Several studies report sensitivity on the following soil properties for hydrology modelling:

1. **Infiltration,** water infiltration into soils occurs during and after storms, allowing soil moisture homogenizes and water transfer in depth. Infiltration is a process in which water mass transfer is function of soil moisture condition and its rate is high when soil are dry and slow down once soils store water until the water flux reach stable state, this former state is more known as basal infiltration or hydraulic conductivity.
2. **Soil water storage**, is a key water volume into the water cycle, it could be considered as a storage volume for short term. Joint to this water that is stored into soils reach an ecological function of water regulation to stream network configuration, atmosphere interchange and percolation transition to groundwater configuration.
3. **Soil depth**, is one of the most important soil characteristic due of capacity to drive the time for the different flow configuration, their spatial distribution is very scarce known with high precision in watershed. Due of this limitation most of hydrological fluxes are susceptible to large errors in their calculation.
4. **Aquifer interaction**, most of the hydrologic models use aquifer interaction to compensate water balance trough revaporation factor to compensates ET and deep aquifer recharge as a water loos.
5. **Water table and percolation**, these two variables are very important in compensate watershed water balance due to its dynamics. However, most of the water table fluctuations are not considered or measured to hydrological modelling, some wells are considered for hydrogeological studies and for surface assessment remains in a secondary plane as water flows difference.

Taking into account that the soil plays an important role in the accuracy of water fluxes most of the soil properties area known at fines scales and its understanding can be useful in water budget at local hydrological analysis.

1.3 Effect of Land Use Land Cover in hydrology dynamics

1.3.1 Rainfed winter cereals

Cereals have been one of the most representative crops in Iberian steppes since early 90's (Rubalcaba and Guillén, 1997). This is the case of the left margin of Duero's river, in which the barley and winter wheat are widely extended in the arable land. In part, because of the cereal-steppes program supported from Common Agricultural Policy (CAP) of the EU during 90s and because of soil suitability and weather regime (Oñate et al., 2007). Besides, the weather regime around 400-600 mm/year, sandy soils and driest summer are factors that fits with wheat and barley physiology reaching extensive profit from land use, in the Mediterranean cereal production systems.

Between barley and wheat, barley is a dominant crop in the area (Gutiérrez García et al., 2016). The planted varieties of barley at the end of the fall season, facilitates the crop management and cultivation success (Pswarayi et al., 2008). This is because of adequate breaking seed dormancy period, soil moisture conditions for optimal germination, temperatures ranges are ideal for winter planting and photoperiod adaptation of the crop (Lister et al., 2009). During the crop season, the precipitation during fall-winter period is around 150 to 200mm (i.e., October, November, December and January), this is essential in terms of soil water storage at the beginning of the crop season (i.e., germination) (Igartua Arregui et al., 2015). In the left margin of Duero's river and in in sandy soils, the soil water storage in early spring is fundamental in tillering due to small precipitation rates and their associated reduced ET rates due to weather characteristics. This set of factors have favoured that wheat and barley have well adapted to these areas.

Cereals are involved in almost all rainfed annual crop rotation schemas in the area (Rivas-Tabares et al., 2019a). However, there are some extensive practices in which barley, fallow, and wheat, in distinct combinations, the crop rotation sequences in the rainfed agricultural area. Increasingly, the reduction of long-term fallow is suppressed from the crop rotation sequence (Poulsen et al., 1998), increasing pressures over soil fertility and availability of water resources for this farming system. This resulting that these three to five years monoculture crop sequences are unsustainable in mid and long-term.

The analysis of long-term monoculture crop sequences from Earth Observations (EO) of the soil-plant-atmosphere system can provide the insights of crop systems trends to investigate the spatial and temporal specific interactions of soil and climate in vegetation dynamics.

1.3.2 Vegetation indexes as a measure of spatial variability

In the Spanish Mediterranean environments, rainfed cereal crops are grown mainly in the arid and semiarid areas, where dryland farming is of renewed interest in the view of sustainability (Lelièvre et al., 2008; Perniola et al., 2015). The main characteristics of the Mediterranean-climatic regions are cool wet winters and hot dry summers. The rainfall pattern coupled with the high rates of evaporation during summer, result in water being an important limitation to agricultural productivity. Some observations with rainfed cereal monoculture sequences have been identified in north-central Spain cereal steppes (Rivas-Tabares et al., 2019b). These monoculture sequences represent an issue for soil degradation and basin water balance in this area. Therefore, a set of combined processes occurs at different times and scales creating complex dynamics during the crop development (Wu and David, 2002).

Monitoring crop development in agricultural zones is a challenging task with several agronomical applications (Xue and Su, 2017). Satellite-derived vegetation indexes (VIs) are measures related to surface reflectance commonly used to characterize the spatial and temporal vegetation dynamics (Joiner et al., 2018; Xue and Su, 2017). Remote sensing provides temporal and spatial patterns of agroecosystem change and has been used to estimate the biophysical characteristics of crops and grasslands (Nagy et al., 2018; Schultz et al., 2016). The variation in climatic conditions (i.e., seasonal and inter-annual changes) allows a wide spectrum of dynamic characteristics (Lazaro et al., 2001; Vicente-Serrano, 2007). In addition, soils in which vegetation has been developed are also an important part to understand VIs response (Mahmoudabadi et al., 2017; Wang et al., 2001; Xu et al., 2015a). The analysis of these series can serve to describe the dynamics driven by soil and climate characteristics. Normalized difference vegetative index (NDVI) is commonly used in this type of evaluation (Moges et al., 2005; Numata et al., 2007; Escribano Rodríguez et al., 2015). The NDVI long-term series from rainfed cereal monoculture sequences have not been studied, although it is an important factor of soil degradation in semiarid areas (Hernanz et al., 2002; Mao et al., 2012; Wu et al., 2017).

NDVI series have been studied in different ways applying several analyses. One of these is based on the persistent character, or long-term memory, of a series studying the time scaling of its variance through Hurst index. One of the first works applying this type of analysis on NDVI series can be found in (Wang et al., 2005). In this line, (Peng et al., 2012) quantified the consistency of vegetation dynamic trends using Hurst index, sometimes named as Hurst exponent too. These works and later several ones (Jiang *et al.*, 2015; Ndayisaba *et al.*, 2016; Tong *et al.*, 2018; Hott *et al.*, 2019; Liu *et al.*, 2019 among others) have used the Rescaled Range Analysis (R/S analysis) method to estimate the Hurst index of NDVI series. Hurst index is one of the Generalized Hurst indexes extracted applying the Generalised Structure Function (GSF) widely used in the turbulence context (Davis et al., 1994). GSF focuses on the absolute

values of the differences that occur at different time scales, and it represents an excellent tool to study the dynamic of a series from a multiscaling point of view. Recently, several works have approached the study of NDVI series using multiscaling analysis (Ba et al., 2020; Li et al., 2017).

1.3.3 Hydrologic response to land cover/use

The land use and land change (LULC) is one of the most important drivers of environmental degradation, and responsible for much of the ongoing soil erosion, land degradation, biodiversity loss, water pollution, and agricultural abandonment, (Navarro and Pereira, 2015; Quintas-Soriano et al., 2016; Smiraglia et al., 2016). LULC is a global concern, with strong implications in the annual water balance, both for surface and groundwater resources (Schilling et al., 2008; Yilmaz et al., 2019). Changes in the vegetation cover and land use (LU) of a basin can have profound effects in the hydrology of the catchment (i.e. how the water is partitioned, and thus the proportion that is evapotranspired and/or flows as runoff) as well as the socio-economic demands that arise with LULC (e.g. irrigation development).

Nowadays, LULC is gaining importance for integrated water management and planning because of its effect on the water balance. Long term LULC effects are little studied across different scales from plot to national. Multipurpose modelling is presented as an alternative to attend the agricultural water demands and attempt to mitigate land degradation (Bangash et al., 2013; Schilling et al., 2008). However, the socio-economic aspects (i.e. more cash and jobs per drop) tend to be more important in water resources planning (Lambin et al., 2001; Kumar and Singh, 2005), hindering the policy effectiveness when it comes to the protection of water bodies.

There are many different expressions of LULC, including deforestation, afforestation, urban development, agricultural intensification-extensification processes, farmland abandonment, etc. All of them are characterized by complex interactions between human behavior, decision-makers and their biophysical environment (Parker et al., 2008). Despite these relations, uncontrolled LULC changes can occur because of individual decision, as response to the rural exodus and market trends. Agricultural activities, such as LULC changes, are also very dynamic in space, and its evaluation is challenging due to all the biophysical processes and human interactions that are involved (Acevedo et al., 2008; Opršal et al., 2016). The multiple connections between the elements and processes (i.e. atmosphere-water-soil-plant and human alterations) are subject of advanced research in recent time (Troch et al., 2009; Sofia and Tarolli, 2017).

Crop choices and rotations are significant land dynamic aspects to be considered when evaluating the environmental impacts of agricultural activities (Franzluebbers et al., 2011; Lemaire et al., 2015). Such processes are driven by farmer's decision, although usually

influenced by policies and regulations, market trends and prices, and by technical advice (Galán-Martín et al., 2015; Louhichi et al., 2017). Plot boundaries are also dynamic, suffering fragmentation and remerging processes (King and Burton, 1982; Botey Fullat, 2009) hindering the data acquisition and management of historic plot data. The knowledge about crop rotations patterns at medium and large scales (spatial and temporal) is still being a subject of research (Schönhart et al., 2011), and some of them are estimated through remote sensing and modelling (Qiu et al., 2003; Ray et al., 2012).

Integrating detailed crop rotations in hydrological assessment suppose adding complexity to the modelling exercise. This is especially true because most of hydrological models do not account this level of details for water balance calculations, and therefore tend to simplify important processes (e.g., phenology and operation scheduling) that largely influence the water budget. Implementing multiple LU's and site-specific farming in the same plot difficult simulation process (Jones et al., 2017). This hinders the understanding of the hydrological responses to the combined biophysical processes (Hively et al., 2009; Lee et al., 2016), moving to an advanced complex system in need of big data (Hutchins et al., 2017; Shafiee et al., 2018) and machine learning (Hosseini and Mahjouri, 2016) for modelling.

1.3.4 Land Use Land Change – LULC modelling scenarios

Land change modelling scenarios is an approach recently used to create the bridge between administrative planning LU perspective and real transfer to local LU context, in which decisions take place. Such approach also allows translating and simulating through modelling tools, a more accurate water balance components quantification based on a participatory methodology. The main purpose of participatory scenarios is to translating narrative scenarios into quantitative assessment of the LU scenario, as well as to assess the stakeholder perception for plausible future use of land at the local context showing the contrasting results to current LU patterns.

However, detailed crop rotation data are limited and the real impact assessment on the natural resources (positive or negative) at larger scales is still poorly understood (Aalders and Aitkenhead, 2006; Jiménez et al., 2016). Modelling approaches are usually the most common tool used to understand and comprehend simultaneous processes of spatial development in time across different LULC scenarios (Veldkamp and Verburg, 2004; Booth et al., 2016). The comparison of different spatial land configurations during a simulation period, provide the environmental responses of different LULC under similar and constant weather regime (Memarian et al., 2014; Singh et al., 2015).

Improving the representation within models of complex processes like crop rotations and other land management decisions is important to make better projections and understand the implications of different land use scenarios. Lack of data and local knowledge is often also an

important barrier. To overcome these barriers and advance in the development of more credible projections and/or scenarios requires engaging with stakeholders and experts to better understand the local realities. Many authors (Kok and van Vliet, 2011; Malek and Boerboom, 2015), have developed successful participatory scenario approaches that are able to better integrate in simulation exercises the local context, in which decision making and stakeholder choices take place, as well as the social and environmental regulatory framework at sub-basin scale. Applied to the context of European agricultural scenarios, the works of Hagemann et al., 2019; Karner et al., 2019 have developed and applied a participatory scenario approach to assess the future agricultural land use scenarios in contrasting European rural landscapes.

1.4 Research objective

Nowadays, the measures for water resources management in semiarid regions at individual water body has to be quantitative based, accurate and participative. For this purpose, the use of hydrological modelling as tool for decision support is crucial to manage water bodies in a sustainable way, especially all related to agricultural water management as the one with higher water demand. The increase in computer processing capacity, the use of inputs from remote sensing, and big data improve hydrological model accuracy when predicting or replicating water fluxes. However, the availability of input data for hydrological models, especially its temporal and spatial resolution, as well as the intrinsic variability of those variables, limits the application of the results for decision making. For this reason, new modelling approaches have been developed to take advantage of available data and mathematical methods (Scull et al., 2003; Szidarovszky, 1983) to improve the model accuracy and carry out a multi-objective assessment of the hydrologic cycle at finer scales (Gupta et al., 1998; Xu et al., 2015b).

The specific research questions of the thesis are:

- Are there any strategies to implement for input data that improve hydrological modelling?
- Could complimentary soil data sources as soil properties used in hydrological modelling to improve water balance accuracy?
- Is it possible to assess the effect of land use and crop rotation on the major components of the water balance in agrarian basins?

The hypothesis of this thesis is:

"Every effort to improve input data, of detailed hydrological models, facilitates calibration and validation procedures, and providing accurate results of water balance components assessment in semiarid agrarian sub-basins. These improvements can be used, as a compliment, to the current management tools from River Basins Authorities, for the for sustainable water management in the near future"

In order to test the former hypothesis, the main objective of this thesis is:

"Evaluate the spatial and temporal variations in the water resources of semiarid basins through novel improvements of input data, increasing the precision of the main components of the water balance in intermediate sub-basins without direct measurements using the SWAT hydrological model".

In order to achieve this goal, the following secondary objectives were considered:

I. Test alternative methods to improve actual data soil, weather input data for hydrological modelling to provide accurate results of hydrologic cycle parameters.

II. Analyse and describes the effect on the water balance components because of spatial heterogeneity of land-use change by using remote sensing data series into the SWAT model.

III. Probe an alternative hydrological modelling method with SWAT for the assessment of water demands in the Duero river basin, incorporating land-use and agricultural management into the modelling.

IV. Analyse and describes the hydrological effects because of the change in land-use in relation to the crucial components of the water balance.

The results obtained from this work are important for different actors involved with water resources management, especially for: 1) the technicians related to the management and allocation of demands at the river basin level and 2) local users, since they allow answering the questions associated with variability in supply and demand. However, the present work is a generic methodological guide for the Mediterranean area, which allows evaluating by means of SWAT modelling the effects on HR from the change in land use foreseen in a participatory exercise.

The applied methodology and the improvements made to the model can contribute as a complementary water resources management strategy used by river basin authorities in the allocation of actual and future water demands. The model developed here can not only be the basis for future hydrological research, but also for environmental management projects, as well as providing the basis for an integrated concept of water legislation related to land use.

1.5 Related publications

This doctoral thesis was developed within the framework of the T.A.L.E. project (Towards multifunctional agricultural landscapes in Europe: Assessing and governing synergies between

food production, biodiversity, and ecosystem services) with reference number (PCIN-2014-085), financed by the Ministry of Economy, Industry and Competitiveness of Spain. As part of the aid line, 2014 International Joint Programming Actions. Which was developed by CEIGRAM (Research Centre for the Management of Agricultural and Environmental Risks) between the years 2017 and 2019.

Rivas David, Willaarts Barbara, de Miguel García Ángel, Tarquis Ana Maria. *Combining integrated models and participatory methods to quantify water and agricultural trade-offs linked to different rural development scenarios*. EGU (2017) (oral presentation PICO-*Present Interactive content*®)

https://meetingorganizer.copernicus.org/EGU2017/EGU2017-10997-1.pdf

Rivas David, Willaarts Bárbara, DeMiguel García Ángel, Tarquis Ana María. *The use of Self Organizing Maps in hydrological modeling with SWAT*. PEDOMETRICS 2017: (Oral Presentation). Pág. 205.

https://static1.squarespace.com/static/5653202ee4b037d305e7fd3e/t/594a53f7e4fcb553cd43b9c0/1498043388899/Abstract+Book+Pedometrics+2017.pdf

Rivas David, de Miguel Angel, Willaarts Bárbara, Zegianini Silvana, Tarquis Ana M.. *Soil properties maps in hydrological modelling with SWAT*. EGU 2018: (Poster).

https://meetingorganizer.copernicus.org/EGU2018/EGU2018-19756.pdf

Volk Martin, Cord Anna, Demiguel Ángel, Holzkämper Annelie, Kaim Andrea, Karner Katrin, Lienhoop Nele, Nitsch Heike, Schmid Erwin, Schönhart Martin, Schramek Jörg, Strauch Michael, Tarquis Alfonso Ana María, van der Zanden Emma H., Verburg Peter, Willaarts Bárbara, Zarrineh Nina, **Rivas David**, Hagemann Nina. *Towards multifunctional agricultural landscapes: assessing and governing synergies between food production, biodiversity and ecosystem services*. LANDSCAPE 2018: (Poster). Pág. 108.

http://communications.ext.zalf.de/sites/land2018/SiteCollectionDocuments/Landscape2018_Book_of_Abstracts.pdf

Rivas-Tabares, D., Tarquis A.M., Willaarts, B., De Miguel A., 2019. An accurate evaluation of water availability in subarid mediterranean watershed through SWAT: Cega-Eresma-Adaja. *Agricultural Water Management*.

DOI: https://doi.org/10.1016/j.agwat.2018.09.012

Rivas-Tabares, D., Willaarts, B., De Miguel A., Tarquis A.M., 2020. Self-organizing map of soil properties in the context of hydrological modeling. *Applied Mathematical Modeling.*

DOI: https://doi.org/10.1016/j.apm.2020.06.044

Rivas-Tabares, D., Willaarts, B., De Miguel A., Tarquis A.M., 2021. Water resources implications linked to the land sharing and land sparing debate: Exploring practical implications in Central Spain. *Water Resources Management.*

DOI: (under review)

Other contributions as co-author in publications with members of the TALE project team:

Katrin Karner, Anna F Cord, Nina Hagemann, Nuria Hernandez-Mora, Annelie Holzkämper, Bernard Jeangros, Nele Lienhoop, Heike Nitsch, **David Rivas**, Erwin Schmid, Catharina JE Schulp, Michael Strauch, Emma H van der Zanden, Martin Volk, Barbara Willaarts, Nina Zarrineh, Martin Schönhart. Developing stakeholder-driven scenarios on land sharing and land sparing–Insights from five European case studies. *Journal of Environmental Management.*

DOI: https://doi.org/10.1016/j.jenvman.2019.03.050

2 Methodology

The methodology applied in this research is the result of combining several methods to address the stated objectives detailed in Chapter one. The interest is to scope hydrological modelling from its conception, enhancing the input data through additional data treatments. This with the aim to foster the importance of it in the accuracy water balance results on decision making in water management of agrarian semiarid watersheds.

2.1 Self-Organizing Map of soil properties in the context of hydrological modelling

2.1.1 Study Area

The Adaja watershed is a tributary subbasin of Duero River and defined as a second order watershed covering an approximate area of 5,263 km^2, comprising two mains tributaries, the Adaja river (left) and Eresma river (right) (see Figure 2). The Adaja watershed presents a regulated stream network in the highlands. To cover water demands, large quantities are stored in reservoirs providing 26.81 hm^3 and 117.06 hm^3 of fresh and irrigation water, respectively. Most of those demands are located in the watershed midlands and lowlands (CHD, 2015). The catchment is gauged at Valdestillas flow gauge (VFG) covering the 98.6% of the total drainage area and daily measurement considered for modelling were selected from 2004 to 2014. This subbasin presents an elevation range between 670–2,426 m., because of this and the landscape variation a proposed division in three parts (lowlands, midland and uplands) is a reasonable approach to assess water balance components of the Cega-Eresma-Adaja system (Rivas-Tabares et al., 2019b). The land use in the Adaja river subbasin is dominated by rainfed agriculture (56.54%), forest (22.27%), urban and transportation (11.22%), shrubs and pastures (7.92%), irrigated crops (1.94%), and water (0.1%) (see Figure 3).

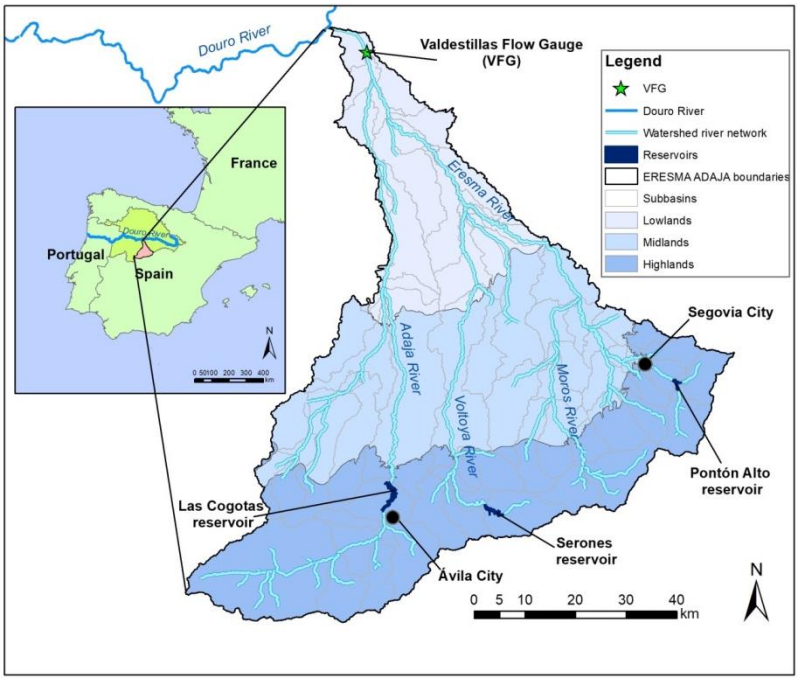

Figure 2. Study area location indicating the gauging station Valdestillas (VFG), subbasin distribution and Adaja river watershed segmentation in North central Spain.

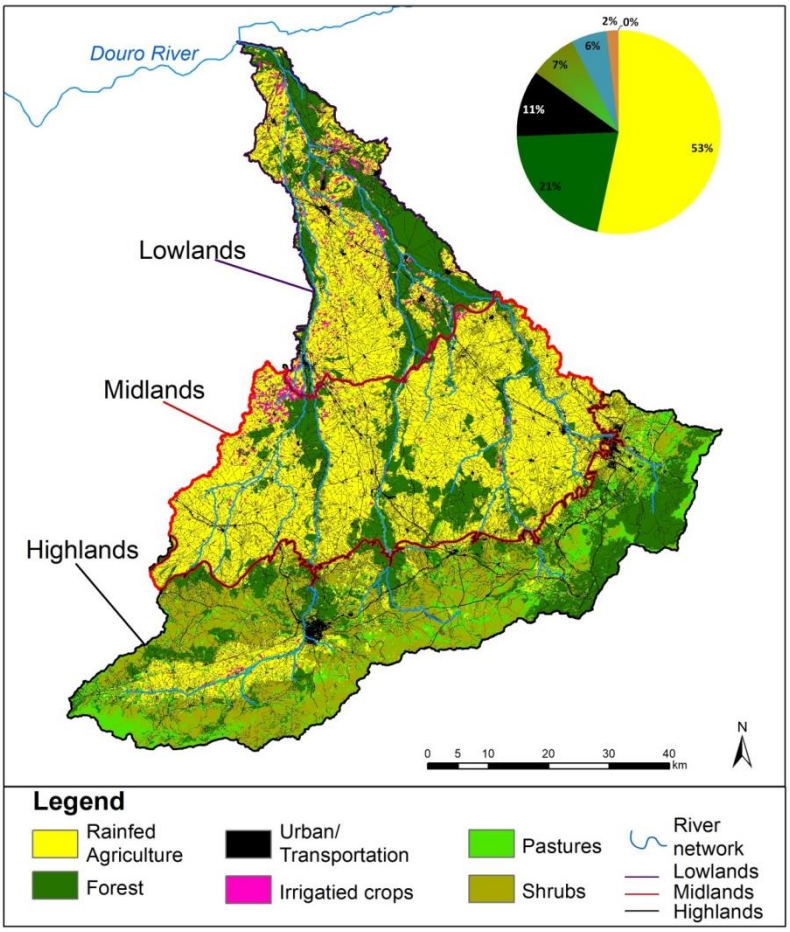

Figure 3. Land Use composition of Adaja river watershed and section division (lowlands, midlands and highlands).

The Adaja watershed contributes with an average discharge over Duero River with 407 hm^3yr^{-1} calculated in short flow series reference. The total water demand (153.94 hm^3yr^{-1}) of the study area is attributable to five main sectors: (1) Agriculture (76%) 117.06 hm^3yr^{-1} (2) Freshwater (17.4%) 26.81 hm^3yr^{-1} (3) Livestock (4.6%) 7.10 hm^3yr^{-1}, (4) Industrial (1.4%) 2.08 hm^3yr^{-1} and (5) recreational (0.6%) 0.89 hm^3yr^{-1} (CHD, 2015). Water abstraction to supply demand comes from surface and groundwater bodies, denoting that groundwater abstraction is the main source of water supply when rivers run with low flow during the spring-summer period.

The predominant soils groups are Cambisols (35.9%), Luvisols (31.4%), Leptosols (12.7%), Arenosols (9.8%), Fluvisols (4.9%), Regosols (1.9%), Solonchack (1.7%), Solonetz (1.7%) and Gleysol (0.1%) (Llera, David A. Nafría et al., 2013).

2.1.2 Soil map properties sources for hydrological modelling

Two different soil data sources were used to obtain three soils mapping and setting up the hydrological model. First, a Harmonized World Soil data base from FAO soil map at 1:1,000,000 scale (HWSD) comprising all soil properties needed for hydrological modelling, including soil depth (Figure 4A). Data of soil properties are shown in Annex 1 in supplementary material.

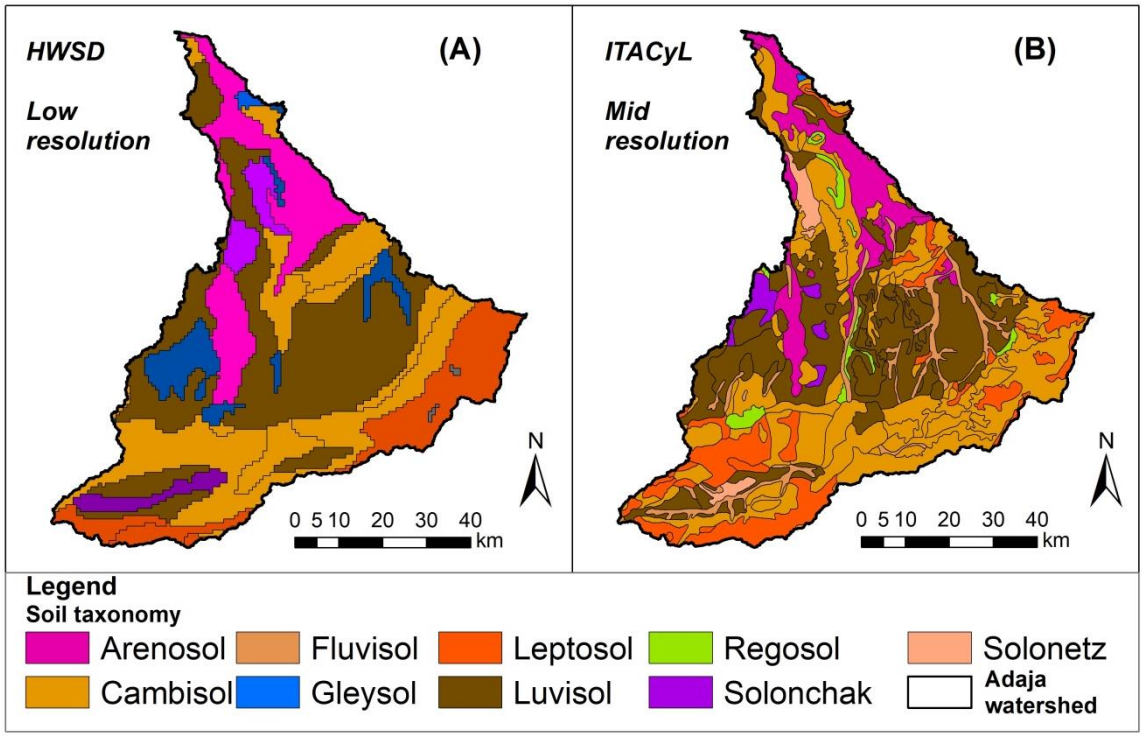

Figure 4. Soils maps of Adaja river watershed from (A) Harmonized World Soil Database - HWSD at 1:1,000,000 (low resolution) and (B) Agricultural Technological Institute of Castilla and Leon – ITACyL at 1:400,000 scale (mid resolution).

Soils maps of Adaja river watershed from (A) Harmonized World Soil Database - HWSD at 1:1,000,000 (low resolution) and (B) Agricultural Technological Institute of Castilla and Leon – ITACyL at 1:400,000 scale (mid resolution).

Second, a database of 407 soil samples of the watershed from different sources (Llera, David A. Nafría et al., 2013) was used to create a griding of 100x100 m resolution starting from a sampling density of approximately 25x25 m. A Kriging method (Matheron, 1963; Wagner et al., 2012) was applied to the original set contained 11 soil variables related to physical and chemical properties, see supplementary material Annex 2. The soil variables grid was used to obtain the other two soil mapping. Soil depth wasn't included in this set.

Based on the taxonomic soil units (TSU) of ITACyL, at 1:400,000 scale (Figure 4B), the average of soil variable grid belonging to the same soil unit was applied to obtain a soil mapping of properties named as TSU. At this point, we would like to bring up that, commonly, soil maps for hydrological modelling set-up are based on the taxonomic approach. In general, those maps were developed using a traditional interpretation of aerial photos, available geology maps, soil samples from field work and performing of laboratory analytics (Tissari et al., 2007). The taxonomic soil units' maps sometimes include additional information about specific soil properties, although this is not the case. However, the inter-spatial variation of properties in the same soil unit is not considered (Lee Ficklin et al., 2014) and in larger units and regional scales this introduce an error forcing to modelers to make some assumptions (Kamali et al., 2017) (Neitsch et al., 2005).

Finally, applying a self-organizing map (SOM) method on the soil variables grid, the third soil map was obtained (SOMM). The SOM method is described in detail in section 2.1.3.

In the runoff's case estimation, the SCS method (Hjelmfelt, 1991) is widely used. In this case, information on the hydrologic soil group for runoff and soil depth are indispensables for routing the water flows. For the three maps, the hydrological soil groups were assigned using lookup tables of the SCS (Hjelmfelt, 1991).

The soil depth for Adaja watershed in HWSD was already included in the dataset, meanwhile the other two maps didn't contain that information. The soil depth for TSU and SOMM was conducted through the implementation of the TOPMODEL approach (Saulnier et al., 1997) and watershed segmentation (Pelletier and Rasmussen, 2009). The TOPMODEL model uses a decreasing linear function of the topographic slope based on the DEM. An adaptation of Saulniers' equation of TOPMODEL was performed due of watershed slope heterogeneity and local geomorphological characteristics, this include spatial and depth restrictions. Firstly, the watershed was segmented in three parts (low, medium and highlands) to establish for each the

restriction values of soil depth for local minimum and maximum values (Rivas-Tabares et al., 2019b). Secondly, the land cover was used to identify the minimum soil depth understood as effective soil depth for root development, because of the sensitivity to this parameter affecting the hydrology dynamics and plant growth (Castro-Franco et al., 2017). The covers considered were cropland, forest and bare soil; and the maximum root depth were assigned from the averages of crops and forest from literature references (Canadell et al., 1996; Padilla and Pugnaire, 2007). The summary of soil depth restrictions is shown in Annex 3 in the supplementary material.

The resulting soil depth map was spatially compared to the available data of 8 complete soil pits that represent the main soil pedogenesis classes of the area and satisfactory validated. This soil profiles were part of the taxonomic soil map documentation at 1:400.000 scale (Llera, David A. Nafría et al., 2013). Moreover, the resulting soil depths do not exceed soil depth values of pits. A reclassification of soil depth was performed to avoid increasing the number of HRUs with tiny soil depth differences. The classes were defined based on spatial variability for each watershed segment and limited to four main depth classes (300, 600, 900, and 1500 mm) see supplementary material Annex 4.

2.1.3 The Self-Organizing Map strategy

A SOM is a technique used to represent and visualize structures of high-dimensional data based on artificial neural network of any continuous function (Kohonen, 2001). It is largely implemented in sciences facilitating interpretation of some physical phenomenon. The algorithm consists in organizing l neurons on a regular grid. For this, a vector is defined with n + m weighted dimension $\mathbf{m}= (m^1 \ldots m^n, m^{n+1} \ldots m^{n+m})$, then those are assigned for each neuron. The neuron l is defined by n= dim($\mathbf{x}$) and m=dim($\mathbf{y}$) dimension arrays, where n denote the dimension of the input data set (in this case the soil properties) and m the dimension of the output (number of soil clusters or soil units). The l neurons are connected to the adjacent neurons by a neighborhood relationship. This characteristic defines the cluster structure of the SOM, Figure 5. This process is based on training samples by following an iterative process. Each iteration k is initialized by an unsupervised training of sample vector $\mathbf{X}_{SOM}$. This training iterates the weight vector $\mathbf{m}_i$ in the domain of the output, in this case was defined in $3 \geq l \leq 50$ clusters to reduce soil units that consequently reduce the number of HRUs compared to the taxonomic soils map with 196 soil units at 1:400.000 scale.

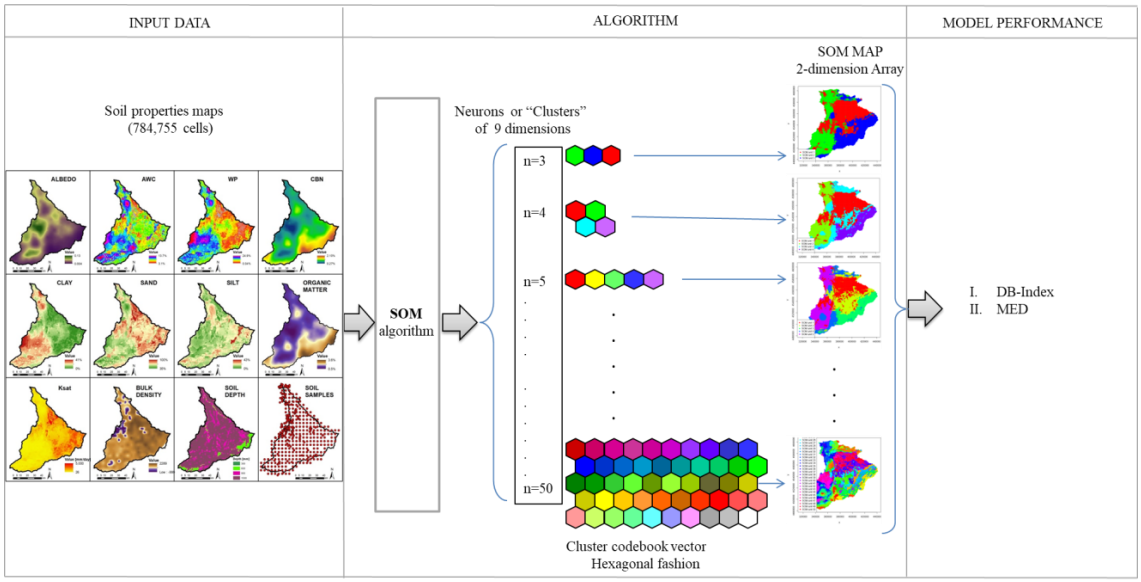

Figure 5. Structure of Self-organizing maps (SOM) to create soil units for SWAT hydrological modelling. The clusters of neurones are represented by pixels with the same size of input data.

The training starts by initializing the SOM when selecting small random values for the initial weight vectors m_i. A typical and reasonable way to achieve faster convergence of the best matching unit is to initialize the $\mathbf{m}_i$ vector with the greatest principal component eigenvalues of the data (Kohonen, 2001). Once the weights are settled in the vector, the iteration k is defined by choosing randomly one vector $\mathbf{X}_{SOM}(k)$ for input data and computing the Euclidean distance $\in_i$ to the weight vectors of the SOM.

$$\in_i = \|X_{SOM}(k) - m_i\| = \sum_{j=1}^{n+m}\left(X_{SOM}^i(k) - m_i^2\right)^2 \quad (1)$$

The neuron that present the smallest distance $\in_i$ to $X_{SOM}(k)$ is the best matching unit (BMU) of X or the 'winning neuron'. This neuron is the map element C, represented by the weight vector $\mathbf{m}_c(k)$.

$$\|X_{SOM}(k) - m_c(k)\| = min\{(X_{SOM}(k) - m_i)\}_i, i = 1,2,\dots,l. \quad (2)$$

The following iterations are completed by updating the weight vectors until the BMU is closer to the input vector. The rule to define the updating the weight vector is defined by (a) the operation ($X_{SOM}(k)$ – $\mathbf{m}_i(k)$), (b) the size of the neighborhood function h_{ci} which decrease monotonically to zero with k and the distance of the wining neuron and (c) a learning rate factor $\alpha_s(k)$ which gradually lowers the height of the neighborhood function as the iteration advances.

$$m_i(k+1) = m_i + \alpha_s(k)h_{ci}(k)[X_{SOM}(k) - m_i(k)] \quad (3)$$

The function h_{ci} is typically represented by a Gaussian function

$$h_{ci}(k) = \exp\left(-\frac{\|r_c - r_i\|^2}{2\sigma^2(k)}\right) \quad (4)$$

In which the expression $\|r_c - r_i\|^2$ is the distance between the map units c and i on the map grid. The σ variable represents the neighborhood radius at iteration k and σ is decreasing monotically during the iterations with k. The value of σ is not explicit required (Kohonen,

2001). It is recommended to initialize the iteration with $\sigma_s(0) \leq 1$ with values near to 1 and then increasing the number of training steps *k*. The vector X_{SOM} is the training data set from the previous Kriging method with the eleven main soil properties, described in section 2.1.2.

For this study, the R package Kohonen was implemented to obtain the soil units through the SOM method (Wehrens and Buydens, 2007). However, the number of cluster will be optimal and some performance metrics are need to ensure an optimal clusters number (Charrad et al., 2014; Khanchouch et al., 2015).

2.1.4 The Self-Organizing Maps performance evaluation

The SOM method provides a map in which the clusters are clearly defined. However, an optimal number of clusters are desirable to reduce even more the complexity of soil properties without losing the soil representativeness of the property into the cluster. For this, this algorithm uses the Davies Boulding index for clustering by using an unsupervised classification learning technique to obtain homogeneous partitions of the object while promoting the heterogeneity between partitions (Khanchouch et al., 2013).

The Davies Bouldin DB Index (Davies and Bouldin, 1979) is characterized by the definition of the compactness and how well are separated the clusters. The DB index is given by the expression,

$$DB = \frac{1}{c}\sum_{i=1}^{c} max \quad _{i \neq j} \left\{ \frac{d(X_i)+d(X_j)}{d(c_i,c_j)} \right\} \tag{5}$$

where variable c defines the number of clusters, i and j denote the clusters, $d(X_i)$ and $d(X_j)$ are the distances between all objects in clusters i and j to their respective centroids, and $d(c_i, c_j)$ is the distance between centroids. Smaller values of DB index show better clustering quality (Fonseka and Alahakoon, 2010; Khanchouch et al., 2013). Once the DB index is defined for a range of clustering domain, a graph that include the lower mean distance of clustering process is reached, indicates that the minimum compromise of those values is an optimal solution for number of clusters.

2.2 Weather Data

The weather data were collected from 47 weather stations of AEMET -Meteorological Agency of Spain. The weather variables and their spatial assignation to sub-basins were reformulated considering the centroids of the resulting boundaries of 79 sub-basins from DEM processing and implementing weighted proportion of each variable using the Thiessen Polygon method TPM (Rivas-Tabares et al., 2019b).

2.3 Hydrological Modelling with SWAT

The SWAT model (Arnold et al., 1998) is a spatial distributed hydrological model, widely used for land management and water resources assessment in very complex watersheds. For this, SWAT use a disaggregation strategy based on two criteria, (i) sub-basins discretization based on DEM (topographic criteria) and (ii) the Hydrologic Response Units - HRUs discretization that is based on soil properties, land use and slope classes. Thereby, the sub-basins are aggregated with several HRUs. The calculation unit for SWAT is attributable to this set of units for all the biophysical modeled processes.

The SWAT model is based on a routines tree that provides a solution of the water balance equation. These routines put up together the hydrological solution for evapotranspiration, surface runoff, soil infiltration and subsurface runoff. Model could be more precise in each routine including sediment, chemical and crop yields depending on the input data setup. Soil is very complex and SWAT model could be settled up to 10 soil layers. Water flux through the soil is based on the saturated capacity of each layer, once the saturation state is achieved, the water flux is coupled as water input of next soil layer but if the following layer in depth is saturated, lateral runoff occurs. If last layer is reached, water flux composes the aquifers recharge volume. Deep aquifer is considered as a lost in water balance, but shallow aquifer overfilling is called return flow from shallow aquifer; this volume is routed directly to the mainstream of each subbasin according to each case.

The runoff is one of the main processes assessed by the SWAT model, this routine is based on the SCS curve number method (Hjelmfelt, 1991), presenting a sensitive factor related with the curve number CN assignation which is in turn related with antecedent moisture condition of soil. The method was developed from experimental abstraction as a non-linear function between rainfall-runoff processes. The definition of three main routine component (1) runoff interception, (2) soil storage variation and (3) infiltrated water in the porous media, expressed as potentials, solve the relation for routing water through the soils of the watershed.

The evapotranspiration ET process can be selected using Presley Taylor method or Penmam-Monteith method. Some differences can be identified by switching the methods but the most universal accepted for modelling purposes with SWAT is the Penman-Monteith method due of the capacity of worldwide accuracy and approximation to the real evapotranspiration measured in different sites and watersheds.

The routing into SWAT is completed once all the water fluxes are calculated and routed into the main channel of each subbasin. In turn, it’s routed into the river network. The SWAT tool is a model still more used for surface calculations due of the complexity of soils and geology of

watersheds. The model is often used for estimating the aquifer recharge as a system lost that could provide an idea of the system, but more precise coupling models are required for estimating the deep aquifer recharge rates.

2.3.1 Calibration-Validation

SWAT model as a distributed model for hydrology assessment requires a calibration and validation process. For this, the HRUs need to reach a moisture condition to initialize the water fluxes estimation. One year at daily time step is a reasonable warming-up period prior calibration and validation processes in sandy soils (Kim et al., 2018), a predominant characteristic of Adaja watershed.

Calibration and validation is conducted through the implementation of the Sequential Uncertainty Fitting SUFI-2 algorithm of the software package SWAT-CUP (Abbaspour, 2011). SUFI-2 is a powerful automatic tool for SWAT model calibration and validation processes due of facility of implementing single or multi-parameter calibration. The iterative algorithm captures most of measured data within the 95% prediction of uncertainty envelope (95PPU) (Abbaspour, 2013). Modeler usually defines a set of parameters from a literature review of similar watersheds or with similar conditions, in this case the parameter area showed in Table A2 in the supplementary material. However, it's advisable to define a valid range for the calibration parameters of the case study. The SUFI-2 algorithm is an iterative process that defines the parameter value over the initial range converging near to the measures through 300-1000 simulations. However, a good correlation between the selected value of the parameters and the measures could provide an erratic model but well represented by model performance metrics (Abbaspour et al., 2004).

2.3.2 Water balance

The SWAT model provides detailed information about main water fluxes at HRU and subbasin scale. In the hydrological cycle, all those fluxes are interconnected and provide different response to soil, surface roughness and ground state relations, Figure 6. The balance of water cycle in the mainstream follows the given mass equation.

$$Q_s = P - ET - \Delta SM - \Delta GW \tag{6}$$

Where Q_s (6) is the surface runoff, ET is evapotranspiration, ΔSM is the change of soil moisture, and ΔGW is the change in groundwater storage. The terms Q_s, ΔSM, and ΔGW are influenced by soil properties, surface roughness and slope. This is also according with the HRU definition but appointed by precipitation behavior as the main water input into the system.

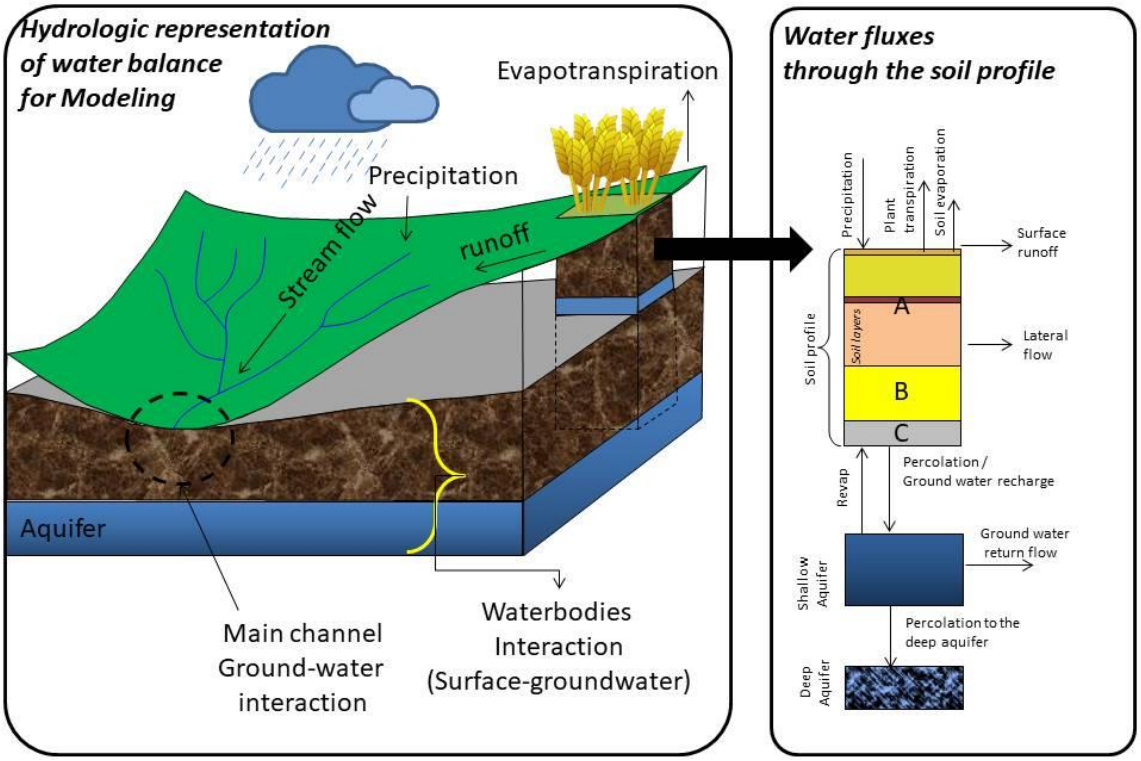

Figure 6. Hydrologic model system representing watershed fluxes: A) main fluxes at basin scale, B) detailed fluxes at soil profile scale.

Water balance is also related with anthropogenic use of soil for vegetation growth, nutrient cycling and for different ecosystem services. Water processes involved in hydrological cycle (runoff, evapotranspiration, soil infiltration and aquifer recharge) are sensitive in sub-arid catchments due of small perturbations of input water into the system in monthly or daily time step. In Adaja watershed, the representation of each of hydrological cycle components could be better analyzed from a watershed segmentation (lowlands, midlands and highlands) (Rivas-Tabares et al., 2019b).

2.3.3 Self-organizing maps in Cega-Eresma-Adaja

Digital soil mapping for Cega-Eresma-Adaja management system was also integrated for modelling evaluation. Cega river watershed was added to previous map described in section 2.1.3, using the same methodology. A soil taxonomic unit map is currently available in the area with a scale of 1:400,000 (Figure 7). However, this map does not include soil properties. A common practice is to use pedotransfer functions to assign the soil properties required to the taxonomic units, affecting the uncertainty of the model (Seeger, 2007). To reduce it, a soil map was created using data from a soil sample database with 11 soil properties (clay percentage, sand percentage, silt percentage, moist soil albedo, available water content, wilting point, field capacity, saturated hydraulic capacity, bulk density, organic carbon content and organic content percentage) and the Kohonen in R tool (Wehrens and Buydens, 2007). Soil units in hydrology

modelling are directly related with the total number of calculation units (i.e., subbasins, Hydrologic Response Units HRUs, etc.). This tool reduces the number of soil units without losing spatial information. The Kohonen tool is based on the self-organising maps (SOMs) approach to delimit soil clusters. Each cluster defines a soil unit with a low variability of physical properties. Spatial variation of each soil parameter is complex in each unit, and different soil map scale analysis is required (Lin et al., 2005). The resulting clusters do not directly correspond to the taxonomic units, although they are interlinked. A close relationship does not apply in this context, (Figure 7). On the one hand, SOM represents clustering of soil properties and on the other, the taxonomy unit represents soil pedogenesis. However, spatial variability of soils properties is more complex. The similar spatial distribution of clusters and taxonomic units is suitable. Therefore, this comparison serves to validate the SOM soils map.

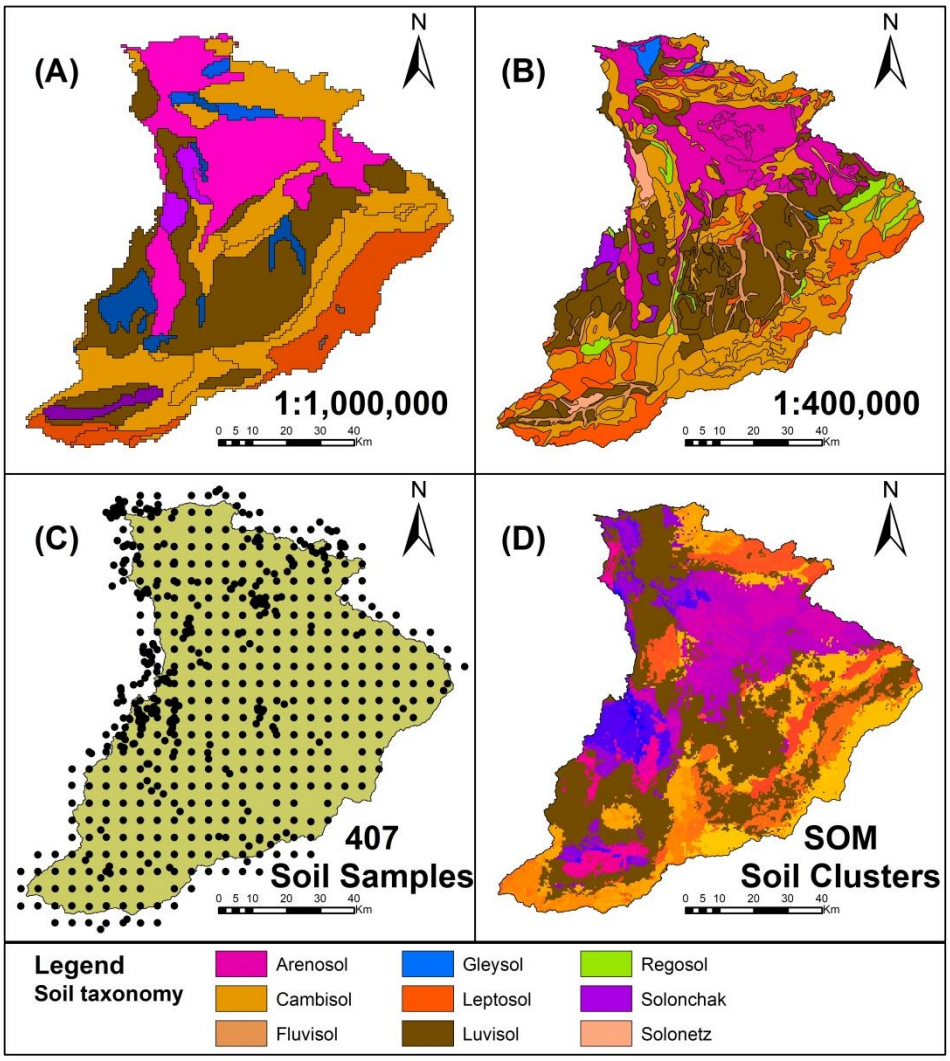

Figure 7. Soil and land use classifications in Cega-Eresma-Adaja (CEA) watershed, colors show the soil taxonomy relationship between the different scales. (A) FAO (HWSD) Soil map at scale 1:1,000,000 (14 soil units), (B) Soils map of CyL at scale 1:400,000 (291 soil units), (C) ITACyL soil samples sites, (D) SOM soil clusters (16 clusters) with depth differentiation (92 soil units) at 20m resolution.

2.4 Evaluation of water availability in sub-arid a Mediterranean watershed

2.4.1 Study area

The Cega-Eresma-Adaja system (CEA) is located in the central north of the Iberian Peninsula, and consists of two adjacent sub-basins that are jointly defined as a hydrological management system by the Duero River Basin Authority (DRBA), Figure 8. The stream network defined by the Eresma and Adaja sub-basins represents 67% of the total CEA area, while the watershed defined by the Cega comprises 33%. The former are regulated at the upper river network, while Cega is not yet regulated.

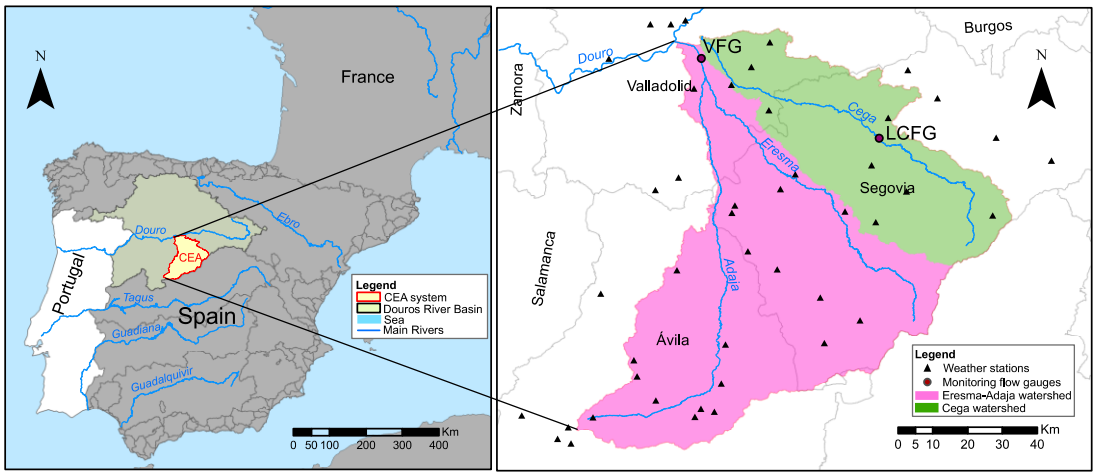

Figure 8. Location of the study area in Duero's River basin, river network and flow gauges.

The Eresma and Adaja sub-basin, with a total discharge of 407 hm^3 yr^{-1}, equivalent to 63% of the total discharge capacity of the CEA and the Cega sub-basin, provides the remaining 37% of CEA discharge (238 hm^3 yr^{-1}). Most of the rivers in the CEA system are directly connected to the aquifers (IGME, 2008). The frequent descent of the water table level, due to overexploitation, is causing a disconnection between the riverbed and the aquifer. This situation is exacerbated in dry periods, where most of the rivers have very low flows (CHD, 2015).

Nine major soil groups could be found in the area: Cambisols (34%), Luvisol (26%), Arenosols (19%), Leptosol (11.5%), Fluvisols (4%), Regosol (3%), Solonetz (1%), Solonchak (1%) and Gleysol (0.5%). The soil genesis is typically developed from moorland limestone in the northeast, Mesozoic carbonates in the headwater area and is detritic in the basin landfill (IGME, 2009). Sandy soils are the representative textures in more than 54% of the area, causing medium-high infiltration rates to subsurface flow to streams and recharge of groundwater bodies.

Agriculture is the main land use, accounting for 54.1% of the total area (Figure 9), followed by forestry (27%), urban (12%), shrubland and pastures (6.7%), and water bodies (0.1%). Rainfed

crops represent 63% of total agricultural land, whereas fallow land accounts for 31%, irrigated annual crops for 5%, and permanent crops represent 1%.

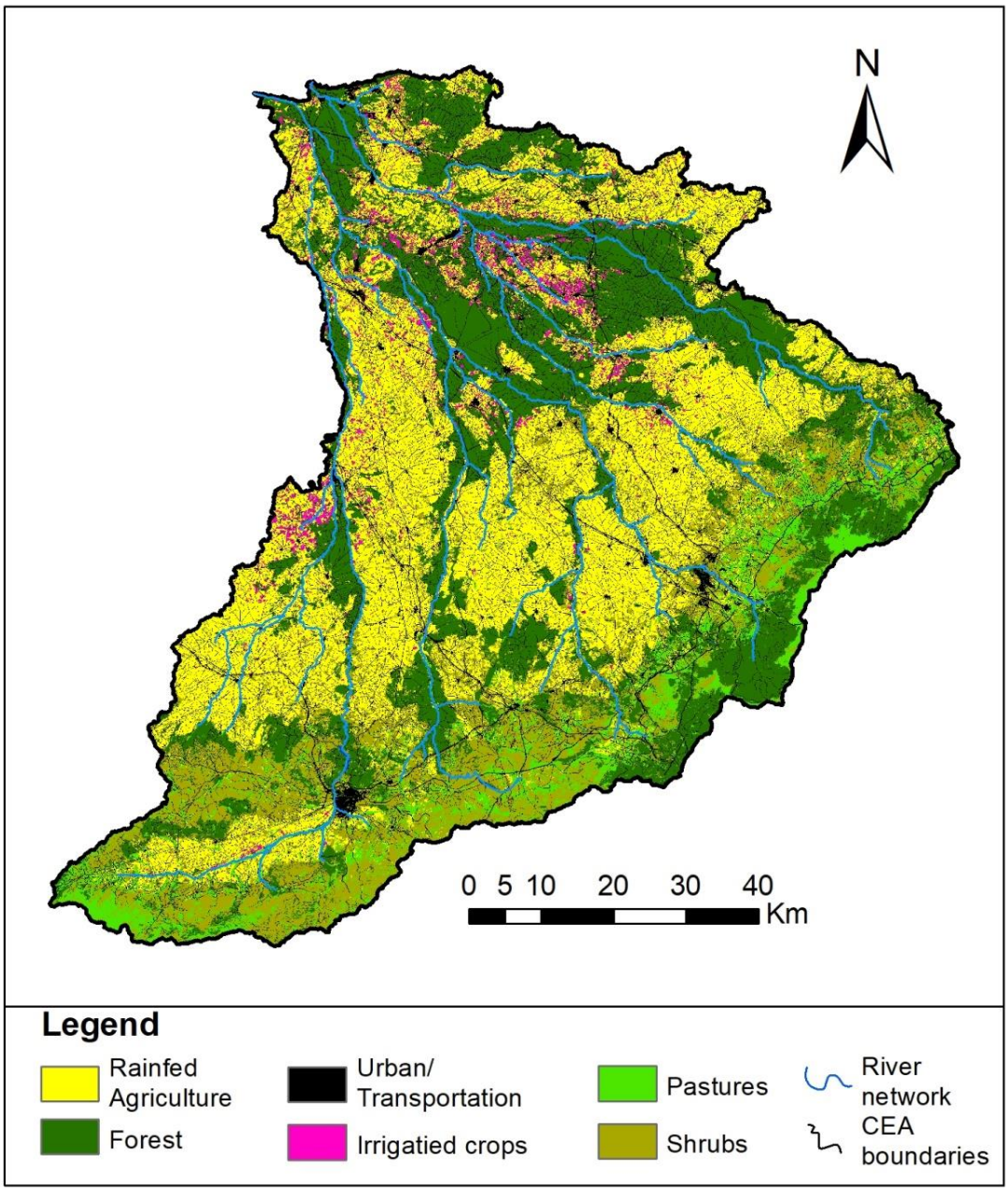

Figure 9. Land use of CEA system.

2.4.2 Hydrological Modelling with SWAT

The SWAT model (Arnold et al., 1998) is a spatial distributed hydrological model, widely used for land management and water resources assessment in very complex watersheds. For this, SWAT use a disaggregation strategy based on two criteria, (i) sub-basins discretization based on DEM (topographic criteria) and (ii) the Hydrologic Response Units - HRUs discretization that is based on soil properties, land use and slope classes. Thereby, the sub-basins are aggregated with

several HRUs. The calculation unit for SWAT is attributable to this set of units for all the biophysical modeled processes.

The SWAT model is based on a routines tree that provides a solution of the water balance equation. These routines put up together the hydrological solution for evapotranspiration, surface runoff, soil infiltration and subsurface runoff. Model could be more precise in each routine including sediment, chemical and crop yields depending on the input data setup. Soil is very complex and SWAT model could be settled up to 10 soil layers. Water flux through the soil is based on the saturated capacity of each layer, once the saturation state is achieved, the water flux is coupled as water input of next soil layer but if the following layer in depth is saturated, lateral runoff occurs. If last layer is reached, water flux composes the aquifers recharge volume. Deep aquifer is considered as a lost in water balance, but shallow aquifer overfilling is called return flow from shallow aquifer; this volume is routed directly to the mainstream of each subbasin according to each case.

The runoff is one of the main processes assessed by the SWAT model, this routine is based on the SCS curve number method (Hjelmfelt, 1991), presenting a sensitive factor related with the curve number CN assignation which is in turn related with antecedent moisture condition of soil. The method was developed from experimental abstraction as a non-linear function between rainfall-runoff processes. The definition of three main routine component (1) runoff interception, (2) soil storage variation and (3) infiltrated water in the porous media, expressed as potentials, solve the relation for routing water through the soils of the watershed.

The evapotranspiration ET process can be selected using Presley Taylor method or Penmam-Monteith method. Some differences can be identified by switching the methods but the most universal accepted for modelling purposes with SWAT is the Penman-Monteith method due of the capacity of worldwide accuracy and approximation to the real evapotranspiration measured in different sites and watersheds.

The routing into SWAT is completed once all the water fluxes are calculated and routed into the main channel of each subbasin. In turn, it’s routed into the river network. The SWAT tool is a model still more used for surface calculations due of the complexity of soils and geology of watersheds. The model is often used for estimating the aquifer recharge as a system lost that could provide an idea of the system, but more precise coupling models are required for estimating the deep aquifer recharge rates.

2.4.3 Model baseline setup

The present study uses the SWAT2012_rev664 version with ArcSWAT 2012.10.19. Simulation is performed based on a daily time step (2004-2014). Model setup is summarised in Figure 10.

In addition to the standard setup process, this work introduces some improvements in the setup related to input data to reduce model uncertainty.

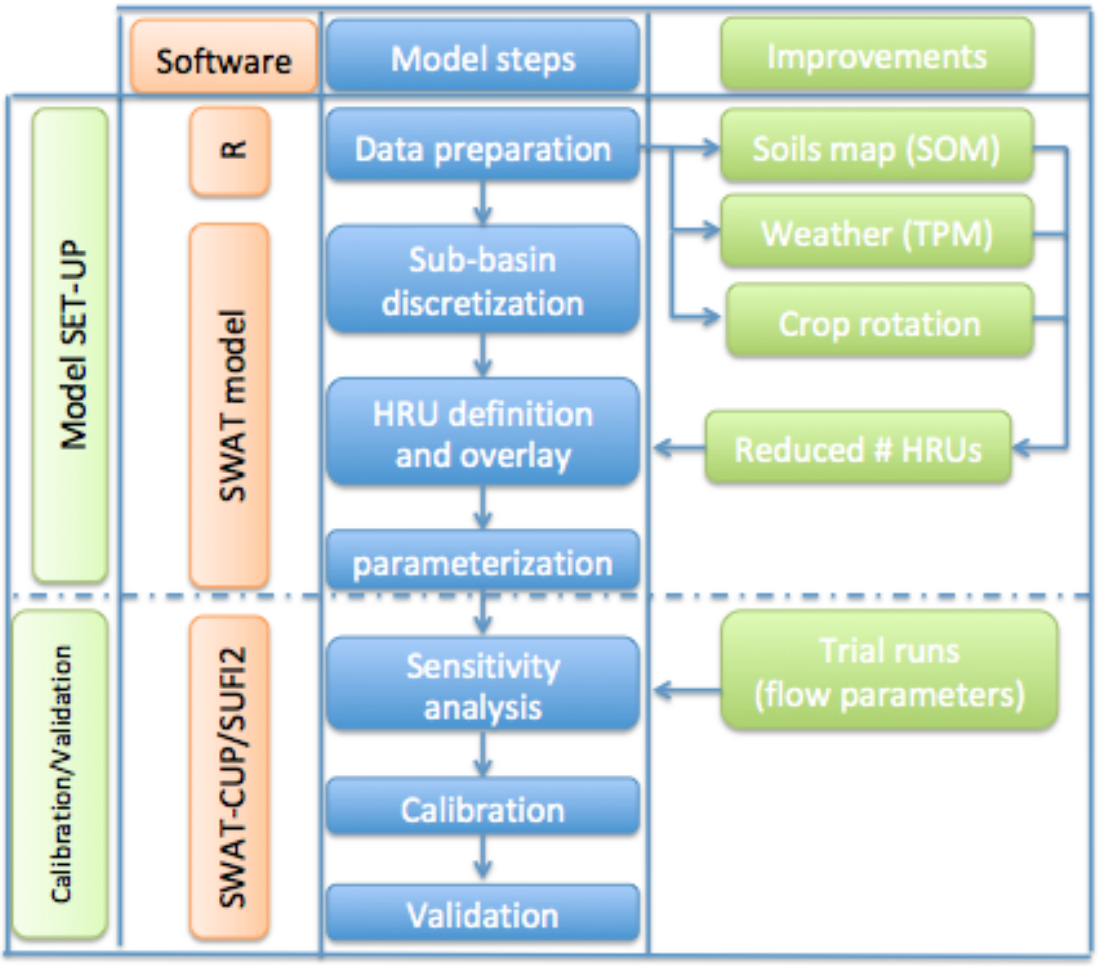

Figure 10. SWAT model development flowchart main steps and implemented software.

Detailed descriptions and sources of the data used to set up the SWAT baseline model are provided in Table 1. The complete data for model setup were based on (i) measured data (e.g. soil samples), (ii) literature values from published studies, reports and official documentation of RBMPs, (iii) assumptions reported in the literature (e.g. soil parameters based on pedotransfer functions PTF) and (iv) SWAT predefined databases (e.g. crop parameters). As the scale of the CEA is wide, detailed management schedules associated with land uses have been included to elucidate their impact on the global water balance. (See Annex 6 for more detailed information).

Table 1. Model input data sources for Cega-Eresma-Adaja (CEA) SWAT baseline model.

Data	Description/properties	Source of data
Digital Elevation model (DEM)	25 m resolution. Map used to define two slope classes 0-3 and >3%	MDT25, LiDAR-PNOA by © Instituto Geográfico Nacional
Flow gauges	Daily discharge (2004-2014) for 2 points: Valdestillas VFG (Adaja river) and Lastras de Cuellar LCFG (Cega river)	CHD – Duero's RBA; CEDEX
Reservoirs	Three reservoirs. Las Cogotas (58,6 hm^3), Pontón Alto (7,4 hm^3) and Serones (6,3 hm^3)	CHD – Duero's RBA
Land use	20 m resolution, 31 basic land-cover categories. Including 18 different crops.	ITACyL, 2013
Soil characteristics	16 soil types were determined using 407 soil samples and introducing (Saulniers et al, 1997) soil depth empirical model to obtain a total of 92 soil different units.	ITACyL, 2013
Weather data	Data for 2004 - 2014. Precipitation, daily maximum and minimum temperature, daily global solar radiation, surface wind speed, daily mean relative humidity.	AEMET
Agricultural management practices	Surveys from ITACyL for INFORIEGO services. Database for irrigation districts with free access.	ITACyL, 2013

CEA boundaries and sub-basins were defined using a 25-m DEM (Digital Elevation Map). An internal sub-basin division was also performed based on interest evaluation points: flow gauge locations, reservoir discharges and predefined sub-basins of DRBA. In total, 121 were defined for the CEA system, including 79 for the EA and 42 for the Cega catchment, each comprising different HRUs.

The CEA system, with ten reservoirs, is considered a hyper-regulated system, with all the reservoirs located in the headwaters of the Eresma-Adaja watershed (capacity of 81.24 hm^3). Discharge data on three reservoirs representing 86.8% of the total capacity are available and therefore considered for the simulations: Las Cogotas (56.8 hm^3), Serones (6.3 hm^3) and Pontón Alto (7.4 hm^3). The discharges from reservoirs were included in the model, following the operation rules and their volume capacity. The input required was estimated and fitted by analysing the global behaviour of gauging discharge series during the simulation period.

From the 20 gauging stations located in the CEA system, only two provided daily stream flow data for the selected period (2004-2014): Valdestillas (VFG) monitored a northerly outlet covering 98.6% of the Eresma-Adaja watershed; and Lastras de Cuellar (LCFG), located in the middle of the Cega watershed, covered just 25% of the total area.

Weather data assignation is a key step in the development of a SWAT model, as any error introduced with the water input would propagate in the whole model. SWAT usually assigns the data of the nearest weather station to the sub-basin centroid, providing a constant value to the whole sub-basin. This could introduce a remarkable model input uncertainty, especially in large sub-basins where weather could be spatially heterogeneous in very steep reliefs. But as (Wagner et al., 2012) remarks, the definition of a composite climatic value by different weights using

diverse interpolation methods significantly improves weather input for the model. This is why the weather data assignation was improved, including a spatial-based representativeness of data for each sub-basin. To do so, an implementation of the Thiessen Polygon Method (TPM) (Thiessen, 1911) was carried out. This method allows the assignment of values by weighted portion of the climate variable to the overlapping polygon area of each sub-basin (Figure 11). Thus, 121 artificial weather stations were created assigning weighted climate values to the centroid for each sub-basin using the TPM method.

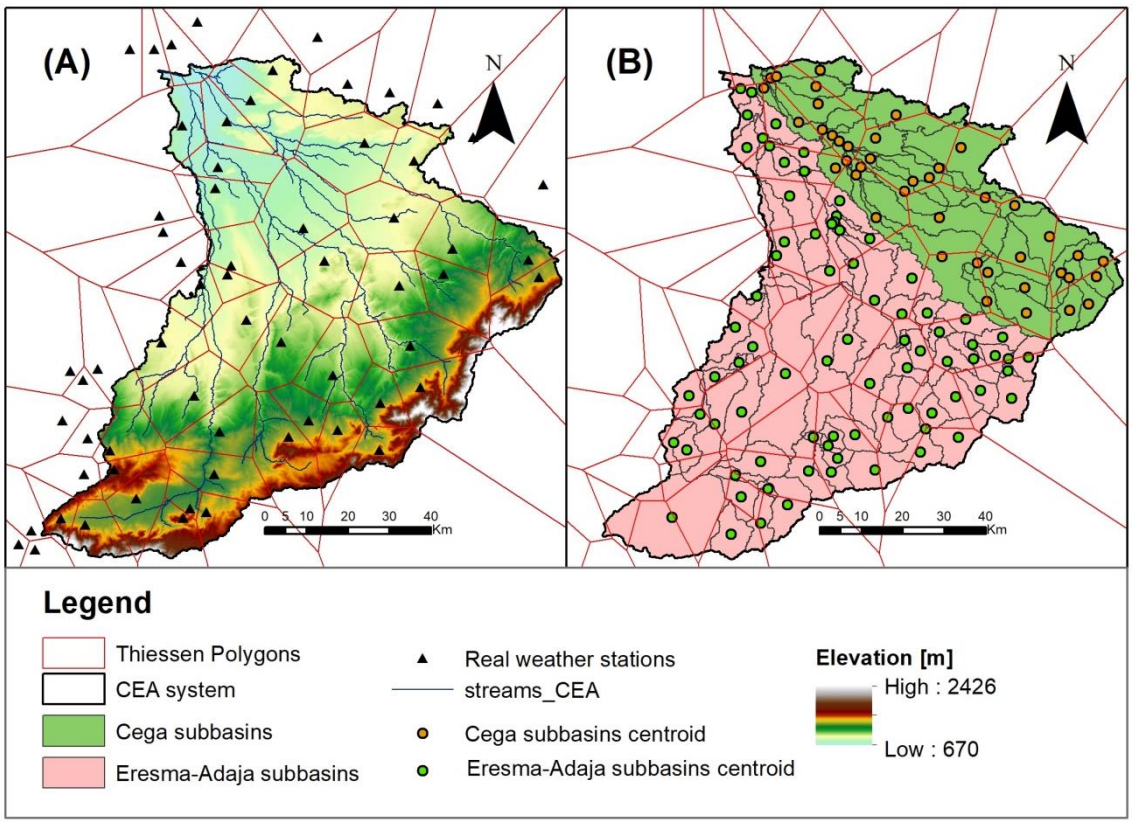

Figure 11. Weather data definition to CEA subbasins (A) and Thiessen Polygon Method (TPM) to define weather stations for SWAT model (B). Weather stations assigned by subbasin centroid for SWAT model.

In a traditional crop rotation setup, once the HRUs are defined, each HRU is assumed to have a homogeneous land use type, and therefore it rotates entirely. However, reality does not follow HRU boundaries for crop rotation. HRUs need to be fragmented (HRU_FR) and crop rotation results in a mosaic of crops representing the crop plots year by year. The land use model setup for crop rotations was improved with respect to traditional rotations by activating the land use change (LUC) module. Specific management operations and scheduling for the HRU_FR (e.g. irrigation, fertilisation, etc.) were considering by adding lines in the crop database with new codes for land uses with different operations. This was in the case of the same crops but with different crop management (e.g. rainfed winter wheat "WWHT", irrigated winter wheat

"WWHI", etc.). The HRU_FR considers the different land operations as an independent calculation. At the end, the HRU water balance values are the results of this land use dynamic.

Data for crop updates were extracted from remote sensing processed images (ITACyl, 2015). The SWAT2009 LUU tool (Pai and Saraswat, 2011) was implemented to assign land cover from the satellite images (2004-2014) to the corresponding spatial HRU (see Table B, in supplementary material for more detailed information). This geospatial tool provides the required files to update the HRUs with the corresponding percentage (HRU_FR) of LUU (Land Use Update) on specific dates defined by the user. The surface flow configuration during rainfall events is related to surface roughness and slope. Consequently, crop rotation is essential for the runoff process. Curve number (CN) is an important parameter for predicting direct runoff and infiltration process.

2.4.4 Calibration and validation

During the modelling run process, a warm-up period must be selected in order to ensure the establishment of basic flow conditions for the simulations. Following Kim et al., 2018, taking into account that sandy soils are predominant in the area, a one-year period (year 2003) was selected to warm up the model. The hydrologic processes need to reach an equilibrium condition for better results during calibration and validation.

Calibration is a procedure to reduce model output uncertainty by adjusting model parameters to obtain a model representation that satisfies pre-agreed criteria. In this research, calibration is performed by comparing the daily streamflow output for the period (2005-2009) with the corresponding measured values. Validation is the process in which the adjusted parameters were assessed in an additional period of time (2010-2014) to corroborate the accuracy of the adjustment, assessing model output uncertainty.

Hydrological models have some parameters that cannot be measured directly (Spaaks and Bouten, 2013). The main measured parameter of water flow in the watersheds is the streamflow, which serves as reference to determine other water flows indirectly (Morán-Tejeda et al., 2010). In hydrology modelling, streamflow is one of the measures used for calibration and validation (Benedini and Tsakiris, 2013). Other measures such as surface runoff, ground water recharge and evapotranspiration, among others, are hard to measure and the data available are limited to specific points in time and space.

Model calibration, validation and sensitivity analysis were performed using the algorithm for Sequential Uncertainty Fitting (SUFI-2). This is included in the SWAT-CUP package (Abbaspour, 2011). This process was settled for each of the two sub-basins of the CEA at a daily time step. SUFI-2 is an algorithm that tries to capture most of the measured data within the

95% prediction uncertainty (95PPU) of the model using the selected parameter ranges during an iteration process consisting of 300-1000 simulations (Abbaspour et al., 2015).

Automatic calibration processes were conducted with a previous parameter analysis through trial runs (10-100 simulations). During this trial, the final selected parameters for calibration and validation were identified by the sensitivity analysis of variables related with stream flow. Homogeneous flow time series lengths for both processes were selected to provide consistent statistical samples and to assess the more recent available data. Nevertheless, a good correlation during validation could be an erratic result due to cumulative model input uncertainties.

2.4.5 Model performance evaluation

The model's performance was assessed through statistical indices of the SUFI2 algorithm, a Bayesian framework to reduce the uncertainty during the sequential and fitting process of some objective function. Suitable ranges for Nash-Sutcliffe efficiency coefficient (NSE) (Nash and Sutcliffe, 1970), coefficient of determination (R^2), and percentage bias (PBIAS) were selected to measure the global matching and relative peak matching of simulated flow with SWAT (Gassman et al., 2007).

The NSE was selected as the objective function for evaluating simulation performance. R^2 and PBIAS are complementary statistical criteria for efficiency statistics. The NSE is valid for ranges between -∞ to 1, where values between 0.0 and 1.0 represent acceptable levels of model performance. However, while values up to 0.5 show a satisfactory rating, even values up to 0.65 are usually considered good results and values between (0.75 - 1.0) are considered very good performance (Moriasi et al., 2007). As statistical criterion of performance, the Kling-Gupta Efficiency (KGE) was selected. Similar to NSE, KGE represents the correlation, bias and relative variability between observed and simulated values. KGE values range from -∞ to 1, and the optimal value is 1.

Model uncertainty was also evaluated, including R-factor (thickness of the 95PPU envelop) and P-factor (as the percentage of observed data enveloped by the modelling results) criteria, to constrain valid parameter ranges for CEA system modelling. Both judge the strength of the calibration and validation processes. Desirable ranges for the P-factor (> 0.7) and R-factor (< 1.5) were targeted to capture most of the matching observed flow into the 95PPU band of the model during an iterative process of a defined group of simulations (Abbaspour et al., 2004).

2.5 Multiscaling NDVI series analysis of rainfed cereal in central Spain.

2.5.1 Site description

The study area is located in north-central Spain in the midlands of the Eresma-Adaja River system (Rivas-Tabares et al., 2019b), overlapping with most of the Avila and Segovia provinces. The area covers 200,197 ha from which 70% is mainly used for rainfed barley and wheat and 14% are other crops (e.g., canola, sunflower, and peas), as the most typical rainfed crops in the area. These rainfed cereals are part of the most representative features of the crop rotation sequence in the area. Two different sites have been chosen based on the SOM digital soil map of Figure 7d. SOM soil unit 5 in subbasin 50 (SOM5) and SOM soil unit 15 in subbasin 24 (SOM15) were selected for this study (Figure 12).

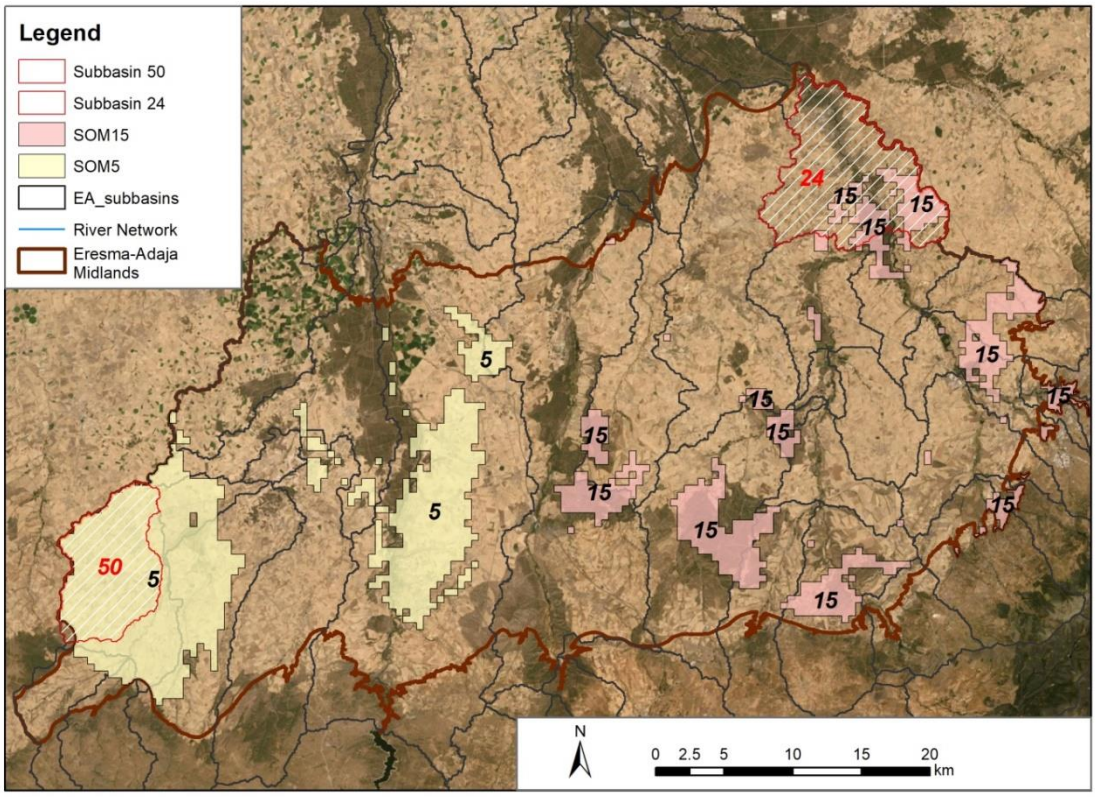

Figure 12. Selected sites for NDVI analysis with similar edaphoclimatic conditions using the Self-organizing maps, units 5 and 15 that overlies with sub basins 50 and 24 respectively. The site is located in the midlands of Eresma-Adaja watershed in north-central Spain.

2.5.2 Data

2.5.2.1 Soil map

The digital soil map used in this work is based in a previous study (Rivas-Tabares et al., 2019b) and is employed to discriminate soils of agroclimatic zones. This map uses the self-organizing map (SOM) algorithm (Kohonen, 1982) to facilitate the clustering of similar soil properties and

provide a spatial arrangement of these in clusters. The map was defined based on similar soil properties in the area (organic matter, carbon content, albedo, clay, sand, silt, available water content, bulk density and hydraulic conductivity) from gridded soil survey points (Llera, David A. Nafría et al., 2013).

In this case, the Eresma-Adaja midland, 15 soil units are defined from the soil property envelope, Figure 7. The Cambisols and Luvisols are the most representative soils in the area, being derived partially from limestone weathering and sand deposits (IGME, 2009). Loamy sand soils are the most predominant texture in the watershed east, while sandy clay loam textures characterise soil in the west of the watershed. The soils of the central part of the watershed are characterized by sandy loam textures, from a soil textures gradient of sandy clay loam from the west to sandy soils to the east. Two soil contrasting characteristics sites were selected to characterize the agroclimatic zones, one in the East (i.e., loamy sand soil) and other in the west (i.e., sandy clay loam soil), Table 2. The physical properties of soil represented through the SOM soils map are a determinant factor for vegetation expression in long-term analysis from earth observations.

Table 2. Soil and topographic characteristics of Self-Organizing soil units SOM5 and SOM15 in the midlands of Eresma-Adaja basin. The deviation is showed in round brackets.

SOM unit	**SOM_05**	**SOM15**
Slope [%]	1-16	1-17
Altitude [MASL]	925-1050	888-912
Clay [%]	29 (5.2)	4 (3)
Sand [%]	56 (4.6)	84 (3.9)
Silt [%]	14 (4.4)	12 (3.5)
Organic Matter [%]	0.9 (0.10)	1.7 (0.15)
Bulk density [g/cm^3]	1420 (145)	1839 (129)
Carbon content [%]	0.5 (0.08)	1.0 (0.09)
Available water content [mm H_2O]	10.1 (0.7)	5.8 (0.7)
Hydraulic Conductivity [mm/hr]	150 (88)	2890 (981)
Albedo [-]	0.08 (0.010)	0.03 (0.005)
Effective Soil depth [mm]	1100	825

2.5.2.2 Weather conditions

The agroclimatic zones definition also requires homogeneous weather conditions. For this, the climate data, such as daily precipitation and mean temperatures, are approximately homogeneous when a smaller order of sub-basins is considered (Ficklin et al., 2013; Kling and Gupta, 2009). The effect of spatial precipitation bias decreases as the spatial scale (i.e. area) increases and this can be explained by the fact that basin perform different degrees of smoothing to the rainfall signal (Obled et al., 1994). In this order of ideas, a 4th order subbasin for climatic data was extracted from a previous study (Rivas-Tabares et al., 2019b). In the referred work, the subbasin weather station of Eresma-Adaja was built from near stations to the subbasin centroid using the Thiessen polygon method – TPM (Thiessen, 1911); more details about weather allocation and TPM subbasin assignation can be found in (Rivas-Tabares et al., 2019b). The monthly weather average conditions of temperature and precipitation are shown in Table 3 for all hydrological years (i.e., starting in October and ending in September) between 2000 and 2019.

Table 3. Monthly average values of precipitation (*Pcp*), maximum temperature (*Tmax*), average temperature (*Tavg*), minimum temperature (*Tmin*). Study period from 2000-2019.

	OCT	NOV	DIC	JAN	FEB	MAR	APR	MAY	JUN	JUL	AUG	SEPT	Annual values
Sub-basin 50 (SOM5)													
Pcp [mm]	67.1	59.7	40.1	52.3	39.0	40.7	56.1	57.0	31.7	14.5	13.8	27.1	499.1
Tmax[°C]	18.2	11.0	8.3	8.0	9.4	13.0	15.6	20.2	26.9	30.2	30.1	25.6	18.0
Tavg[°C]	12.8	6.9	4.4	4.0	4.6	7.4	9.4	13.0	18.8	21.3	21.7	18.1	11.9
Tmin [°C]	7.3	2.8	0.4	0.0	-0.1	1.8	3.2	5.8	10.6	12.5	13.3	10.6	5.7
Sub-basin 24 (SOM15)													
Pcp [mm]	61.2	45.5	34.2	36.5	30.7	36.0	50.3	50.5	31.2	12.6	16.4	25.3	430.4
Tmax[°C]	17.9	11.0	8.3	8.1	9.4	12.8	15.4	20.0	26.8	30.0	29.9	25.4	17.9
Tavg [°C]	12.6	6.9	4.4	3.9	4.6	7.2	9.2	12.8	18.5	21.0	21.4	17.9	11.7
Tmin [°C]	7.2	2.8	0.4	-0.2	-0.2	1.6	3.0	5.7	10.2	12.1	12.8	10.4	5.5

2.5.2.3 Earth observation data

The MODIS-Terra MOD13Q1 V06 product at 250 m spatial resolution and 16-day composite images (Didan, 2015) from 2000 to 2019 (460 images) were used for single spectral bands (blue, red, NIR and MIR) and for the NDVI.

The extracted bands and NDVI from MOD13Q1 comprise data from 02-01-2000 to 24-12-2019 that were checked through the quality and reliability pixel index of MODIS data, and only high-quality pixels (rank key =0) were filtered for the series. It is important to highlight that the 16-day composite NDVI series are generated using the two 8-day composite surface reflectance granules (MOD09A1) in the 16-day period considered one of the most spatiotemporal reliable products of MODIS (Didan, 2015).

The data extraction from the MODIS product was performed using the Google Earth Engine (Gorelick et al., 2017), and the scripts are provided in Annex 5.

2.5.3 Plots and pixels selection criteria

A workflow that illustrates the procedure of the sampling methodology of this work is shown in Figure 13. In both sites selected, SOM5 and SOM15, 4,911 plots of monoculture cereal patterns were identified from the crop rotations analysing of the land cover classification data of the Agrarian Technological Institute of Castilla and Leon (ITACyL) (Llera, David A. Nafría et al., 2013) in the Eresma-Adaja midlands.

Based on (Valverde-Arias et al., 2019) work, two conditions were applied for the site pixel selection in these plots: the selected centroid plot has to (i) buffer in at least 2 pixels from the subbasin bounds and (ii) guarantee a minimal distance of two times the diagonal pixel size plus 1 m (D=707.1 m) between centroids to avoid resampling the same pixel and avoid the subbasin bounds effect.

Finally, pixels from ten plots were selected and considered representative monoculture parcels during the study period, five plots located in each zone.

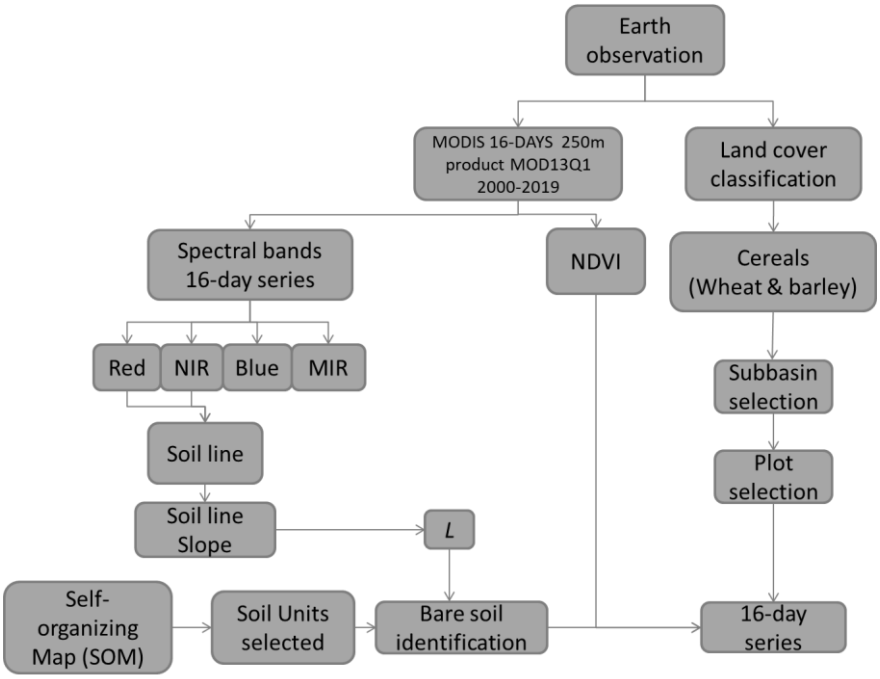

Figure 13. Workflow of the sampling methodology and information extraction from Earth observations and soils map.

2.5.4 Soil reflectance characteristics

With the purpose to validate the difference in soils between SOM5 and SOM15, the soil reflectance was analysed to see if statistically significant differences were found. The time window for bare soil identifications was chosen from the tillage operation dates of the selected

plots. This information was extracted from surveys of the INFORIEGO survey (Llera, David A. Nafría et al., 2013). In the studied zones, the spectral response from soils can be obtained in the 2nd week of February (February 18th), the beginning of the growing season.

An ANOVA was applied for each spectral band values at that date during the study years to compared SOM5 and SOM15. Previously, a normality test was conducted for each spectral band and zone to confirm the suitability to apply this type of analysis.

Additionally, the relation between NIR (0.7 - 1.1 μm) and red (0.6 - 0.7 μm) reflectance bands over bare soils, named the soil line (SL) (Baret et al., 1993; Gitelson et al., 2002), was used to compare both zones.

The SL is identified from a graph of the NIR band against the red band. The function for bare soil line (BSL) was used to calculate it from Landsat package in R (Goslee and Goslee, 2019) for each site. This algorithm uses the quantile method to take the lowest set of points, those with an NIR/red ratio less than the limit-th quantile, in this case, defined as 0.1. Thus, the minimum value of NIR for each level of red was chosen and then these points were used in a linear regression to estimate the slope that is identify as BSL.

2.5.5 NDVI series and statistics

The NDVI time series was calculated as the average from the 5 selected parcels per zone and each date (NDVI original). These series cover from 2000 till 2019, having 23 data points per year (n=23) and a length of 460 values.

Some of the depressed values of the series were pre-processed through the Savitzky–Golay filter (Savitzky and Golay, 1964) to smooth the time series, specifically those that were caused primarily by cloud contamination and atmospheric variability (Chen et al., 2004).

A cycle pattern was extracted from NDVI original series calculating the average per date in each zone. Based on this cycle pattern, an NDVI average value from the crop cycle was used to compare both zones. Additionally, the relation between the precipitation and NDVI was study through the correlation of the accumulated variables during the period that a clear increase of the vegetation index is observed, January to May (Reed et al., 1996).

Finally, the Mann-Kendall test was applied for each NDVI original series to determine whether there was any significant trend following Jiang et al., 2015. This is an important point, as if a trend is detected a detrended should be applied before the multiscaling analysis (Davis et al., 1994).

Beside the NDVI original series two more were extracted. The first one was obtained subtracting from NDVI original series the cycle pattern naming it as NDVI residual. Performing this operation, the seasonality of the series was removed. In many studies this NDVI residual is considered as anomaly and it is employed to assess the current state of crops and rangelands (Moges et al., 2005). However, different types of anomalies can be found in the literature (Numata et al., 2007). In this study z-score anomaly were chosen as a differece between the NDVI average and its value at a date in a year could be signingicant or not depending in the dispersion that NDVI values have normally at that date. Terefore, the second series obtained was dividing the NDVI residual by the standard deviation (SD) of the NDVI values per date obtaining the NDVI anomaly commonly used in the studies of extreme events (Xue and Su, 2017).

These three types of series, for each site, were analysed with the Generalised Structure Function that is explained in the next section.

2.5.6 Generalized structure function (GSF)

The GSF consists of the statistical assessment of nonoverlapping fluctuations across different increments of scales in the time series. The analysis consists of the comparison of statistical moments of the series for each scale increment (Monin and Yaglom, 1999). A multiscale behaviour of the series can be identified when statistical moments are invariant at different scale increments (Davis et al., 1994).

The time series is considered a $f(t_i)$, (i = 1,2,3,…, N) in which the fluctuations are assessed. These fluctuations can follow a random behaviour (Brownian motion) in which the variance is proportional to time intervals of t_i and can be computed through the Hurst exponent H: $\sqrt{\langle \Delta f \rangle^2} \propto (\Delta t)^H$ where H is the power exponent in the range of $0.00 < H < 1.00$ (Lacasa et al., 2009). A Hurst equal to 0.50 indicates Brownian motion and characterizes non-memory signals. Values from $0.50 < H < 1.00$, the signal is persistent, showing a trending behaviour in which the past signal influences the following data sequence and for H Values ranging $0.00 < H < 0.50$ are referred to as the most common signal in nature and indicate anti-persistent behaviour. When the series is anti-persistent, this suggests that the series is sensitivity to external forces with short-term variations. Thus, an increase will most likely be followed by a decrease or vice-versa (i.e., values will tend to revert to a mean). This means that future values have a tendency to return to a long-term mean.

Nevertheless, the scaling analyses consist of generalizing the structure function S (equation 1) with stationary gradients for q>0 (Yu et al., 2003) defined as:

$$S_q(\Delta i) \equiv \langle (|f(t_i + \Delta i) - f(t_i)|)^q \rangle \quad (1)$$

$$S_q(\Delta i) = C_q \Delta i^{\zeta(q)} = C_q \Delta i^{qH(q)} \approx \Delta i^{\zeta(q)} \quad (2)$$

where i is the i[th] data of the sequence, and q can be any real number including negative values (Davis et al., 1994). The C_q parameter is scalar depending on q at any power of Δi, suggesting in this case that q has a variable relationship with H and $\zeta(q)$ is the exponent of the structure function (equation 2). Thus, the exponent H can be defined for a hierarchy using the $\zeta(q)$ as:

$$H(q) = \frac{\zeta(q)}{q} \quad (3)$$

If the plot $\zeta(q)$ against q shows a linear behaviour, this behaviour is related to monofractal signals. However, if the line is nonlinear, the behaviour is related to multifractal signals (Lovejoy et al., 2001). The multifractality of the signal is defined when the different windows of the data sequence (series fragments) are equivalent to the different zones of the fractal object defining the various values of the fractal dimension.

2.6 Land Use Land Cover change through scenario modelling

2.6.1 Study Area

The sub-basin "*Arroyo de la Balisa*" (AdlB) comprises 242 km^2 and is located in the middle section of the Duero Basin, Figure 14. The sub-basin stream persists under unregulated regime inside the CEA system. The former is regulated by some reservoirs in the uplands. In addition, the ecological status of the water bodies within the sub-basin is deficient due of low IPS (Specific Pollution Sensitivity Index) a biological water quality indicator related to benthic organisms (CHD, 2015). The sub-basin is slightly sloped and elevation range between 747 and 1011 m. The common soils are Luvisols, Fluvisols and Cambisols based on FAO soil classes (Nachtergaele et al., 2009), presenting moderate infiltration rates. Its agro-climate is dominated by a Mediterranean sub-arid regime, highlighted by a very dry summer and a mean annual precipitation of 427 mm yr^{-1}(AEMET, 2013). In addition, the sub-basin is fundamentally devoted to agriculture (70% land allocated for this purpose), and mainly used for rainfed agriculture for cereal production (e.g. winter wheat and barley), Figure 15. Although irrigation is an occasional practice, this is more and more expanded. This is linked with a very high-water demand and intensive tillage and fertilization.

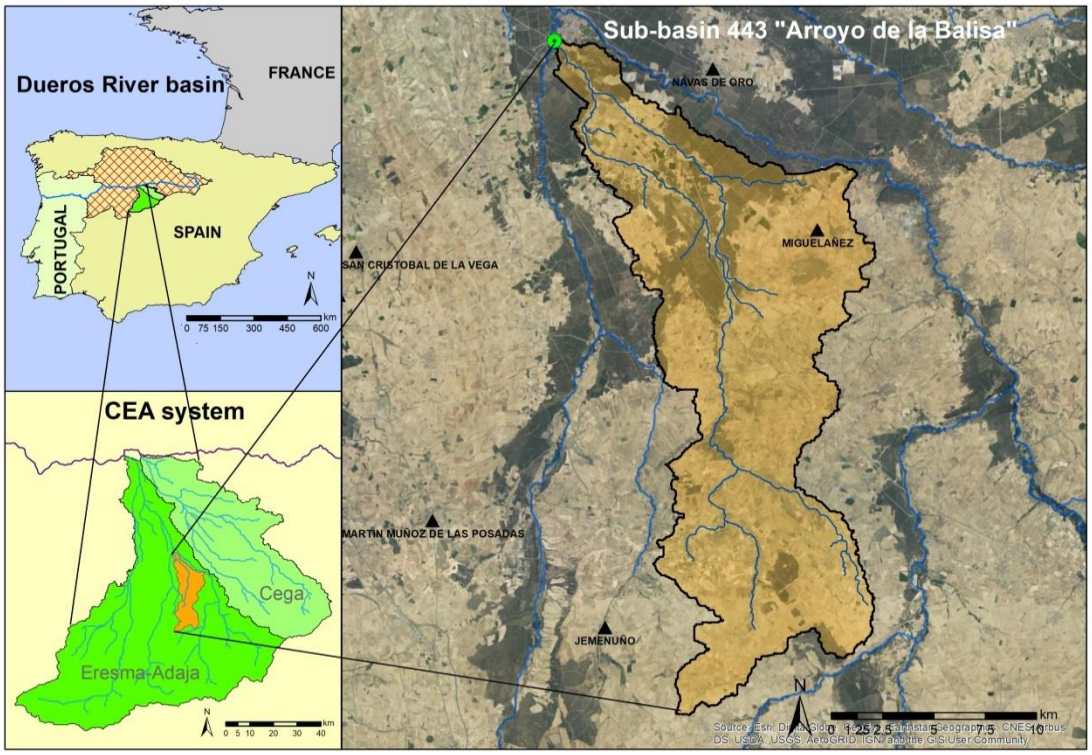

Figure 14. Case study area for LULC scenario modelling. Subbasin 443 "Arroyo de la Balisa" AdlB in North Central Spain.

2.6.2 Pre-processing of LULC mapping

Prior to participatory scenario definition, a LULC map was performed to allocate crop rotation and management operations and then this was used for baseline model set-up (Figure 15), since it represent properly the average distribution of LUs during the interval of analysis (Rivas-Tabares et al., 2019a). To allocate temporal the LUs, specifically to identify crop rotation for the period 2004 to 2014, two sources of information where used: satellite images already classified by ITACyL for the period 2011-2014 (https://atlas.itacyl.es/descarga/); and data from a regional survey of JCyL (The Junta of Castile and Leon) for the period 2004 to 2010. As a result of overlapping the former data sources, a hybrid set of LU maps at a resolution of 20m were defined for the period 2004-2011. This was conducted to represent the LU spatially-matching to the survey area for each land cover. In addition, cadastral maps were additionally used to improve the spatial matching of LULC time-series for the simulation period. The LU classes were defined in detail for agriculture (crops), forest, grassland, shrubs, urban-transportation and water.

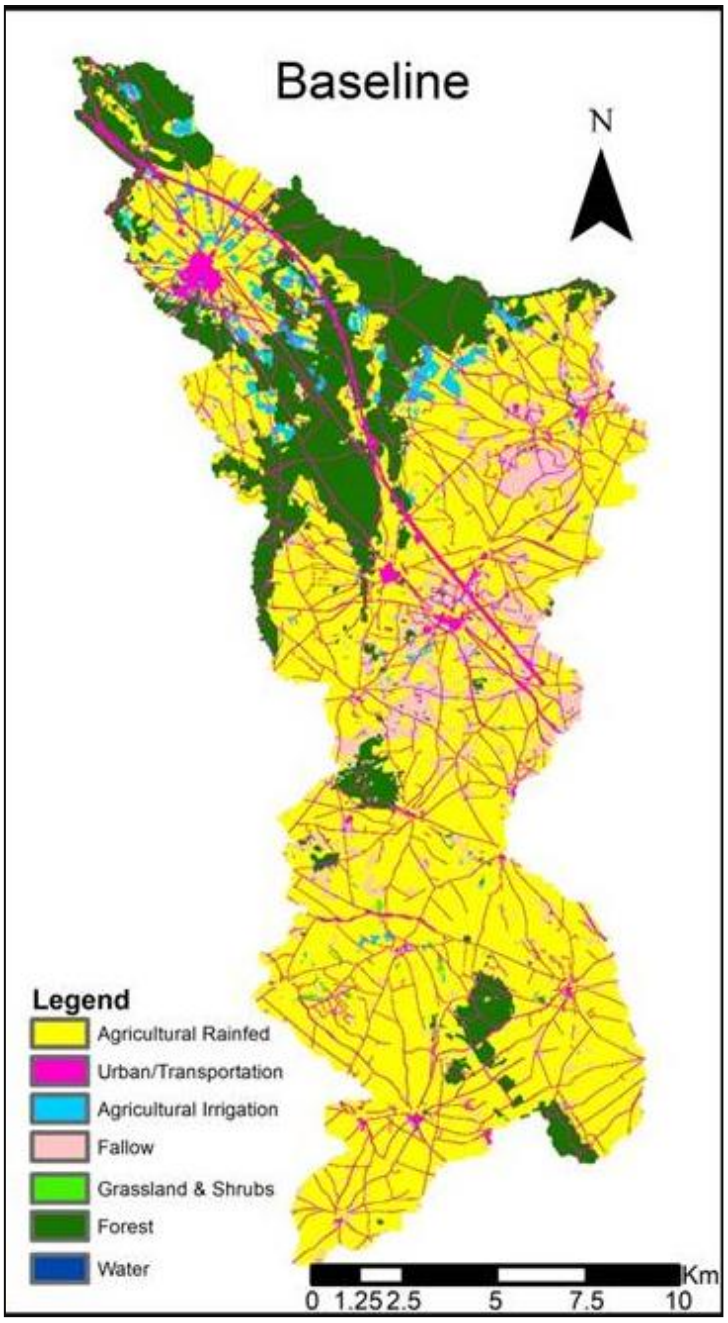

Figure 15. Land use (LU) of sub-basin "Arroyo de la Balisa - AdlB" used as baseline scenario.

The definitions of LU management include all human activities on a given system (Neitsch et al., 2002). In this case, the assessment of those activities was focused on cropland practices. The crop rotational patterns described by stakeholder were posteriorly adjusted to a graphical template to facilitate management information assignation, Figure 16. This template facilitates the allocation of management rules from stakeholders and from secondary sources, as surveys. The template is intuitive for crop cycle and at the same time is in concordance to hydrological year. However, this template is also flexible and could be adapted to other crop pattern cycles.

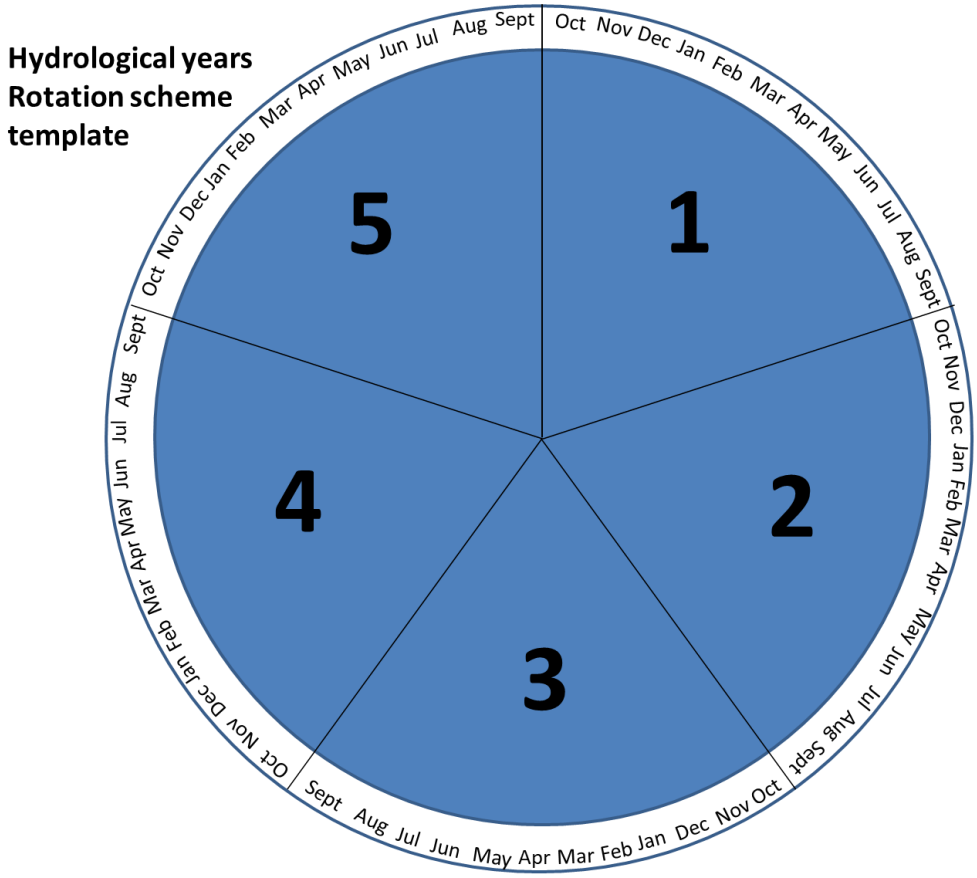

Figure 16. Template for crop rotation cycle assignation for 5 years cycle corresponding to hydrological year (from October till September). Numbers from 1 to 5 indicates the year number.

The template also allows identifying other farm practices, such as plantation dates, tillage, irrigation, fertilizer and pesticides application, intermediate cropping, harvesting dates, etc. Although, the assigned dates are estimates due to variability of weather conditions of each year but fixed for modelling purposes. Once the template was completed with crop pattern and its management, modeler translates those results into data input for modelling. However, the introduced values into model assuming that operations for each crop occurs at the same date over the whole sub-basin. A summary of management practices by crop is presented in Table 4.

Table 4. Summary of management practices by land use (LU) crop in Sub-Basin "Arroyo de la Balisa" AdlB, Spain.

Land Use		Planting	Tillage		Fertilization			Harvest
Crop	SWAT Code	Date	Operation	Date	Date	N-P-K	Total (kg)	Date
Winter Wheat	**WWHT**	08-dic	Fallow	03-dic	12-oct	27-00-00	350	28-jul
			Field Cultivator Lt15ft	05-dic				
			Roller Packer Flat Roller	07-dic				
Barley	**BARL**	25-feb	Fallow	23-feb	24-feb	27-00-00	350	21-jul
Maize	**CORN**	01-abr	Subsoil Chisel Plow	10-abr	06-may	08-15-15	1000	15-sep
			Rotary Hoe	25-abr				
			Field Cultivator Lt15ft	25-may				
			Roller Packer Flat Roller	30-may				
Potato	**POTA**	16-abr	Spring Ploughing	05-abr	04-abr	08-15-15	1000	22-ago
			Field Cultivator Lt15ft	09-abr				
			Bedded disk-row	12-abr				
			Beet cultivator 8 row	14-abr				
Sugar beet	**SGBT**	01-mar	Spring Ploughing	20-feb	01-mar	27-00-00	1200	15-may
			Field Cultivator Lt15ft	27-feb				
			Disk Plow Lt23ft	28-feb				
Sunflower	**SUNF**	25-abr	Spring tooth Harrow Ge15ft	23-mar	22-mar	08-15-15	600	02-sep
Alfalfa	**ALFA**	01-oct	Fallow	04-oct	02-oct	00-20-20	200	05-may
								05-jun
								01-jul
								05-ago
								01-sep
								30-sep
Horticulture	**HORT**	03-mar	Fallow	02-mar	01-mar	Elem-N	500	01-ago
Aromatic herbs	**AROM**	15-feb	Fallow	02-mar	04-mar	Elem-N	500	01-ago
Peas	**PEAS**	15-nov	Fallow	14-feb	13-feb	Elem-N	300	01-jul
Canola	**CANA**	06-oct	Fallow	16-oct	17-oct	08-15-15	250	20-jul
Olives	**OLIV**	already planted	Spring Ploughing	02-mar	01-mar	Elem-N	250	15-oct
Vineyard	**GRAP**	already planted	Spring Ploughing	15-mar	13-abr	Elem-N	250	15-ago

2.6.3 Scenario definition

The LULC scenarios used in this research build on the participatory process developed in the TALE project (Towards multifunctional agricultural landscapes in Europe: Assessing and governing synergies between food production, biodiversity, and ecosystem services)(Volk and Hagemann, 2018). The purpose of TALE was to ground the debate on land sharing and sparing to the reality of different European Agricultural Landscapes by developing participatory agricultural scenarios, consistent with European policies (Common agricultural Policy, Water Framework Directive, Birds and Habitat Directive) and global socioeconomic drivers as determined by the IPCC Shared Socioeconomic Pathway, and explore quantitatively the ecosystem services synergies and trade-offs linked to different land use trajectories. The project involved five case studies, and AdlB sub-basin of CEA basin was one of the case studies (see Figure 14). Thus, the LULC scenarios of this sub-basin build on the participatory exercise of the TALE project. The details of the scenario process are described in Hagemann et al., (2019) and

the resulting scenarios are discussed in Karner et al., (2019). In summary, the land use scenarios represent contrasting visions about how to balance regional agricultural development and the continuous provision of key ecosystem services such as water supply, and biodiversity conservation.

What was sought with the scenarios was to first develop narratives at a regional level about possible regional developments in agriculture and their compatibility with environmental objectives (ecosystem services), which were consistent with narratives of policies at the European and global socioeconomic levels. Based on these narratives, elaborated in a participatory way, they were translated into scenarios of LU changes, where types of uses, spatial allocation, and management practices, including crop rotations, are quantitatively detailed. These scenarios, before being used for hydrological simulation, were validated with actors. Further details on the participatory scenario process, stakeholder composition group, narratives and outcomes are provided in the supplementary material Annex 7.

2.6.4 Modelling

The SWAT model was used to assess water budget differences from the three contrasting visions of agricultural development through LULC scenarios in the sub-basin AdlB of CEA system. This assessment includes in detail: the stream flow out regime variation and depth aquifer recharge volume fluctuations. The model set-up, calibration and validation procedures were used from a previous SWAT model of CEA system (Rivas-Tabares et al., 2019b) from which was extracted the model for AdlB sub-basin and was established as baseline scenario. The outflow series of CEA model was considered to analyze if any regulation effect of flow from *Las Cogotas* reservoir has effect on flow series at the outlet of case study. To do that, a comparison between Coca flow gauge values and CEA previous model was done, finding that in case study there is no alteration of reservoir effect on outflow series, Figure 17. For this reason, the calibration and validation parameters values of the of CEA model were used to adjust LU scenario models (LSH, LBA and LSP).

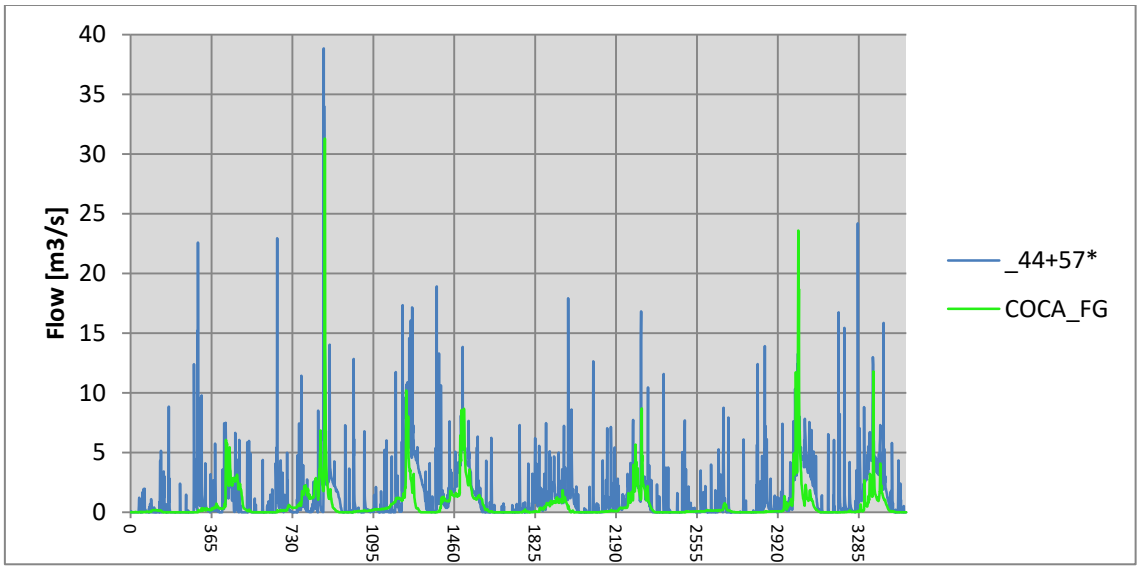

Figure 17. Flowout series comparison between Coca flow gauge (COCA_FG) and subbasin,"Arroyo de la Balisa – AdlB", flow gauge (_44+57*) from Ceja-Eresma-Adaja (CEA) model.

Nonetheless, the definition of HRU during modelling of LULC scenarios is crucial due of its spatial representativeness. The HRUs are spatially and dimensionally different depending on LU, soils and slope. Achieve a spatial matching of HRU would allow a common framework for a direct comparison between HRUs through the different scenarios. Hydrologic implications due of LULC change were evaluated through consistent HRU spatial distribution. This means, that the HRUs for this study are spatially coincident independent of crop and management schedule of the LU scenarios.

For this, the baseline model was defined with 224 HRUs based on LU reference map (Figure 15) for the simulation period. Considering baseline model as reference for HRU definition, the 224 HRUs polygons are common through the four models (Baseline, LSH, LBA and LSP). According with LU's, we classified the HRU condition, distinguishing between static and dynamic for LULC change. Some of the HRUs keep it static in time due of invariant LU condition (e.g. water bodies, transportation, urban, irrigated areas and, some forest patches). Meanwhile, most of agriculturally based HRUs are more dynamic. Thus, within the dynamic HRUs, the crop rotations and crop management were assigned for each scenario. A group of 208 units were classified as static HRUs (49.4% of the total area), they represent polygons less than 100 hectares each and the other complimentary 16 HRUs (dynamic) were bigger than 100 hectares, Figure 18. From the static HRUs (208), 192 HRUs are dedicated to agriculture in a fragmented mosaic representing the 10.4% of the area, the resting 16 static HRUs were assigned by the following: four for urban/transportation, four grassland and shrubs, six forest and two for horticulture. In the other hand, the 16 dynamic HRUs represent the 50.6% of the total area and the 83% of rainfed agriculture, depicted mainly for extensive cereals 57.4%.

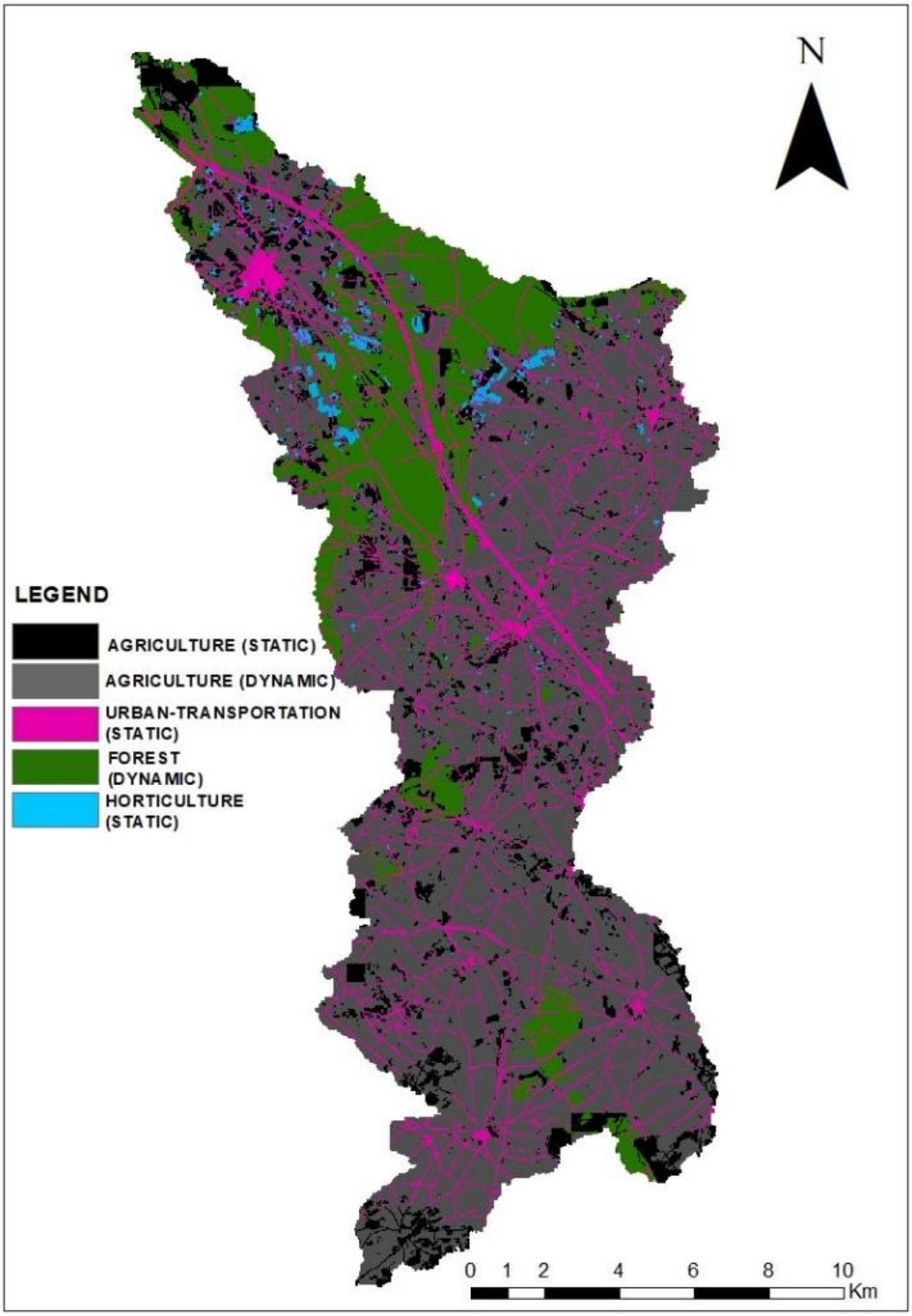

Figure 18. Hydrological Response Unit (HRU) template for static and dynamic HRUs of subbasin, "Arroyo de la Balisa - AdlB".

3 Results and Discussion

3.1 Self-Organizing maps of soil properties

3.1.1 Soil mapping for hydrological modelling

In the first model based on HWSD map, the HRU definition was based on the 14 soil units. In this case, 79 of the Adaja River sub-basins were defined using a unique soil unit, contrary to the high spatial variability expected in soils properties within the subbasin. Larger sub-basins could be defined to capture more soil units, but the river network is regulated in highlands and narrows in midlands-lowlands sections, causing a diverse size of sub-basins. The lack of finer soils data resolution could force to merge the sub-basins to get more soil units per subbasin, but this is not desirable because of limiting outflow results. This suggests that the movement of water within the subbasin is homogeneous due of soil properties and variability in the model is only explained by land use and its management. Therefore, soil representativeness at subbasin scale is not accurately captured by HWSD in the watershed studied. The soil map scale 1:1,000,000 is not recommended for Adaja River hydrological modelling with SWAT due to the lack of soil variability representativeness at subbasin scale. In addition, soil depth for the soil units only considers two depths in the whole area, 300mm in the north and 1,000mm in the rest being an excessive simplification for the complex schema of this subbasin. The HRUs should contain accurate information in soils and land use as the subbasin outflows are the summation of different water flows from the HRUs.

The TSU soil map obtained provides an identical map from the taxonomic point of view from the original. The difference is that TSU map now includes the soil properties. The quantification of the eleven soil properties and the soil depth was done by averaging the raster values of each one into the taxonomic units' boundaries (see Annex 8). With this approach, the soil depth obtained will be the average of soil depths belonging to the inside of the boundaries and this could be a source of uncertainty in water fluxes through soils.

In the case of SOMM, the soil clusters are equivalent to the soil units (Figure 19). From 3 to 50 number of cluster two different metrics were used to obtain the optimum number: (i) the lowest value between the sum of normalized mean distance and (ii) the lowest DB index. The SOMM clusters from 13 to 19 present an optimal range (showed in Figure 19). However, we found that the 16 clusters array meets both criteria with a minimum local DB index value that provides a good performance metric pointing it as the best map. At the same time, they are also in concordance to a topographic distribution as showed in Figure 20.

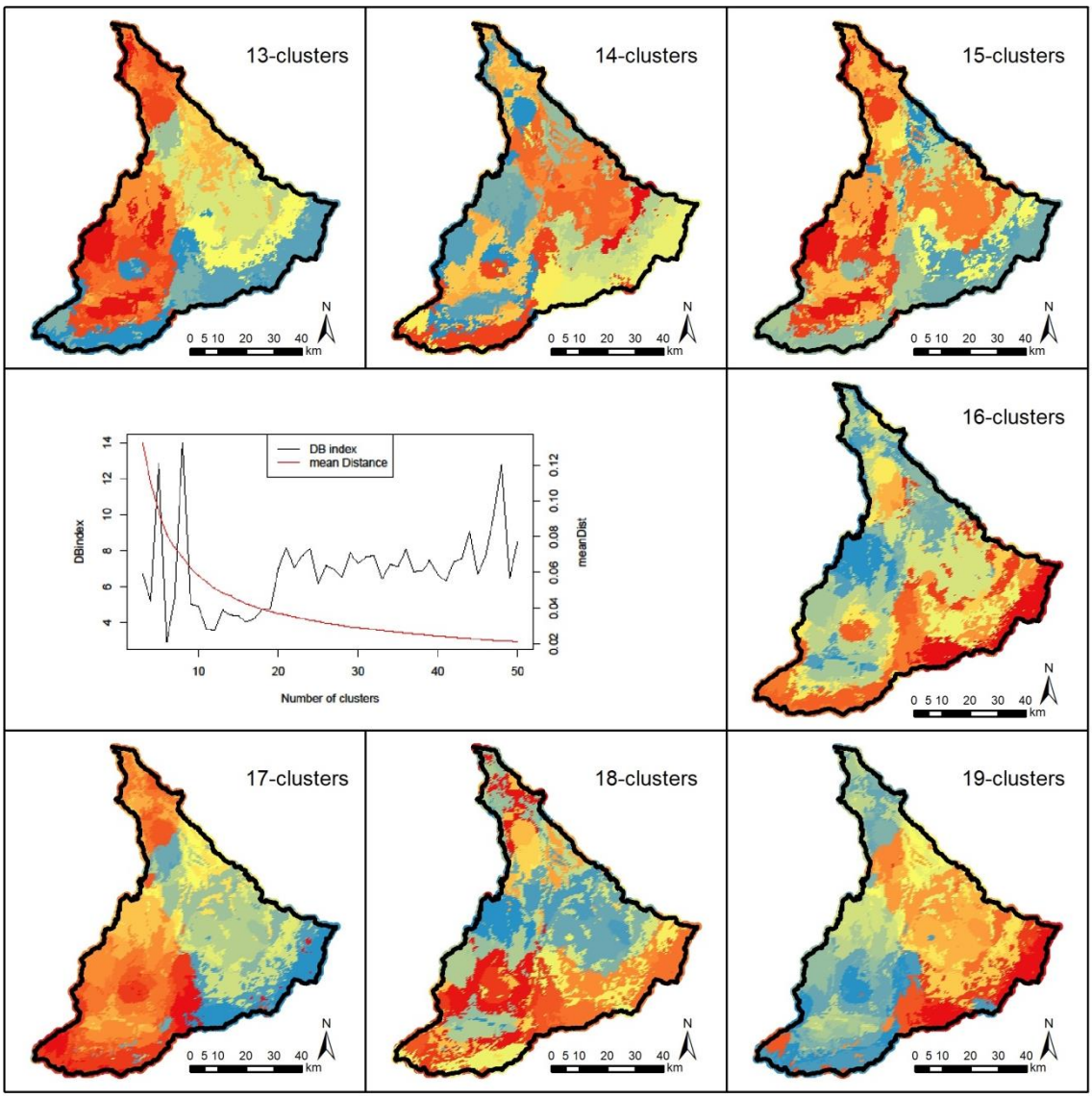

Figure 19. Self-organizing maps assessment testing from 3-50 clusters for soils mapping in Adaja river watershed.

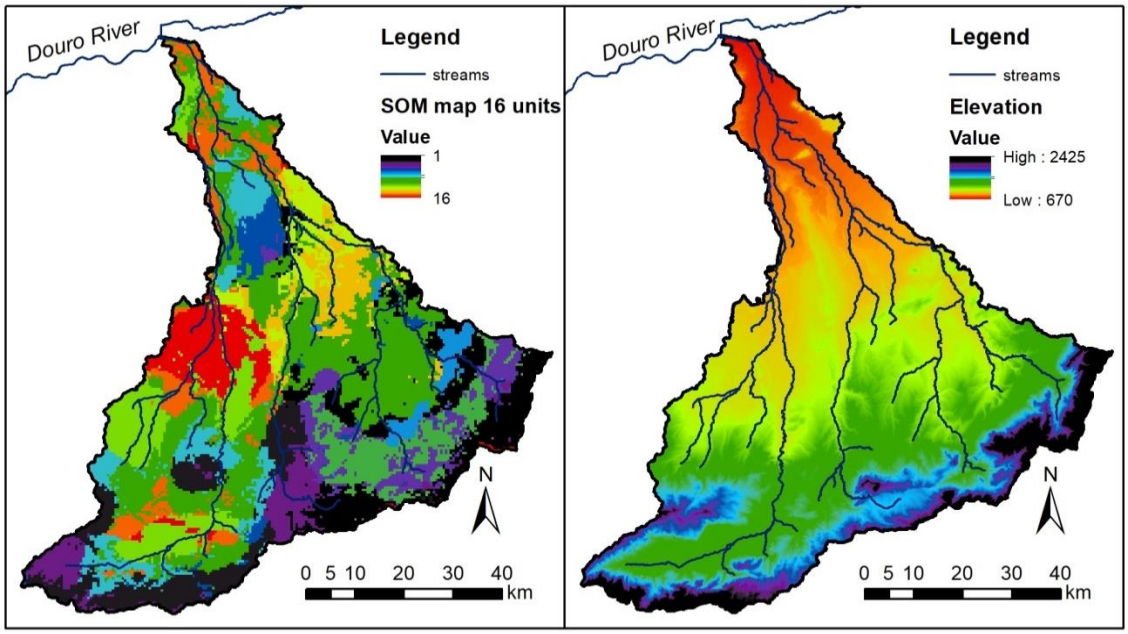

Figure 20. Self-Organizing Map (SOMM) with 16 soil clusters used for SWAT hydrological modelling for Adaja watershed and topographic comparison to the elevation map.

Soil mapping for hydrological purposes differs from edaphological mapping point of view (Burrough, 1983). If a pedogenesis soil clustering is the goal, other neural network different from SOM should be used for this purpose. The method selected depends on the application requested. In this case, SOMM was based on a learning algorithm from the Kriging interpolation input maps and do not require additional validation than the metrics evaluation.

Some soil properties vary with time, whereas the SWAT soil data base remains constant for all the studied period. For this reason, several studies find that hydrological models present different stream flow effect because of different soil resolution during model set up (Geza and McCray, 2008; Romanowicz et al., 2005), even suggesting that most of the model uncertainty is driven by a scale-dependence for water balance in sub-arid watersheds (Muttiah and Wurbs, 2002). Not only land use scenarios and land management are the sources to optimize the human activities in watersheds. It is desirable that soil properties changes should be included as part of land use scenarios (Bormann et al., 2007). This point out that field work its necessary to update soil sampling sites due to temporal soil properties variations such as infiltration rates, organic matter content, among others.

Soil mapping for hydrological modelling is still under continued development and the techniques as Kriging and SOM are valuable contributions to develop soil scenarios for hydrological modelling in SWAT.

3.1.2 SWAT parameters analysis

During model calibration, 25 parameters were selected (Table 5) based on a literature review of sub-arid basins (Rivas-Tabares et al., 2019b). The parameters selection depends on the main hydrological modeled processes and the measured data used to calibrate the model. In this case, parameters associated to processes like the runoff, internal soil fluxes, watershed configuration and stream routing characteristics were considered performing model calculations through the SUFI-2 algorithm simulations for stream flow calibration.

Table 5. Comparison of sensitivity parameters during calibration of three different SWAT model set-up in Adaja watershed.

	HWSD			**TSU**			**SOMM**		
Parameter	Sensitivity Ranking	*t*-stat	p-value	Sensitivity Ranking	*t*-stat	p-value	Sensitivity Ranking	*t*-stat	p-value
GW_DELAY.gw	18	0.767	0.445	24	0.064	0.956	1	6.043	0.000
OV_N.hru	3	3.429	0.001	6	1.524	0.131	2	-3.168	0.002
CN2.mgt	1	-41.823	0.000	1	-13.616	0.000	3	-2.903	0.004
REVAPMN.gw	11	-1.272	0.207	22	0.292	0.772	4	-1.421	0.159
SOL_AWC.sol	7	1.762	0.082	4	2.339	0.022	5	-1.291	0.200
SURLAG.bsn	21	-0.236	0.813	9	-1.191	0.237	6	-1.039	0.301
ESCO.hru	20	0.254	0.800	10	-1.178	0.242	7	0.994	0.324
SHALLST.gw	6	-1.763	0.082	3	-3.185	0.002	8	-0.952	0.344
GWQMN.gw	25	-0.007	0.994	16	0.579	0.564	9	-0.925	0.357
ALPHA_BF.gw	22	0.205	0.837	20	-0.309	0.758	10	-0.884	0.379
LAT_TIME.hru	13	-1.202	0.233	14	-0.732	0.466	11	-0.843	0.401
SLSOIL.hru	8	-1.503	0.137	13	-0.944	0.348	12	-0.723	0.472
HRU_SLP.hru	14	-1.127	0.264	17	0.573	0.568	13	0.688	0.494
CH_K2.rte	24	0.040	0.968	21	-0.305	0.761	14	-0.636	0.527
SOL_Z.sol	4	2.855	0.005	2	4.357	0.000	15	0.544	0.610
CH_K1.sub	10	1.378	0.172	19	-0.341	0.734	16	-0.607	0.546
SLSUBBSN.hru	2	4.026	0.001	8	1.273	0.207	17	-0.595	0.553
CANMX.hru	16	0.899	0.371	23	0.146	0.883	18	0.387	0.699
CH_N2.rte	19	0.588	0.558	18	-0.386	0.700	19	0.387	0.700
CH_N1.sub	15	1.048	0.298	7	1.350	0.181	20	-0.377	0.707
EVRCH.bsn	23	0.152	0.879	15	-0.707	0.481	21	-0.179	0.857
GW_REVAP.gw	9	-1.492	0.139	12	-1.167	0.247	22	0.166	0.868
RCHRG_DP.gw	12	1.250	0.215	11	-1.167	0.247	23	-0.076	0.939
EPCO.hru	17	-0.774	0.441	25	0.056	0.955	24	0.041	0.967
PLAPS.sub	5	1.800	0.076	5	1.623	0.108	25	-0.016	0.987

Table 5 shows the sensitivity metrics for each calibrated parameter for the three maps obtained. A p-value close to zero and larger values for t-stat indicates the most sensitive parameter, and both are used to establish a sensitively ranking (Abbaspour, 2013) that could serve as a guide to reveal from where uncertainty comes from. The parameters related with groundwater fluxes, HRU definition and soils are the most sensitive. Within these, the soil depth and available water content remains in the first seven more sensitive parameters in the three models. It's important to remind that from the parameters related with HRU definition, land use and soil units are included. It is also notorious that soil depth remains as an important parameter in model sensitivity. Knowing that parameters' sensitivity analysis is unique for each studied catchment (van Griensven et al., 2006), some of them (CN_2, SOL_Z, SOL_AWC) are presented too in some sub-arid basins in the first 10 of the sensitivity rank (Aouissi et al., 2016; Gao et al., 2018; Li et al., 2010).

3.1.3 Calibration-Validation implications

Considering the large extension of the Adaja watershed and its regulated river network situation in the up waters, the calibration and validation process at a daily time step is well captured by the SWAT model. During the calibration and validation processes of the three soil sources, it is notorious that a stepped improvement has been achieved through the three models, getting the best result with the SOMM strategy (Table 6). The statistical criteria (Nash-Sutcliffe efficiency coefficient - NSE, R^2 and PBIAS)(Nash and Sutcliffe, 1970) values were well captured above the satisfactory criteria during both the calibration and validation periods following Moriasi`s work in 2007 (Moriasi et al., 2007). More details of SOMM set-up, calibration, and validation process and their performances can be found in (Rivas-Tabares et al., 2019b).

Table 6. Comparison of three soil sources models implemented in SWAT model for Adaja watershed at daily time step using 25 parameters with the SUFI-2 Algorithm.

SWAT Model Soils Set-Up	Period	R^2	NS	bR^2	PBIAS	KGE	p_factor	r_factor
HWSD	Calibration	0.61	0.46	0.54	10.90	0.71	0.46	0.70
	Validation	0.57	0.44	0.53	12.02	0.69	0.44	0.66
TSU	Calibration	0.64	0.42	0.59	24.80	0.73	0.52	1.51
	Validation	0.64	0.40	0.58	20.20	0.70	0.50	1.50
SOMM	Calibration	0.86	0.84	0.70	-10.80	0.84	0.63	0.39
	Validation	0.85	0.82	0.61	-9.10	0.86	0.61	0.37

In the three cases the objective function for calibration was the Nash-Sutcliffe efficiency coefficient (NSE), showing a better result with SOMM improving a 0.46 NSE value in HWSD map set-up to 0.84 in SOMM map set-up. A p_factor larger than 0.5 shows that more than 50% of observations are included inside the 95PPU band. A r_factor smaller than 1.5 indicates a reasonable prediction of uncertainties (Kamali et al., 2017). Comparing these values with the ones showed in Table 6, the best prediction rank was SOMM, then ITACyL and the third HWSD soil model configurations.

As far as we know, no other authors report similar improvements using SOM strategy for setting up SWAT model in soils database. Nevertheless, similar work were conducted to use artificial neural networks for digital soil mapping in the Iberian peninsula (Freire et al., 2013). The referred work suggests that for digital soil mapping the Multi-layer Perceptron (MPL) strategy show better results for edaphological mapping of soil properties rather than the SOM strategy. Nevertheless, the MPL is too sensitive of soil sample data used to develop the model and SOM is better to reduce the dimension of soil units minimizing soil properties error. The soil database properties with a sampling of 25x25 m were collected from three different sampling campaigns and at analysis were carried out at different laboratories. Hence, SOM strategy is preferable to avoid the sampling bias effect during the clustering configuration.

It's important to note that the HRUs number was reduced to 600 units as a strategy for soil data aggregation for hydrologic simulations (Luo et al., 2012) but different HRU sizes between the three soil set-up will might affect the hydrological processes at subbasin scale. This could be because of slope value and length differences of each HRU. As result of this situation, stream flow predicted is overestimated during peak flows or precipitation events over wet soil. The opposite is true with an underestimation of the flow when there are over 20 to 30 days with low humidity in the soil. This is in agreement with a similar situation reported by Geza's work in 2008 (Geza and McCray, 2008), in which a different model set-up was compared between State Soil Geographic database (STATSGO) and the Soil Survey Geographic database (SSURGO) soil data bases in the Turkey Creek watershed in Colorado. Other work reported by Romanowicz et al., 2005 show the SWAT model sensitivity to soil data parameterization with two data sets at 1:500.000 and 1:25.000 scale soil maps in Belgium. This work suggests that SWAT model is sensitive to data quality of soils properties.

An interesting characteristic of soil database sets comparison is that a larger quantity of HRUs doesn't imply better calibration-validation procedures to achieve satisfactory adjustment of model parameters. The soil units and their properties are a source of uncertainty and any effort to reduce the soil properties dimension could improve calibration and validation procedures.

3.1.4 Water balance and flows assessment

The main water cycle components were estimated and presented in Table 7 for the period 2004 to 2014. The values are presented for an average year showing the overall behaviour of the water balance components. This result shows that HWSD present larger differences in CN average value influencing the surface runoff that it's too high for this area suggesting a runoff overestimation. This is visible again in calibration series during storms days (series not showed). The model setup with HWSD was discharged at this point, suggesting that the soil map scale do not respond to the observed outflow at VFG. One difference related with runoff process is that this depends on infiltration rates which, in turn, are associated with the soil group (Figure 21).

Table 7. Summary of the main water balance components from three soil sources (HWSD, TSU and SOMM strategy) assessed with SWAT model for Adaja river watershed. Values in [mm/yr].

Water balance component	HWSD	TSU	SOMM
Precipitation	438.5	438.5	438.5
ET	355.5	326.2	339.3
Surface runoff	29.09	21.41	16.1
Lateral flow	14.17	15.01	1.89
Return Flow	18.01	31.57	26.87
Percolation to shallow aquifer	32.12	66.08	68.89
Revap from shallow aquifer	35.47	31.40	23.80
Recharge to deep aquifer	1.61	6.66	2.81

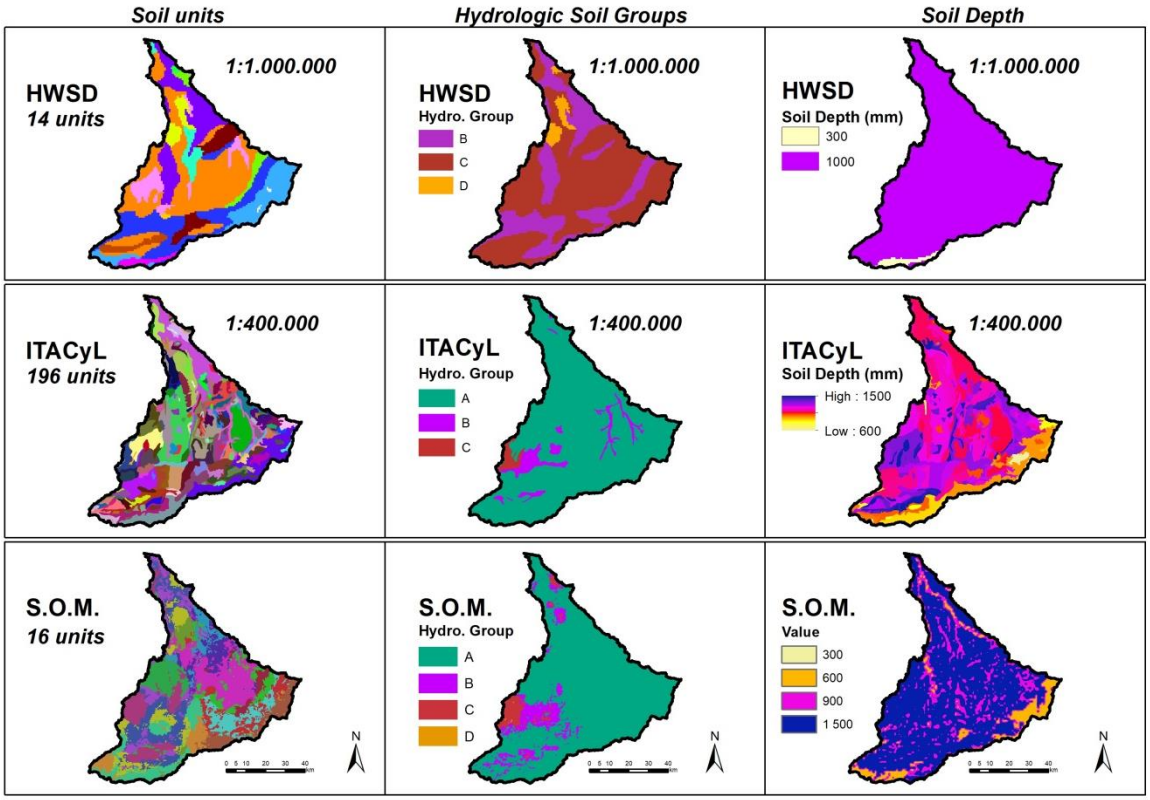

Figure 21. Hydrological group and soil depth comparison of the three soil maps for SWAT set up of Adaja river watershed.

The ITACyL map and SOMM present similar behaviour during calibration for CN and surface runoff, suggesting that for both soil sources were similar in surface water flows. However, larger differences of water fluxes through the soil profile are more evident. Comparing the final soil depth for soil units and clusters, it's clear that TSU soil depth has an influence on lateral flow regulation and lag time in configuring discharge hydrogram at VFG. When soil layer is thin and hydraulic conductivity are slightly higher, the return flow as lateral contribution to streams is higher, as showed in Table 7. The SOMM shows a more regulated behaviour of flow contribution to streams because of peak matching during calibration as showed in Figure 22.

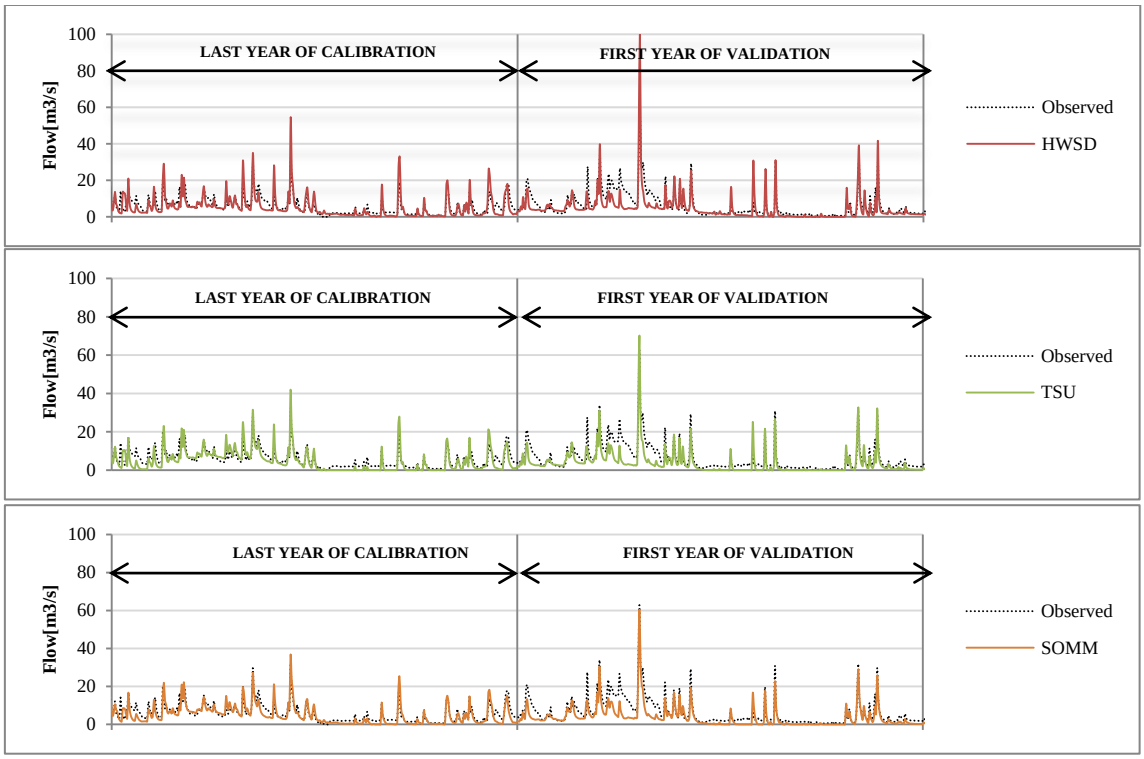

Figure 22. Observed and simulated daily streamflow for calibration and validation at Valdestillas flow gauge (VFG) for the three models. The last year of calibration is 2010 and first year of validation 2011.

The model calibration for each soil data set provides an idea of how well the model is representing the stream flow. The results from this comparison shows that the SOMM presents the best fitting values to stream flow at VFG, requiring less effort during the calibration process. The clustering strategy of soil properties provides very good results for stream flow prediction in sub-arid watersheds as Adaja river watershed.

The Adaja river network, as a sub-arid watershed, is very sensitive to soil properties set up during modelling with SWAT. Others clustering algorithms for soil properties could be also used reducing the calibration-validation effort and achieving more precise models. However, top quality soil survey with fieldwork is always desirable even for the efforts and time that consumes.

3.2 The water availability in a sub-arid Mediterranean watershed

3.2.1 SWAT model setup improvements

In the case of the weather data assignment, a water input difference of around +14% (59mm/yr) was found between the method of weather direct assignation by centroid and the proposed TPM methodology (Figure 11). This is a considerable volume difference compared to the mean stream flow of the CEA system (EA with 57mm/yr and Cega River with 83 mm/yr) and to mean rainfall in CEA (427mm/yr). Other authors also found differences between both methods. For example, Pande et al., (1978) reported a water input difference of +13% from the arithmetic

mean method with respect to the TPM method in Kings river, California. On the contrary, (Fiedler, 2003) estimated -3% in the Cumberland Plateau (United States). This situation was also reported by (Strauch et al., 2012), who showed variations in model streamflow arround (+1,5% in calibration and +3.5% in validation) among different rainfall estimation methods (including the TPM). Independently of the method used for weather assignation, the precipitation data are one of the most significant sources of uncertainty of hydrology modelling with SWAT (Aouissi et al., 2013; Rouhani et al., 2009). As other studies have reported and the current research findings support, rainfall datasets tend to drag most of the input model uncertainty along with them. This is the only parameter considered for water input in the model, especially in Mediterranean basins, where the precipitation varies in space and time.

For the soil map, soil clusters for the range from 3 to 50 soil clusters were tested (Figure 23). The selected set of clusters must present the lowest value between the sum of the normalised mean distance and the normalised DB index (Wehrens and Buydens, 2007). The number of soil clusters with low values for both indices was in the range of 13 to 19 clusters. The comparison between clusters and spatial taxonomic distribution serves as validation of the SOM soil clustering map for SWAT, noting that 16 units is the most suitable number of clusters (Figure 24). Thus, the number of HRUs was reduced from 34,037 to 1,000 HRUs as an improvement proposed by (Luo et al., 2012). This method differs from the use of taxonomic soil units which, in many cases, are not based on soil properties (Burrough, 1983). Using this number of soil clusters, a reduced number of HRUs for each sub-basin was obtained, even for the wide extension of the CEA. SOM is a technique increasingly used in water resources for different environmental datasets due to the robustness of the method (Kalteh et al., 2008). However, there is no evidence of the use of SOM in soil clustering for SWAT modelling. Several studies use a similar approach of soil clusters with SOM (Merdun, 2011; Rivera et al., 2015), but not for hydrological modelling purposes. Comparisons between taxonomic units and SOM for the SWAT model are expected to be included in future research.

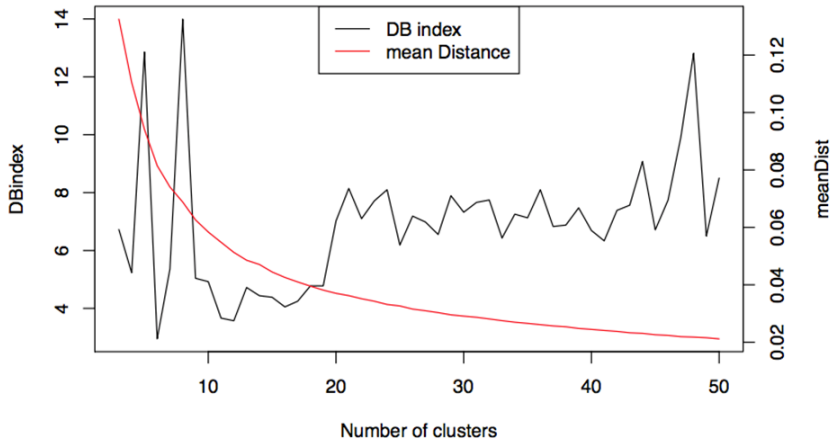

Figure 23. Comparison of D-B index and mean Distance of soil map clustering in Self-Organizing Map (SOM) procedure.

From the land use cover map series, more than 75,000 different crop rotation possibilities were found in the CEA system during the study period. To include more realistic crop rotations and facilitate management scheduling, the LUU field was updated using the SWAT2009LUU tool, considering only the nine most representative crops, covering in total 86% of total crops (Table 8). As previously mentioned, the land use update of HRUs employs the (HRU_FR) variable, which allows us to consider the fragmented crop rotation patterns from remote sensing. This setup proposal results in a composite CN value of the HRUs. From CN values, patterns associated with row crops, such as potatoes (data not shown), present the highest CN values (higher runoff potential); this situation is also true for fallow land, while the opposite is true for forage cover (lower runoff potential). HRUs with HRU_FR of fallow land in more than 30% also present high CN values, and runoff is increased during rainfall events. Proportional values of CN by HRU could be provided by the different land use composition of the HRUs.

Table 8. Cega-Eresma-Adaja (CEA) main crop rotation patterns during simulation period.

Crop dominant	Number of crop patterns	Percentage	Area [ha]	CN[1]
Barley	19.762	26,11%	128.354	64,56
Wheat	16.992	22,45%	109.940	63,13
Fallow	7.493	9,90%	48.481	80,07
Sunflower	7.183	9,49%	46.474	67,79
Other cereals	5.480	7,24%	35.455	64,07
Horticulture	3.096	4,09%	20.029	67,00
Bean legumes	2.006	2,65%	12.977	67,80
Forrages	1.809	2,39%	11.704	35,00
Peas	1.082	1,43%	7.003	67,00
Others crops*	10.786	14,25%	150.010	----*

[1] Average calibrated of Curve Number (CN) value for different crops
*Other crops include different land covers (forest and 17 other crops with different CN).

The model setup for improvement of land use using the SWAT LUU tool results in a CN envelope for the HRUs. The composite value of CN is related with the amount of surface runoff in a HRU scale. The CEA watershed CN is the average of CNs of the HRUs. The average of

CN in CEA is 51.6, similar to mixed forest value of CN2 of the SCS method. In this case, the value of CN of an HRU is a result of grouped land covers. Normally, hydrologic models provide an insight into runoff causes and a reduced strategy in this way is expected to avoid soil erosion and nutrient transport (Bundy et al., 2008). Nevertheless, a strategy to reduce runoff is difficult to define at HRU level with a CN envelope, but the assessment of the runoff slowdown effect of crop patterns is plausible for decision makers using this approach. To this end, HRU analysis by sub-basins is required. Individual land use fragmentation (plot detailed crop rotation) of HRUs is possible by increasing the complexity and computational requirements of the model. Analysis of results in the fragmented HRUs dynamics is not reported in the literature and their analysis is limited to the assessment of global effect at sub-basin scale, due to the complexity and computational requirements to consider individual effect of the land cover over the HRU.

3.2.2 SWAT model sensitivity analysis, calibration and validation

Following Neitsch et al. (2002), a previous analysis was performed to detect the most influential parameters in the streamflow calibration process. This process reveals that 25 parameters are the most sensitive to stream flow changes (Table 10). Parameters related with water dynamics of groundwater recharge (GW_DELAY, REVAPMN, ESCO, SHALLST, GWQMN and ALPHA_BF), runoff (OV_N, CN2 S, SURLAG) and infiltration (SOL_AWC) were respectively the most sensitive in the ranking. Similar parameters for sensitivity ranking were found in other Mediterranean catchments (Galván et al., 2009; Mateus et al., 2014; Salmoral et al., 2017). As in the present study, they also found that the GW_DELAY parameter is one of the most sensitive during the streamflow calibration process. This parameter is related with the lateral flow configuration between the root zone and shallow aquifer connection to the river bed, pointing out the importance of the shallow aquifer and main channel relationship in sub-arid zones. This situation is also reported for other Mediterranean catchments in France (Sellami et al., 2014), Spain (Jimeno-Sáez et al., 2018) or Turkey (Karnez, 2017).

Table 9. Daily calibration and validation statistics for SWAT model.

Statistical Index	VFG		LCFG	
	Calibration	Validation	Calibration	Validation
R^2	0.86 (very good)	0.85 (very good)	0.69 (good)	0.67 (good)
NS	0.84 (very good)	0.82 (very good)	0.65 (good)	0.61 (good)
bR^2	0.70	0.61	0.70	0.61
PBIAS	-10.8 (good)	-9.1 (very good)	-15,8 (good)	-18.6 (good)
KGE	0.84	0.86	0.70	0.71
p_factor	0.63	0.61	0.57	0.53
R_factor	0.39	0.37	0.22	0.21

Table 10. Summary of calibration parameters implemented with SUFI2.

Parameter	Definition	Units	Default range	Calibrated value	Sensitivity Ranking	*t*-stat	P-value
GW_DELAY.gw	Groundwater delay	days	30 – 450	218.79	1	6.043	0.000
OV_N.hru	Manning's "n" value for overland flow	na	0.01 – 30	2.13	2	-3.168	0.002
CN2.mgt	SCS runoff curve number for moisture condition 2	na	(-0.2) – 0.2	0.32	3	-2.903	0.004
REVAPMN.gw	Threshold depth of water in the shallow aquifer for "REVAP" to occur	mm	0 – 500	534.74	4	-1.421	0.159
SOL_AWC.sol	Available water capacity of the soil layer	mm/mm	0 – 0.5	0.54	5	-1.291	0.200
SURLAG.bsn	Surface runoff lag time	days	0 – 24	10.41	6	-1.039	0.301
ESCO.hru	Soil evaporation compensation factor	na	0 – 1	0.23	7	0.994	0.324
SHALLST.gw	Initial depth of water in the shallow aquifer	mm	0 – 1000	612.32	8	-0.952	0.344
GWQMN.gw	Threshold depth of water in the shallow aquifer required for return flow to occur	mm	0 – 5000	1.06	9	-0.925	0.357
ALPHA_BF.gw	Baseflow alpha factor	days	0 – 1	0.057	10	-0.884	0.379
LAT_TIME.hru	Lateral flow travel time	days	0 – 180	160.84	11	-0.843	0.401
SLSOIL.hru	Slope length for lateral subsurface flow	mm	0 – 150	65.97	12	-0.723	0.472
HRU_SLP.hru	Average slope steepness	m/m	0 – 0.6	0.28	13	0.688	0.494
CH_K2.rte	Effective hydraulic conductivity in main channel alluvium	mm/hr	0 – 500	181.17	14	-0.636	0.527
SOL_z.sol	Depth from soil surface to bottom of layer	mm	0 – 1000	776.57	15	0.544	0.610
CH_K1.sub	Effective hydraulic conductivity in tributary channel alluvium	mm/hr	0 – 300	24.10	16	-0.607	0.546
SLSUBBSN.hru	Average slope length	m	10 – 150	137.96	17	-0.595	0.553
CANMX.hru	Maximum canopy storage	mm	0 – 100	57.62	18	0.387	0.699
CH_N2.rte	Manning's "n" value for the main channel	na	0 – 0.3	0.10	19	0.387	0.700
CH_N1.sub	Manning's "n" value for the tributary channels	na	0.01 – 30	5.54	20	-0.377	0.707
EVRCH.bsn	Reach evaporation adjustment factor	na	0.5 – 1	0.85	21	-0.179	0.857
GW_REVAP.gw	Groundwater "REVAP" coefficient	na	0 – 0.3	0.08	22	0.166	0.868
RCHRG_DP.gw	Deep aquifer percolation fraction	fraction	0 – 1	0.20	23	-0.076	0.939
EPCO.hru	Plant uptake compensation factor	na	0 – 1	0.39	24	0.041	0.967
PLAPS.sub	Precipitation lapse rate	mm/km	0 – 100	77.58	25	-0.016	0.987

Another sensitive parameter is CN2 (3th place in the sensitivity ranking). This parameter is related with runoff of the watershed. But the use of composite values of CN per HRUs is complex, as it allows us to include realistic crop rotation, which makes it difficult to define specific measures to manage the runoff per specific land use. Some of the uncertainty related with the runoff component of water balance is based on variability of HRU definition, and analysis of single HRUs is required.

Daily stream flow performance during calibration (2004-2010) and validation (2011-2014) is compared in Table 9. According to the performance ratings established by (Moriasi et al., 2007), the VFG monitoring point fits a "very good" class with an NSE of 0.84 (in calibration) and 0.82

(in validation). In the case of LCFG, although the values found are lower, it is still considered a "good" class streamflow performance. Similar values of NSE and R^2 were also found in several SWAT hydrological calibration studies in Mediterranean watersheds (Dechmi et al., 2012; Galván et al., 2009; Mateus et al., 2014; Salmoral et al., 2017). For the quality model assessment, the PBIAS is considered good if its value is in the ± 25% range (Abbaspour, 2011). The resulting PBIAS for VFG is around -10% and for LCFG is around -18%. Accordingly, model performance is correct, although it underestimates values during the peak flows.

The stream flow calibration and validation shows that VFG (Figure 24) is absolutely influenced by the operation of the reservoirs (Las Cogotas and Pontón Alto). If reservoir operation is not included, no more than an R^2 of 0.13 could be achieved (series not shown).

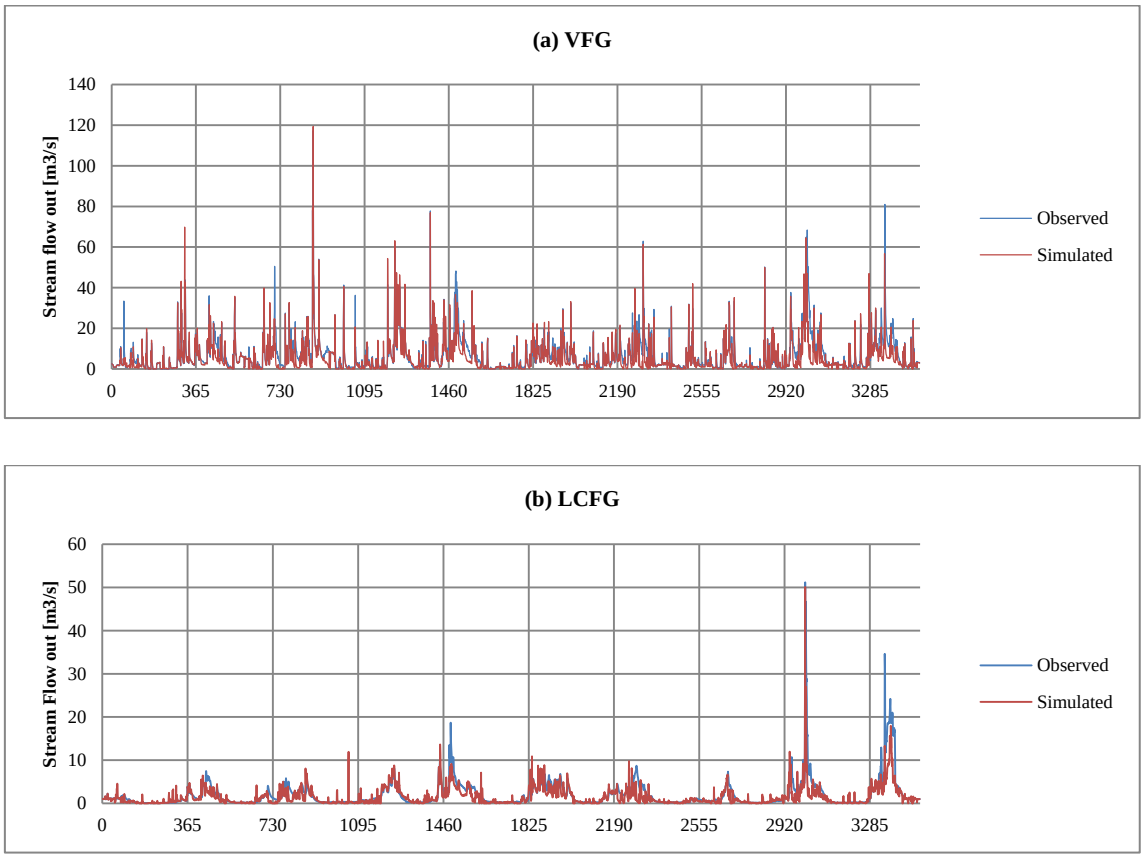

Figure 24. Observed and simulated daily streamflow using SWAT model for (a) VFG, (b) LCFG.

It is important to note that the weather regime during the calibration and validation period is not balanced; the calibration was established over three wet years and the validation period was basically during dry years, Figure 25. Moreover, during validation the outflow series show a slight inaccuracy for peak events, when comparing observed and measured flows, resulting in underestimates. During dry years (2009 and 2013) these underestimations are more evident. On the other hand, calibration was settled with wet years (2007, 2008 and 2010). Considering the unbalanced weather regime in the simulation period, the statistical performance indices for

validation were expected to be less accurate. Nevertheless, flows are well fitted between simulated and measured LCFG and VFG for calibration and validation. The majority of the unadjusted values are inside the 95PPU band.

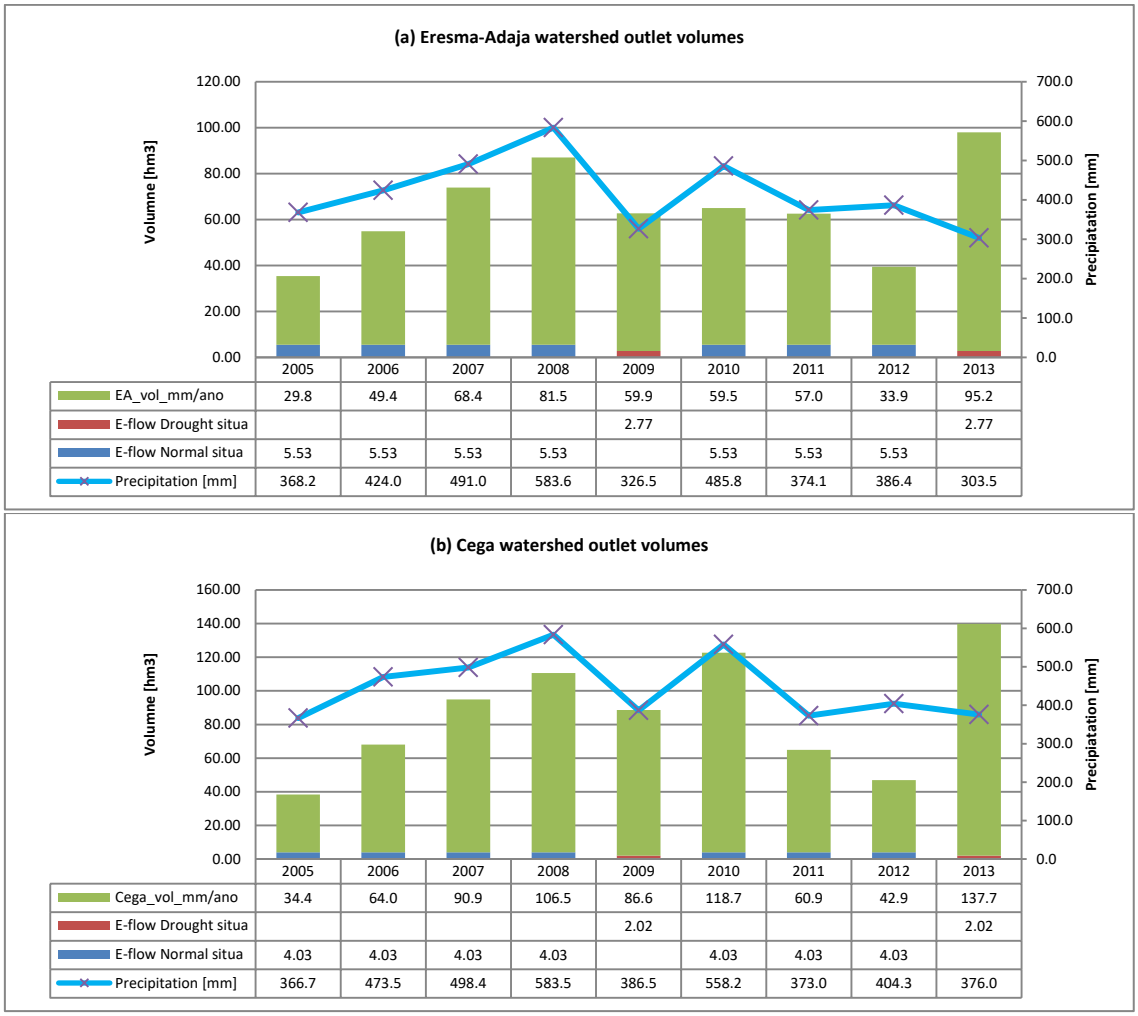

Figure 25. Yearly watershed total volumes outlet and ecological flow in comparison to precipitation for (a) Eresma0Adaj watershed and (b) Cega watershed.

Another point to consider is the situation when the model simulates low flow measures, between no flow and 0.4 m^3/s. Nonetheless, the simulated zero flow situations are found in the 95PPU band. Thus, simulated low flows were in part responsible for negative values of PBIAS. Further analysis during very low flow days (measured data) is necessary (Bisantino et al., 2010; Skoulikidis et al., 2017). A calibration based on a seasonal scheme is needed (Ricci et al., 2018) and differentiated dynamic baseline flow could provide a strategy to follow (Arnold et al., 1995). Although there are some studies that report very low flows in regulated rivers in Europe (Kirkby et al., 2011), or in Spain (Martinez - Capel et al., 2011; Salmoral et al., 2017), no discussion about this condition related with PBIAS is provided.

It should be noted that LCFG is a gauging station that only depicts 25% of the Cega upstream watershed. Consequently, downstream hydrology of this point is not gauged, and only indirect evaluation is considered. After the LCFG point is where agricultural water demand increases. Further studies involving a methodology for ungauged watersheds are necessary to validate the Cega downwater calculations of the SWAT model results.

3.2.3 Model uncertainty

Model uncertainty is assessed through the statistical performance indices, P-factor and R-factor. Those indices are correlated and a balance must be achieved during the calibration process. Values of approximately 0.6 for P-factor and between 0.22-0.39 for R-factor, show the model uncertainty degree for the calibrated ranges of parameters. The suggested values are >0.7 and <1.5 respectively (Abbaspour, 2013). Abbaspour's work noted that for P-factor and R-factor they should be as large as possible, although for large and regulated basins these values could be lower. Large-scale and very complex systems (hyper-regulated watersheds) present high variance due to climate conditions. P-factor and R-factor could be targeting close to the range values proposed by Abbaspour in 2004, but these parameters do not necessarily entirely explain the biophysical process. Modellers look for the balance between several factors: the objective function, the function weight, the initial and boundary conditions, and the type and length of measured data used to calibrate (Abbaspour, 2013). Consequently, the parameter-combination band is very complex in large watersheds; other research at daily time scale and large watershed also refers to values in the range of our P-factor and R-factor results (Begou et al., 2016; Roth et al., 2016). Further study is needed on a sub-basin scale to expand on details to reach higher performance values of the uncertainties.

3.2.4 Water balance

The water balance components (Inflow, outflows and storage volumes) and values are represented in the schema of Figure 26, for each two sub-basins within CEA.

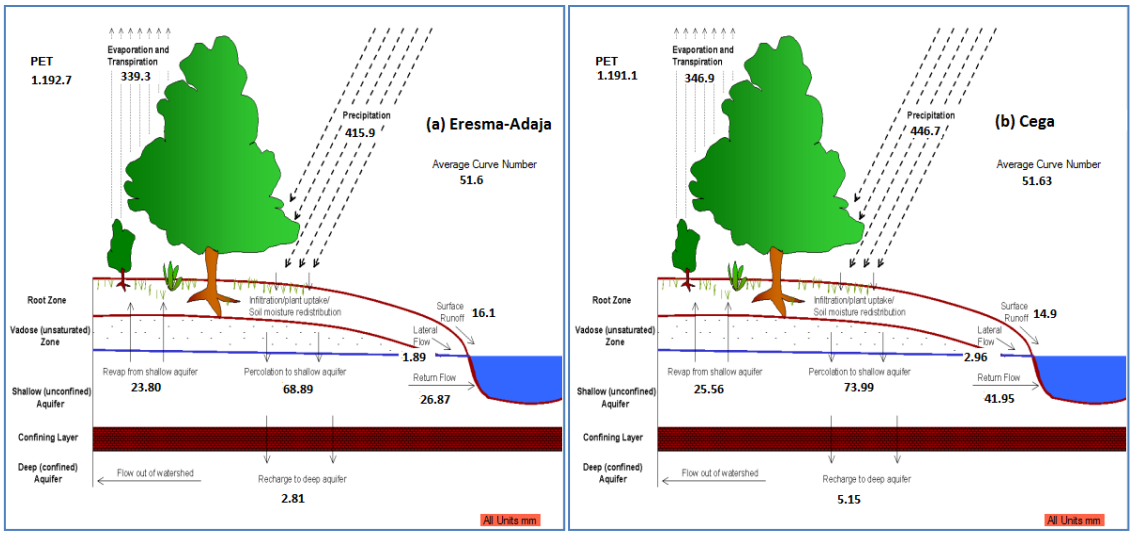

Figure 26. The SWAT model balance components of CEA subbasins. Cega river (left) and EA(Eresma-Adaja) (right).

The streamflow/rainfall ratio for regulated catchments is usually lower than in watersheds with natural flow. This statement is borne out in the present study, with a ratio of 0.14 for EA (regulated) and 0.18 for Cega (unregulated). Similar values were reported for different Mediterranean basins (Merheb et al., 2016). This situation highlights the implications of streamflow regulation in catchments similar to EA and Cega. Thus, reservoir regulation rules must be seasonally compared to maintain similar runoff ratios between regulated and unregulated stream regimes in these similar catchments. This could be a target to preserve the natural streamflow behaviour in spite of the regulation of large headwater reservoirs.

Streamflow volume is a key element for river authorities. The model estimates a streamflow of 59.4 mm/yr for EA and 82.5 mm/yr for Cega. Similar results were reported by the DURERO project (Vicente Gonzalez et al., 2016) for the whole Douro watershed, with a streamflow value of 60.8 mm/yr. The more accurate water balance in ungauged areas of the watershed provided by the present study could serve as complimentary information for planning purposes at the local scale.

Runoff is a complex component, being the sum of surface runoff and the river baseflow. The latter is the contribution of lateral flow and the groundwater return flow. In this case, the groundwater contribution to the baseflow is higher than the surface runoff, as shown in Table 11. During dry years or dry seasons, the disconnection between riverbed and aquifer is more frequent; this causes very low stream flows. The situation is evident in stream flow series and in the decrease of groundwater level in piezometers.

SWAT model results show that the CEA system is a deficit watershed. The negative average net balance (-850.2 mm/yr) proves it during the simulation period. The comparison of the

potential evapotranspiration (ETP=1,192.1 mm/yr) and real evapotranspiration (ET= 341.9 mm/yr) shows a large water deficit (Table 11). The simulation results for CEA indicate on average that only 15.7% of precipitation is converted into surface flow. This finding indicates that all processes during the soil-plant-atmosphere interaction (>80%) are quantitatively more relevant than surface flow. For this reason, the vadose zone interface is a key factor in water dynamics in the CEA and merits more in-depth study. For more details on simulation ratios of hydrophysical processes, see supplementary material Annex 9.

Table 11. Water balance components for Eresma-Adaja and Cega watersheds with SWAT model.

Type	Period	Calibration					Validation				Simulation mean values
	Hydrologic Year	2005	2006	2007	2008	2009	2010	2011	2012	2013	
	year type	Average	Average	wet	wet	dry	wet	average	average	dry	
Eresma-Adaja	Precipitation	368.2	424.0	491.0	583.6	326.5	485.8	374.1	386.4	303.5	415.9
	ETP	1346.8	1272.1	1162.4	1154.3	1315.1	1193.8	1298.0	1301.1	690.5	1192.7
	Deficit	978.6	848.1	671.4	570.7	988.6	708.0	923.9	914.7	387.0	776.8
	ET	269.5	413.8	409.3	389.7	332.2	363.6	362.1	294.0	219.2	339.3
	Flow	29.8	49.4	68.4	81.5	59.9	59.5	57.0	33.9	95.2	59.4
	VFG-$Flow_{obs}$	29.31	48.54	67.2	80.09	58.89	58.44	56.04	33.28	80.79	57.0
	Surface runoff	13.2	15.4	24.1	25.9	10.2	16.8	13.6	14.4	11.3	16.1
	Baseflow	16.6	34	44.3	55.6	49.7	42.7	43.4	19.5	83.9	43.3
	Deep aquifer recharge	3.05	3.51	4.07	4.83	2.70	4.03	3.1	3.2	2.51	2.81
	Soil storage	13.45	15.48	17.93	21.31	11.92	17.74	13.66	14.11	11.08	15.19
	SAV + Reservoir regulation	52.4	-58.19	-8.7	86.26	-80.22	40.94	-61.76	41.19	-24.49	-0.8
Cega	Precipitation	366.7	473.5	498.4	583.5	386.5	558.2	373.0	404.3	376.0	446.7
	ETP	1345.2	1248.1	1133.5	1127.4	1303.9	1176.3	1334.7	1333.0	717.3	1191.1
	Deficit	978.5	774.6	635.1	543.9	917.4	618.1	961.7	928.7	341.3	744.3
	ET	274.7	420.9	425.9	394.9	325.1	371.5	355.0	319.4	235.2	346.9
	Flow	34.4	64.0	90.9	106.5	86.6	118.7	60.9	42.9	137.7	82.5
	LCFG-$Flow_{obs}$	144.42	269.14	382.02	447.77	363.89	498.76	255.74	180.11	507.83	338.85
	Surface runoff	12.3	15.6	20.2	20.7	11.2	17.3	11.6	12.6	12.7	14.9
	Baseflow	22.1	48.4	70.7	85.8	75.4	101.4	49.3	30.3	125	67.6
	Deep aquifer recharge	4.23	5.46	5.75	6.73	4.46	6.44	4.3	4.66	4.33	5.15
	Soil storage	13.39	17.29	15.56	21.31	14.11	20.39	13.62	14.76	13.73	16.31
	SAV	39.28	-34.15	-39.71	54.06	-43.77	41.17	0.08	65.48	122.74	78.34

Values in [mm/yr]

Note: VFG-$Flow_{obs}$: observed flow at Valdestillas Flow gauge; LCFG-$Flow_{obs}$: observed flow at Lastras de Cuellar Flow gauge; ETP: potential evapotranspiration; ET: evapotranspiration; Flow: simulated flow; Surface runoff: simulated surface runoff; SAV: Shallow aquifer variation.

The CEA system is a large sub-basin of the River Douro with a variety of landscapes, which suggest that water balance is not homogeneous in the system. Three zones were defined based on environmental experts' knowledge of landscapes and water management (Figure 27). SWAT model results show that Cega highlands present the highest rainfall in comparison of Eresma-Adaja watershed headwaters. Regarding this difference, it is important to note that stream fluxes are different in volume and water management could be different in middle and lowland areas. In addition, Cega has an absence of regulation infrastructures. Peak flows and flashes were more frequent in the Cega River; these events were reported in communication media during the simulation period. The Eresma-Adaja river tributary zone presents lower rainfall volumes, suggesting that tougher conditions of scarcity could be located in this zone. This suggests that agriculture in this zone is more feasible under a rainfed regime.

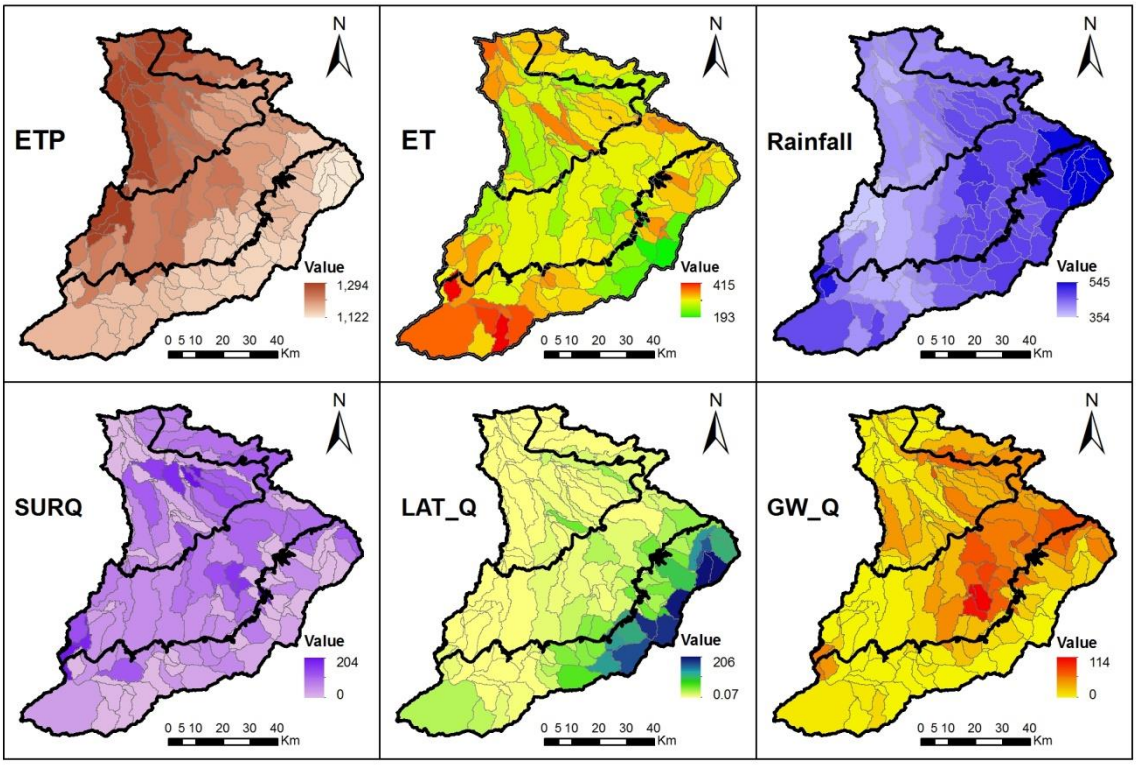

Figure 27. Mean annual water balance components of CEA subbasins. Values in [mm]. ET (real evapotranspiration), ETP (potential evapotranspiration), SURQ (surface runoff), LAT_Q(lateral flow), GW_Q(ground water recharge). Headwaters in the south and low lands in north-west.

In contrast, potential evapotranspiration shows a differentiated trend of higher values in the lowlands and lower in the headwaters. The average ETP of all land covers in the headwater shows a lower value compared to the lowlands, which is due to altitude, predominance of forest (stomatal resistance to ET) and lower temperatures during the spring-summer period. Moreover, real evapotranspiration values in the southern west of Eresma-Adaja are more affected by the recent agricultural development in this area, allocating a pressure in water demand in this area that affects the Eresma-Adaja water availability in the middle and lowlands.

In general, surface runoff in volume is less than groundwater fluxes in both watersheds (Eresma-Adaja and Cega). However, this relation is true in the lowlands and midland, but different in the headwaters due to water movement through the soil. The roughness of forest and pastures in headwaters for surface runoff slows down the flux. These fluxes enter these shallow soils until they meet rocks and start moving by gravitational forces as lateral flows. This situation limits the deep aquifer recharge in headwaters. The opposite processes of recharge occur in the midlands, where the materials are sandy composites, soil depths are higher and slopes are more flattened. Deep aquifer recharge is higher in the Cega River than in Eresma-Adaja, as higher volumes of lateral flow that comes from the headwaters infiltrates the sandy soils. Lateral flow in headwaters of Eresma-Adaja (south west) could be increased by changing the land use to natural forest covers and pastures. Reservoir and agricultural demand in the Eresma-Adaja headwaters limit the lateral flow and the deep aquifer recharge in the midlands.

Annual water balance shows that there is no water surplus to support new demands, including the expected 18% irrigation expansion (49 hm^3/yr). Moreover, a tendency of decreasing precipitation is an issue that the watershed must be adapted to. Capture of precipitation peak events with more reservoirs, as suggested by stakeholders, will have a negative impact on stream flow and consequently on aquifer recharge and soil water scarcity of the ecosystem. In sub-arid watersheds, the reservoirs limit riverbed water transfer to aquifer in the downwaters, resulting in a lower water table without capillarity contribution to bottomland crops (Lin, 2011). This effect could be expected in a reduction of groundwater "revap" volume to plants. This situation in CEA could affect "Tierra de Pinares", a valuable ecosystem of conifer forest (900 ha) in watershed midlands that are rooted connected (2 m deep) to the water table.

3.2.5 CEA water demand assessment

According to our results, 86.64% of water demand for the CEA is allocated to agricultural purposes. Figure 28 shows the average real evapotranspiration (ET) of HRUs during simulation and the area of the dominant rotation crop pattern (9 crops). Annual rainfed crops use on average the same water compared to the permanent crops, but annual rainfed crops consume this amount of water in only 5-6 months. Furthermore, during the rest of the year when precipitation events are more frequent, fallow land contributes to reduce shallow aquifer recharge. This dynamic is explained by the runoff being privileged in slope land > 5%. During the rotation schema, fallow land is characterised by the lack of surface roughness, causing a quick response with the precipitation-runoff process. This situation prevents a prolonged time of infiltration before the start of surface runoff. Vegetated cover could be used to slow down runoff and increase water use efficiency. Vegetated cover is a strategy to be included in crop rotation schemes, mainly in schemes that include annual rainfed and irrigated row crops for Mediterranean watersheds (Taboada-Castro et al., 2015). Water efficiency can be achieved, but

only if annual ET of vegetated cover is approximately 350 mm/yr. This assertion is based on permanent crop average water consumption. In addition, ET for vegetated cover for inter-annual rotations could be approximately 16 mm/month during the fall-winter period and 42 mm/month during the spring-summer period.

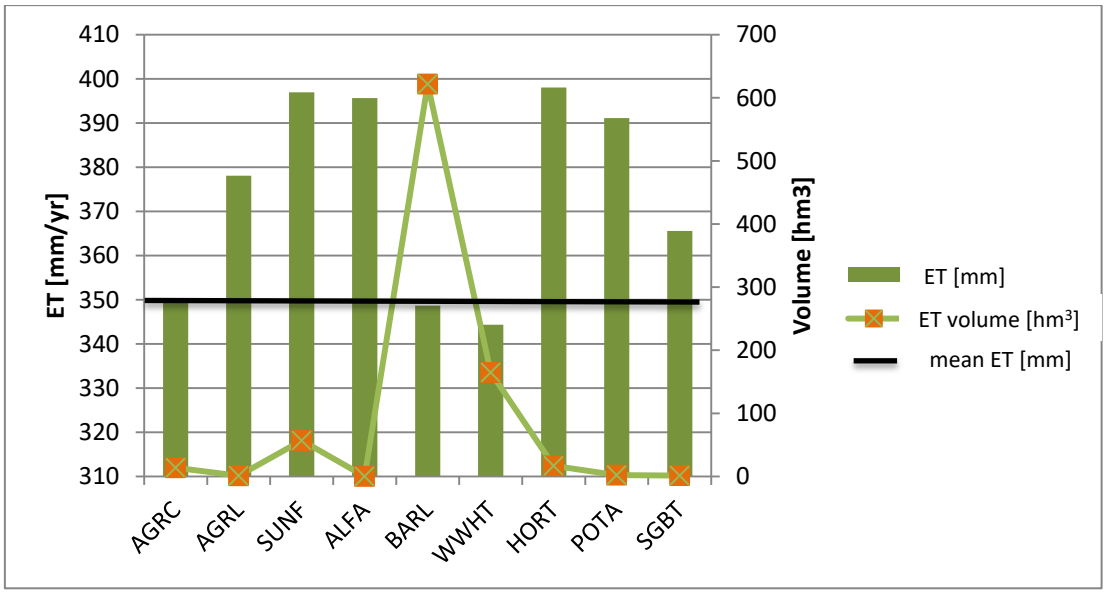

Figure 28. Summary of land use water demand in Cega-Eresma-Adaja (CEA) watershed simulated with SWAT: Evapotranspiration (ET), mean ET and water volume (Volume).

Irrigated crops represent the major water consumption use. A strategy to spatially redistribute crop area in quantity provides a feasible solution to homogenise agricultural water demand. Similar to the situation in rainfed crops, the CEA watershed needs to decrease agricultural irrigation area that uses more than 350 mm/yr, including crops that demand less water. Focus on barley dominant patterns could be an insight to achieve a balanced water demand. In addition, an economic analysis is also needed to assess a more convenient solution to reduce agricultural water consumption.

Deep aquifer simulated recharge is estimated at 2 mm/yr (15.7 hm^3/yr). On average, a rate of 25.4 mm/yr (196.26 hm^3/yr) was used for irrigation during the simulation. Comparing this value with the agricultural water demand established by RBMP (170.42 hm^3), there is a difference of 26.26 hm^3 (3.34 mm/yr) that could be extracted from aquifers. This finding indicates that possibly shallow aquifers and deep aquifers have been used to extract 26.26 hm^3, but only 15.7 hm^3 comes from renewable resources. The overexploitation is more associated with the groundwater bodies of "Los Arenales" located downstream, and it is difficult to measure global overdraft due to shared boundaries with other watersheds. Further developments of aquifer recharge could be provided by simulating the entire watershed and aquifer shares with SWAT and MODFLOW.

Most of the groundwater recharge is related to wheat and pasture land cover patterns. In addition to aquifer recharge, groundwater quality tracking in these sandy soils is mandatory. Diffuse pollution of aquifer in this zone is very sensitive, and responsible for the poor status of the water bodies. Fertilisation operation in wheat and pasture improvements needs to be included in further studies on this issue. This situation is also related to diffuse pollution of groundwater bodies due to the fertilisation rates and timing. In SWAT, the CN is relatively easy to manipulate, and any strategy or measure to reduce runoff can be included in the model. Hence, priority strategies for runoff control in potato and barley are needed. See supplementary material Annex 10.

3.3 Vegetation dynamics

3.3.1 Soil reflectance statistics

The descriptive statistics of the spectral bands at the time that bare soil is predominant are shown in Table 12. For both zones, SOM5 and SOM15, skewness and kurtosis values are in the range of -2 to +2, indicating that the band samples probably come from a normal distribution. However, to confirm normality of these values Shapiro-Wilk and Kolmogorov-Smirnov tests were conducted with a positive result (see Table 12). Observing the mean values of the spectral bands studied, always SOM5 presents lower values than SOM15.

Table 12. Statistics of MOD13Q spectral bands series for SOM5 and SOM15 for the 18th of February associated to bare soil as predominant condition for the period 2000 to 2019.

	Reflectance bands							
	NIR		**RED**		**Blue**		**MIR**	
SOM soil unit	**5**	**15**	**5**	**15**	**5**	**15**	**5**	**15**
	Bare soil (February 18th)							
Mean	0.294	0.343	0.133	0.161	0.063	0.076	0.177	0.232
Typical error	0.009	0.011	0.004	0.006	0.002	0.003	0.011	0.016
Median	0.290	0.332	0.136	0.161	0.064	0.076	0.185	0.222
Standard deviation	0.038	0.051	0.018	0.028	0.010	0.012	0.049	0.071
Kurtosis	-0.553	-0.707	-0.122	-0.906	-0.548	-0.636	-1.184	-0.421
Skewness	0.005	0.412	-0.607	0.006	-0.229	-0.217	-0.331	0.583
Count	20	20	20	20	20	20	20	20
	Normality test							
Shapiro Wilk								
Statistic	0.932	0.922	0.955	0.965	0.971	0.973	0.964	0.959
P-value	0.170	0.108	0.442	0.644	0.971	0.808	0.624	0.523
Kolmogorov-Smirnov								
P-value	0.776	0.749	0.932	0.898	0.934	0.912	0.969	0.987

The dates in which tillage operations match with sensed dates serve as references to assess and compare the soil reflectance from SOM5 and SOM15. From those dates, analysis of variance (ANOVA) was performed, indicating that there are significant differences between the two soil units across all the single bands (Table 13). These results suggest that the mean confidence

intervals between SOM5 and SOM15 of reflectance responses are statistically different (Figure 29) confirming the difference of both soils.

Table 13. Analysis of variance (ANOVA) showing significant statistical differences (*p*-value < 0.01) for single bands (NIR, Red, Blue and MIR) for the two soil units SOM5 and SOM15.

Source	Sum of Squares	Degrees of freedom	Mean Square	F-Ratio	P-Value
NIR					
Between SOMs	0.024	1	0.024	11.93	0.001
Within SOMs	0.078	38	0.002		
Total (Corrected)	0.103	39			
Red					
Between SOMs	0.008	1	0.008	14.67	0.001
Within SOMs	0.021	38	0.001		
Total (Corrected)	0.029	39			
Blue					
Between SOMs	0.002	1	0.002	13.51	0.001
Within SOMs	0.005	38	0.000		
Total (Corrected)	0.006	39			
MIR					
Between SOMs	0.030	1	0.030	8.03	0.007
Within SOMs	0.142	38	0.004		
Total (Corrected)	0.172	39			

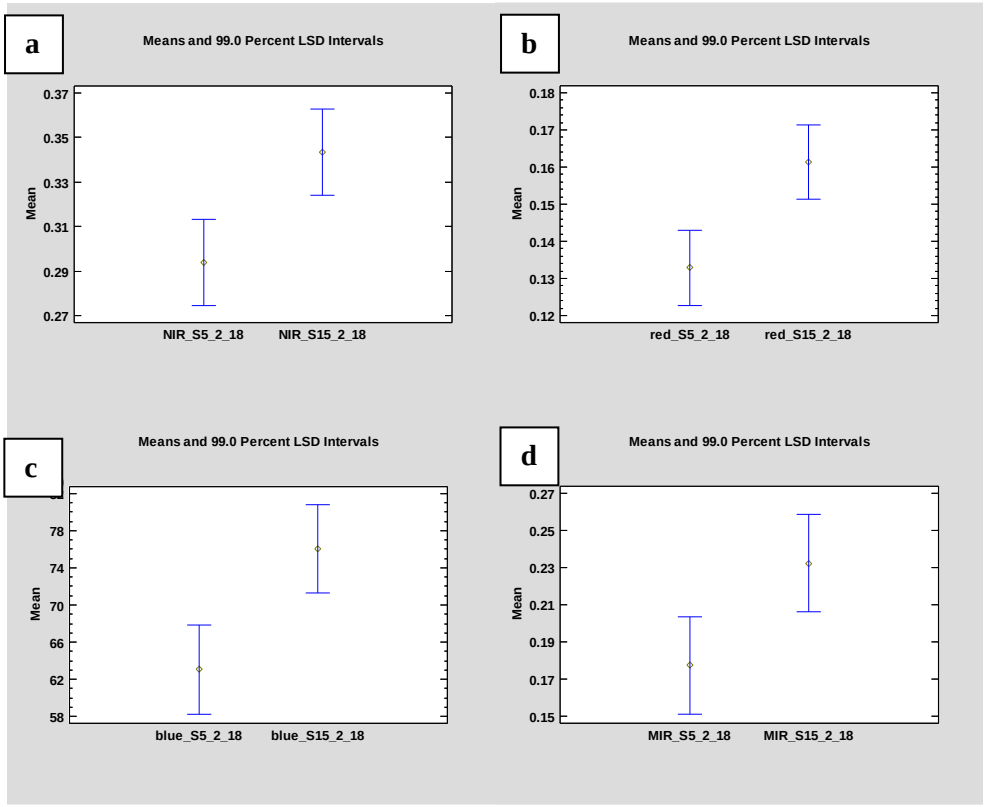

Figure 29. Intervals of confidence plots from the Least Significant Difference test (LSD) for SOM5 and SOM15. a) NIR*, b) Red*, c) Blue*, d) MIR* mean band values and, e) NDVI**. *for February the 18th;** Growing season.

The estimation of BSL for both zones presented different values (Figure 30). The SOM5 unit presents a higher slope value than that of SOM15. The P-value < 0.05 for the ANOVA test applied to these results confirms statistical differences in slopes and intercepts (Table 14).

Table 14. Statistical significance of bare soil lines (BSL) for SOM5 and SOM15.

Source	Sum of Squares	Df	Mean Square	F-Ratio	P-Value
Intercepts	0.0016	1	0.0016	79.53	0.0000
Slopes	0.0001	1	0.0001	4.46	0.0383

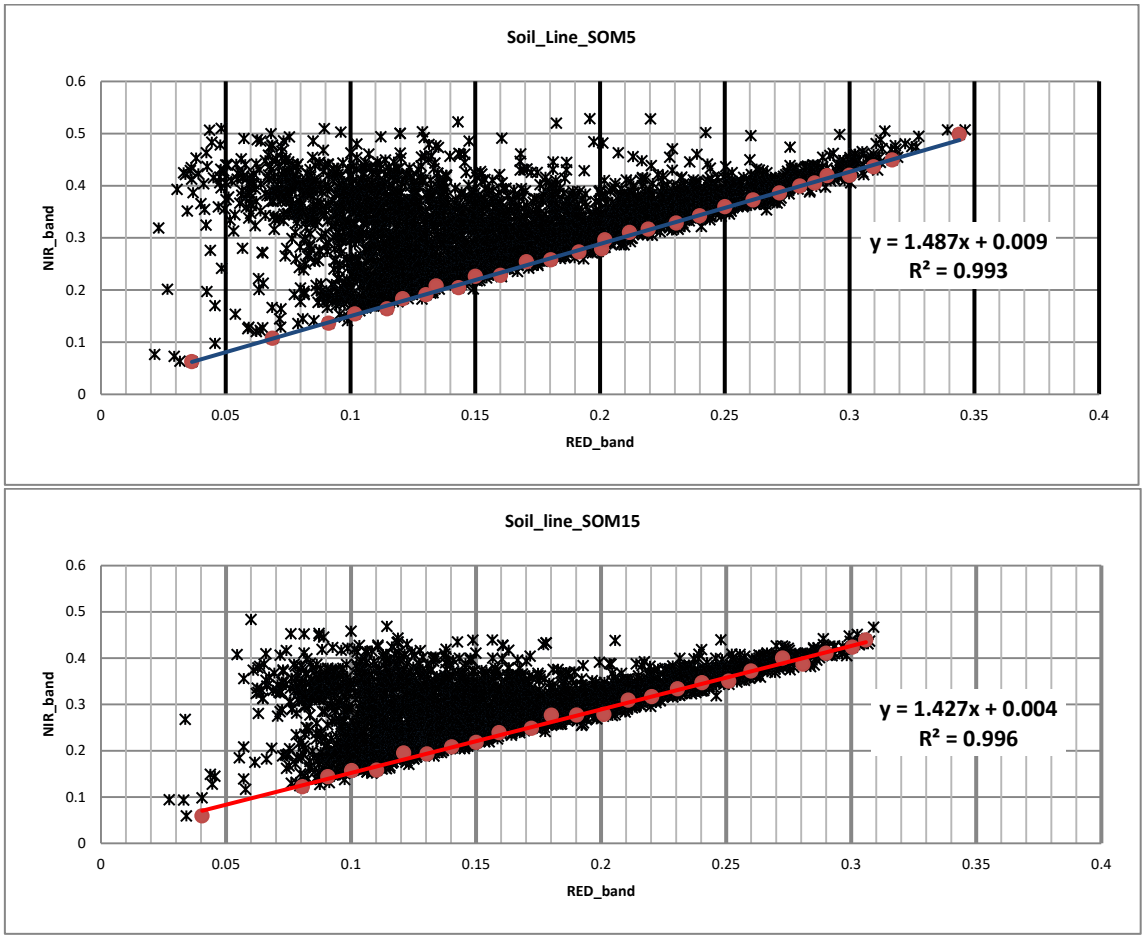

Figure 30. Soil lines for SOM5 and SOM 15 soil units. NIR and Red values for February 18th in the period 2000 to 2019. Slope of linear regression indicates bare soil line (BSL) value.

3.3.2 NDVI statistics

NDVI series patterns for SOM5 and SOM15 are shown in Figure 31. From October to February there is a smooth increase. Then, March and April present significant increases in the NDVI values followed by a decrease during May and June when the crop cycle finished. The range of mean NDVI values in the yearly cycle goes from 0.22, in a wide part of fallow, till 0.60 at the end of April.

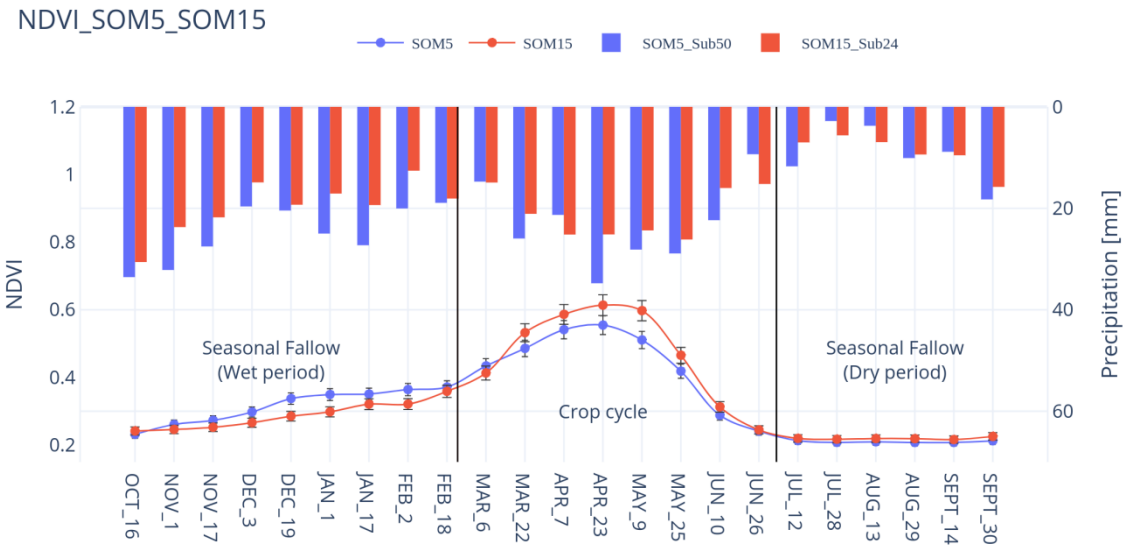

Figure 31. Average of NDVI every15-days for monoculture cereals crop cycle of SOM5 and SOM15 in comparison with precipitation for the period 2000 to 2019.

The rain series patterns are shown in Figure 31 too. The months with highest rain are October, April, and May for both sites. Looking at Figure 31 and at Table 2, SOM5 presents a higher precipitation than SOM15 in almost all the months. However, during the crop cycle the highest NDVI values are achieved at SOM15. When an ANOVA is applied to the average NDVI value of the crop cycle, March to June, of each zone a significant difference, with a confidence level of 99% and *p*-values < 0.01 (Table 15), is obtained. This confirms the visual observation of Figure 31.

Table 15. Analysis of variance (ANOVA) of NDVI for the two sampling sites SOM5 and SOM15 using the average index value of the plots for each sensing date range between March and June from 2000 to 2019.

Source	Sum of Square	Degrees of freedom	Mean Square	F-Ratio	P-Value
NDVI					
Between SOMs	0.112	1	0.112	10.15	0.002
Within SOMs	2.635	238	0.011		
Total (Corrected)	2.747	239			

To study the correlation of both variables, NDVI and precipitation, first they were accumulated from January till May for each zone (Figure 32). There is a linear relation between the accumulated precipitation and the accumulated NDVI values with a R^2 higher than 0.95 in both sites. However, the slope of each one present unique value.

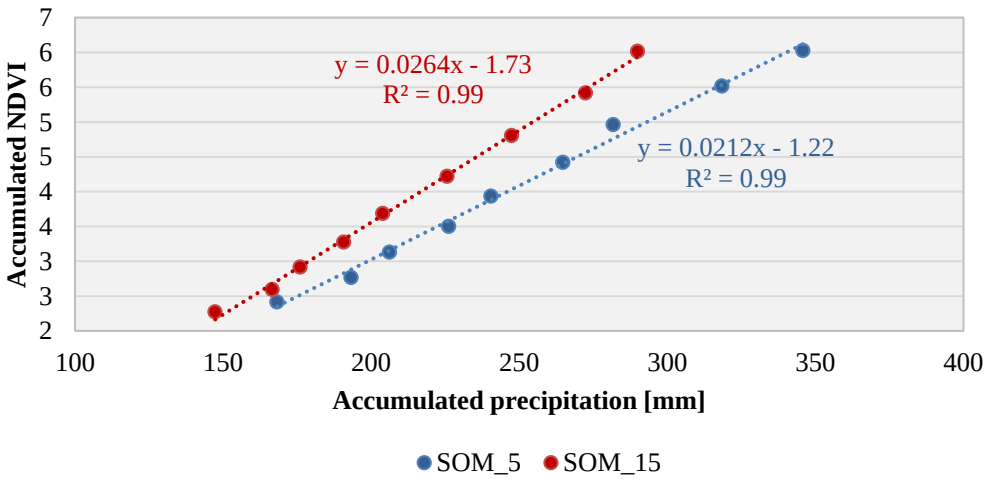

Figure 32. Linear correlation between accumulated values of precipitation and NDVI from January to May.

Linear correlation between accumulated values of precipitation and NDVI from January to May. Finally, both NDVI original series did not present a significant trend in the range of years study in this work at a confidence level of 0.05 ($-1.96 \leq Z \leq +1.96$).

3.3.3 Scaling characteristics of NDVI original series

The NDVI original series for each zone are showed in Figure 33a. The yearly cycle is easily recognized with valleys presenting values around 0.2 and peaks that some years are above 0.6 and other presents lower values. In SOM5 there is a clear year, 2009, with the lowest values of NDVI that in SOM15 does not present. However, in SOM15 there is a peak in 2000 and low NDVI values in 2009 and 2014.

The multiscaling analysis of both sites is showed in Figure 34. The scaling pattern was obtained approximately with lags from 1 till 8, corresponding to 16 days till 4 months approximately. Both present a strong persistent character with a GSF above the straight line of the uncorrelated noise. As we can see in the Generalised Hurst exponents (GHE), they present a significant variation in the Hurst exponent depending on q value showing their multifractality. This can be observed in the difference of both extremes ($\Delta H(q)$) showed in Table 15 for both sites. In all the parameters, SOM5 presents higher values than SOM15.

The NDVI original signals present a global seasonal pattern in which monoculture sequence was clearly identified and all years where planted. The variability involved in the process (i.e., climate, crop types and soils) are continuously changing in time or exhibit trended behaviour, as presented in the former section. This was observed by analysing their overall variability across the study period.

The persistent condition of the NDVI signature is mainly coming from the yearly cycle that composes its pattern. The noise in cereal sequences may be due to different mechanisms, as reported by other authors (Igbawua et al., 2019; Liu and Huete, 1995). As both sites selected presented cereals, the difference can only be attributable to climatic conditions, wet or dry years, terrain slopes or seed varieties. Other sources of noise can be attributable to soil brightness; when soil brightness increases during the fallow season period, the NDVI can be lower. The former was also corroborated from July to February and distinguished the dry and wet periods by seasonal behaviour (Figure 33a). However, during the growing season, most of the reflectance comes from vegetation and not from soil.

The scaling property of these NDVI original series agrees with earlier works in which the persistence condition for crops is also reported through H(q=2) or Hurst index using R/S method (Liu et al., 2019; Peng et al., 2012). However, the results have shown that this series could have a multifractal nature. Li *et al.*, 2017 and Ba *et al.*, 2020 investigated the vegetation dynamic of areas affected by the fire through multifractal analysis achieving the same conclusion. Several parameters can be calculated, as the ones showed in Table 16, given more possibilities to classified the NDVI series studied.

This multifractal analysis in NDVI have been wider used in the spatial scaling context (Alonso et al., 2017; Duffaut Espinosa et al., 2017; Escribano Rodríguez et al., 2015; Lovejoy et al., 2008; Martin-Sotoca et al., 2018).

Looking at the common Hurst index (H(q=2)), both series present persistent values of 0.70 in SOM5 and 0.70 in SOM15. As both GSFs present a slight curvature and H(q=1) is higher than 0.50 the extraction of the seasonal trend is recommended (Davis et al., 1994).

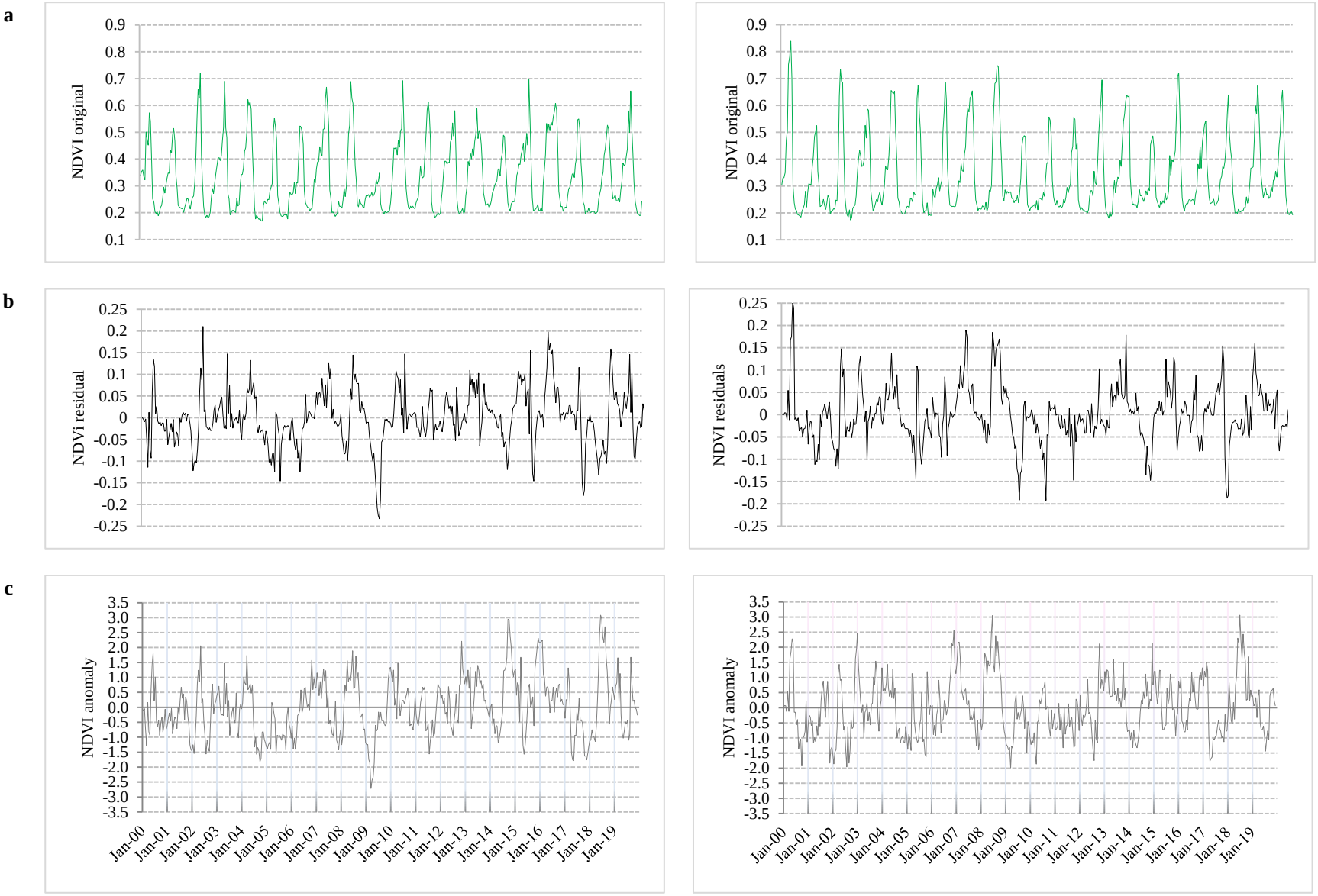

Figure 33. NDVI time series from SOM5 (right column) and SOM15 (left column): (a) NDVI original, (b) NDVI residual, (c) NDVI anomaly.

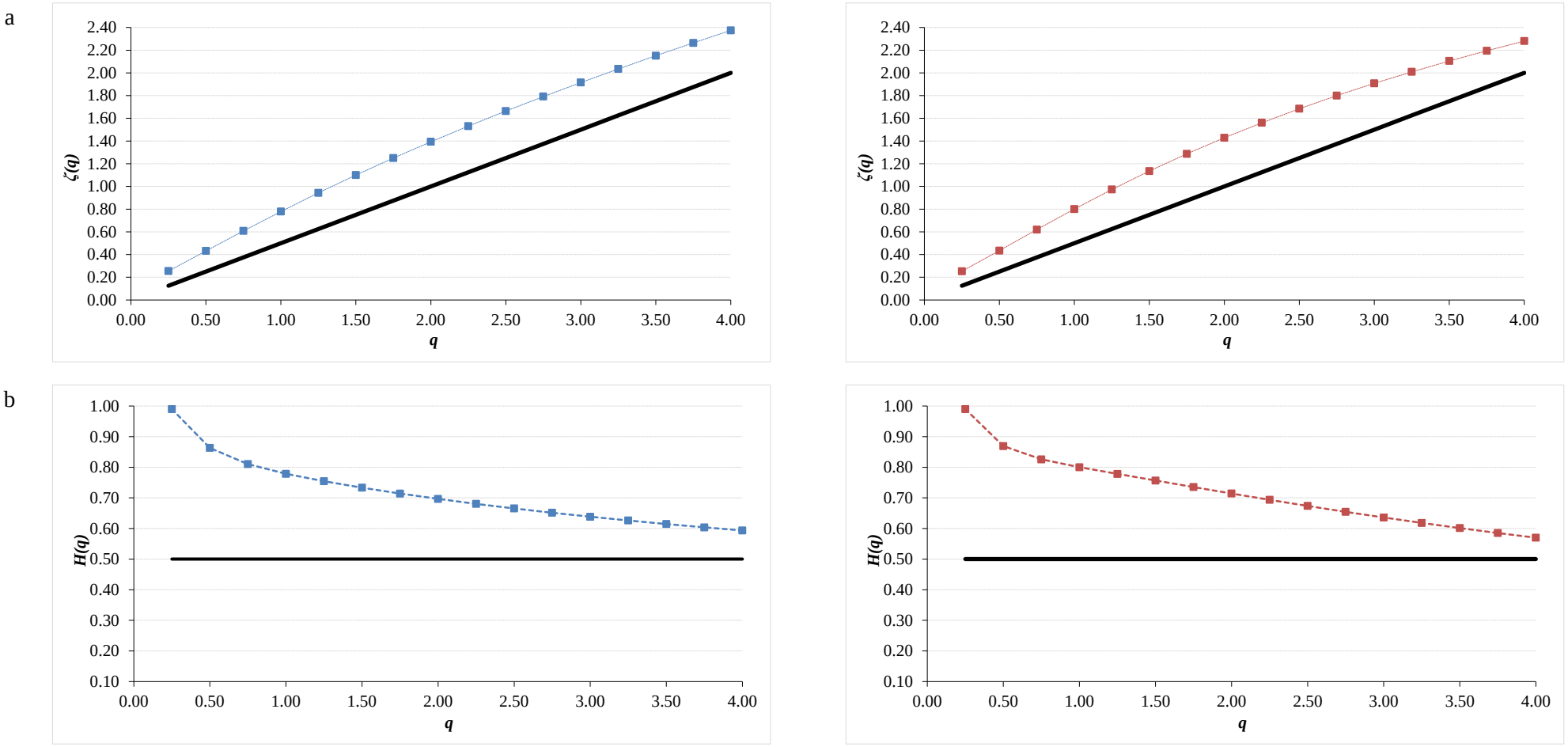

Figure 34. Generalized Structure Function plots for NDVI original series of SOM5 (left column in blue) and SOM15 (right column in red) for: (a) ζ(q) curve and (b) Generalized Hurst exponent H(q), continuous line correspond to non-correlated noise with Hurst value of 0.5.

3.3.4 Scaling characteristics of NDVI residual and anomaly series

Once that from the original NDVI series the seasonal cycle has been extracted, NDVI residual series present a different pattern (Figure 33b). All the differences are in the range of 0.25 and -0.25, pointing out with positive values the moments above the mean for that date of the year and with negative values the moments under the mean for that date of the year. The observations mentioned in the NDVI original series are more marked here. The highest negative value is found in 2009 in SOM5 and the highest positive value is founded in 2000 in SOM15.

The GSF and GHE reflect the change in the pattern of these series (Figure 35). Again, the scaling behaviour is founded from 16 days till 4 months. Both present a strong anti-persistent character with a GSF under the straight line of the uncorrelated noise. As we can see in the Generalised Hurst exponents (GHE), they present a significant variation in the Hurst exponent depending on q value showing their multifractality. This can be observed in the difference of both extremes ($\Delta H(q)$) showed in Table 16 for both sites. Both curves, GSF and GHE, are similar for both sites. However, SOM15 presents higher values than SOM5 but very similar $\Delta H(q)$.

Table 16. Multifractal parameters for each zone and each one of NDVI series. H(q=1), generalized Hurst index for q=1; H(q=2), generalizes Hurst index for q=2; $\Delta H(q)$=H(q=0.25)-H(q=4).

ZONE	NDVI SERIES	H(q=1)	H(q=2)	Δ H(q)
SOM5	Original	0.78	0.70	0.40
	Residual	0.41	0.37	0.12
	anomaly	0.40	0.37	0.09
SOM15	Original	0.80	0.70	0.40
	Residual	0.46	0.43	0.14
	anomaly	0.37	0.34	0.09

Looking at the common Hurst index (H(q=2)), both series present anti-persistent values of 0.37 and 0.43 in SOM5 and SOM15 respectively.

The NDVI anomaly series have been obtained applying a z-score to the NDVI original series and present a similar pattern that NDVI residual one (Figure 33c). Comparing these last two series, the z-score has a smooth effect as it has been divided by the standard deviation of the NDVI values of that date. Therefore, dates with high SD reduce the value obtained in the anomaly series compare to residual one.

This effect of smoothing in certain dates of the z-score is reflected in the multifractal parameters obtained. The GSF and GHE presents less curvature and a visual inspection reflect almost a straight line (Figure 36). Again, the scaling behaviour is founded from 16 days till 4 months. Both present an anti-persistent character with a GSF under the straight line of the uncorrelated noise.

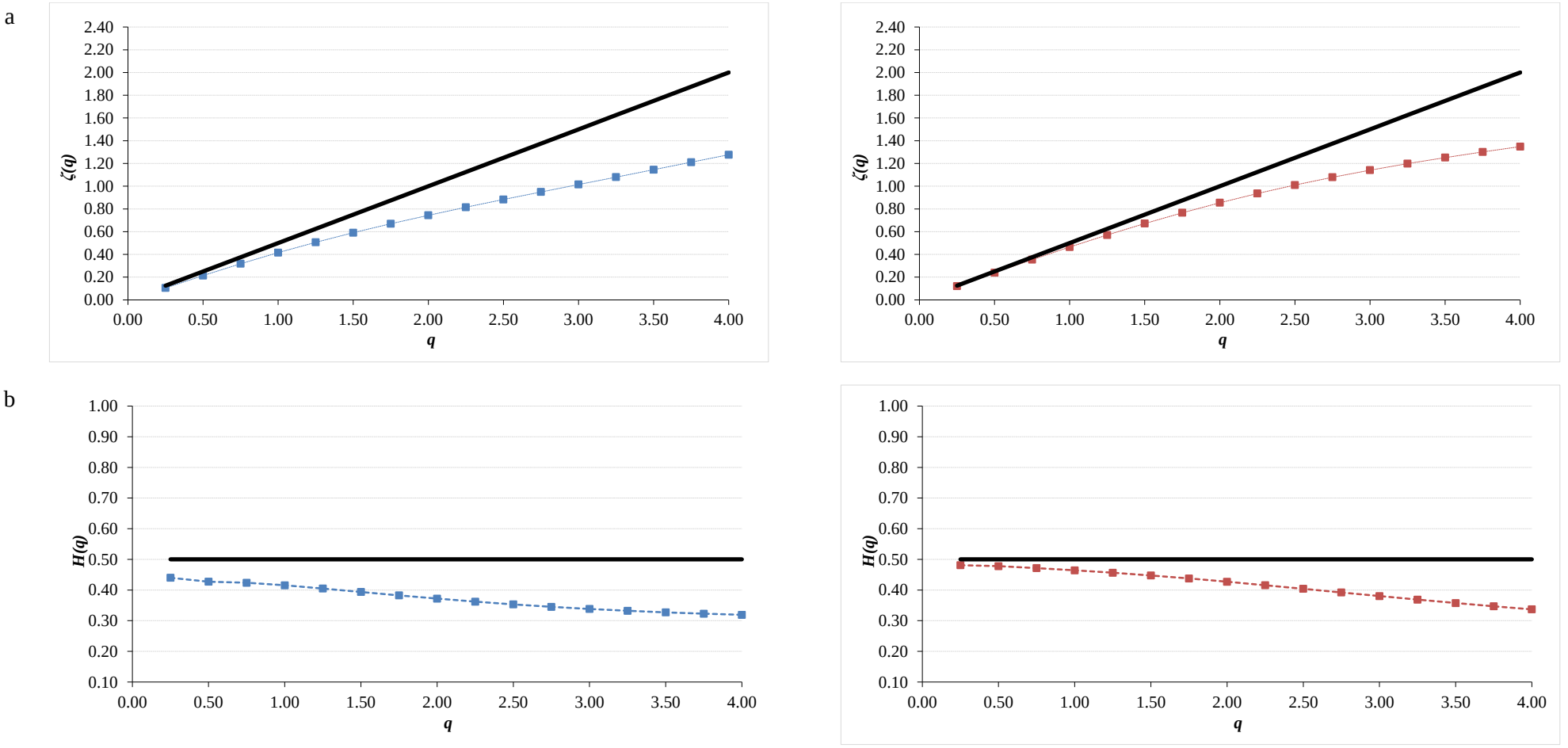

Figure 35. Generalized Structure Function plots for NDVI residual series of SOM5 (left column in blue) and SOM15 (right column in red) for: (a) ζ(q) curve and (b) Generalized Hurst exponent H(q), continuous line correspond to non-correlated noise with Hurst value of 0.5.

This can be observed in the difference of both extremes ($\Delta H(q)$) showed in Table 16 for both sites showing a value lower than 0.10. Both curves, GSF and GHE, are similar for both sites. However, SOM5 presents higher values than SOM15, as the NDVI original series.

Both series present anti-persistent values in $H(q=2)$, of 0.37 in SOM5 and 0.34 in SOM15. These values are higher than in the case of NDVI residual series. Therefore, NDVI anomaly series are less anti-persistent and with a weaker multifractal character than NDVI residual series.

Thus, the most noticeable source of noise in NDVI residual series, in cereal crops once that cycle average pattern has been extracted from the original series, is the reflectance variation under different soil moisture conditions. These, in turn, are related to the rainfall variation from its cycle average pattern and the properties of the soil against the rainfall regime. This situation is especially evident when analysing the reflectance values of the red and NIR bands. Accordingly, NDVI residual signal results in a mixture of noises coming from both spectral bands.

A visual observation of NDVI residual series (Figure 33b) in both sites remind to a residual noise. However, this noise exhibited a scaling behaviour pointing out a structure and, therefore, it is not an uncorrelated noise. Even more, NDVI residual series presents multiscaling behaviour as the GSF and the GHE are not straight lines. This implies that once the clear seasonal pattern is extracted from NDVI series, the residual has still structure, but antipersistent, keeping the multifractal nature from the original series. The MFA normally used by some authors (Igbawua et al., 2019; Li et al., 2017) applied a detrended fluctuation analysis as many of the series analized presented a significant trend in time. In this work, the two series analised did not present a significant trend, the detreded applied was to extract first the average cycle pattern and then the GSF was calculated. This is a different way to approach the study but more suitable for monoculture crops.

NDVI anomaly series presents a smoother behaviour than the residual one. This is reflected in more straight lines in GFS and GHE that originate a weaker multifractal nature in these series but keeps the antipresistant character. This is revealing that the different dispersion of NDVI values in each date has an influence in the multifractal character of the series. The higher dispersion is presented in the crop cycle during seasons where the rain presents higher dispersion too. This point out that NDVI anomaly series is reflecting the variability created mainly by the rain interacting with the characteristics of that site. The analysis of this type of series could be another factor to be incorporated in the agroclimatic zone definition as it is adding an evaluation of the crop risk.

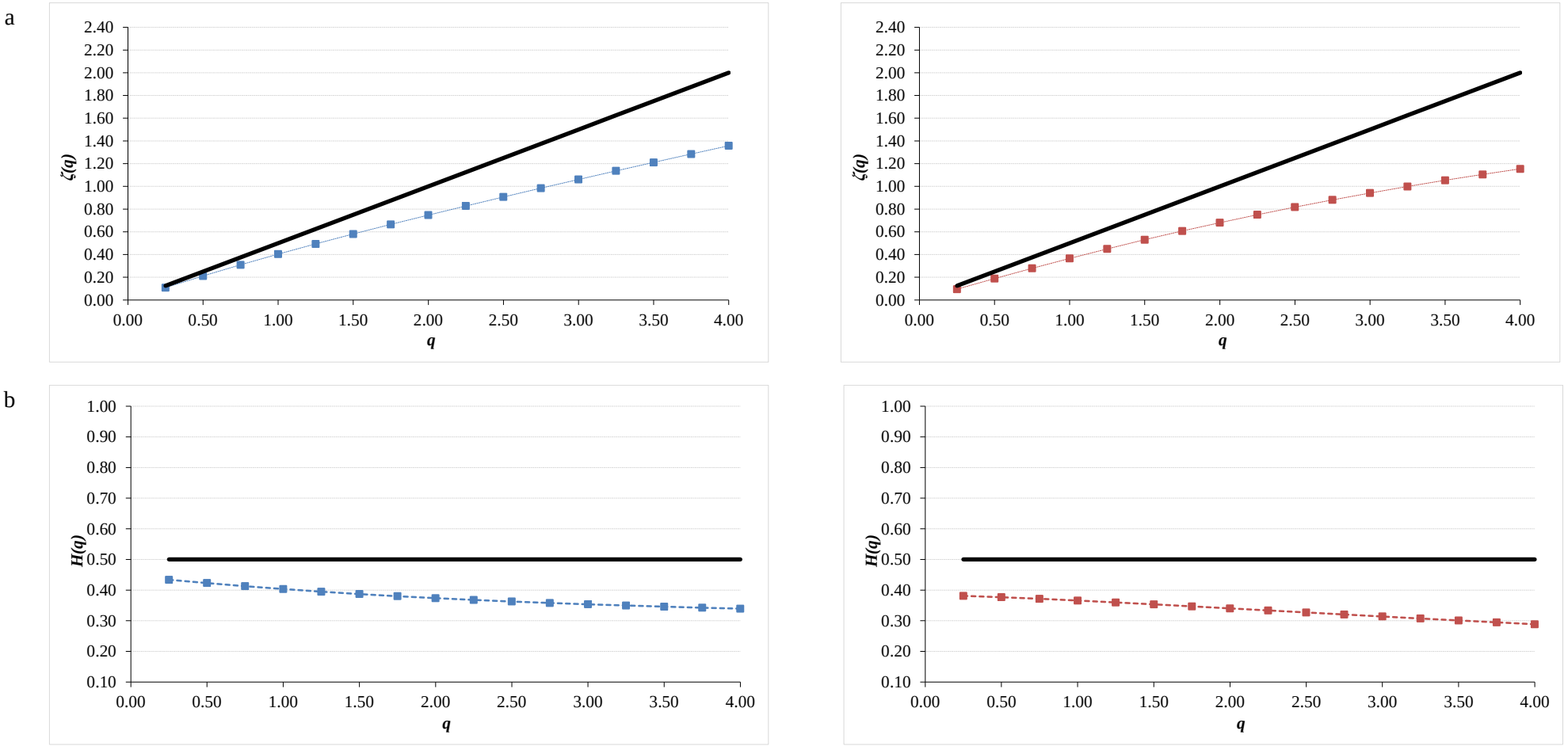

Figure 36. Generalized Structure Function plots for NDVI anomaly series of SOM5 (left column in blue) and SOM15 (right column in red) for: (a) ζ(q) curve and (b) Generalized Hurst exponent H(q), continuous line correspond to non-correlated noise with Hurst value of 0.5.

3.3.5 Agroclimatic zone and NDVI patterns

NDVI series in this case covers two reflectance surfaces, bare soil from inter-crop period (i.e., fallow) and cereal crop season. From the first one, is clearly defined and is the date on which bare soil is completely exposed to the atmosphere is after tillage operations. On these dates, analysis of variance indicates that the SOM5 and SOM15 units are spectrally different. This situation is probably true due to topsoil soil property differences (textural, physical, and chemical) and can be supported by the SOM soil unit algorithm data. From Table 2, which lists the topsoil properties of SOM5 and SOM15, the clay and sand contents are the main properties that vary between the soil units. There is an agreement between low clay content and high reflectance values. Similar findings were reported using Landsat sensors by (Demattê et al., 2009), who stated the usefulness of band data to quantify topsoil attributes related to a previous soil classification, such as clay content.

However, the previous soil moisture condition is essential and influences the soil reflectance of each band (Kaleita et al., 2005; Lobell and Asner, 2002). Furthermore, reflectance differences are also observed between the years. This result can be compared by analysing the subbasin precipitation regime (see Figure 31). From this, we can suggest that reflectance is not only different between soil units but also important, bearing in mind that previous soil moisture conditions influence reflectance in soils. This was described in the early 2000s by (Muller and Décamps, 2001). Nevertheless, the least significant difference (LSD) plots of Figure 29 consider the soil moisture state under the two situations, both with dry soil and wet soil years. The reflectance of dry soil is frequently higher than that of wet soils (Mzuku et al., 2015; Weidong et al., 2002), and in this case, SOM15 site is drier than SOM5. This is because some moisture is needed for tillage, and in SOM5, most of the previous days were rainy days. This situation suggests that bare soil reflectance can also be different due to a combination of soil properties and the soil moisture content. However, the mean difference in the LSD plots of bands over a 20-year period with diverse previous conditions of soil moisture remains different. The reflectance differences are also corroborated by comparing the BSL from each site, in which the slopes are also different (Figure 30). The slope in SOM5 is higher than that in SOM15.

In this sense, the SOM5 unit and SOM15 exhibit two fundamental elements of differentiation from the classical statistics of bare soil reflectance. The first one is related to the intrinsic physical soil properties attributable to each soil unit of the classification. The second is related to the weather regime, specifically accentuated on the soil wetting behaviour of precipitation.

Soil saturation can be reached several times when precipitation rates exceed infiltration rates in the case of SOM5, also because spring storms exceeded 50 mm/month for all years except 2002, 2005, 2011, 2015 and 2019 (Rivas-Tabares et al., 2019b). This situation can be an effect of soil

affecting the maximum value of NDVI over the growing season of cereals in SOM5. However, in areas in which the vegetation response is highly influenced by rainfall, the variations in NDVI can also be attributed to other agronomic management practices of crops (e.g., trends towards earlier sowing, nitrogen fertilizer rates, or semi-dwarf varieties with high early vigour, etc.) as reported in wheat fields with Mediterranean environments (Smith et al., 1995). In the area, barley and wheat varieties are quite similar year by year (Llera, David A. Nafría et al., 2013), and only timing management (i.e., 1 – 2 weeks lag) is the main source of variability and is related to crop timing.

For the reflectance during crop season, the NDVI averages from SOM5 and SOM15 are significantly different as shown in Table 14. These results suggest that the NDVI signal is also different between the zones, suggesting that soils and weather conditions are motivating the spectral variability of sites. The NDVI pattern differences of SOM5 and SOM 15 are due to a mixture of biophysical processes over time and space. The spatial domain is mostly related to soil properties, and the timing domain is related to the atmospheric interaction of the soil-crop, mainly in relation to rainfall. SOM5 is a soil with higher clay content and is exposed to higher rainfall rates during the spring, and SOM15 is more like a sandy soil and exhibits a drier spring than that of SOM5. However, SOM15 reaches maximum values of NDVI during the growing season of cereals between April and May, depending on intra- and inter-annual variability. Similar results were found in the NDVI series comparing different vegetation covers at the regional scale (Martínez and Gilabert, 2009).

The different slopes obtained from the regression of accumulated NDVI against accumulated precipitation (Precp), shown in Figure 32, confirm the differences in the vegetation response to both agroclimatic conditions. The slope can be interpreting as how much ΔNDVI is achieved per ΔPrecp. Higher slope implies that for a certain ΔPrecp the ΔNDVI will be higher. In this sense, SOM15, with sandy soils, obtain a higher ΔNDVI than SOM5, with clay soils, for each ΔPrecp. In summary, there is a linear relationship between the accumulated NDVI with respect to accumulated precipitation, and the slope of this relation could be related to soil characteristics as the temperature in both sites is very similar. This higher correlation between NDVI and accumulated precipitation can be found in other works on Mediterranean zones (Al-Bakri and Suleiman, 2004).

On the other hand, high precipitation during the growing season, in combination with clay soils of SOM5 can advance crop development during the first months. By the end of the growing season, in SOM15, with less accumulated precipitation, accumulated NDVI reach similar values to SOM5 once that a total rainfall of 250 mm is accumulated. Despite accumulative NDVI is similar in both cases, the growth is altered by water availability and soil characteristics.

3.4 Participatory Land Use Land Cover modelling

To assess LULC scenarios into quantitative maps, two main products were developed: the mapping template, for spatial location of the changes to create LU maps, and the crop rotation template, that allows extracting and completing crop cycles and its management across different crop sequences.

3.4.1 LULC scenarios

The interpretation of crop rotation maps from ITACyL, form a group up to 7.000 different rotational crop sequences considering individual parcels (series not showed). However, the sequence was reduced by identifying recurrent patterns in 5 years cycle basis. The crop rotation types (1-6) were defined based on remote sensing identification and grouping by major frequencies and area representativeness, see Figure 37. Each pattern represents the most common cropland rotation system in case study.

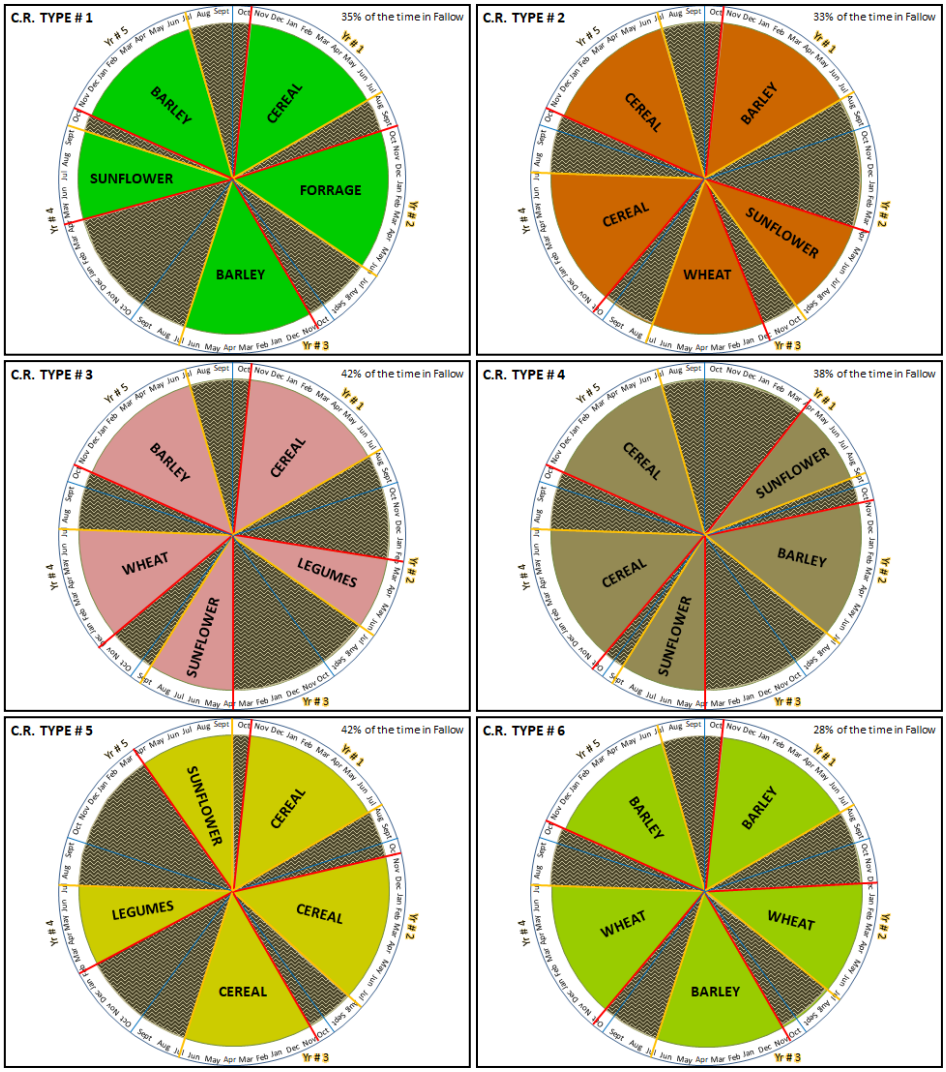

Figure 37. The six cropland rotation patterns (C.R. TYPE #) identified from remote sensing in subbasin 443, "Arroyo de la Balisa". The sowing dates are in red lines, the harvest dates in yellow line and the hydrologic year bounds in blue lines.

The LULC scenarios from stakeholder mapping activity of the LU distribution are showed in Figure 38. However, it represents a general overview of the LU and the final land dynamics include also the land management of cropping patterns at HRU level. The agricultural land is the more dynamic LU for the analysis period and most of the variations are attributable to this LU. The rainfed agricultural land is the major change across the scenarios followed by grassland. Another change is the lightly increase of irrigated agriculture in LBA scenario. Due to the expansion of irrigation schemes in the basin, some plots are from the moment planned to be irrigated in the area following the River Basin Management Plan (RBMP). Urban and forest land covers were mainly accorded from stakeholders as constant LU in the three scenarios for this sub-basin. It's also important to note that fallow as LU in baseline scenario represent a bigger area (7.94%) respect to LSH (0.24%), LBA (0.24%) and LSP (0.24%).

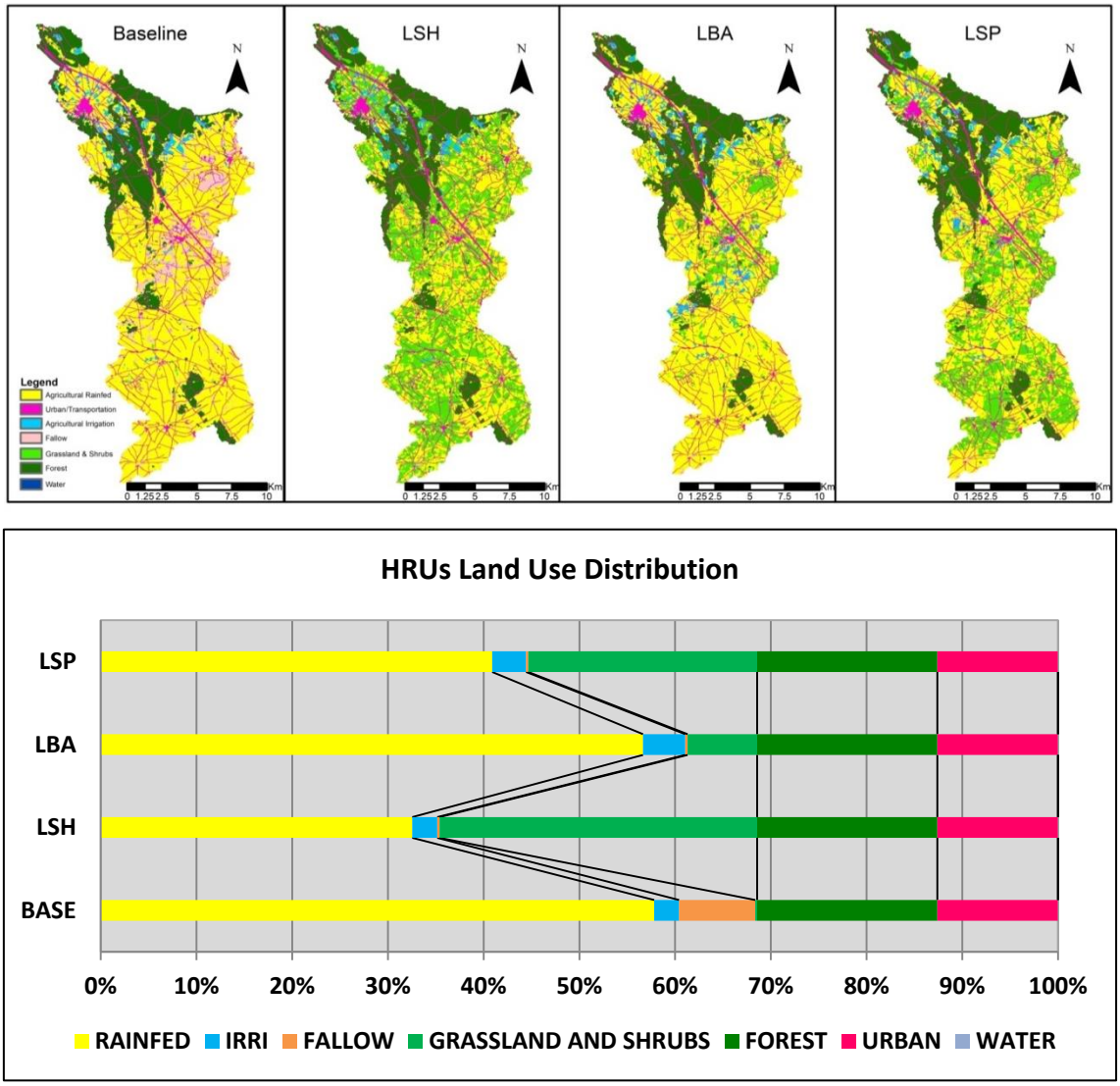

Figure 38. Land use distribution for the scenarios land sharing (LSH), land balance (LBA) and land sparing (LSP) in comparison to Baseline scenario (BASE) for the subbasin studied ("*Arroyo de la Balisa* - AdlB").

The fallow practice in rainfed productive systems, in central Spain, is a common and important practice of actual cereal scheme (Alonso, 1980; Moret et al., 2006). This practice was considered in this study only as an intermediate practice during yearly crop rotation scheme. Regularly, the fallow is also considered as a yearly or two-years practice in the rotational schemes. However, stakeholders' perception was directed to reduce it using crop rotation strategies to compensate the nutrient cycling and soil properties recovery. The yearly fallow suppresion in management schedulling tries to respond to a very common questioning for different stakeholders. There are three main reasons: (a) low area representativeness from the total area, (b) in Duero's middlands responds especially to a farmer decision (schedulling, soil fertility and water storage, market behavious of rainfed products and machinery disposal) and (c) cereal under monocrop situation as a historical extensive practice.

The crop rotation dynamics over the 16 HRUs represents the active and variable fact across the scenario assessment. The sequences were assigned in order to preserve the actual pattern plus the adjustment of workshop translation to storylines. The resulting crop rotation sequence for the 16 HRUs of each LU scenario are showed in Figure 39. The major LU change sequence dynamics from Figure 39 is evidenced in LSH scenario, where 8 HRUs are fixed with grassland cover for all years of the simulation period. In LSP, monocrop sequences are fixed in six HRUs including 4 grassland HRUs. There are some HRUs for irrigation crop, three in the LBA scenario and one in LSP, in both cases depicted to horticulture. Once the grassland and the irrigated horticulture were included in the crop rotation schema, they maintain the static condition across the scenarios.

In the context of future land scenarios in the Mediterranean, the agriculture is also facing to most of the global changes, where desertification risk is a major concern with a significant part of the territories with a highly/very highly susceptibility to landscape degradation. For example, Spain is accounting to 240,000 km^2 risked area (49% of the territory) and Portugal to 24,000 km^2 (28%) (Prăvălie et al., 2017). Semi-arid conditions and rainfall variability are common climate drivers for Spanish and Portuguese farmers, who are forced to convert the traditional rainfed agriculture to a more productive agro-system (Castro and Castro, 2019), by improving the water use efficiency (Ortega et al., 2005), by introducing high-value crops varieties (Kropff et al., 2001; García Morillo et al., 2015) or by managing multifunctional pastures (Teixeira et al., 2014). However, this situation is intensifying the impacts (more production in less land, more water and inputs required), the abandonment of marginal land in extensive rainfed areas (García-Ruiz, 2010), causing a landscape effect in the reallocation of agriculture and a shift from traditional rainfed crops to intensive irrigated agriculture (Fornés et al., 2005; Pinilla, 2006). The evolution of the current socio-ecological system, on the one hand is trending towards to the greening-up and in the other towards land degradation, each with enormous consequences for the environment (van Leeuwen et al., 2019).

BASELINE

HRU	2004_2005*	2005_2006*	2006_2007*	2007_2008*	2008_2009*	2009_2010*	2010_2011*	2011_2012*	2012_2013*	2013_2014*
1	AGRC	PEAS	SUNF	WWHT	BARL	AGRC	PEAS	SUNF	WWHT	BARL
2	BARL	SUNF	WWHT	AGRC	AGRC	BARL	SUNF	WWHT	AGRC	AGRC
3	HAY	BARL	BARL	SUNF	BARL	HAY	BARL	BARL	SUNF	BARL
4	SUNF	BARL	SUNF	WWHT	BARL	SUNF	BARL	SUNF	WWHT	BARL
5	WWHT	BARL	AGRC	PEAS	BARL	WWHT	BARL	AGRC	PEAS	BARL
6	AGRC	PEAS	SUNF	WWHT	BARL	AGRC	PEAS	SUNF	WWHT	BARL
7	BARL	SUNF	WWHT	BARL	BARL	BARL	SUNF	WWHT	BARL	BARL
8	SUNF	BARL	WWHT	SUNF	BARL	SUNF	BARL	WWHT	SUNF	BARL
9	WWHT	BARL	BARL	WWHT	SUNF	WWHT	BARL	BARL	WWHT	SUNF
10	BARL	AGRC	SUNF	WWHT	PEAS	BARL	AGRC	SUNF	WWHT	PEAS
11	WWHT	BARL	BARL	SUNF	BARL	WWHT	BARL	BARL	SUNF	BARL
12	BARL	WWHT	BARL	BARL	WWHT	BARL	WWHT	BARL	BARL	WWHT
13	WWHT	WWHT	SUNF	WWHT	BARL	WWHT	WWHT	SUNF	WWHT	BARL
14	BARL	BARL	AGRC	PEAS	SUNF	BARL	BARL	AGRC	PEAS	SUNF
15	WWHT	AGRC	PEAS	WWHT	SUNF	WWHT	AGRC	PEAS	WWHT	SUNF
16	BARL	HAY	BARL	AGRC	SUNF	BARL	HAY	BARL	AGRC	SUNF

LAND SHARING (LSH)

HRU	2004_2005*	2005_2006*	2006_2007*	2007_2008*	2008_2009*	2009_2010*	2010_2011*	2011_2012*	2012_2013*	2013_2014*
1	BARL	SUNF	WWHT	AGRC	AGRC	BARL	SUNF	WWHT	AGRC	AGRC
2	WWHT	BARL	AGRC	PEAS	BARL	WWHT	BARL	AGRC	PEAS	BARL
3	RNGE	RNGE	RNGE	RNGE	RNGE	RNGE	RNGE	RNGE	RNGE	RNGE
4	RNGE	RNGE	RNGE	RNGE	RNGE	RNGE	RNGE	RNGE	RNGE	RNGE
5	RNGE	RNGE	RNGE	RNGE	RNGE	RNGE	RNGE	RNGE	RNGE	RNGE
6	RNGE	RNGE	RNGE	RNGE	RNGE	RNGE	RNGE	RNGE	RNGE	RNGE
7	RNGE	RNGE	RNGE	RNGE	RNGE	RNGE	RNGE	RNGE	RNGE	RNGE
8	RNGE	RNGE	RNGE	RNGE	RNGE	RNGE	RNGE	RNGE	RNGE	RNGE
9	RNGE	RNGE	RNGE	RNGE	RNGE	RNGE	RNGE	RNGE	RNGE	RNGE
10	AGRC	PEAS	SUNF	WWHT	BARL	AGRC	PEAS	SUNF	WWHT	BARL
11	RNGE	RNGE	RNGE	RNGE	RNGE	RNGE	RNGE	RNGE	RNGE	RNGE
12	BARL	WWHT	BARL	BARL	WWHT	BARL	WWHT	BARL	BARL	WWHT
13	WWHT	WWHT	SUNF	WWHT	BARL	WWHT	WWHT	SUNF	WWHT	BARL
14	BARL	BARL	AGRC	PEAS	SUNF	BARL	BARL	AGRC	PEAS	SUNF
15	WWHT	AGRC	PEAS	WWHT	SUNF	WWHT	AGRC	PEAS	WWHT	SUNF
16	BARL	HAY	BARL	AGRC	SUNF	BARL	HAY	BARL	AGRC	SUNF

LAND BALANCE (LBA)

HRU	2004_2005*	2005_2006*	2006_2007*	2007_2008*	2008_2009*	2009_2010*	2010_2011*	2011_2012*	2012_2013*	2013_2014*
1	BARL	SUNF	WWHT	AGRC	AGRC	BARL	SUNF	WWHT	AGRC	AGRC
2	HAY	BARL	BARL	SUNF	BARL	HAY	BARL	BARL	SUNF	BARL
3	WWHT	BARL	BARL	WWHT	SUNF	WWHT	BARL	BARL	WWHT	SUNF
4	BARL	SUNF	WWHT	BARL	BARL	BARL	SUNF	WWHT	BARL	BARL
5	WWHT	BARL	BARL	WWHT	SUNF	WWHT	BARL	BARL	WWHT	SUNF
6	BARL	SUNF	WWHT	BARL	BARL	BARL	SUNF	WWHT	BARL	BARL
7	HORT	HORT	HORT	HORT	HORT	HORT	HORT	HORT	HORT	HORT
8	BARL	SUNF	WWHT	BARL	BARL	BARL	SUNF	WWHT	BARL	BARL
9	WWHI	BARI	BARI	WWHI	BARI	WWHI	BARI	BARI	WWHI	BARI
10	SUNF	BARL	WWHT	SUNF	BARL	SUNF	BARL	WWHT	SUNF	BARL
11	SUNF	BARL	WWHT	SUNF	BARL	SUNF	BARL	WWHT	SUNF	BARL
12	BARL	WWHT	BARL	BARL	WWHT	BARL	WWHT	BARL	BARL	WWHT
13	WWHT	WWHT	SUNF	WWHT	BARL	WWHT	WWHT	SUNF	WWHT	BARL
14	BARL	BARL	AGRC	PEAS	SUNF	BARL	BARL	AGRC	PEAS	SUNF
15	WWHT	AGRC	PEAS	WWHT	SUNF	WWHT	AGRC	PEAS	WWHT	SUNF
16	BARL	HAY	BARL	AGRC	SUNF	BARL	HAY	BARL	AGRC	SUNF

LAND SPARING (LSP)

HRU	2004_2005*	2005_2006*	2006_2007*	2007_2008*	2008_2009*	2009_2010*	2010_2011*	2011_2012*	2012_2013*	2013_2014*
1	RNGE	RNGE	RNGE	RNGE	RNGE	RNGE	RNGE	RNGE	RNGE	RNGE
2	RNGE	RNGE	RNGE	RNGE	RNGE	RNGE	RNGE	RNGE	RNGE	RNGE
3	BARL	SUNF	WWHT	BARL	BARL	BARL	SUNF	WWHT	BARL	BARL
4	RNGE	RNGE	RNGE	RNGE	RNGE	RNGE	RNGE	RNGE	RNGE	RNGE
5	BARL	SUNF	WWHT	BARL	BARL	BARL	SUNF	WWHT	BARL	BARL
6	BARL	SUNF	WWHT	BARL	BARL	BARL	SUNF	WWHT	BARL	BARL
7	BARL	SUNF	WWHT	BARL	BARL	BARL	SUNF	WWHT	BARL	BARL
8	BARL	SUNF	WWHT	BARL	BARL	BARL	SUNF	WWHT	BARL	BARL
9	HORT	HORT	HORT	HORT	HORT	HORT	HORT	HORT	HORT	HORT
10	SUNF	BARL	WWHT	SUNF	BARL	SUNF	BARL	WWHT	SUNF	BARL
11	RNGE	RNGE	RNGE	RNGE	RNGE	RNGE	RNGE	RNGE	RNGE	RNGE
12	BARL	WWHT	BARL	BARL	WWHT	BARL	WWHT	BARL	BARL	WWHT
13	WWHT	WWHT	SUNF	WWHT	BARL	WWHT	WWHT	SUNF	WWHT	BARL
14	BARL	BARL	AGRC	PEAS	SUNF	BARL	BARL	AGRC	PEAS	SUNF
15	WWHT	AGRC	PEAS	WWHT	SUNF	WWHT	AGRC	PEAS	WWHT	SUNF
16	BARL	HAY	BARL	AGRC	SUNF	BARL	HAY	BARL	AGRC	SUNF

Figure 39. Template for the main crop rotation patterns in Sub-basin 443, "*Arroyo de la Balisa* - AdlB", for the baseline and the three scenarios**.**

3.4.2 Water balance simulations

The central fact, related to hydrologic modelling, is the variation of the main water balance components respect to the reference model, the baseline scenario, Figure 40. The variation of water balance components showed in mm yr^{-1} represents small values Table 17. However, interpreting these variations based on the hydrological year cycle, in the context of Mediterranean basins, makes the monthly volumes variations very important for the environment provision and regulation as water scarcity is a key factor (Figure 40). The variation of the ET across the scenarios is the most relevant change, Figure 41. This is directly related to the LULC distribution, crop management and the main hydrologic effects are related to the stream flow out and the deep aquifer recharge during the spring-summer period. The ET during the period (March-July) presents a higher variability respect to baseline, highlighting a lower ET of LSH during April and May (Figure 41).

Table 17. Variation of water balance components across the scenarios respect to baseline in mm/yr.

Scenario	Precipitation [mm/yr]	Evapotranspiration [mm/yr]	Flow Out [mm/yr]	Soil Water Storage [mm/yr]	DA recharge [mm/yr]
Baseline	435.6	341.2	70.39	20.40	3.61
LSH	435.6	340.1	71.48	20.35	3.67
LBA	435.6	342.3	70.03	19.68	3.59
LSP	435.6	341.3	70.87	19.79	3.64

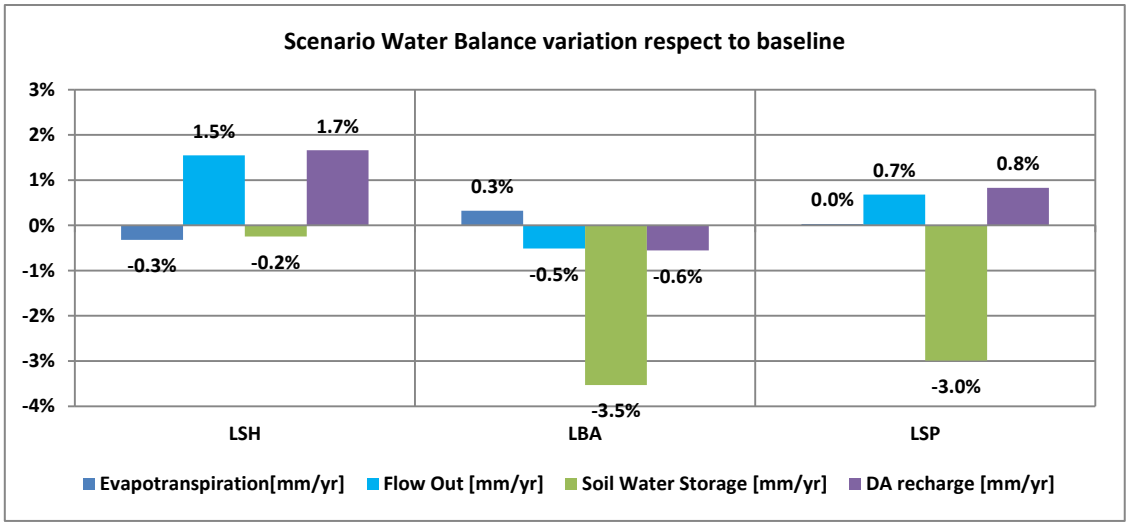

Figure 40. Water balance components variations of the three land use scenarios (LBA: land balance, LSH; land sharing and LSP; land sparing) in comparison to baseline scenario. Calculation based on 10-years average.

Figure 41. Box plots of the main water balance components across the three LULC scenarios: Land sharing (LSH), Land Sparing (LSP) and Land Balance (LBA). Calculation based on 10-years average.

In the case of LSH, a slightly diminution of ET (-0.3%) is compensated into an augmentation of flow out (1.5%) of the sub-basin and depth aquifer recharge (1.7%), annually showed in Figure 39. However, the ET during June and July in LSH is higher than the other scenarios due to grassland coverage but despite this the stream flow out (median and Q3) is a little bit higher as similar in lateral flow because stream flow is composed by surface run off, lateral flow and

groundwater contribution. This is partly explained due to a diminution of the fallow land area (-7.7%) and pastures increase of 33% in LSH, 23.7% in LSP and, 7.1% in LBA with respect to baseline. This suggests, that the increase of ET's in the scenarios respect to baseline's is a key fact and, the reduction of ET in LSH turns into beneficial management for surface and groundwater bodies' protection by increasing its flows. Similar finding related to soil-vegetation in Mediterranean ephemeral small basins were described in Italy under climate change scenarios (Pumo et al., 2016).

However, the ET diminution is not only responsible for water bodies' augmentation in LSH scenario. The soil is a determining factor for watershed regulation in Mediterranean basins and constitutes the place in which the water components change the water cycle direction and make it sensitive and variable. A diminution of soil moisture is revealed in this sub-basin as a very important source for water regulation (-3.5% in LBA and – 3.0% in LSP) due to soil characteristics, Figure 39. Despite, the soils moisture is favored in fallow land, the water retention in sandy soils is very low, for this reason the aquifer recharge was increased (+1.7% in LSH) and the lateral flow contributes to stream flow increasing in 1.5% the watershed flow out. A similar finding of this process was reported for Duero's basin (Morán-Tejeda et al., 2011). In contrast, the LBA scenario is showed as closer as baseline, highlighting that this scenario made the situation worse in terms of deep aquifer recharge especially during the summer flows. The ET in LBA was higher than baseline in March and April and very closer to baseline during the late spring and summer. This suggests that LBA strategy is worse than baseline for the water bodies' regulation (surface and groundwater) in late spring and during the summer, the critical period of hydric stress.

In the other hand, a small increase of the ET in LSP result of 3.0% diminution of soil water storage while an augmentation of 0.3% of ET in LBA is traduce in -3.5% of soil water storage (Figure 40). However, while in LSP the deep aquifer recharge was augmented in 0.8% in LBA was -0.6%. As it's confirmed the relation between ET and land cover, it's important to note the importance of LULC in which a reduction of 7.7% of unseeded fallow area and an increase of pastures area (+33% in LSH, 23.7% in LSP and +7.1% in LBA) with respect to baseline, affect the water bodies flows. Despite the diminution of fallow land in LSH scenario and pastures augmentation, it shows hydrological benefits for the watershed in terms of water bodies protection. Although water quantity regulation is very important in semi-arid watersheds, the water quality and sediments assessment is needed to optimize the scenarios.

The unseeded fallow, as yearly practice in Mediterranean basins, is very important as part of rainfed cropping system because this practice allowing the ET reduction (i.e. plant transpiration) favoring the water storage through the soil profile and nutrient mineralization (Lacasta, 1995;

Gómez De Barreda Ferraz, 2011). Similar findings were detected in semi-arid conditions in central Chaco Paraguay (Cáceres and Ratzlaff, 2013) but highlighting that it also depends on the soils and tillage types. Other works also emphasize in the high variability of the monthly soil moisture in comparison to single year water balance in Duero's watersheds (Vicente Gonzalez et al., 2016). Also, the latter, pointing up the relationship of soil moisture with ET from different LU's in water regulation, treating the ET separately from rainfed crops and ET from natural covers (i.e. pastures and forest). In contrast, the unseeded fallow land in central Spain is subjected to an intensive tillage, four tillage operations: 1st plow (after harvest), 2nd plow (fall)", 3rd plow (winter) and rotary hoe for weeds suppression (summer), all of them associated with erosion processes (De Alba et al., 1999; Boellstorff and Benito, 2005) and water quality problems (Alba et al., 2011; Nadal-Romero et al., 2019), risking the semi-arid ecosystems in central Spain. For this reason, we suggest that for further research the fallow yearly practice must be lightly reduced but included as a strategy for rainfed crop rotation scheme in Mediterranean ephemeral streams.

4 Conclusions

4.1 General and specific conclusions

This research present join novel improvements to hydrological modelling, tying up input data treatment, spatiotemporal vegetation dynamics, and human-induced land use/cover scenarios to get accurate values for water balance components in semiarid watersheds. These elements have been shown as very sensitive in hydrological modelling with the SWAT model; its treatment contributes to addressing water demands issues from an integrated schema for water resources management bi-directionally, this is from first-order basins to subbasin scales and from HRUs to agroclimatic zones. Thus the detailed knowledge of water interaction between managed and natural systems contributes to protecting water bodies sustainably for future decision-making. Specifically, this work highlights the sensitivity of soils data, land use/cover temporal dynamics, temporal water demand of vegetation, in hydrology modelling. Every simplification in the input data of hydrology modelling affects systems interaction representation, for this reason when the hydrology model represents these interactions at finer scales, the model can provide results allowing improvement in territorial water demand trade-offs. The most relevant contributions and outputs of this work are outlined as follows.

4.1.1 On the value of soil data treatment in hydrology modelling

The hydrological effect using different soil data sources confirms that spatial resolution is essential for subbasin and HRU aggregation definition during SWAT model Set-Up. Although the hydrological behavior of the basin is stable, important variations at the level of sub-basins and HRUs were identified. Flow out series show that accuracy during peak events are the challenge focus during calibration/validation process using the different soil data sets. SWAT set-up is an essential stage in which scale and quality data play an important role regarding the multi-objective assessment of the hydrologic cycle processes.

The SOM strategy and high-quality data for model parameterization could be a valuable tool to improve hydrological model calibration and validation processes in sub-arid areas, this study presents a significant improvement in the overall process of calibration-validation of SWAT model.

One of the most sensitive model parameters, related to soil variables, is soil depth which is essential for water fluxes and soil water content. The estimation of soil depth for each HRU impacts on water balance components, specially related with aquifer recharge volumes in sub-arid watershed, as Adaja River in Spain.

4.1.2 On the importance of including vegetation dynamics for the understanding of coupled processes in hydrological modelling

The inclusion of vegetation dynamics reinforces the idea that the knowledge of soil properties and climate spatial variability is a key component in understanding patterns of vegetation at large scales. The conclusions of this study are as follows:

- Data from Earth observation, in this case, the MODIS satellite, through the soil reflectance differences validated the soil units from a digital soil mapping approach with the self-organizing map (SOM) algorithm. The main differences between the two areas are related to the soil physical properties and the precipitation regime.
- NDVI statistics show a significant difference between the two areas that mainly differ in soil physical properties and the precipitation regime.
- NDVI series under rainfed monoculture activity in the semiarid climate in Spain exhibits a persistent structure and a clear multiscaling nature.
- NDVI residual and anomalies series analysis under rainfed monoculture activity in the semiarid climate in Spain exhibits an anti-persistent structure and a weaker multiscaling nature.

4.1.3 An accurate evaluation of water availability in a sub-arid Mediterranean watershed

CEA, as part of Mediterranean sub-arid catchments with low precipitation rates and accentuated water scarcity during summer, is a fragile ecosystem and some measures are needed to mitigate water resources overexploitation, as commented by other authors (Ricci et al., 2018).

This study shows the ability of SWAT to simulate many complex processes as well as the importance of including detailed land use information to achieve satisfactory model performance. The model can be used to guide water management decisions by stakeholders who have water provision targets to meet, especially in the assigning of more realistic agricultural water demands. Setup improvements assessed through global statistic indices confirm this. Land use and soils are the most important data for the HRUs definition step; any effort to achieve more accurate data and maps will reduce the model uncertainty. The model in a daily time step has closely simulated the observation streamflow. However, calibration of the SWAT model with very low flows is still under study, as intermittent zero flows occurred during simulations with low flows and observation values kept measures under 0.1 m^3/s.

Flow regulation and infrastructure, such as reservoirs and artificial aquifer recharge, were made to respond to the agricultural demand in the CEA system. These are elements that define a stream's hydric behaviour in meagre flow watersheds such as the CEA. Any improvement to reduce agricultural water demand is a factor that directly increases availability of stream flow. Flow stream increment could be achieved by a redefinition of operating rules for reservoir

discharge and reduced volumes for artificial aquifer recharge. All measures addressing the reduction of net irrigation land, deficit irrigation strategies, and less water-demanding crops, among others, are suitable elements to mitigate drought periods with less economic impact.

The main effort to preserve water resources in the CEA under the current water deficit state (very low flows at the outlet) must be directed to soil conservation strategy, due to the importance to water transfer to vegetation and to aquifer recharge. A reduction in water consumption of crop vegetation could contribute directly to increased water availability in stream flows as lateral and return flows. The increase in vegetated covers in fallow areas during (fall-winter) period in slopes > 5% could help slow down runoff and allow an increase in infiltration time and rates. Thus, the increment of water flux to aquifer recharge could allow the lag time of subsurface flow to streams. Further analysis is needed in headwaters through the application of land use scenarios in this sense.

Finally, many applications are foreseen, such as conducting policy and impact studies, using the model for climate and LUC studies and analysing the implications of inter-sub-basin transfers, among others.

4.1.4 Land Use change through participatory scenario modelling with SWAT.

The scenario modelling provides the following conclusions:

- Participatory scenario is a very useful approach to integrate stakeholder knowledge into the development of quantitative and credible LULC, which are a fundamental input for modelling and quantifying the hydrological and water resources implications.
- The land sharing (LSH) scenario represents among the three scenarios the most likely LU strategy to favor stream flow configuration and deep aquifer recharge in this semiarid sub basin.
- LSH scenario could be used as a driver for land management of midlands on Duero's river basin to achieve environmental goals related to water volume availability.
- The fallow should be included as an important yearly practice in rainfed crop rotation schemas in Mediterranean basins. Since this choice suppose an important strategy for water balance regulation in this sub-basin. However, despite fallow suppression also fulfills strategic measure for water quality regulation, a balance about the amount of yearly fallow land is needed. The assessment, through modelling, of this effect should be coupled for water quantity and quality to analyze the overall effect.
- In Mediterranean and agricultural basins, the crop rotations schemas are very sensitive to water resources variability. The schemas and their location in basins must be rethinking and modeled to achieve the environmental goals.

4.2 Limitations and further research

4.2.1 Limitations

Hydrological modelling is a representation of very complex processes of the soil-plant-atmosphere system. However, the model itself is a simplification of these processes and to capture all involved processes is an impossible task. For this reason, modellers deal with reducing the different uncertainties sources as much as possible and thus, defining model limitations. Most of the uncertainties of the processes are related to the date in which the processes take place and its temporal availability, data quality, and its spatial and temporal scale. The SWAT model also aggregates processes at HRU level which limit the capacity to understand the process at a finer level than HRUs. Even though, the HRU definition was improved during the parameterization process, to reach a balance between finer resolutions of input data representation, simulation computational time, and calibration-validation resources using a personal computer. The complete run of SWAT model, that comprises all the HRUs, need supercomputer resources to get calculations for all possible HRUs. This means, a precision of daily time step for areas up to one hectare.

Self-organizing maps (SOM) as a method used in this work to improve the edaphological input for the SWAT model is based on the spatial availably of soil pits or soil survey data. For this reason, an increase of soil survey points can increase the performance of spatial clustering. However, the use of DB index allow to avoid get randomly results when defining the desirable number of clusters, but the inclusion of new soil data points can improve the bounds of soil units from the SOM. The SOM join to DB index provide a region of high performance for digital soil mapping of soil properties for hydrological modelling but clustering final selection also need comparison to taxonomic soil maps to corroborate that clustering from SOM follow the same bounds pattern.

Quality of precipitation data is one of the most sensitive parameters for hydrological modelling since this is in most of the cases the only water input into the model. The only exceptions are the sub-basins downstream of the reservoirs, in which the release counts as additional surface water input into the system or from basins water transfers. Using TPM for precipitation assignation per watershed also is a source of uncertainty. This approach does not consider finer gradients between rain gauges and assumes a uniform distribution of precipitation in the subbasin. The TPM provides weighted values between rain gauges overlapped with sub-basins limits. However, the use of TPM provides more accurate results in surface flow configuration in combination with the SWAT model because of the use of HRUs approach to split the sub-basins. Some bias in streamflow estimations could be attributed to several precipitation extreme events as hail or spring-summer storms in ungauged areas, but in the Mediterranean, these

events represent small volumes at the basin scale. This could be part of the system water input and usually attributable to the peak matching in extreme events. Despite this situation, the SWAT model captured the streamflow at daily time step for a long-term period with accurate series behaviour.

Land use land cover information, is also one of the most difficult but relevant information to get a reliable hydrological model. Every managed system is susceptible to change from one day to other. This especially true for agricultural areas, in which crop campaigns change larger areas in a matter of days. This is attributable to sowing dates, tillage operations, growing season, irrigation timing, and harvesting dates. Most of these dates from every parcel are almost unknown. With the aid of EO and farmers surveys, an approximate of this timing can be estimated. However, these dates are essential for flow routing in the SWAT model. For model simplification, the dates for each agrarian activity and for each crop was settled at the same time in the whole basin. This is not true in reality and this situation affect flows specially with time response of the precipitation-run off configuration process and from phonological point of view the vegetation is exposed to weather hazards in different states. Therefore, the aim of this model was not related to cropping phenology and was performed with hydrological purposes considering cropping details in a uniform way.

The inclusion of cropping sequences, approximate dates for each operation is actually a significant improvement for hydrological modelling at basin scales for long-term period as present in this work. Most of the models used to evaluate water demands at basin scales do not uses crop sequences, and do not consider crop operations neither fixing dates for operations. Actually, the models used to evaluate water resources allocation are based on mass transfer optimization routines, fixing most of the principal processes as evapotranspiration, uniform soil hydraulic properties, unique land use maps or vegetation cover over simulation period. All of these do not represent accurately the complexity of the soil-plant-atmosphere system interaction of a watershed. However, models as SWAT are present as a technical complement for these management models. The limitation for SWAT model implementation for its massive usage for basin water resources management and planning is data availability, limited computational resources and technicians training.

There are also some limitations regarding EO data. The pixel size of the product, revisit period, and atmospheric noise are part of the main concerns of uncertainty for vegetation dynamic analysis. Despite this, the analysis of long-term series evidences the strong relation between weather conditions and vegetation. This is especially true for rainfed crops and for natural vegetation in Mediterranean area. This relation is important since rained agriculture and

hydrology dynamics in Mediterranean zone is very sensitive to weather dynamics face to climate change scenarios.

4.2.2 Further research

- The improvement of operation scheduling. This can be possible integrating the tool SWATFarmR to scheduling of management operations based on climate data and operation schedules for the specific land uses in a SWAT model.

- Calibrate and validate a SWAT model of the CEA system with all possible HRUs using super computer resources.

- Adopted criteria guideline to facilitate multi-variable and multi-site calibration and validation of the SWAT model in Mediterranean zone.

- Improve the analysis to calibrate and validate ephemeral streams in Mediterranean zone.

- Use the EO data to train a SOM soil map for hydrological purposed coupled to taxonomic soil unit approach, including diverse soil depth models.

- Create soil properties scenarios for hydrological modelling of agrarian watersheds in the Mediterranean zone.

- Include annual fallow as a valuable practice in crop rainfed sequences to optimize stream flows trade-off in river basin management and planning.

- Include water quality calibration and validation in a SWAT model of the CEA system.

- Integrate data from CAP Spanish system can provide valuable data to monitor crop growth and evaluate crop yields also with the SWAT model. An economic valuation of agrarian productivity could be performed.

- The CEA system offer a diversity of managed systems that represent traditional, moderate and advanced managed systems of Iberian Peninsula and serve as an example for multiple agrarian and environmental studies.

5 References

Aalders, I.H., Aitkenhead, M.J., 2006. Agricultural census data and land use modelling. Comput. Environ. Urban Syst. 30, 799–814. https://doi.org/https://doi.org/10.1016/j.compenvurbsys.2005.06.003

Abbaspour, K.C., 2013. SWAT-CUP 2012: SWAT calibration and uncertainty programs–a user manual. Eawag Dübendorf, Switz. 103.

Abbaspour, K.C., 2011. Swat-Cup2: SWAT Calibration and Uncertainty Programs Manual Version 2, Department of Systems Analysis, Integrated Assessment and Modelling (SIAM).

Abbaspour, K.C., Johnson, C.A., van Genuchten, M.T., 2004. Estimating Uncertain Flow and Transport Parameters Using a Sequential Uncertainty Fitting Procedure. Vadose Zo. J. 3, 1340–1352.

Abbaspour, K.C., Rouholahnejad, E., Vaghefi, S., Srinivasan, R., Yang, H., Kløve, B., 2015. A continental-scale hydrology and water quality model for Europe: Calibration and uncertainty of a high-resolution large-scale SWAT model. J. Hydrol. 524, 733–752. https://doi.org/https://doi.org/10.1016/j.jhydrol.2015.03.027

Acevedo, M.F., Baird Callicott, J., Monticino, M., Lyons, D., Palomino, J., Rosales, J., Delgado, L., Ablan, M., Davila, J., Tonella, G., Ramírez, H., Vilanova, E., 2008. Models of natural and human dynamics in forest landscapes: Cross-site and cross-cultural synthesis. Geoforum 39, 846–866. https://doi.org/https://doi.org/10.1016/j.geoforum.2006.10.008

AEMET, 2013. Daily precipitation, maximum temperature and minimum temperature. period 2000-2015.

Al-Bakri, J.T., Suleiman, A.S., 2004. NDVI response to rainfall in different ecological zones in Jordan. Int. J. Remote Sens. 25, 3897–3912.

Alba, S. de, Alcázar Torralba, M., Cermeño Martín, F., Barbero Abolafio, F., 2011. Erosión y manejo del suelo. Importancia del laboreo ante los procesos erosivos naturales y antrópicos.

Alonso, A.C., 1980. El barbecho en los secanos españoles. Finisterra 15.

Alonso, C., Tarquis, A.M., Zúñiga, I., Benito, R.M., 2017. Spatial and radiometric

characterization of multi-spectrum satellite images through multi-fractal analysis. Nonlin. Process. Geophys. 24, 141–155. https://doi.org/10.5194/npg-24-141-2017

Aouissi, J., Benabdallah, S., Chabaâne, Z.L., Cudennec, C., 2013. Sensitivity analysis of SWAT model to the spatial rainfall distribution and watershed subdivision in streamflow simulations in the Mediterranean context: A case study in the Joumine watershed. Tunisia, in: 2013 5th International Conference on Modeling, Simulation and Applied Optimization (ICMSAO). pp. 1–6. https://doi.org/10.1109/ICMSAO.2013.6552706

Aouissi, J., Benabdallah, S., Lili Chabaâne, Z., Cudennec, C., 2016. Evaluation of potential evapotranspiration assessment methods for hydrological modelling with SWAT—Application in data-scarce rural Tunisia. Agric. Water Manag. 174, 39–51. https://doi.org/https://doi.org/10.1016/j.agwat.2016.03.004

Arnold, J., Srinivasan, R., Muttiah, R., Williams, J., 1998. Large area hydrologic modeling and assessment - Part 1: Model development. J. Am. Water Resour. Assoc. 34, 73–89.

Arnold, J.G., Allen, P.M., Muttiah, R., Bernhardt, G., 1995. Automated Base Flow Separation and Recession Analysis Techniques. Ground Water 33, 1010–1018. https://doi.org/10.1111/j.1745-6584.1995.tb00046.x

Asa, E., 2012. Comparison of Linear and Nonlinear Kriging Methods for Characterization and Interpolation of Soil Data. J. Comput. Civ. Eng. 26, 11–19. https://doi.org/10.1061/(ASCE)CP.1943-5487.0000118

Ba, R., Song, W., Lovallo, M., Lo, S., Telesca, L., 2020. Analysis of Multifractal and Organization/Order Structure in Suomi-NPP VIIRS Normalized Difference Vegetation Index Series of Wildfire Affected and Unaffected Sites by Using the Multifractal Detrended Fluctuation Analysis and the Fisher–Shannon Analysis. Entropy 22, 415.

Bai, W., Chen, X., Tang, Y., He, Y., Zheng, Y., 2019. Temporal and spatial changes of soil moisture and its response to temperature and precipitation over the Tibetan Plateau. Hydrol. Sci. J. 64, 1370–1384.

Bangash, R.F., Passuello, A., Sanchez-Canales, M., Terrado, M., López, A., Elorza, F.J., Ziv, G., Acuña, V., Schuhmacher, M., 2013. Ecosystem services in Mediterranean river basin: Climate change impact on water provisioning and erosion control. Sci. Total Environ. 458–460, 246–255. https://doi.org/https://doi.org/10.1016/j.scitotenv.2013.04.025

Baret, F., Jacquemoud, S., Hanocq, J.F., 1993. The soil line concept in remote sensing. Remote Sens. Rev. 7, 65–82.

Baveye, P.C., Laba, M., 2015. Moving away from the geostatistical lamppost: Why, where, and how does the spatial heterogeneity of soils matter? Ecol. Modell. 298, 24–38. https://doi.org/https://doi.org/10.1016/j.ecolmodel.2014.03.018

Begou, J., Jomaa, S., Benabdallah, S., Bazie, P., Afouda, A., Rode, M., 2016. Multi-Site Validation of the SWAT Model on the Bani Catchment: Model Performance and Predictive Uncertainty. Water 8, 178. https://doi.org/10.3390/w8050178

Benedini, M., Tsakiris, G., 2013. Model Calibration and Verification BT - Water Quality Modelling for Rivers and Streams, in: Benedini, M., Tsakiris, G. (Eds.), . Springer Netherlands, Dordrecht, pp. 223–229. https://doi.org/10.1007/978-94-007-5509-3_18

Bennie, A.T.P., Hensley, M., 2001. Maximizing precipitation utilization in dryland agriculture in South Africa—a review. J. Hydrol. 241, 124–139.

Berbel, J., Expósito, A., Gutiérrez-Martín, C., Mateos, L., 2019. Effects of the irrigation modernization in Spain 2002–2015. Water Resour. Manag. 33, 1835–1849.

Berbel, J., Gutiérrez-Martín, C., Rodríguez-Díaz, J.A., Camacho, E., Montesinos, P., 2015. Literature review on rebound effect of water saving measures and analysis of a Spanish case study. Water Resour. Manag. 29, 663–678.

Bisantino, T., Gentile, F., Milella, P., Liuzzi, G.T., 2010. Effect of Time Scale on the Performance of Different Sediment Transport Formulas in a Semiarid Region. J. Hydraul. Eng. 136, 56–61. https://doi.org/10.1061/(ASCE)HY.1943-7900.0000125

Boellstorff, D., Benito, G., 2005. Impacts of set-aside policy on the risk of soil erosion in central Spain. Agric. Ecosyst. Environ. 107, 231–243. https://doi.org/https://doi.org/10.1016/j.agee.2004.11.002

Booth, E.G., Qiu, J., Carpenter, S.R., Schatz, J., Chen, X., Kucharik, C.J., Loheide, S.P., Motew, M.M., Seifert, J.M., Turner, M.G., 2016. From qualitative to quantitative environmental scenarios: Translating storylines into biophysical modeling inputs at the watershed scale. Environ. Model. Softw. 85, 80–97. https://doi.org/https://doi.org/10.1016/j.envsoft.2016.08.008

Bormann, H., Breuer, L., Gräff, T., Huisman, J.A., 2007. Analysing the effects of soil properties changes associated with land use changes on the simulated water balance: A comparison of three hydrological catchment models for scenario analysis. Ecol. Modell. 209, 29–40. https://doi.org/https://doi.org/10.1016/j.ecolmodel.2007.07.004

Botey Fullat, M., 2009. La concentración parcelaria en Castilla y León : caracterización de la parcelación a través del análisis multivariante. Tesis - Universidad Politécnica de Madrid. E.T.S.I. Agrónomos, Madrid.

Brears, R.C., 2015. The circular economy and the water-food nexus. Futur. Food J. Food, Agric. Soc. 3, 53–59.

Bundy, L.G., Mallarino, A.P., Good, L.W., 2008. 12. Field-Scale Tools for Reducing Nutrient Losses to Water Resources.

Bünemann, E.K., Bongiorno, G., Bai, Z., Creamer, R.E., De Deyn, G., de Goede, R., Fleskens, L., Geissen, V., Kuyper, T.W., Mäder, P., Pulleman, M., Sukkel, W., van Groenigen, J.W., Brussaard, L., 2018. Soil quality – A critical review. Soil Biol. Biochem. 120, 105–125. https://doi.org/https://doi.org/10.1016/j.soilbio.2018.01.030

Burrough, P.A., 1983. Multiscale sources of spatial variation in soil. I. The application of fractal concepts to nested levels of soil variation. J. soil Sci. 34, 577–597.

Caballero, T.M.N., 2019. Gestión compartida de recursos hídricos entre España y Portugal: Veinte años del Convenio de Albufeira. Rev. Adm. pública 391–427.

Cáceres, S.H.R., Ratzlaff, L.D., 2013. Período de barbecho del suelo y crecimiento radicular del cártamo Carthamus tinctorius L. en función al contenido de agua en el Chaco Central. Investig. Agrar. 13, 13–18.

Calbó, J., 2010. Possible Climate Change Scenarios with Specific Reference to Mediterranean Regions BT - Water Scarcity in the Mediterranean: Perspectives Under Global Change, in: Sabater, S., Barceló, D. (Eds.), . Springer Berlin Heidelberg, Berlin, Heidelberg, pp. 1–13. https://doi.org/10.1007/698_2009_28

Canadell, J., Jackson, R.B., Ehleringer, J.B., Mooney, H.A., Sala, O.E., Schulze, E.-D., 1996. Maximum rooting depth of vegetation types at the global scale. Oecologia 108, 583–595.

Castro-Franco, M., Domenech, M., Costa, J.L., Aparicio, V.C., 2017. Modelling effective soil depth at field scale from soil sensors and geomorphometric indices. Acta Agronómica 66, 228–234.

Castro, H., Castro, P., 2019. Mediterranean Marginal Lands in Face of Climate Change: Biodiversity and Ecosystem Services, in: Climate Change-Resilient Agriculture and Agroforestry. Springer, pp. 175–187.

Charrad, M., Ghazzali, N., Boiteau, V., Niknafs, A., 2014. NbClust: An R Package for

Determining the Relevant Number of Clusters in a Data Set. J. Stat. Softw. 61, 1–36. https://doi.org/10.18637/jss.v061.i06

CHD, 2015. Plan Hidrológico de la Demarcación Hidrográfica del Duero 2015-2021.

Chen, J., Jönsson, P., Tamura, M., Gu, Z., Matsushita, B., Eklundh, L., 2004. A simple method for reconstructing a high-quality NDVI time-series data set based on the Savitzky–Golay filter. Remote Sens. Environ. 91, 332–344.

Clark, M.P., Fan, Y., Lawrence, D.M., Adam, J.C., Bolster, D., Gochis, D.J., Hooper, R.P., Kumar, M., Leung, L.R., Mackay, D.S., 2015. Improving the representation of hydrologic processes in Earth System Models. Water Resour. Res. 51, 5929–5956.

Custodio, E., Andreu-Rodes, J.M., Aragón, R., Estrela, T., Ferrer, J., García-Aróstegui, J.L., Manzano, M., Rodríguez-Hernández, L., Sahuquillo, A., del Villar, A., 2016. Groundwater intensive use and mining in south-eastern peninsular Spain: Hydrogeological, economic and social aspects. Sci. Total Environ. 559, 302–316. https://doi.org/https://doi.org/10.1016/j.scitotenv.2016.02.107

Davies, D.L., Bouldin, D.W., 1979. A cluster separation measure. IEEE Trans. Pattern Anal. Mach. Intell. 224–227.

Davis, A., Marshak, A., Wiscombe, W., Cahalan, R., 1994. Multifractal characterizations of nonstationarity and intermittency in geophysical fields: Observed, retrieved, or simulated. J. Geophys. Res. Atmos. 99, 8055–8072.

De Alba, S., Benito, G., Pérez González, A., 1999. El barbecho convencional, una práctica convencional que intensifica la degradación del suelo por erosión hídrica en los sistemas agrícolas de ambientes semiáridos, in: Congreso Europeo de Agricultura Sostenible En Ambientes Mediterráneos. Escuela de Ingenierías Agrarias de La Universidad de Extremadura-Junta de Extremadura. pp. 262–266.

de Miguel, Á., Hoekstra, A.Y., García-Calvo, E., 2015. Sustainability of the water footprint of the Spanish pork industry. Ecol. Indic. 57, 465–474.

Dechmi, F., Burguete, J., Skhiri, A., 2012. SWAT application in intensive irrigation systems: model modification, calibration and validation. J. Hydrol. 470, 227–238.

Del Tánago, M.G., De Jalón, D.G., Román, M., 2012. River restoration in Spain: theoretical and practical approach in the context of the European Water Framework Directive. Environ. Manage. 50, 123–139.

Demattê, J.A.M., Fioriob, P.R., Ben-Dorc, E., 2009. Estimation of soil properties by orbital and laboratory reflectance means and its relation with soil classification. Open Remote Sens. J. 2, 12–23.

Devia, G.K., Ganasri, B.P., Dwarakish, G.S., 2015. A Review on Hydrological Models. Aquat. Procedia 4, 1001–1007. https://doi.org/https://doi.org/10.1016/j.aqpro.2015.02.126

Didan, K., 2015. MOD13Q1 MODIS/Terra vegetation indices 16-day L3 global 250m SIN grid V006. NASA EOSDIS L. Process. DAAC.

Dodds, F., Bartram, J., 2016. The water, food, energy and climate Nexus: Challenges and an Agenda for action. Routledge.

Duffaut Espinosa, L.A., Posadas, A.N., Carbajal, M., Quiroz, R., 2017. Multifractal downscaling of rainfall using normalized difference vegetation index (NDVI) in the Andes Plateau. PLoS One 12, e0168982.

Duffy, C.J., 2017. The terrestrial hydrologic cycle: an historical sense of balance. Wiley Interdiscip. Rev. Water 4, e1216.

Duque, C., Fontalva, J.M.G., Díaz, J.M.M., Calvache, M.L., 2018. Estimating the water budget in a semi-arid region (Torrevieja aquifer—south-east Spain) by assessing groundwater numerical models and hydrochemical data. Environ. earth Sci. 77, 78.

Escribano Rodríguez, J., Tarquis, A.M., Saa-Requejo, A., Díaz-Ambrona, C.G.H., 2015. Relation of NDVI obtained from different remote sensing at different space and resolutions sensors in Spanish Dehesas. EGUGA 15416.

European Comission, 2012. Report on the Review of the European Water Scarcity and Droughts Policy.

European Environment Agency, 2015. The european environment : state and outlook 2015 : synthesis report. Copenhagen European Environment Agency, Copenhagen.

EUROSTAT, 2017. Annual freshwater abstraction by source and sector in Europe.

Expósito, A., Berbel, J., 2017. Agricultural irrigation water use in a closed basin and the impacts on water productivity: The case of the Guadalquivir river basin (Southern Spain). Water 9, 136.

Fatichi, S., Vivoni, E.R., Ogden, F.L., Ivanov, V.Y., Mirus, B., Gochis, D., Downer, C.W., Camporese, M., Davison, J.H., Ebel, B., 2016. An overview of current applications,

challenges, and future trends in distributed process-based models in hydrology. J. Hydrol. 537, 45–60.

Fernández, J.M., Selma, M.A.E., 2004. The dynamics of water scarcity on irrigated landscapes: Mazarrón and Aguilas in south-eastern Spain. Syst. Dyn. Rev. J. Syst. Dyn. Soc. 20, 117–137.

Fernandez, R., Quiroga, A., Noellemeyer, E., Funaro, D., Montoya, J., Hitzmann, B., Peinemann, N., 2008. A study of the effect of the interaction between site-specific conditions, residue cover and weed control on water storage during fallow. Agric. Water Manag. 95, 1028–1040. https://doi.org/https://doi.org/10.1016/j.agwat.2008.03.010

Ficklin, D.L., Stewart, I.T., Maurer, E.P., 2013. Climate change impacts on streamflow and subbasin-scale hydrology in the Upper Colorado River Basin. PLoS One 8, e71297–e71297. https://doi.org/10.1371/journal.pone.0071297

Fiedler, F., 2003. Simple, Practical Method for Determining Station Weights Using Thiessen Polygons and Isohyetal Maps. J. Hydrol. Eng. 8, 219–221. https://doi.org/10.1061/(ASCE)1084-0699(2003)8:4(219)

Fonseka, A., Alahakoon, D., 2010. Exploratory data analysis with Multi-Layer Growing Self-Organizing Maps. Inf. Autom. Sustain. (ICIAFs), 2010 5th Int. Conf. https://doi.org/10.1109/ICIAFS.2010.5715648

Fornés, J.M., Hera, Á. la, Llamas, M.R., 2005. The silent revolution in groundwater intensive use and its influence in Spain. Water Policy 7, 253–268.

Franzluebbers, A.J., Sulc, R.M., Russelle, M.P., 2011. Opportunities and challenges for integrating North-American crop and livestock systems, in: Grassland Productivity and Ecosystem Services. CAB International Wallingford, UK, pp. 208–218.

Freire, S., de Lisboa, N., Fonseca, I., Brasil, R., Rocha, J., Tenedório, J.A., 2013. Using Artificial Neural Networks for Digital Soil Mapping–a comparison of MLP and SOM approaches. AGILE.

Galán-Martín, Á., Pozo, C., Guillén-Gosálbez, G., Antón Vallejo, A., Jiménez Esteller, L., 2015. Multi-stage linear programming model for optimizing cropping plan decisions under the new Common Agricultural Policy. Land use policy 48, 515–524. https://doi.org/https://doi.org/10.1016/j.landusepol.2015.06.022

Galván, L., Olías, M., de Villarán, R.F., Santos, J.M.D., Nieto, J.M., Sarmiento, A.M., Cánovas,

C.R., 2009. Application of the SWAT model to an AMD-affected river (Meca River, SW Spain). Estimation of transported pollutant load. J. Hydrol. 377, 445–454.

Gao, X., Chen, X., Biggs, T.W., Yao, H., 2018. Separating Wet and Dry Years to Improve Calibration of SWAT in Barrett Watershed, Southern California. Water 10, 274.

García-Ruiz, J.M., 2010. The effects of land uses on soil erosion in Spain: A review. CATENA 81, 1–11. https://doi.org/https://doi.org/10.1016/j.catena.2010.01.001

García Morillo, J., Rodríguez Díaz, J.A., Camacho, E., Montesinos, P., 2015. Linking water footprint accounting with irrigation management in high value crops. J. Clean. Prod. 87, 594–602. https://doi.org/https://doi.org/10.1016/j.jclepro.2014.09.043

Gassman, P.W., Reyes, M.R., Green, C.H., Arnold, J.G., 2007. The Soil and Water Assessment Tool: Historical Development, Applications, and Future Research Directions. Iowa State Univ.

GESSLER, P.E., MOORE, I.D., McKENZIE, N.J., RYAN, P.J., 1995. Soil-landscape modelling and spatial prediction of soil attributes. Int. J. Geogr. Inf. Syst. 9, 421–432. https://doi.org/10.1080/02693799508902047

Geza, M., McCray, J.E., 2008. Effects of soil data resolution on SWAT model stream flow and water quality predictions. J. Environ. Manage. 88, 393–406. https://doi.org/https://doi.org/10.1016/j.jenvman.2007.03.016

Giorgi, F., Lionello, P., 2008. Climate change projections for the Mediterranean region. Glob. Planet. Change 63, 90–104. https://doi.org/https://doi.org/10.1016/j.gloplacha.2007.09.005

Giorgi, F., Lionello, P., Bangash, R.F., Passuello, A., Sanchez-Canales, M., Terrado, M., López, A., Elorza, F.J., Ziv, G., Acuña, V., Schuhmacher, M., Arnold, J.G.J., Fohrer, N., García-Ruiz, J.M., López-Moreno, J.I., Vicente-Serrano, S.M., Lasanta–Martínez, T., Beguería, S., Arnold, J.G.J., Srinivasan, R., Muttiah, R., Williams, J., Lloyd-Hughes, B., Saunders, M.A., Korres, W., Reichenau, T.G., Fiener, P., Koyama, C.N., Bogena, H.R., Cornelissen, T., Baatz, R., Herbst, M., Diekkrüger, B., Vereecken, H., Schneider, K., Kleidon, A., Schymanski, S., Stieglitz, M., Kauffman, G.J., 2015. Spatio-temporal soil moisture patterns – A meta-analysis using plot to catchment scale data. J. Hydrol. 29, 326–341. https://doi.org/https://doi.org/10.1016/j.jhydrol.2014.11.042

Gitelson, A.A., Stark, R., Grits, U., Rundquist, D., Kaufman, Y., Derry, D., 2002. Vegetation and soil lines in visible spectral space: a concept and technique for remote estimation of vegetation fraction. Int. J. Remote Sens. 23, 2537–2562.

Gober, P., White, D.D., Quay, R., Sampson, D.A., Kirkwood, C.W., 2017. Socio-hydrology modelling for an uncertain future, with examples from the USA and Canada. Geol. Soc. London, Spec. Publ. 408, 183–199.

Gómez De Barreda Ferraz, D., 2011. El barbecho.

Goovaerts, P., 1999. Geostatistics in soil science: state-of-the-art and perspectives. Geoderma 89, 1–45. https://doi.org/https://doi.org/10.1016/S0016-7061(98)00078-0

Gorelick, N., Hancher, M., Dixon, M., Ilyushchenko, S., Thau, D., Moore, R., 2017. Google Earth Engine: Planetary-scale geospatial analysis for everyone. Remote Sens. Environ. 202, 18–27.

Goslee, S., Goslee, M.S., 2019. Package 'landsat.' R Packag. Doc. Available online https//cran. r-project. org/web/packages/landsat/landsat. pdf (accessed 16 December 2019).

Grizzetti, B., Lanzanova, D., Liquete, C., Reynaud, A., Cardoso, A.C., 2016. Assessing water ecosystem services for water resource management. Environ. Sci. Policy 61, 194–203. https://doi.org/https://doi.org/10.1016/j.envsci.2016.04.008

Gupta, H.V., Sorooshian, S., Yapo, P.O., 1998. Toward improved calibration of hydrologic models: Multiple and noncommensurable measures of information. Water Resour. Res. 34, 751–763. https://doi.org/10.1029/97WR03495

Gutiérrez García, A., Villarino Barrera, I., Nafría García, D.A., Garrido del Pozo, N., Abia Llera, I., Fernández Sánchez, M., Rodríguez, L., 2016. Nuevo sistema de predicción de cosechas de cereales de Castilla y León.

Hagemann, N., van der Zanden, E.H., Willaarts, B., Holzkämper, A., Volk, M., Rutz, C., Schönhart, M., 2019. Bringing the Sharing-Sparing Debate Down to the Ground – Lessons Learnt for Participatory Scenario Development. Unpubl. Manuscr.

Hernanz, J.L., López, R., Navarrete, L., Sanchez-Giron, V., 2002. Long-term effects of tillage systems and rotations on soil structural stability and organic carbon stratification in semiarid central Spain. Soil Tillage Res. 66, 129–141.

Hively, W.D., Lang, M., McCarty, G.W., Keppler, J., Sadeghi, A., McConnell, L.L., 2009. Using satellite remote sensing to estimate winter cover crop nutrient uptake efficiency. J. soil water Conserv. 64, 303–313.

Hjelmfelt, A.T., 1991. Investigation of Curve Number Procedure. J. Hydraul. Eng. 117, 725–737. https://doi.org/10.1061/(ASCE)0733-9429(1991)117:6(725)

Hoff, H., Iceland, C., Kuylenstierna, J., te Velde, D.W., 2012. Managing the Water-Land-Energy Nexus for Sustainable Development. Chronicle 49.

Hosseini, S.M., Mahjouri, N., 2016. Integrating support vector regression and a geomorphologic artificial neural network for daily rainfall-runoff modeling. Appl. Soft Comput. 38, 329–345.

Hott, M.C., Carvalho, L.M.T., Antunes, M.A.H., Resende, J.C., Rocha, W.S.D., 2019. Analysis of Grassland Degradation in Zona da Mata, MG, Brazil, Based on NDVI Time Series Data with the Integration of Phenological Metrics. Remote Sens. 11, 2956.

Hrachowitz, M., Benettin, P., Van Breukelen, B.M., Fovet, O., Howden, N.J.K., Ruiz, L., Van Der Velde, Y., Wade, A.J., 2016. Transit times—The link between hydrology and water quality at the catchment scale. Wiley Interdiscip. Rev. Water 3, 629–657.

Hutchins, M.G., McGrane, S.J., Miller, J.D., Hagen-Zanker, A., Kjeldsen, T.R., Dadson, S.J., Rowland, C.S., 2017. Integrated modeling in urban hydrology: reviewing the role of monitoring technology in overcoming the issue of 'big data'requirements. Wiley Interdiscip. Rev. Water 4, e1177.

i Canals, L.M., de Baan, L., 2015. Land Use, in: Life Cycle Impact Assessment. Springer, pp. 197–222.

Igartua Arregui, E., Gracia Gimeno, M.P., Casas Cendoya, A.M., 2015. ¿ Cebadas de invierno, de primavera, o hay otras?

Igbawua, T., Zhang, J., Yao, F., Ali, S., 2019. Long Range Correlation in Vegetation Over West Africa From 1982 to 2011. IEEE Access 7, 119151–119165.

IGME, 2009. Identificación y caracterización de la interrelación que se presenta entre aguas subterráneas, cursos fluviales, descargas por manantiales, zonas húmedas y otros ecosistemas naturales de especial interés hídrico. Demarcación Hidrográfica 021 Duero. SISTEM.

IGME, 2008. Integración de las masas de agua subterranea en el modelo de gestión de la cuenca hidrográfica del Duero. Determinación de los parámetros de simulación (coeficientes de agotamiento).

Jiang, W., Yuan, L., Wang, W., Cao, R., Zhang, Y., Shen, W., 2015. Spatio-temporal analysis of vegetation variation in the Yellow River Basin. Ecol. Indic. 51, 117–126.

Jiménez, D., Dorado, H., Cock, J., Prager, S.D., Delerce, S., Grillon, A., Bejarano, M.A.,

Benavides, H., Jarvis, A., 2016. From observation to information: data-driven understanding of on farm yield variation. PLoS One 11, e0150015.

Jimeno-Sáez, P., Senent-Aparicio, J., Pérez-Sánchez, J., Pulido-Velazquez, D., 2018. A comparison of SWAT and ANN models for daily runoff simulation in different climatic zones of peninsular Spain. Water (Switzerland) 10, <xocs:firstpage xmlns:xocs=""/>. https://doi.org/10.3390/w10020192

Joiner, J., Yoshida, Y., Anderson, M., Holmes, T., Hain, C., Reichle, R., Koster, R., Middleton, E., Zeng, F.-W., 2018. Global relationships among traditional reflectance vegetation indices (NDVI and NDII), evapotranspiration (ET), and soil moisture variability on weekly timescales. Remote Sens. Environ. 219, 339–352.

Jones, J.W., Antle, J.M., Basso, B., Boote, K.J., Conant, R.T., Foster, I., Godfray, H.C.J., Herrero, M., Howitt, R.E., Janssen, S., Keating, B.A., Munoz-Carpena, R., Porter, C.H., Rosenzweig, C., Wheeler, T.R., 2017. Toward a new generation of agricultural system data, models, and knowledge products: State of agricultural systems science. Agric. Syst. 155, 269–288. https://doi.org/https://doi.org/10.1016/j.agsy.2016.09.021

Kaleita, A.L., Tian, L.F., Hirschi, M.C., 2005. Relationship between soil moisture content and soil surface reflectance. Trans. ASAE 48, 1979–1986.

Kalogeropoulos, K., Chalkias, C., Pissias, E., Karalis, S., 2011. Application of the SWAT model for the investigation of reservoirs creation BT - Advances in the Research of Aquatic Environment: Volume 2, in: Lambrakis, N., Stournaras, G., Katsanou, K. (Eds.), . Springer Berlin Heidelberg, Berlin, Heidelberg, pp. 71–79. https://doi.org/10.1007/978-3-642-24076-8_9

Kalteh, A.M., Hjorth, P., Berndtsson, R., 2008. Review of the self-organizing map (SOM) approach in water resources: Analysis, modelling and application. Environ. Model. Softw. 23, 835–845. https://doi.org/https://doi.org/10.1016/j.envsoft.2007.10.001

Kamali, B., Abbaspour, C.K., Yang, H., 2017. Assessing the Uncertainty of Multiple Input Datasets in the Prediction of Water Resource Components. Water . https://doi.org/10.3390/w9090709

Karabulut, A., Egoh, B.N., Lanzanova, D., Grizzetti, B., Bidoglio, G., Pagliero, L., Bouraoui, F., Aloe, A., Reynaud, A., Maes, J., 2016. Mapping water provisioning services to support the ecosystem–water–food–energy nexus in the Danube river basin. Ecosyst. Serv. 17, 278–292.

Karner, K., Cord, A.F., Hagemann, N., Hernandez-Mora, N., Holzkämper, A., Jeangros, B., Lienhoop, N., Nitsch, H., Rivas, D., Schmid, E., Schulp, C.J.E., Strauch, M., van der Zanden, E.H., Volk, M., Willaarts, B., Zarrineh, N., Schönhart, M., 2019. Developing stakeholder-driven scenarios on land sharing and land sparing – Insights from five European case studies. J. Environ. Manage. 241, 488–500. https://doi.org/https://doi.org/10.1016/j.jenvman.2019.03.050

Karnez, E., 2017. Modeling Agricultural Land Management to Improve Understanding of Nitrogen Leaching in an Irrigated Mediterranean Area in Southern Turkey, in: Sagir, H. (Ed.), . IntechOpen, Rijeka, p. Ch. 7. https://doi.org/10.5772/65809

Khadra, R., Sagardoy, J.A., 2019. Irrigation Modernization and Rehabilitation Programs, A Spectrum of Experiences: Analysis and Lessons Learnt, in: Irrigation Governance Challenges in the Mediterranean Region: Learning from Experiences and Promoting Sustainable Performance. Springer, pp. 45–78.

Khanchouch, I., Boujenfa, K., Limam, M., 2013. AN IMPROVED MULTI-SOM ALGORITHM. Int. J. Netw. Secur. Its Appl. 5, 181. https://doi.org/10.5121/ijnsa.2013.5414

Khanchouch, I., Charrad, M., Limam, M., 2015. A Comparative Study of Multi-SOM Algorithms for Determining the Optimal Number of Clusters. Int. J. Futur. Comput. Commun. 4, 198–202. https://doi.org/10.7763/IJFCC.2015.V4.384

Kim, K.B., Kwon, H.-H., Han, D., 2018. Exploration of warm-up period in conceptual hydrological modelling. J. Hydrol. 556, 194–210.

King, R., Burton, S., 1982. Land Fragmentation: Notes on a Fundamental Rural Spatial Problem. Prog. Geogr. 6, 475–494. https://doi.org/10.1177/030913258200600401

Kirkby, M., Gallart, F., Kjeldsen, T., Irvine, B., Froebrich, J., Porto, A., De Girolamo, A., Team, the, 2011. Classifying low flow hydrological regimes at a regional scale. Hydrol. Earth Syst. Sci. 15, 3741. https://doi.org/10.5194/hess-15-3741-2011

Kleidon, A., Schymanski, S., Stieglitz, M., 2009. Thermodynamics, irreversibility, and optimality in land surface hydrology, in: Bioclimatology and Natural Hazards. Springer, pp. 107–118.

Kling, H., Gupta, H., 2009. On the development of regionalization relationships for lumped watershed models: The impact of ignoring sub-basin scale variability. J. Hydrol. 373, 337–351. https://doi.org/https://doi.org/10.1016/j.jhydrol.2009.04.031

Kohonen, T., 2001. Self-organizing maps, 3rd ed. ed. Berlin Springer, Berlin.

Kohonen, T., 1982. Self-organized formation of topologically correct feature maps. Biol. Cybern. 43, 59–69. https://doi.org/10.1007/BF00337288

Kok, K., van Vliet, M., 2011. Using a participatory scenario development toolbox: added values and impact on quality of scenarios. J. Water Clim. Chang. 2, 87–105. https://doi.org/10.2166/wcc.2011.032

Kropff, M.J., Bouma, J., Jones, J.W., 2001. Systems approaches for the design of sustainable agro-ecosystems. Agric. Syst. 70, 369–393. https://doi.org/https://doi.org/10.1016/S0308-521X(01)00052-X

Krysanova, V., White, M., 2015. Advances in water resources assessment with SWAT—an overview. Hydrol. Sci. J. 60, 771–783.

Kumar, M.D., Singh, O.P., 2005. Virtual Water in Global Food and Water Policy Making: Is There a Need for Rethinking? Water Resour. Manag. 19, 759–789. https://doi.org/10.1007/s11269-005-3278-0

Lacasa, L., Luque, B., Luque, J., Nuno, J.C., 2009. The visibility graph: A new method for estimating the Hurst exponent of fractional Brownian motion. EPL (Europhysics Lett. 86, 30001.

Lacasta, C., 1995. Investigaciones sobre el secano en Castilla-La Mancha. Madrid, Spain Cons. Super. Investig. Cientıficas-Junta Comunidades Castilla-La Mancha.

Lambin, E.F., Turner, B.L., Geist, H.J., Agbola, S.B., Angelsen, A., Bruce, J.W., Coomes, O.T., Dirzo, R., Fischer, G., Folke, C., George, P.S., Homewood, K., Imbernon, J., Leemans, R., Li, X., Moran, E.F., Mortimore, M., Ramakrishnan, P.S., Richards, J.F., Skånes, H., Steffen, W., Stone, G.D., Svedin, U., Veldkamp, T.A., Vogel, C., Xu, J., 2001. The causes of land-use and land-cover change: moving beyond the myths. Glob. Environ. Chang. 11, 261–269. https://doi.org/https://doi.org/10.1016/S0959-3780(01)00007-3

Lampurlanes, J., Angas, P., Cantero-Martınez, C., 2002. Tillage effects on water storage during fallow, and on barley root growth and yield in two contrasting soils of the semi-arid Segarra region in Spain. Soil Tillage Res. 65, 207–220.

Lazaro, R., Rodrigo, F.S., Gutiérrez, L., Domingo, F., Puigdefábregas, J., 2001. Analysis of a 30-year rainfall record (1967–1997) in semi–arid SE Spain for implications on vegetation. J. Arid Environ. 48, 373–395.

Lee Ficklin, D., Luo, Y., Zhang, M., E. Gatzke, S., 2014. The Use of Soil Taxonomy as a Soil Type Identifier for the Shasta Lake Watershed Using SWAT. Trans. ASABE 57, 717–728. https://doi.org/https://doi.org/10.13031/trans.57.9557

Lee, S., Yeo, I.-Y., Sadeghi, A.M., McCarty, G.W., Hively, W.D., Lang, M.W., 2016. Impacts of Watershed Characteristics and Crop Rotations on Winter Cover Crop Nitrate-Nitrogen Uptake Capacity within Agricultural Watersheds in the Chesapeake Bay Region. PLoS One 11, e0157637.

Lelièvre, F., Norton, M.R., Volaire, F., 2008. Perennial grasses in rainfed Mediterranean farming systems—Current and potential role. Options Méditerranéennes. Série A Séminaires Méditerranéens 79, 137–146.

Lemaire, G., Gastal, F., Franzluebbers, A., Chabbi, A., 2015. Grassland–Cropping Rotations: An Avenue for Agricultural Diversification to Reconcile High Production with Environmental Quality. Environ. Manage. 56, 1065–1077. https://doi.org/10.1007/s00267-015-0561-6

Li, C., Qi, J., Feng, Z., Yin, R., Zou, S., Zhang, F., 2010. Parameters optimization based on the combination of localization and auto-calibration of SWAT model in a small watershed in Chinese Loess Plateau. Front. Earth Sci. China 4, 296–310. https://doi.org/10.1007/s11707-010-0114-5

Li, X., Lanorte, A., Lasaponara, R., Lovallo, M., Song, W., Telesca, L., 2017. Fisher–Shannon and detrended fluctuation analysis of MODIS normalized difference vegetation index (NDVI) time series of fire-affected and fire-unaffected pixels. Geomatics, Nat. Hazards Risk 8, 1342–1357.

Lin, H., Wheeler, D., Bell, J., Wilding, L., 2005. Assessment of soil spatial variability at multiple scales. Ecol. Modell. 182, 271–290.

Lin, Q., 2011. Influence of dams on river ecosystem and its countermeasures. J. Water Resour. Prot. 3, 60.

Lister, D.L., Thaw, S., Bower, M.A., Jones, H., Charles, M.P., Jones, G., Smith, L.M.J., Howe, C.J., Brown, T.A., Jones, M.K., 2009. Latitudinal variation in a photoperiod response gene in European barley: insight into the dynamics of agricultural spread from 'historic' specimens. J. Archaeol. Sci. 36, 1092–1098. https://doi.org/https://doi.org/10.1016/j.jas.2008.12.012

Liu, H.Q., Huete, A., 1995. A feedback based modification of the NDVI to minimize canopy

background and atmospheric noise. IEEE Trans. Geosci. Remote Sens. 33, 457–465.

Liu, X., Tian, Z., Zhang, A., Zhao, A., Liu, H., 2019. Impacts of climate on spatiotemporal variations in vegetation NDVI from 1982–2015 in Inner Mongolia, China. Sustainability 11, 768.

Llera, David A. Nafría, Del, G.N.G., Álvarez, P.M.V., Cubero, A.D., Miriam, J., Ignacio, F.S., Barrera, V., García, A.G., 2013. Atlas agroclimático de Castilla y León [WWW Document]. Junta Castilla y León. URL http://atlas.itacyl.es/

Lobell, D.B., Asner, G.P., 2002. Moisture effects on soil reflectance. Soil Sci. Soc. Am. J. 66, 722–727.

Louhichi, K., Ciaian, P., Espinosa, M., Colen, L., Perni, A., Paloma, S.G. y, 2017. Does the crop diversification measure impact EU farmers' decisions? An assessment using an Individual Farm Model for CAP Analysis (IFM-CAP). Land use policy 66, 250–264. https://doi.org/https://doi.org/10.1016/j.landusepol.2017.04.010

Lovejoy, S., Schertzer, D., Stanway, J.D., 2001. Fractal behavior of ozone, wind and temperature in the lower stratosphere. Phys. Rev. Lett. 86, 5200–5203.

Lovejoy, S., Tarquis, A.M., Gaonac'h, H., Schertzer, D., 2008. Single-and Multiscale Remote Sensing Techniques, Multifractals, and MODIS-Derived Vegetation and Soil Moisture. Vadose Zo. J. 7, 533–546.

Luo, Y., Ficklin, D.L., Zhang, M., 2012. Approaches of soil data aggregation for hydrologic simulations. J. Hydrol. 464–465, 467–476. https://doi.org/10.1016/j.jhydrol.2012.07.036

Mahmoudabadi, E., Karimi, A., Haghnia, G.H., Sepehr, A., 2017. Digital soil mapping using remote sensing indices, terrain attributes, and vegetation features in the rangelands of northeastern Iran. Environ. Monit. Assess. 189, 500.

Malek, Ž., Boerboom, L., 2015. Participatory scenario development to address potential impacts of land use change: an example from the Italian Alps. Mt. Res. Dev. 35, 126–139.

Mao, R., Zeng, D.-H., Li, L.-J., Hu, Y.-L., 2012. Changes in labile soil organic matter fractions following land use change from monocropping to poplar-based agroforestry systems in a semiarid region of Northeast China. Environ. Monit. Assess. 184, 6845–6853.

Martin-Sotoca, J.J., Saa-Requejo, A., Borondo, J., Tarquis, A.M., 2018. Singularity maps applied to a vegetation index. Biosyst. Eng. 168, 42–53.

Martinez - Capel, F., Belmar, O., Velasco, J., 2011. Hydrological classification of natural flow regimes to support environmental flow assessments in intensively regulated Mediterranean rivers, Segura River Basin (Spain) 47. https://doi.org/10.1007/s00267-011-9661-0

Martínez, B., Gilabert, M.A., 2009. Vegetation dynamics from NDVI time series analysis using the wavelet transform. Remote Sens. Environ. 113, 1823–1842.

Mateus, M., Almeida, C., Brito, D., Neves, R., 2014. From Eutrophic to Mesotrophic: Modelling Watershed Management Scenarios to Change the Trophic Status of a Reservoir. Int. J. Environ. Res. Public Health 11, 3015–3031. https://doi.org/10.3390/ijerph110303015

Matheron, G., 1963. Principles of geostatistics. Econ. Geol. 58, 1246–1266.

Matheron, G., 1962. Traité de géostatistique appliquée. 1 (1962). Editions Technip.

Memarian, H., Balasundram, S.K., Abbaspour, K.C., Talib, J.B., Boon Sung, C.T., Sood, A.M., 2014. SWAT-based hydrological modelling of tropical land-use scenarios. Hydrol. Sci. J. 59, 1808–1829.

Merdun, H., 2011. Self-organizing map artificial neural network application in multidimensional soil data analysis. Neural Comput. Appl. 20, 1295–1303. https://doi.org/10.1007/s00521-010-0425-1

Merheb, M., Moussa, R., Abdallah, C., Colin, F., Perrin, C., Baghdadi, N., 2016. Hydrological response characteristics of Mediterranean catchments at different time scales: a meta-analysis. Hydrol. Sci. J. 61, 2520–2539.

Moges, S.M., Raun, W.R., Mullen, R.W., Freeman, K.W., Johnson, G. V, Solie, J.B., 2005. Evaluation of green, red, and near infrared bands for predicting winter wheat biomass, nitrogen uptake, and final grain yield. J. Plant Nutr. 27, 1431–1441.

Monin, A.S., Yaglom, A.M., 1999. Statistical Fluid Mechanics: The Mechanics of Turbulence.

Mook, W.G., Custodio, E., 2002. Isótopos ambientales en el ciclo hidrológico : principios y aplicaciones. Madrid IGME, Madrid.

Morán-Tejeda, E., Ceballos-Barbancho, A., Llorente-Pinto, J.M., 2010. Hydrological response of Mediterranean headwaters to climate oscillations and land-cover changes: The mountains of Duero River basin (Central Spain). Glob. Planet. Change 72, 39–49.

Morán-Tejeda, E., López-Moreno, J.I., Ceballos-Barbancho, A., Vicente-Serrano, S.M., 2011.

River regimes and recent hydrological changes in the Duero basin (Spain). J. Hydrol. 404, 241–258. https://doi.org/https://doi.org/10.1016/j.jhydrol.2011.04.034

Moreno, F., Arrúe, J.L., Cantero-Martínez, C., López, M. V, Murillo, J.M., Sombrero, A., López-Garrido, R., Madejón, E., Moret, D., Álvaro-Fuentes, J., 2010. Conservation agriculture under Mediterranean conditions in Spain, in: Biodiversity, Biofuels, Agroforestry and Conservation Agriculture. Springer, pp. 175–193.

Moret, D., Arrúe, J.L., López, M. V, Gracia, R., 2006. Influence of fallowing practices on soil water and precipitation storage efficiency in semiarid Aragon (NE Spain). Agric. Water Manag. 82, 161–176. https://doi.org/https://doi.org/10.1016/j.agwat.2005.07.019

Moriasi, D.N., Arnold, J.G., Van Liew, M.W., Bingner, R.L., Harmel, R.D., Veith, T.L., 2007. Model evaluation guidelines for systematic quantification of accuracy in watershed simulations. Trans. ASABE 50, 885–900.

Muller, E., Décamps, H., 2001. Modeling soil moisture–reflectance. Remote Sens. Environ. 76, 173–180. https://doi.org/https://doi.org/10.1016/S0034-4257(00)00198-X

Muñoz, I., Milà-I-Canals, L., Fernández-Alba, A.R., 2010. Life Cycle Assessment of Water Supply Plans in Mediterranean Spain. J. Ind. Ecol. 14, 902–918. https://doi.org/10.1111/j.1530-9290.2010.00271.x

Muttiah, R.S., Wurbs, R.A., 2002. Scale-dependent soil and climate variability effects on watershed water balance of the SWAT model. J. Hydrol. 256, 264–285. https://doi.org/https://doi.org/10.1016/S0022-1694(01)00554-6

Mzuku, M., Khosla, R., Reich, R., 2015. Bare Soil Reflectance to Characterize Variability in Soil Properties. Commun. Soil Sci. Plant Anal. 46, 1668–1676. https://doi.org/10.1080/00103624.2015.1043463

Nachtergaele, F., Velthuizen, H. V, Verelst, L., Wiberg, D., 2009. Harmonized World Soil Database (HWSD). Food Agric. Organ. United Nations, Rome.

Nadal-Romero, E., Khorchani, M., Lasanta, T., García-Ruiz, J.M., 2019. Runoff and Solute Outputs under Different Land Uses: Long-Term Results from a Mediterranean Mountain Experimental Station. Water 11, 976.

Nagy, A., Fehér, J., Tamás, J., 2018. Wheat and maize yield forecasting for the Tisza river catchment using MODIS NDVI time series and reported crop statistics. Comput. Electron. Agric. 151, 41–49.

Narsimlu, B., Gosain, A., Chahar, B., 2013. Assessment of Future Climate Change Impacts on Water Resources of Upper Sind River Basin, India Using SWAT Model. An Int. J. - Publ. Eur. Water Resour. Assoc. 27, 3647–3662. https://doi.org/10.1007/s11269-013-0371-7

Nash, J.E., Sutcliffe, J. V, 1970. River flow forecasting through conceptual models part I — A discussion of principles. J. Hydrol. 10, 282–290. https://doi.org/https://doi.org/10.1016/0022-1694(70)90255-6

Navarro, L.M., Pereira, H.M., 2015. Rewilding abandoned landscapes in Europe, in: Rewilding European Landscapes. Springer, Cham, pp. 3–23.

Ndayisaba, F., Guo, Hao, Bao, A., Guo, Hui, Karamage, F., Kayiranga, A., 2016. Understanding the spatial temporal vegetation dynamics in Rwanda. Remote Sens. 8, 129.

Neitsch, S.L., Arnold, J.G., Kiniry, J.R. e a1, Srinivasan, R., Williams, J.R., 2002. Soil and water assessment tool user's manual version 2000. GSWRL Rep. 202.

Neitsch, S.L., Arnold, J.G., Kiniry, J.R., Srinivasan, R., Williams, J.R., 2005. Soiland Water Assessment Tool, Theorical Documentation Version 2005. Grassland Soiland Water Research Laboratory. Agric. Res. Serv. Blackl. Res. Center-Texas Agric. Exp. Station. USA.

Newbold, T., Hudson, L., Hill, S., Contu, S., Gray, C., Scharlemann, J., Börger, L., Phillips, H., Sheil, D., Lysenko, I., Purvis, A., 2016. Global patterns of terrestrial assemblage turnover within and among land uses. Ecography (2016).

Numata, I., Roberts, D.A., Chadwick, O.A., Schimel, J., Sampaio, F.R., Leonidas, F.C., Soares, J. V, 2007. Characterization of pasture biophysical properties and the impact of grazing intensity using remotely sensed data. Remote Sens. Environ. 109, 314–327.

Nyamadzawo, G., Nyamugafata, P., Chikowo, R., Giller, K., 2008. Residual effects of fallows on selected soil hydraulic properties in a kaolinitic soil subjected to conventional tillage (CT) and no tillage (NT). Agrofor. Syst. 72, 161–168. https://doi.org/10.1007/s10457-007-9057-6

Obled, C., Wendling, J., Beven, K., 1994. The sensitivity of hydrological models to spatial rainfall patterns: an evaluation using observed data. J. Hydrol. 159, 305–333.

Oñate, J.J., Atance, I., Bardají, I., Llusia, D., 2007. Modelling the effects of alternative CAP policies for the Spanish high-nature value cereal-steppe farming systems. Agric. Syst. 94, 247–260. https://doi.org/https://doi.org/10.1016/j.agsy.2006.09.003

Opršal, Z., Kladivo, P., Machar, I., 2016. The role of selected biophysical factors in long-term land-use change of cultural landscape. Appl. Ecol. Environ. Res. 14, 23–40.

Ortega, J.F., de Juan, J.A., Tarjuelo, J.M., 2005. Improving water management: The irrigation advisory service of Castilla-La Mancha (Spain). Agric. Water Manag. 77, 37–58. https://doi.org/https://doi.org/10.1016/j.agwat.2004.09.028

Padilla, F.M., Pugnaire, F.I., 2007. Rooting depth and soil moisture control Mediterranean woody seedling survival during drought. Funct. Ecol. 21, 489–495.

Pai, N., Saraswat, D., 2011. SWAT2009_LUC: A Tool to Activate the Land Use Change Module in SWAT 2009. Trans. ASABE v. 54, 1649-1658–2011 v.54 no.5.

Pande, G., Al-Mashidani, B.B., Lal, B.B., 1978. TECHNIQUE FOR THE DETERMINATION OF AREAL AVERAGE RAINFALL. J Phys D Appl Phys 23, 445–453.

Parker, D.C., Hessl, A., Davis, S.C., 2008. Complexity, land-use modeling, and the human dimension: Fundamental challenges for mapping unknown outcome spaces. Geoforum 39, 789–804. https://doi.org/https://doi.org/10.1016/j.geoforum.2007.05.005

Patel, M., Kok, K., Rothman, D.S., 2007. Participatory scenario construction in land use analysis: An insight into the experiences created by stakeholder involvement in the Northern Mediterranean. Land use policy 24, 546–561. https://doi.org/https://doi.org/10.1016/j.landusepol.2006.02.005

Pelletier, J.D., Rasmussen, C., 2009. Geomorphically based predictive mapping of soil thickness in upland watersheds. Water Resour. Res. 45.

Peng, J., Liu, Z., Liu, Y., Wu, J., Han, Y., 2012. Trend analysis of vegetation dynamics in Qinghai–Tibet Plateau using Hurst Exponent. Ecol. Indic. 14, 28–39.

Pérez-Blanco, C.D., Delacámara, G., Gómez, C.M., 2015. Water charging and water saving in agriculture. Insights from a Revealed Preference Model in a Mediterranean basin. Environ. Model. Softw. 69, 90–100. https://doi.org/https://doi.org/10.1016/j.envsoft.2015.03.006

Perniola, M., Lovelli, S., Arcieri, M., Amato, M., 2015. Sustainability in cereal crop production in Mediterranean environments, in: The Sustainability of Agro-Food and Natural Resource Systems in the Mediterranean Basin. Springer, Cham, pp. 15–27.

Pinilla, V., 2006. The development of irrigated agriculture in twentieth-century Spain: a case study of the Ebro basin. Agric. Hist. Rev. 54, 122–141.

Poulsen, J.G., Sotherton, N.W., Aebischer, N.J., 1998. Comparative nesting and feeding ecology of skylarks Alauda arvensis on arable farmland in southern England with special reference to set-aside. J. Appl. Ecol. 35, 131–147.

Prăvălie, R., Patriche, C., Bandoc, G., 2017. Quantification of land degradation sensitivity areas in Southern and Central Southeastern Europe. New results based on improving DISMED methodology with new climate data. Catena 158, 309–320.

Psomas, A., Dagalaki, V., Panagopoulos, Y., Konsta, D., Mimikou, M., 2016. Sustainable Agricultural Water Management in Pinios River Basin Using Remote Sensing and Hydrologic Modeling. Procedia Eng. 162, 277–283. https://doi.org/https://doi.org/10.1016/j.proeng.2016.11.059

Pswarayi, A., Van Eeuwijk, F.A., Ceccarelli, S., Grando, S., Comadran, J., Russell, J.R., Francia, E., Pecchioni, N., Li Destri, O., Akar, T., 2008. Barley adaptation and improvement in the Mediterranean basin. Plant Breed. 127, 554–560.

Pulido-Velazquez, D., García-Aróstegui, J.L., Molina, J.-L., Pulido-Velazquez, M., 2015. Assessment of future groundwater recharge in semi-arid regions under climate change scenarios (Serral-Salinas aquifer, SE Spain). Could increased rainfall variability increase the recharge rate? Hydrol. Process. 29, 828–844. https://doi.org/10.1002/hyp.10191

Pumo, D., Caracciolo, D., Viola, F., Noto, L. V, 2016. Climate change effects on the hydrological regime of small non-perennial river basins. Sci. Total Environ. 542, 76–92. https://doi.org/https://doi.org/10.1016/j.scitotenv.2015.10.109

Qiu, J., Tang, H., Frolking, S., Boles, S., Li, C., Xiao, X., Liu, J., Zhuang, Y., Qin, X., 2003. Mapping Single-, Double-, and Triple-crop Agriculture in China at 0.5° × 0.5° by Combining County-scale Census Data with a Remote Sensing-derived Land Cover Map. Geocarto Int. 18, 3–13. https://doi.org/10.1080/10106040308542268

Quintas-Soriano, C., Castro, A.J., Castro, H., García-Llorente, M., 2016. Impacts of land use change on ecosystem services and implications for human well-being in Spanish drylands. Land use policy 54, 534–548. https://doi.org/https://doi.org/10.1016/j.landusepol.2016.03.011

Rafael, M., Àngel, R.-A.M., Carlos, G.J., Joan, A., 2010. El Niño Southern Oscillation and climate trends impact reservoir water quality. Glob. Chang. Biol. 16, 2857–2865. https://doi.org/10.1111/j.1365-2486.2010.02163.x

Ramanathan, V., Crutzen, P., Kiehl, J., Rosenfeld, D., 2001. Atmosphere - Aerosols, climate,

and the hydrological cycle. Science (80-.).

Ray, D.K., Ramankutty, N., Mueller, N.D., West, P.C., Foley, J.A., 2012. Recent patterns of crop yield growth and stagnation. Nat. Commun. 3, 1293.

Reed, B.C., Loveland, T.R., Tieszen, L.L., 1996. An approach for using AVHRR data to monitor US Great Plains grasslands. Geocarto Int. 11, 13–22.

Rekolainen, S., Kämäri, J., Hiltunen, M., Saloranta, T.M., 2003. A conceptual framework for identifying the need and role of models in the implementation of the water framework directive. Int. J. River Basin Manag. 1, 347–352. https://doi.org/10.1080/15715124.2003.9635217

Ricci, G.F., De Girolamo, A.M., Abdelwahab, O.M.M., Gentile, F., 2018. Identifying sediment source areas in a Mediterranean watershed using the SWAT model. L. Degrad. Dev. 29, 1233–1248. https://doi.org/10.1002/ldr.2889

Ries, J.B., Seeger, M., Marzolff, I., 2004. Influencia del pastoreo en la cubierta vegetal y la geomorfodinámica en el transecto Depresión del Ebro-Pirineos. Geographicalia 5–19.

Rivas-Tabares, D., Tarquis, A.M., Willaarts, B., De Miguel, Á., 2019a. An accurate evaluation of water availability in sub-arid Mediterranean watersheds through SWAT: Cega-Eresma-Adaja. Agric. Water Manag. 212, 211–225. https://doi.org/https://doi.org/10.1016/j.agwat.2018.09.012

Rivas-Tabares, D., Tarquis, A.M., Willaarts, B., De Miguel, Á., 2019b. An accurate evaluation of water availability in sub-arid Mediterranean watersheds through SWAT: Cega-Eresma-Adaja. Agric. Water Manag. 212, 211–225. https://doi.org/https://doi.org/10.1016/j.agwat.2018.09.012

Rivera, D., Sandoval, M., Godoy, A., 2015. Exploring soil databases: a self-organizing map approach. Soil Use Manag. 31, 121–131. https://doi.org/10.1111/sum.12169

Romanowicz, A.A., Vanclooster, M., Rounsevell, M., La Junesse, I., 2005. Sensitivity of the SWAT model to the soil and land use data parametrisation: a case study in the Thyle catchment, Belgium. Ecol. Modell. 187, 27–39.

Roth, V., Nigussie, T., Lemann, T., 2016. Model parameter transfer for streamflow and sediment loss prediction with SWAT in a tropical watershed. Environ. Earth Sci. 75, 1–13. https://doi.org/10.1007/s12665-016-6129-9

Rouhani, H., Willems, P., Feyen, J., 2009. Effect of watershed delineation and areal rainfall

distribution on runoff prediction using the SWAT model. Hydrol. Res. 40, 505–519.

Rubalcaba, J.J.O., Guillén, P.Á., 1997. El programa de Estepas Cerealistas en Castilla y León.

Rubiano, J., Otero, M., Johnson, N., 2006. Guest Editorial: Why do scales matter in water resources management? Water Int. 31, 338–342. https://doi.org/10.1080/02508060608691936

Salmoral, G., Willaarts, B.A., Garrido, A., Guse, B., 2017. Fostering integrated land and water management approaches: Evaluating the water footprint of a Mediterranean basin under different agricultural land use scenarios. Land use policy 61, 24–39. https://doi.org/https://doi.org/10.1016/j.landusepol.2016.09.027

Santra, P., Chopra, U.K., Chakraborty, D., 2008. Spatial variability of soil properties and its application in predicting surface map of hydraulic parameters in an agricultural farm. Curr. Sci. 937–945.

Saulnier, G.-M., Beven, K., Obled, C., 1997. Including spatially variable effective soil depths in TOPMODEL. J. Hydrol. 202, 158–172. https://doi.org/10.1016/S0022-1694(97)00059-0

Savitzky, A., Golay, M.J.E., 1964. Smoothing and differentiation of data by simplified least squares procedures. Anal. Chem. 36, 1627–1639.

Schilling, K.E., Jha, M.K., Zhang, Y., Gassman, P.W., Wolter, C.F., 2008. Impact of land use and land cover change on the water balance of a large agricultural watershed: Historical effects and future directions. Water Resour. Res. 44.

Schönhart, M., Schmid, E., Schneider, U.A., 2011. CropRota – A crop rotation model to support integrated land use assessments. Eur. J. Agron. 34, 263–277. https://doi.org/https://doi.org/10.1016/j.eja.2011.02.004

Schultz, M., Clevers, J.G.P.W., Carter, S., Verbesselt, J., Avitabile, V., Quang, H.V., Herold, M., 2016. Performance of vegetation indices from Landsat time series in deforestation monitoring. Int. J. Appl. earth Obs. Geoinf. 52, 318–327.

Scull, P., Franklin, J., Chadwick, O.A., McArthur, D., 2003. Predictive soil mapping: a review. Prog. Phys. Geogr. 27, 171–197.

Seeger, M., 2007. Uncertainty of factors determining runoff and erosion processes as quantified by rainfall simulations. CATENA 71, 56–67. https://doi.org/https://doi.org/10.1016/j.catena.2006.10.005

Sellami, H., Jeunesse, I., Benabdallah, S., Baghdadi, N., Vanclooster, M., 2014. Uncertainty analysis in model parameters regionalization: a case study involving the SWAT model in Mediterranean catchments (Southern France). Hydrol. Earth Syst. Sci. 18, 2393. https://doi.org/10.5194/hess-18-2393-2014

Shafiee, M.E., Barker, Z., Rasekh, A., 2018. Enhancing water system models by integrating big data. Sustain. Cities Soc. 37, 485–491. https://doi.org/https://doi.org/10.1016/j.scs.2017.11.042

Sigua, G.C., Hudnall, W.H., 2008. Kriging analysis of soil properties. J. Soils Sediments 8, 193. https://doi.org/10.1007/s11368-008-0003-7

Singh, H.V., Kalin, L., Morrison, A., Srivastava, P., Lockaby, G., Pan, S., 2015. Post-validation of SWAT model in a coastal watershed for predicting land use/cover change impacts. Hydrol. Res. 46, 837–853.

Singh, V.P., Frevert, D.K., Morán-Tejeda, E., Ceballos-Barbancho, A., Llorente-Pinto, J.M., Salmoral, G., Willaarts, B.A., Garrido, A., Guse, B., Riegger, J., Günter, A., van der Schrier, G., Briffa, K.R., Jones, P.D., Osborn, T.J., Zlotnik, V.A., Wang, T., Nieber, J.L., Šimunek, J., Zhou, T., Haddeland, I., Nijssen, B., Lettenmaier, D.P., Zalidis, G., Stamatiadis, S., Takavakoglou, V., Eskridge, K., Misopolinos, N., Willaarts, B.A., Ballesteros, M., Hernández-Mora, N., Weingartner, R., Viviroli, D., Schädler, B., Dürr, H.H., Messerli, B., Meybeck, M., Weingartner, R., Vidal-Abarca, M.R., Santos-Martín, F., Martín-López, B., Sánchez-Montoya, M.M., Alonso, M.L.S., van Wesemael, B., Mulligan, M., Poesen, J., Udias, A., Pastori, M., Malago, A., Vigiak, O., Nikolaidis, N.P., Bouraoui, F., Uchida, E., Swallow, S.K., Gold, A.J., Opaluch, J., Kafle, A., Merrill, N.H., Michaud, C., Gill, C.A., Terrado, M., Acuña, V., Ennaanay, D., Tallis, H., Sabater, S., Stoate, C., Boatman, N.D., Borralho, R.J., Carvalho, C.R., De Snoo, G.R., Eden, P., Starosolszky, O., Speich, M.J.R., Zappa, M., Lischke, H., Smakhtin, V.U., 2018. Verification of numerical solutions of the Richards equation using a traveling wave solution. Sci. Total Environ. 240, 99–120. https://doi.org/https://doi.org/10.1016/j.landusepol.2016.09.027

Skoulikidis, N.T., Sabater, S., Datry, T., Morais, M.M., Buffagni, A., Dörflinger, G., Zogaris, S., Del Mar Sánchez-Montoya, M., Bonada, N., Kalogianni, E., Rosado, J., Vardakas, L., De Girolamo, A.M., Tockner, K., 2017. Non-perennial Mediterranean rivers in Europe: Status, pressures, and challenges for research and management. Sci. Total Environ. 577, 1–18. https://doi.org/10.1016/j.scitotenv.2016.10.147

Smiraglia, D., Ceccarelli, T., Bajocco, S., Salvati, L., Perini, L., 2016. Linking trajectories of land change, land degradation processes and ecosystem services. Environ. Res. 147, 590–

600. https://doi.org/https://doi.org/10.1016/j.envres.2015.11.030

Smith, R.C.G., Adams, J., Stephens, D.J., Hick, P.T., 1995. Forecasting wheat yield in a Mediterranean-type environment from the NOAA satellite. Aust. J. Agric. Res. 46, 113–125.

Sofia, G., Tarolli, P., 2017. Hydrological response to~ 30 years of agricultural surface water management. Land 6, 3.

Spaaks, J.H., Bouten, W., 2013. Resolving structural errors in a spatially distributed hydrologic model using ensemble Kalman filter state updates. Hydrol. Earth Syst. Sci. 17, 3455–3472.

Stigter, T.Y., Nunes, J.P., Pisani, B., Fakir, Y., Hugman, R., Li, Y., Tomé, S., Ribeiro, L., Samper, J., Oliveira, R., Monteiro, J.P., Silva, A., Tavares, P.C.F., Shapouri, M., Cancela da Fonseca, L., El Himer, H., 2014. Comparative assessment of climate change and its impacts on three coastal aquifers in the Mediterranean. Reg. Environ. Chang. 14, 41–56. https://doi.org/10.1007/s10113-012-0377-3

Strauch, M., Bernhofer, C., Koide, S., Volk, M., Lorz, C., Makeschin, F., 2012. Using precipitation data ensemble for uncertainty analysis in SWAT streamflow simulation. J. Hydrol. 414–415, 413–424. https://doi.org/https://doi.org/10.1016/j.jhydrol.2011.11.014

Szidarovszky, F., 1983. Optimal observation network in geostatistics and underground hydrology. Appl. Math. Model. 7, 25–32. https://doi.org/https://doi.org/10.1016/0307-904X(83)90159-2

Taboada-Castro, M.M., Rodríguez-Blanco, M.L., Palleiro, L., Taboada-Castro, M.T., 2015. Soil crusting and surface runoff in agricultural land in Galicia (NW Spain). Spanish J. Soil Sci. 5.

Teixeira, R.F.M., Proença, V., Valada, T., Crespo, D., Domingos, T., 2014. Sown biodiverse pastures as a win-win approach to reverse the degradation of Mediterranean ecosystems., in: EGF at 50: The Future of European Grasslands. Proceedings of the 25th General Meeting of the European Grassland Federation, Aberystwyth, Wales, 7-11 September 2014. IBERS, Aberystwyth University, pp. 258–260.

Teshager, A.D., Gassman, P.W., Secchi, S., Schoof, J.T., Misgna, G., 2016. Modeling Agricultural Watersheds with the Soil and Water Assessment Tool (SWAT): Calibration and Validation with a Novel Procedure for Spatially Explicit HRUs. Environ. Manage. 57, 894–911. https://doi.org/10.1007/s00267-015-0636-4

Tharme, R.E., 2003. A global perspective on environmental flow assessment: emerging trends in the development and application of environmental flow methodologies for rivers. River Res. Appl. 19, 397–441. https://doi.org/10.1002/rra.736

Thiessen, A.H., 1911. Precipitation averages for large areas. Mon. Weather Rev. 39, 1082–1089.

Tian, Z., Ingjerd, H., Bart, N., P., L.D., 2016. Human-Induced Changes in the Global Water Cycle. Terr. Water Cycle Clim. Chang., Geophysical Monograph Series. https://doi.org/doi:10.1002/9781118971772.ch4

Tissari, S., Nykänen, V., Lerssi, J., Kolehmainen, M., 2007. Classification of Soil Groups Using Weights-of-Evidence-Method and RBFLN-Neural Nets. Nat. Resour. Res. 16, 159–169. https://doi.org/10.1007/s11053-007-9040-y

Tong, S., Zhang, J., Bao, Yuhai, Lai, Q., Lian, X., Li, N., Bao, Yongbin, 2018. Analyzing vegetation dynamic trend on the Mongolian Plateau based on the Hurst exponent and influencing factors from 1982–2013. J. Geogr. Sci. 28, 595–610.

Troch, P.A., Carrillo, G.A., Heidbüchel, I., Rajagopal, S., Switanek, M., Volkmann, T.H.M., Yaeger, M., 2009. Dealing with Landscape Heterogeneity in Watershed Hydrology: A Review of Recent Progress toward New Hydrological Theory. Geogr. Compass 3, 375–392. https://doi.org/10.1111/j.1749-8198.2008.00186.x

Ullrich, A., Volk, M., 2009. Application of the Soil and Water Assessment Tool (SWAT) to predict the impact of alternative management practices on water quality and quantity. Agric. Water Manag. 96, 1207–1217. https://doi.org/10.1016/j.agwat.2009.03.010

Valverde-Arias, O., Garrido, A., Saa-Requejo, A., Carreño, F., Tarquis, A.M., 2019. Agro-ecological variability effects on an index-based insurance design for extreme events. Geoderma 337, 1341–1350.

van Griensven, A., Meixner, T., Grunwald, S., Bishop, T., Diluzio, M., Srinivasan, R., 2006. A global sensitivity analysis tool for the parameters of multi-variable catchment models. J. Hydrol. 324, 10–23. https://doi.org/https://doi.org/10.1016/j.jhydrol.2005.09.008

van Leeuwen, C.C.E., Cammeraat, E.L.H., de Vente, J., Boix-Fayos, C., 2019. The evolution of soil conservation policies targeting land abandonment and soil erosion in Spain: A review. Land use policy 83, 174–186. https://doi.org/https://doi.org/10.1016/j.landusepol.2019.01.018

Veldkamp, A., Verburg, P.H., 2004. Modelling land use change and environmental impact. J. Environ. Manage. 72, 1–3. https://doi.org/https://doi.org/10.1016/j.jenvman.2004.04.004

Vesanto, J., Alhoniemi, E., 2000. Clustering of the self-organizing map. IEEE Trans. neural networks 11, 586–600.

Vicente-Serrano, S.M., 2007. Evaluating the impact of drought using remote sensing in a Mediterranean, semi-arid region. Nat. Hazards 40, 173–208.

Vicente Gonzalez, D.J., Rodríguez Sinobas, L., Garrote de Marcos, L., Sánchez Calvo, R., 2016. Application of the System of Environmental Economic Accounting for Water SEEAW to the Spanish part of the Duero basin: lessons learned. Sci. Total Environ. ISSN 0048-9697, 2016-09, Vol. 563-4.

Vieux, B.E., 2001. Distributed Hydrologic Modeling Using GIS BT - Distributed Hydrologic Modeling Using GIS, in: Vieux, B.E. (Ed.), . Springer Netherlands, Dordrecht, pp. 1–17. https://doi.org/10.1007/978-94-015-9710-4_1

Volk, M., Hagemann, N., 2018. TALE-Towards multifunctional agricultural landscapes in Europe: Assessing and governing synergies between biodiversity and ecosystem services. Impact 2018, 39–41.

Vörösmarty, C.J., Fekete, B.M., Meybeck, M., Lammers, R.B., 2000. Global system of rivers: Its role in organizing continental land mass and defining land-to-ocean linkages. Global Biogeochem. Cycles 14, 599–621.

Wagner, P.D., Fiener, P., Wilken, F., Kumar, S., Schneider, K., 2012. Comparison and evaluation of spatial interpolation schemes for daily rainfall in data scarce regions. J. Hydrol. 464–465, 388–400. https://doi.org/10.1016/j.jhydrol.2012.07.026

Wang, G., Mang, S., Cai, H., Liu, S., Zhang, Z., Wang, L., Innes, J.L., 2016. Integrated watershed management: evolution, development and emerging trends. J. For. Res. 27, 967–994. https://doi.org/10.1007/s11676-016-0293-3

Wang, J., Price, K.P., Rich, P.M., 2001. Spatial patterns of NDVI in response to precipitation and temperature in the central Great Plains. Int. J. Remote Sens. 22, 3827–3844.

Wang, X., Wang, C., Niu, Z., 2005. Application of R/S method in analyzing NDVI time series. Geogr. Geo-Information Sci. 21, 20–24.

Wehrens, R., Buydens, L.M.C., 2007. Self- and Super-organizing Maps in R: The kohonen Package. J. Stat. Softw. 21. https://doi.org/10.18637/jss.v021.i05

Weidong, L., Baret, F., Xingfa, G., Qingxi, T., Lanfen, Z., Bing, Z., 2002. Relating soil surface moisture to reflectance. Remote Sens. Environ. 81, 238–246.

Willaarts, B.A., Ballesteros, M., Hernández-Mora, N., 2014. Ten years of the Water Framework Directive in Spain: An overview of the ecological and chemical status of surface water bodies. Integr. Water Resour. Manag. 21st Century Revisiting Paradig. Taylor Fr. Leiden 99–120.

Wu, H., Wu, L., Zhu, Q., Wang, J., Qin, X., Xu, J., Kong, L., Chen, J., Lin, S., Khan, M.U., 2017. The role of organic acids on microbial deterioration in the Radix pseudostellariae rhizosphere under continuous monoculture regimes. Sci. Rep. 7, 1–13.

Wu, J., David, J.L., 2002. A spatially explicit hierarchical approach to modeling complex ecological systems: theory and applications. Ecol. Modell. 153, 7–26.

Xu, Y.-T., Zhang, Y., Wang, S.-G., 2015a. A modified tunneling function method for non-smooth global optimization and its application in artificial neural network. Appl. Math. Model. 39, 6438–6450. https://doi.org/https://doi.org/10.1016/j.apm.2015.01.059

Xu, Y.-T., Zhang, Y., Wang, S.-G., 2015b. A modified tunneling function method for non-smooth global optimization and its application in artificial neural network. Appl. Math. Model. 39, 6438–6450. https://doi.org/https://doi.org/10.1016/j.apm.2015.01.059

Xue, J., Su, B., 2017. Significant remote sensing vegetation indices: A review of developments and applications. J. Sensors 2017.

Yilmaz, Y.A., Sen, O.L., Turuncoglu, U.U., 2019. Modeling the hydroclimatic effects of local land use and land cover changes on the water budget in the upper Euphrates – Tigris basin. J. Hydrol. 576, 596–609. https://doi.org/https://doi.org/10.1016/j.jhydrol.2019.06.074

Yu, C.X., Gilmore, M., Peebles, W.A., Rhodes, T.L., 2003. Structure function analysis of long-range correlations in plasma turbulence. Phys. Plasmas 10, 2772–2779.

Zhao, A., Zhu, X., Liu, X., Pan, Y., Zuo, D., 2016. Impacts of land use change and climate variability on green and blue water resources in the Weihe River Basin of northwest China. CATENA 137, 318–327. https://doi.org/https://doi.org/10.1016/j.catena.2015.09.018

6 Annexes

Annex 1. Harmonized world soil database HWSD for SWAT modelling of Adaja Watershed in Spain.

MUID	S5ID	NLAYERS	HYDGRP	SOL_ZMX	SOL_Z1	SOL_BD1	SOL_AWC1	SOL_K1	SOL_CBN1	CLAY1	SILT1	SAND1	ROCK1	SOL_ALB1	SOL_Z2	SOL_BD2	SOL_AWC2	SOL_K2	SOL_CBN2	CLAY2	SILT2	SAND2	ROCK2	SOL_ALB2
7003	FAO	2	C	1000	300	1.1	0.05	17.20	2.72	23	36	41	8	0.01	700	1.16	0.02	18.96	1.07	24	32	44	6	0.01
9673	FAO	2	C	1000	300	1.39	0.25	4.00	0.6	18	48	34	15	0.01	700	1.41	0.11	5.36	0.4	18	46	36	10	0.01
9677	FAO	1	C	300	300	1.45	0.00	30.25	1.4	9	18	73	21	0.01	0	0	0.00	0.00	0	0	0	0	0	0.01
9678	FAO	2	B	1000	300	1.54	0.33	50.00	0.3	5	6	89	1	0.01	700	1.55	0.14	50.00	0.3	5	6	89	1	0.01
9696	FAO	2	B	1000	300	1.5	0.33	41.51	0.7	9	13	78	19	0.01	700	1.5	0.14	40.66	0.31	10	13	77	14	0.01
9697	FAO	2	C	1000	300	1.1	0.05	17.20	2.72	23	36	41	8	0.01	700	1.16	0.02	18.96	1.07	24	32	44	6	0.01
9699	FAO	2	C	1000	300	1.41	0.17	10.17	0.65	21	43	36	6	0.01	700	1.45	0.07	9.24	0.43	23	43	34	10	0.01
9703	FAO	2	D	1000	300	1.28	0.50	1.35	0.87	49	32	19	5	0.01	700	1.35	0.21	3.61	0.39	42	35	23	5	0.01
9705	FAO	2	C	1000	300	1.41	0.17	10.17	0.65	21	43	36	6	0.01	700	1.45	0.07	9.24	0.43	23	43	34	10	0.01
9706	FAO	2	D	1000	300	1.28	0.17	1.35	0.87	49	32	19	5	0.01	700	1.35	0.07	3.61	0.39	42	35	23	5	0.01
9715	FAO	2	C	1000	300	1.53	0.17	16.87	0.83	24	28	48	12	0.01	700	1.51	0.07	12.98	0.4	34	25	41	8	0.01
9719	FAO	2	C	1000	300	1.44	0.50	25.66	0.4	15	13	72	4	0.01	700	1.55	0.21	25.65	0.27	28	14	58	5	0.01
9725	FAO	2	C	1000	300	1.36	0.25	25.65	0.86	21	40	39	4	0.01	700	1.39	0.11	25.65	0.38	21	38	41	7	0.01
9736	FAO	2	C	1000	300	1.53	0.5	16.87	0.83	24	28	48	12	0.01	700	1.33	0.5	12.98	0.4	34	25	41	8	0.01
9744	FAO	2	C	1000	300	1.33	0.50	14.58	1.39	21	37	42	19	0.01	700	1.48	0.21	17.75	0.6	20	34	46	26	0.01

Annex 2. Soil properties of Adaja watershed using the Kriging interpolation method from soil samples.

AWC: available water content in [%], WP: wilting point in [%], CBN: Organic carbon content in [%] and Ksat: Hydraulic conductivity in [mm/day].

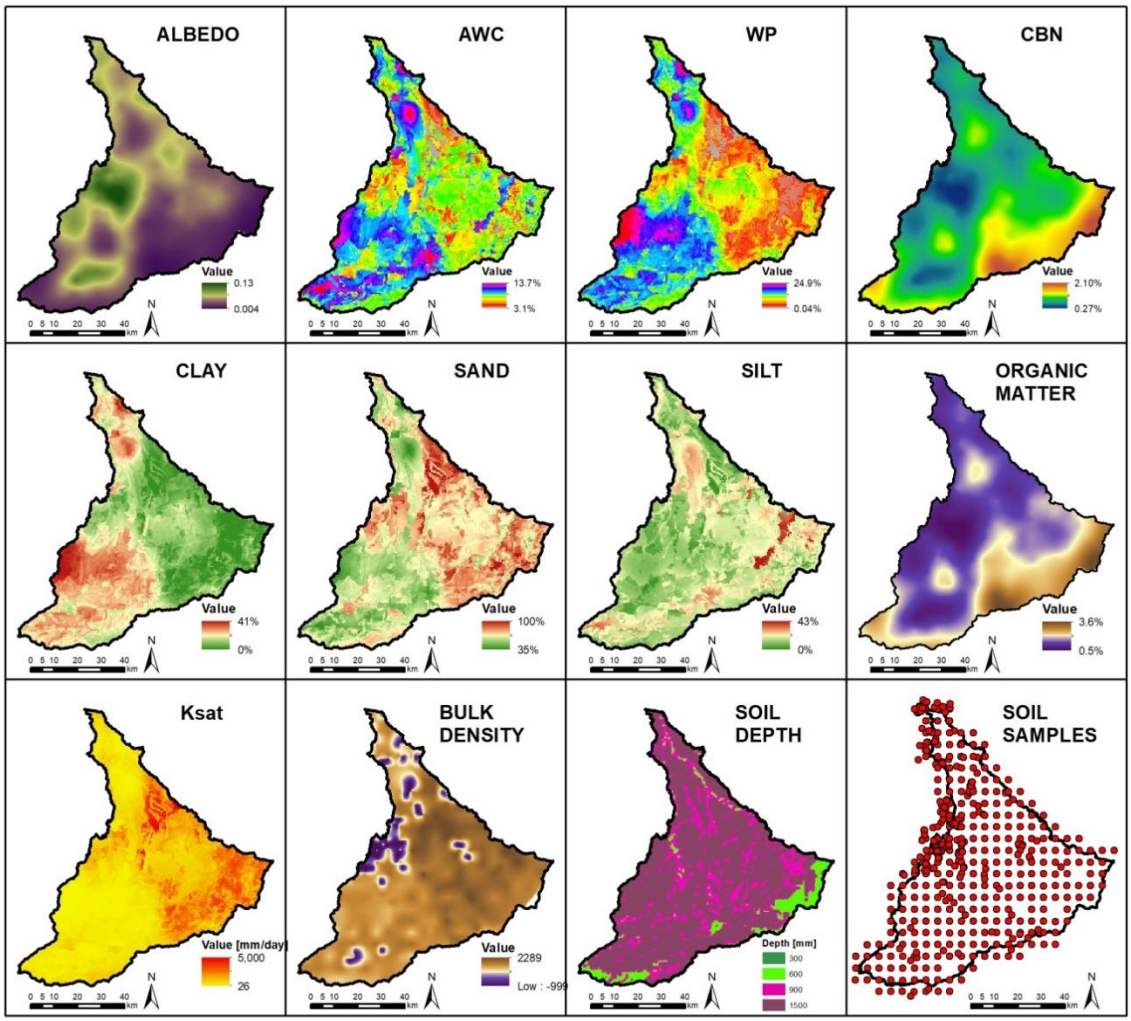

Annex 3. Soil depth restrictions for soil depth mapping of Adaja watershed.

Watershed Segment	Minimun soil depth of pits [mm]	Maximun soil depth of pits [mm]	Effective minimum soil depth for root development [mm]	Effective maximun soil depth for root development [mm]
Low	850	1500	800 (cropland) 120 (forest) 0.0 (bare soil)	1200 (cropland) 2000 (forest) 50 (bare soil)
Medium	850	1200	800 (cropland) 100 (forest) 0.0 (bare soil)	1200 (cropland) 2000 (forest) 50 (bare soil)
High	100	800	100 (cropland) 85 (forest) 0.0 (bare soil)	350 (cropland) 60 (forest) 50 (bare soil)

Annex 4. Soil depth model developed for Adaja watershed.

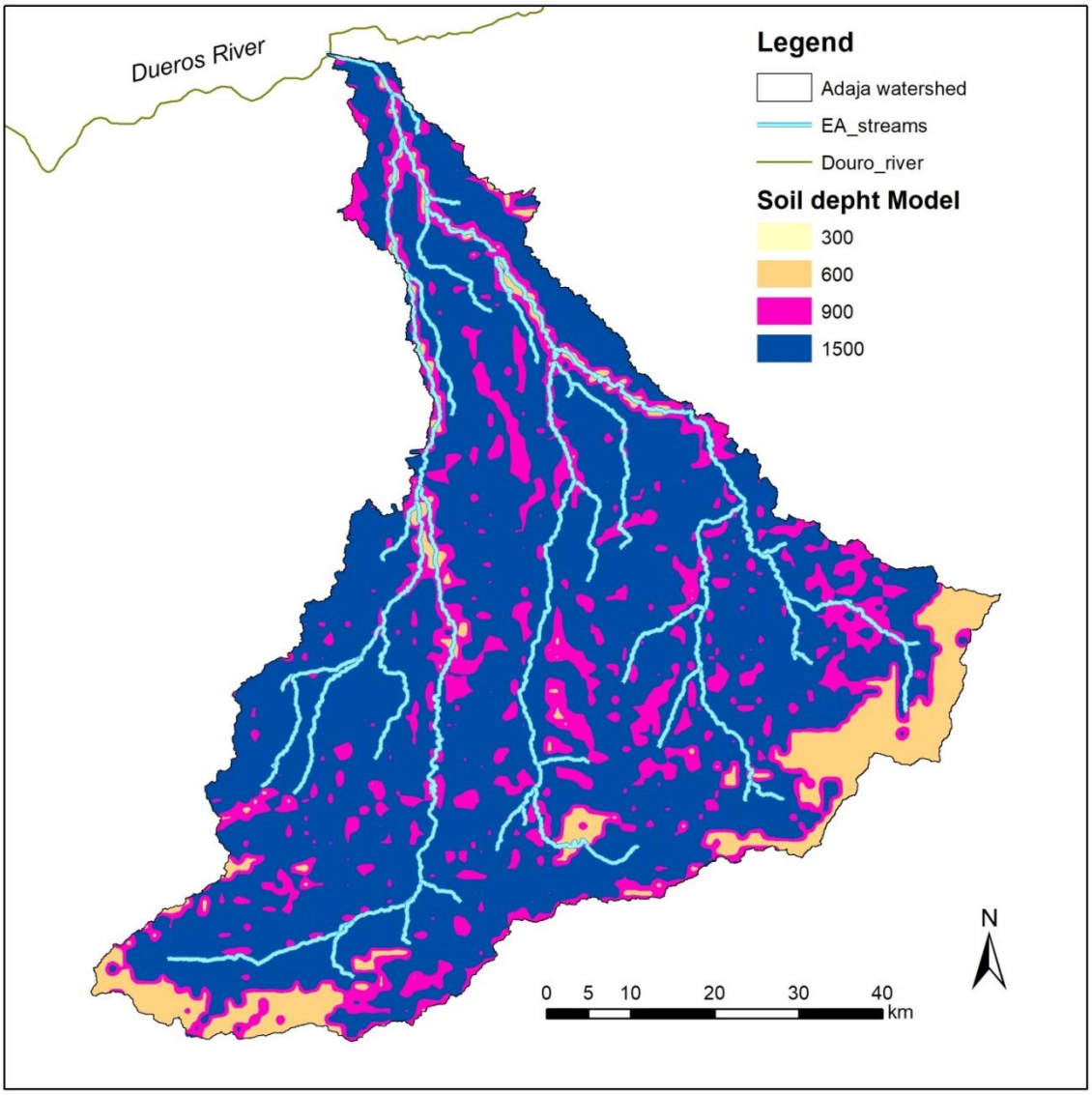

Annex 5. Google Earth Engine script to extract MOD13Q1 reflectance bands and Vegetation indices for SOM 5 and SOM15.

Script for SOM5 plots

```
var MOD13Q1 = ee.ImageCollection('MODIS/006/MOD13Q1').
        filterDate('2000-02-18', '2019-10-01').
        select('NDVI','EVI','sur_refl_b01', 'sur_refl_b02','sur_refl_b03','sur_refl_b07');
// Define a region of interest as a point.
var SOM15_5 = ee.Feature(
        ee.Geometry.Point(-4.942608705,      40.86418543), {'label': ' som15_5'});
var SOM15_9 = ee.Feature(
        ee.Geometry.Point(-4.949504594,      40.82555542), {'label': ' som15_9'});
var SOM15_12 = ee.Feature(
        ee.Geometry.Point(-4.938772086,      40.83156543), {'label': ' som15_12'});
var SOM15_19 = ee.Feature(
        ee.Geometry.Point(-4.966845778,      40.8048759), {'label': ' som15_19'});
var SOM15_41 = ee.Feature(
        ee.Geometry.Point(-4.944333386,      40.85712406), {'label': ' som15_41'});
// Add to map point of interest
Map.addLayer(SOM15_5);
Map.addLayer(SOM15_9);
Map.addLayer(SOM15_12);
Map.addLayer(SOM15_19);
Map.addLayer(SOM15_41);
// Create and print the chart.
print(ui.Chart.image.series(MOD13Q1, SOM15_5),10000);
print(ui.Chart.image.series(MOD13Q1, SOM15_9),10000);
print(ui.Chart.image.series(MOD13Q1, SOM15_12),10000);
print(ui.Chart.image.series(MOD13Q1, SOM15_19),10000);
print(ui.Chart.image.series(MOD13Q1, SOM15_41),10000);
```

Script for SOM15 plots

```
// Load MOD13Q1 product input imagery.
var MOD13Q1 = ee.ImageCollection('MODIS/006/MOD13Q1').
        filterDate('2000-02-18', '2019-10-01').
        select('NDVI','EVI','sur_refl_b01', 'sur_refl_b02','sur_refl_b03','sur_refl_b07');
// Define a region of interest as a point.
var SOM15_13 = ee.Feature(
        ee.Geometry.Point(-4.224098023, 41.06509693), {'label': ' som15_13'});
var SOM15_15 = ee.Feature(
        ee.Geometry.Point(-4.224782776, 41.0750117),  {'label': ' som15_15'});
var SOM15_16 = ee.Feature(
        ee.Geometry.Point(-4.226666651, 41.08117623), {'label': ' som15_16'});
var SOM15_17 = ee.Feature(
        ee.Geometry.Point(-4.233210781, 41.07385135), {'label': ' som15_17'});
var SOM15_23 = ee.Feature(
        ee.Geometry.Point(-4.244248046, 41.06830756), {'label': ' som15_23'});
// Add to map point of interest
Map.addLayer(SOM15_13);
Map.addLayer(SOM15_15);
Map.addLayer(SOM15_16);
Map.addLayer(SOM15_17);
Map.addLayer(SOM15_23);
```

```
// Create and print the chart.
print(ui.Chart.image.series(MOD13Q1, SOM15_13),10000);
print(ui.Chart.image.series(MOD13Q1, SOM15_15),10000);
print(ui.Chart.image.series(MOD13Q1, SOM15_16),10000);
print(ui.Chart.image.series(MOD13Q1, SOM15_17),10000);
print(ui.Chart.image.series(MOD13Q1,                                    SOM15_23)
```

Annex 6. Detailed crop management operations of Cega-Eresma-Adaja (CEA) case study.

Land use crop	SWAT Landuse code	Planting Date	Tillage operation name	Tillage date	Auto-Fertilization initial date	Fertilizer composition	Fertilizer total amount	Harvest operation date
Winter Wheat	WWHT	08-dec	Fallplow	03-dec	12-oct	27-00-00	350 kg	28-jul
			Field Cultivator Lt15ft	05-dec				
			Roller Packer Flat Roller	07-dec				
Barley	BARL	25-feb	Fallplow	23-feb	24-feb	27-00-00	350 kg	21-jul
Maize	CORN	01-apr	Subsoil Chisel Plow	10-apr	06-may	08-15-15	1000 kg	15-sep
			Rotary Hoe	25-apr				
			Field Cultivator Lt15ft	25-may				
			Roller Packer Flat Roller	30-may				
Potato	POTA	16-apr	Generic Spring Plowing Operation	05-apr	04-apr	08-15-15	1000 kg	22-aug
			Field Cultivator Lt15ft	09-apr				
			Bedder disk-row	12-apr				
			Beet cultivator 8 row	14-apr				
Sugar beet	SGBT	01-mar	Generic Spring Plowing Operation	20-feb	01-mar	27-00-00	1200 kg	15-may
			Field Cultivator Lt15ft	27-feb				
			Disk Plow Lt23ft	28-feb				
Sunflower	SUNF	25-apr	Springtooth Harrow Ge15ft	23-mar	22-mar	08-15-15	600 kg	02-sep
Alfalfa	ALFA	01-oct	Fallplow	04-oct	02-oct	00-20-20	200 kg	05-may
								05-jun
								01-jul
								05-aug
								01-sep
								30-sep
Horticulture	HORT	03-mar	Fallplow	02-mar	01-mar	Elem-N	500 kg	01-aug
Aromatic herbs	AROM	15-feb	Fallplow	02-mar	04-mar	Elem-N	500 kg	01-aug
Peas	PEAS	15-nov	Fallplow	14-feb	13-feb	Elem-N	300 kg	01-jul
Canola	CANA	06-oct	Fallplow	16-oct	17-oct	08-15-15	250 kg	20-jul
Olives	OLIV	already planted	Sprgplow	02-mar	01-mar	Elem-N	250 kg	15-oct
Vineyard	GRAP	already planted	Sprgplow	15-mar	13-apr	Elem-N	250 kg	15-aug

Annex 7. Participatory scenario process

The use of this participatory scenario approach is intended to create the bridge, between global LU narratives and the local context in which LU decisions take place. Such approach also allows translating and simulating through modelling tools, a more accurate water balance components quantification. The main purpose of these participatory scenarios is to translating narrative scenarios into quantitative assessment of the LU scenario, as well as to assess the stakeholder perception for plausible future use of land at the local context showing the contrasting results to current LU patterns.

Workshop and stakeholder composition group

The workshop was held on November 28th 2016, in the town of Coca (Segovia), located in the study area and selected for its proximity to the location where most participants resided or worked. It was designed and developed by two external facilitators (the first two authors of this report) in close collaboration with the UPM team. Additionally, two external rapporteurs were hired to provide support in taking notes during the event. Participants were selected by the TALE technical team in close collaboration with the two external facilitators, using as main selection criteria their in-depth knowledge of the study area and the search for a well-balanced diversity of interests and expertise. Invitations were sent by email and follow-up phone calls conducted as needed. The workshop was attended by 24 people including: 3 participants from the Duero River Basin Authority (RBA), 2 from the Castilla y León regional agricultural authority, 4 irrigators or members of irrigator farmer associations, 2 rainfed farmers members of farming associations, 2 from the Castilla y León regional environmental authority, 3 environmental agents, 3 members of regional or national environmental groups, 2 representatives of municipalities located in the CEA region, and 3 members of Academia. The event was hosted in a facility made available by the Municipality of Coca and received the explicit support of the Duero RBA (the study is located within the Duero River Basin). The organizing team included three facilitators and three rapporteurs.

Narratives and outcomes

A summarized description for the three scenarios is described as follows.

- Scenario LSH (Land Sharing)

  The scenario drivers related with LULC for LSH were highlighted by the adoption of pastures and shrubs over the abandoned agricultural parcels due of non-productive characteristics and the transitory suppression of fallow in the crop rotation annual scheme keeping as a permanent condition. Also, reductions of fertilization amounts were globally reduced in a 30% for N and 10% for P. The LULC were conducted specifically using protocol rules for middle part of CEA system.

- Scenario LSP (Land Sparing)

  The LSP scenario was highlighted by the privileging of a specialized agriculture, a more intensive agriculture. Those areas follow strategies oriented to increase water efficiency producing more with fewer resources. A lightly augmentation of irrigation areas was defined at the expense of higher abandon non-productive parcels. An agricultural land concentration of irrigated parcels and rainfed crops around municipal headers were defined, trying to optimize the efforts of high-tech practices and infrastructures in time and costs. The LULC were conducted specifically using the defined protocol rules for middle part of CEA system.

- Scenario LBA (Land Balance)

  The LBA scenario was considered as a consensus between the maintaining of agricultural rainfed practices in most of the area but a remarkable need to attend external demand of horticulture, the augmentation of irrigation efficiency as a good practice and the suppression of fallow from rotation scheme of non/productive parcels and let them fall in natural recover of vegetated surface (mosaic of spontaneous pastures and shrubs).

During the workshop, the LU factors associated to trade-offs between the agricultural landscapes, food production and biodiversity in a 10 year's horizon were jointly discussed, fulfilling the WFD (Water Framework Directive) targets following each of the storylines. The three local scenarios were drafted by stakeholders making use of basin maps as template to allocate the major LU change of the basin and the associated land management practices to each LU change, Figure A1.

LU maps from drafting from baseline scenario to each narrative.

The scenario comparison is possible considering the following elements : i) a stakeholder workshop formed by experts in resources management, agriculture, administration and regional planning, ii) a standardized protocol (Patel et al., 2007) developed and adapted to local circumstance for TALE consortium (Hagemann et al., 2019; Karner et al., 2019) as guideline for scenario building, iii) using common model biophysical elements as weather regime, time simulation and soils and, iv) the stakeholder validation feedback. However, complete missing information, qualitative to quantitative, requires that technical modeler's uses complimentary

information as planning documents to infer plausible targets and allocate them spatially. The LULC scenarios and its spatial arrangements were conducted for the CEA system thought a mapping activity. The workshop final results were the creation of LULC reference maps for each storyline which in turn the latter were used in this work for setting up each scenario for modelling.

In sub-basin 443, through the three scenarios were considered that there was no significant augmentation of urban-transportation and forest areas. For this reason, urban-transportation and forest LU's were considered as static area whereas the agricultural and semi-natural (pastures and shrubs) were considered as more dynamical land. The focus of this reasoning was foreseen inferring the environmental effect of LULC and land management at sub-basin scale.

With the aim to compare scenarios with a realistic approach, a baseline scenario was defined, in which the calibration and validation were assessed. The effort of compare physically the scenario modelling performance, were developed upgrading the parameters from calibration sensitivity ranking to make it transferable before assessing results for LSH, LBA and LSP scenarios.

Once the LU reference maps have been defined (Baseline, LSH. LBA and LSP), the maps were validated through a survey to the same group of stakeholders. The modelling structure needs to be spatially coincident for comparisons and analysis. Thus, a spatial unit was established to allow the spatial direct comparison. The spatial unit selected was the Hydrologic Response Unit (HRU) of SWAT model. The model set-up is detailed in section 2.3.

Annex 8. Soil database for SWAT model using the Kriging strategy for soil properties assignation to taxonomic units of ITACyL soil map (TSU) al 1:400,000 scale.

MUID	S5ID	NLAYERS	HYDGRP	SOL_ZMX	SOL_Z1	SOL_BD1	SOL_AWC1	SOL_K1	SOL_CBN1	CLAY1	SILT1	SAND1	ROCK1	SOL_ALB1	USLE_K1
50000	ITACYL	1	B	1300	300	1.38013	0.107845	7.89307	1	27.1017	19.5217	53.3766	0	0.024503	0.142798
50001	ITACYL	1	A	1256	300	1.8563	0.077623	65.2473	1	9.02159	18.0901	72.9673	0	0.024503	0.142798
50002	ITACYL	1	A	1350	300	1.39177	0.084943	18.4875	1.012488	19.5751	14.3669	66.058	0	0.032286	0.149578
50003	ITACYL	1	A	1300	300	1.73977	0.08313	56.1983	1.645349	9.12188	19.95892	70.9192	0	0.009429	0.164496
50004	ITACYL	1	A	300	300	1.79244	0.079341	106.011	1.018157	3.9175	22.1475	73.935	0	0.031932	0.170777
50005	ITACYL	1	A	1227	300	1.61227	0.104359	18.414	1.192797	20.3898	22.2722	57.338	0	0.022736	0.161809
50006	ITACYL	1	A	1300	300	1.21697	0.101756	13.2898	0.496904	22.1962	20.4581	57.3457	0	0.088	0.159561
50007	ITACYL	1	A	300	300	1.65743	0.093959	36.428	0.821163	12.3354	20.9166	66.748	0	0.046839	0.168494
50008	ITACYL	1	A	300	300	1.98966	0.092247	54.1825	0.609506	9.43645	24.79245	65.7711	0	0.070693	0.177081
50009	ITACYL	1	A	300	300	1.72884	0.102354	28.2749	0.500233	14.8961	25.1791	59.9248	0	0.087432	0.172518
50010	ITACYL	1	A	300	300	0.940075	0.127755	9.34198	1.143238	25.7975	31.385	42.8175	0	0.025037	0.164908
50011	ITACYL	1	B	300	300	0.992624	0.133468	4.51901	2.616279	19.8615	17.8806	62.2579	0	0.001427	0.155781
50012	ITACYL	1	B	300	300	1.13122	0.124694	6.54603	0.86661	28.6659	28.4833	42.8508	0	0.042877	0.161471
50013	ITACYL	1	A	1050	300	1.21317	0.099661	18.281	0.480899	18.9804	22.2056	58.814	0	0.090782	0.165033
50014	ITACYL	1	A	1033	300	1.32442	0.101033	15.2684	0.729081	21.8287	20.3345	57.8368	0	0.056025	0.159417
50015	ITACYL	1	B	300	300	1.12441	0.105043	7.44492	1.36282	27.1592	17.4889	55.3519	0	0.016335	0.148063
50016	ITACYL	1	B	300	300	1.11526	0.139108	4.27834	1.119849	31.963	36.9462	31.0908	2.2989	0.026202	0.16394
50017	ITACYL	1	A	300	300	1.93787	0.104926	89.9006	0.968953	2.5099	34.0527	63.4374	0	0.035138	0.191547
50018	ITACYL	1	A	300	300	1.79255	0.074783	126.098	1.141302	2.84839	19.56451	77.5871	0	0.025131	0.157286
50019	ITACYL	1	A	300	300	1.73783	0.068654	150.605	1.426326	0.811042	16.96986	82.2191	0	0.014437	0.135877
50020	ITACYL	1	A	300	300	1.74475	0.09454	103.065	0.884814	2.27411	29.38369	68.3422	0	0.041385	0.187341
50021	ITACYL	1	A	300	300	1.76499	0.091693	114.582	0.626773	1.61303	27.48067	70.9063	0	0.068359	0.184638
50022	ITACYL	1	A	1500	300	1.3955	0.082486	20.5583	0.720907	18.7052	13.8835	67.4113	0	0.056923	0.149551
50023	ITACYL	1	A	300	300	1.14053	0.08307	29.7884	0.768576	15.899	16.1948	67.9062	0	0.051883	0.15675
50024	ITACYL	1	A	1269	300	1.19302	0.106567	10.1425	0.883878	26.4886	19.7268	53.7846	0	0.041461	0.153721
50025	ITACYL	1	A	300	300	1.30067	0.087666	23.2158	1.459099	18.7406	14.6744	66.585	0	0.013546	0.149302
50026	ITACYL	1	A	1350	300	1.62845	0.078566	42.1971	1.180337	16.3743	12.319	71.3067	0	0.023294	0.144006

MUID	S5ID	NLAYERS	HYDGRP	SOL_ZMX	SOL_Z1	SOL_BD1	SOL_AWC1	SOL_K1	SOL_CBN1	CLAY1	SILT1	SAND1	ROCK1	SOL_ALB1	USLE_K1
50027	ITACYL	1	B	300	300	1.2802	0.11354	4.50946	2.057291	31.564	19.7333	48.7027	0	0.004232	0.146396
50028	ITACYL	1	A	814	300	1.36143	0.073787	42.6118	0.904919	12.4822	15.0989	72.4189	0	0.039799	0.153165
50029	ITACYL	1	A	1227	300	2.03046	0.084377	60.5134	0.755262	8.87672	21.75188	69.3714	0	0.053244	0.171887
50030	ITACYL	1	A	300	300	1.19464	0.086785	18.3691	0.624651	19.6875	16.5925	63.72	1.8349	0.068641	0.152406
50031	ITACYL	1	A	300	300	1.24701	0.086065	20.0917	0.831634	18.6464	15.0197	66.3339	0	0.045895	0.152292
50032	ITACYL	1	A	1500	300	1.20001	0.096986	9.50311	0.746895	27.499	14.3611	58.1399	0	0.054117	0.143856
50033	ITACYL	1	A	300	300	1.12702	0.080036	23.7191	1.205994	17.5964	14.0997	68.3039	1.6393	0.02216	0.146032
50034	ITACYL	1	A	1200	300	1.6174	0.076881	104.902	3.410244	4.38309	17.57131	78.0456	0	0.000305	0.148826
50035	ITACYL	1	A	1250	300	1.738639	0.08164	89.3936	1.617616	5.66669	19.68941	74.6439	0	0.009952	0.161385
50036	ITACYL	1	A	1248	300	1.62004	0.07713	96.529	2.304936	6.07521	17.37309	76.5517	0	0.002615	0.151901
50037	ITACYL	1	A	1317	300	1.6557	0.069725	124.652	2.300465	3.43321	16.59269	79.9741	0	0.002637	0.141415
50038	ITACYL	1	A	1288	300	1.7238	0.064042	151.352	0.928971	1.12911	15.77479	83.0961	0	0.03798	0.131483
50039	ITACYL	1	A	1150	300	1.69813	0.087271	93.2526	1.180366	4.29966	23.96034	71.74	0	0.023293	0.175159
50040	ITACYL	1	A	300	300	1.21758	0.101475	21.4308	3.249901	20.375	17.7584	61.8666	0	0.000416	0.153332
50041	ITACYL	1	A	300	300	1.02896	0.104963	10.0231	5.041465	25.6379	18.1902	56.1719	0	1.28E-05	0.149197
50042	ITACYL	1	A	300	300	1.01423	0.096496	14.3393	4.476709	22.4363	17.0087	60.555	0	3.83E-05	0.150197
50043	ITACYL	1	A	1350	300	1.50556	0.103629	28.174	2.613581	17.8614	20.3012	61.8374	0	0.001435	0.159612
50044	ITACYL	1	A	1300	300	1.19529	0.082845	13.5549	2.692081	23.3875	7.7658	68.8467	0	0.001231	0.123277
50045	ITACYL	1	A	300	300	1.8914	0.076921	116.819	1.677076	2.47956	19.05804	78.4624	0	0.008865	0.152237
50046	ITACYL	1	A	300	300	1.82	0.102399	51.0442	1.52907	7.98324	29.42166	62.5951	0	0.011822	0.180221
50047	ITACYL	1	A	1500	300	1.89677	0.100373	100.216	1.04964	2.26239	31.35541	66.3822	0	0.030035	0.189169
50048	ITACYL	1	A	1277	300	1.62334	0.107816	11.8453	2.644343	23.7961	22.6001	53.6038	0	0.001351	0.156783
50049	ITACYL	1	A	300	300	1.74522	0.098139	114.795	1.835878	1.80809	28.98721	69.2047	0	0.00651	0.183818
50050	ITACYL	1	A	300	300	1.75785	0.085847	44.9176	0.842355	12.2466	19.0519	68.7015	0	0.044948	0.164701
50051	ITACYL	1	A	300	300	1.83709	0.100634	25.6063	1.730895	17.4961	21.9423	60.5616	0	0.007984	0.162667
50052	ITACYL	1	A	300	300	1.88078	0.11177	31.9993	1.187919	14.5644	29.3804	56.0552	0	0.022953	0.174472
50053	ITACYL	1	A	300	300	1.84628	0.103929	54.9785	1.205326	9.62706	29.24134	61.1316	0	0.022189	0.179674
50054	ITACYL	1	A	300	300	1.92348	0.090656	78.4672	0.883157	5.61853	26.55587	67.8256	0	0.041519	0.181536
50055	ITACYL	1	A	300	300	1.27686	0.090952	43.3184	1.313256	12.0575	21.0717	66.8708	0	0.017988	0.16711
50056	ITACYL	1	A	300	300	1.81107	0.093672	39.6834	0.773488	12.0575	23.0008	64.9417	0	0.05139	0.171885
50057	ITACYL	1	A	300	300	1.43298	0.10072	28.0492	1.007442	15.5673	22.7934	61.6393	0	0.032604	0.167971

MUID	S5ID	NLAYERS	HYDGRP	SOL_ZMX	SOL_Z1	SOL_BD1	SOL_AWC1	SOL_K1	SOL_CBN1	CLAY1	SILT1	SAND1	ROCK1	SOL_ALB1	USLE_K1
50058	ITACYL	1	A	300	300	0.970133	0.081114	37.5747	2.810983	14.6479	13.6787	71.6734	0	0.000977	0.146093
50059	ITACYL	1	A	300	300	0.999547	0.093254	17.2511	0.967006	21.4192	14.66	63.9208	0	0.035272	0.149134
50060	ITACYL	1	A	300	300	0.927	0.123544	21.137	3.197674	20.0755	33.4626	46.4619	2.2222	0.000461	0.167923
50061	ITACYL	1	A	300	300	1.0799	0.09494	19.6638	1.088221	20.4066	16.7994	62.794	0	0.027864	0.153996
50062	ITACYL	1	A	300	300	1.79647	0.065141	143.914	0.485412	3.79731	13.80849	82.3942	0	0.089989	0.130103
50063	ITACYL	1	A	1484	300	1.46498	0.099624	10.7844	1.941209	24.5107	18.1246	57.3647	0	0.005304	0.150392
50064	ITACYL	1	A	1408	300	1.1654	0.099145	9.28116	0.759762	26.3758	16.1032	57.521	0	0.05278	0.148291
50065	ITACYL	1	A	1445	300	1.31134	0.087532	18.2864	0.694	21.8217	14.0866	64.0917	0	0.059981	0.148149
50066	ITACYL	1	A	1282	300	2.00283	0.094114	124.38	1.144814	0.625724	29.71038	69.6639	0	0.02496	0.187269
50067	ITACYL	1	A	300	300	1.55139	0.082378	35.1884	0.87657	15.5605	15.2726	69.1669	0	0.042054	0.154161
50068	ITACYL	1	A	300	300	1.95773	0.083283	104.615	0.7645	3.94572	22.80548	73.2488	0	0.052296	0.173279
50069	ITACYL	1	A	300	300	1.86156	0.107896	27.4105	0.944924	14.7865	27.5204	57.6931	0	0.036819	0.173792
50070	ITACYL	1	A	300	300	1.86156	0.101749	24.7715	0.789558	17.1728	23.6703	59.1569	0	0.049808	0.168069
50071	ITACYL	1	A	300	300	1.842	0.11731	39.3182	2.325581	10.2664	34.1091	55.6245	0	0.002512	0.179665
50072	ITACYL	1	A	300	300	1.88834	0.113525	24.1099	1.082203	16.0862	29.383	54.5308	0	0.028192	0.1733
50073	ITACYL	1	A	300	300	1.6713	0.080042	105.622	0.980994	4.82659	21.52541	73.648	0	0.034325	0.169244
50074	ITACYL	1	C	300	300	1.33977	0.127919	4.28656	1.264517	33.7709	27.4761	38.753	0	0.019776	0.155153
50075	ITACYL	1	C	1500	300	1.45308	0.097766	3.71178	0.25893	32.6767	8.3502	58.9731	0	0.139791	0.123289
50076	ITACYL	1	B	1267	300	1.35859	0.095018	5.90858	0.331206	29.2543	10.4151	60.3306	0	0.12146	0.132802
50077	ITACYL	1	A	300	300	1.7319	0.100204	87.4995	0.712145	2.90633	31.67627	65.4174	0	0.057901	0.190158
50078	ITACYL	1	A	300	300	1.59448	0.075076	120.308	0.720587	3.69418	20.70462	75.6012	0	0.056958	0.165531
50079	ITACYL	1	A	300	300	1.72081	0.109394	26.7733	0.826942	16.3162	26.6428	57.041	0	0.046316	0.171792
50080	ITACYL	1	A	300	300	1.23183	0.087429	19.8973	1.030558	20.2297	14.1822	65.5881	0	0.031171	0.148639
50081	ITACYL	1	A	300	300	1.97101	0.090659	15.7076	1.144	21.2319	14.4382	64.3299	0	0.025	0.148154
50082	ITACYL	1	A	300	300	1.24601	0.086199	20.9317	1.245994	20.1131	12.5581	67.3288	0	0.020502	0.143528
50083	ITACYL	1	A	300	300	1.14992	0.103486	17.0674	0.74036	20.6135	19.5531	59.8334	0	0.054809	0.159467
50084	ITACYL	1	A	300	300	1.25162	0.107737	21.0378	1.06411	18.9736	24.8667	56.1597	0	0.029202	0.166277
50085	ITACYL	1	B	300	300	1.09051	0.142786	7.138	1.095285	27.3845	38.9424	33.6731	0	0.027484	0.170023
50086	ITACYL	1	B	1335	300	1.37209	0.096443	5.21965	0.808209	30.3137	9.2842	60.4021	0	0.048034	0.127848
50087	ITACYL	1	A	1500	300	1.54529	0.079734	16.6822	0.52581	20.8712	10.6629	68.4659	0	0.083189	0.138812
50088	ITACYL	1	A	1140	300	1.573	0.080882	17.6511	0.154115	19.908	12.7363	67.3557	0	0.171399	0.146162

MUID	S5ID	NLAYERS	HYDGRP	SOL_ZMX	SOL_Z1	SOL_BD1	SOL_AWC1	SOL_K1	SOL_CBN1	CLAY1	SILT1	SAND1	ROCK1	SOL_ALB1	USLE_K1
50089	ITACYL	1	A	300	300	1.01357	0.111247	15.5124	1.194186	20.9973	24.9801	54.0226	0	0.022675	0.164098
50090	ITACYL	1	B	300	300	1.0832	0.131716	4.80997	1.398983	31.6066	32.1391	36.2543	1.3157	0.015226	0.159409
50091	ITACYL	1	A	300	300	1.12976	0.118233	10.5767	1.024802	24.842	27.5622	47.5958	0	0.031522	0.162825
50092	ITACYL	1	B	300	300	0.984469	0.14149	6.19673	1.338581	26.7118	41.7283	31.5599	6.4516	0.017123	0.167502
50093	ITACYL	1	A	1500	300	1.34251	0.070164	38.4862	0.491547	13.9317	11.6839	74.3844	0	0.088922	0.141031
50094	ITACYL	1	A	300	300	1.17213	0.078384	29.7934	1.40986	17.8785	13.0429	69.0786	0	0.014907	0.145248
50095	ITACYL	1	A	1300	300	1.264	0.086915	19.4502	0.803052	19.8551	14.8392	65.3057	0	0.048518	0.151146
50096	ITACYL	1	A	300	300	1.80251	0.103489	23.3149	1.23507	17.7148	23.9905	58.2947	0	0.020942	0.166264
50097	ITACYL	1	A	1092	300	1.28703	0.106778	12.028	0.981233	25.5313	20.832	53.6367	0	0.034309	0.155813
50098	ITACYL	1	A	300	300	1.2799	0.093958	27.3991	1.166198	18.2169	18.909	62.8741	0	0.023943	0.159327
50099	ITACYL	1	A	300	300	1.09811	0.09966	17.5846	1.199808	20.5313	19.4462	60.0225	0	0.022428	0.156677
50100	ITACYL	1	A	1171	300	1.18309	0.098238	13.5597	0.639872	22.8378	18.4053	58.7569	0	0.066639	0.155955
50101	ITACYL	1	A	300	300	1.3	0.105829	18.1721	1.744186	20.7173	20.5258	58.7569	0	0.007781	0.157688
50102	ITACYL	1	A	300	300	1.31053	0.11225	16.5094	2.512209	21.1708	24.2032	54.626	0	0.001747	0.161054
50103	ITACYL	1	A	1300	300	1.36472	0.116011	14.9955	1.663855	22.4986	25.2749	52.2265	0	0.009096	0.161426
50104	ITACYL	1	A	1260	300	1.19931	0.114943	5.64103	3.369064	30.2271	21.0918	48.6811	0	0.00033	0.149161
50105	ITACYL	1	A	1260	300	1.42781	0.048439	106.996	0.771709	4.64217	7.59153	87.7663	0	0.051568	0.094407
50106	ITACYL	1	A	1450	300	1.65014	0.070906	67.624	2.676762	10.212	14.1096	75.6784	0	0.001269	0.143934
50107	ITACYL	1	A	1267	300	1.86201	0.054171	157.537	0.78936	2.79406	9.96934	87.2366	0	0.049828	0.10409
50108	ITACYL	1	A	995	300	1.64897	0.08508	29.9366	1.364773	15.6646	17.0177	67.3177	0	0.016273	0.156791
50109	ITACYL	1	A	1118	300	1.94752	0.058211	101.297	0.63336	6.11157	10.65123	83.2372	0	0.067488	0.116804
50110	ITACYL	1	A	300	300	1.94315	0.050633	114.833	0.703733	3.5274	6.8216	89.651	0	0.058856	0.089105
50111	ITACYL	1	A	300	300	1.84791	0.063917	93.7348	0.590552	6.59214	14.03586	79.372	0	0.073348	0.139122
50112	ITACYL	1	A	300	300	1.92632	0.04638	106.838	0.611343	5.29489	5.92541	88.7797	0	0.070441	0.086366
50113	ITACYL	1	A	1500	300	1.86075	0.043543	108.77	0.463405	4.62241	3.35569	92.0219	0	0.093924	0.072069
50114	ITACYL	1	A	1187	300	1.66576	0.093723	45.6255	1.134651	16.83	20.3131	62.8569	0	0.025458	0.16302
50115	ITACYL	1	A	300	300	1.91587	0.056751	97.1987	0.450708	4.97023	10.94087	84.0889	0	0.096272	0.115185
50116	ITACYL	1	A	300	300	1.80639	0.04931	91.5947	0.137915	6.23308	7.27192	86.495	0	0.176885	0.096055
50117	ITACYL	1	A	1500	300	1.51248	0.07052	27.8898	0.471474	16.4553	9.1459	74.3988	0	0.092461	0.131041
50118	ITACYL	1	A	300	300	1.71693	0.053175	68.0912	0.471344	9.12229	7.08231	83.7954	0	0.092485	0.101867
50119	ITACYL	1	B	1267	300	1.3991	0.093448	6.78242	0.89907	29.0447	8.7539	62.2014	0	0.040254	0.126743

MUID	S5ID	NLAYERS	HYDGRP	SOL_ZMX	SOL_Z1	SOL_BD1	SOL_AWC1	SOL_K1	SOL_CBN1	CLAY1	SILT1	SAND1	ROCK1	SOL_ALB1	USLE_K1
50120	ITACYL	1	A	1500	300	1.45273	0.085825	16.1209	1.916459	22.1638	10.8486	66.9876	0	0.005565	0.135832
50121	ITACYL	1	C	300	300	1.28215	0.111545	3.93585	1.277448	32.8813	17.4839	49.6348	0	0.019285	0.143356
50122	ITACYL	1	A	1500	300	1.72197	0.077972	33.6533	1.026459	16.1854	12.8562	70.9584	0	0.03142	0.146031
50123	ITACYL	1	A	600	300	1.3536	0.087079	32.5398	3.235436	15.6509	16.8409	67.5082	0	0.000428	0.154971
50124	ITACYL	1	A	921	300	1.40233	0.092624	22.5064	1.67039	17.8993	18.8084	63.2923	0	0.008981	0.157867
50125	ITACYL	1	A	1500	300	1.30759	0.119344	9.46553	2.537384	26.4729	25.3129	48.2142	0	0.001664	0.157181
50126	ITACYL	1	A	1164	300	1.42874	0.108008	17.5052	2.260593	21.7199	21.7319	56.5482	0	0.00285	0.157837
50127	ITACYL	1	B	1274	300	1.31553	0.102385	6.93371	1.229523	28.5897	14.1686	57.2417	0	0.021169	0.141065
50128	ITACYL	1	A	300	300	1.38631	0.117491	9.53141	1.572215	25.2175	26.1124	48.6701	1.5384	0.010871	0.158423
50129	ITACYL	1	A	300	300	1.83053	0.06389	71.6772	0.670488	7.50209	13.00511	79.4928	0	0.062787	0.135459
50130	ITACYL	1	A	1133	300	1.98594	0.063491	117.195	1.052936	3.66393	13.97427	82.3618	0	0.029843	0.128834
50131	ITACYL	1	A	1500	300	1.71599	0.079154	58.4708	1.364971	9.25284	17.75996	72.9872	0	0.016267	0.158722
50132	ITACYL	1	A	1140	300	2.00699	0.078109	53.6288	0.760413	9.89256	17.72154	72.3859	0	0.052713	0.161263
50133	ITACYL	1	A	1350	300	1.66859	0.07049	114.48	0.905215	2.94177	17.82213	79.2361	0	0.039776	0.149161
50134	ITACYL	1	A	1100	300	1.84181	0.079023	57.3554	0.927413	9.26061	18.56369	72.1757	0	0.038095	0.16303
50135	ITACYL	1	A	300	300	1.80312	0.080064	63.6489	1.183994	8.21967	19.12063	72.6597	0	0.023129	0.163229
50136	ITACYL	1	A	1270	300	1.89147	0.075047	60.3333	0.923762	9.62598	16.51052	73.8635	0	0.038366	0.156187
50137	ITACYL	1	A	300	300	1.81243	0.073152	69.1115	0.975227	8.1537	15.6825	76.1638	0	0.034712	0.150475
50138	ITACYL	1	A	300	300	1.77287	0.067254	67.7999	0.833006	7.80391	14.40089	77.7952	0	0.045773	0.143758
50139	ITACYL	1	A	300	300	1.65745	0.092225	68.4971	1.048727	6.30223	25.85687	67.8409	0	0.030089	0.179382
50140	ITACYL	1	A	300	300	1.76848	0.059386	123.075	0.733448	3.49642	13.15888	83.3447	0	0.055551	0.124098
50141	ITACYL	1	A	300	300	1.89864	0.085945	87.0096	0.982453	4.77359	23.93551	71.2909	0	0.034228	0.176118
50142	ITACYL	1	A	300	300	1.75598	0.056105	128.202	0.704116	3.94737	12.27283	83.7798	0	0.058812	0.120037
50143	ITACYL	1	A	1347	300	1.49503	0.097247	12.1418	1.340669	24.5246	15.0655	60.4099	0	0.017054	0.146113
50144	ITACYL	1	A	1357	300	1.55565	0.102356	8.93943	0.384727	25.8743	17.8557	56.27	0	0.109453	0.152249
50145	ITACYL	1	A	1332	300	1.37664	0.088723	11.6459	0.637308	27.3449	9.0898	63.5653	0	0.066972	0.129627
50146	ITACYL	1	A	1192	300	1.42915	0.088775	17.5281	0.75232	22.403	12.9513	64.6457	0	0.053549	0.144755
50147	ITACYL	1	A	300	300	1.2629	0.095156	11.2534	1.86475	24.8868	14.3406	60.7726	0	0.006154	0.143198
50148	ITACYL	1	A	1239	300	1.43446	0.062717	43.8682	0.564351	14.1961	7.8989	77.905	0	0.077182	0.120222
50149	ITACYL	1	A	300	300	0.962232	0.124448	17.6395	0.636942	21.9003	32.4031	45.6966	0	0.06702	0.170125
50150	ITACYL	1	A	300	300	1.10627	0.104912	15.1651	0.641715	21.6172	20.0478	58.335	0	0.066401	0.159384

MUID	S5ID	NLAYERS	HYDGRP	SOL_ZMX	SOL_Z1	SOL_BD1	SOL_AWC1	SOL_K1	SOL_CBN1	CLAY1	SILT1	SAND1	ROCK1	SOL_ALB1	USLE_K1
50151	ITACYL	1	A	300	300	0.913757	0.134177	8.2638	1.027942	25.6355	35.1313	39.2332	0	0.03133	0.167915
50152	ITACYL	1	B	300	300	1.07137	0.128049	8.18784	0.867919	25.8001	31.2776	42.9223	1.5385	0.042768	0.164992
50153	ITACYL	1	B	300	300	0.913757	0.141897	6.13008	1.51575	24.1556	47.6327	28.2117	15.7895	0.012132	0.167352
50154	ITACYL	1	C	300	300	1.07137	0.144648	4.08229	1.470901	34.1341	38.6472	27.2187	0	0.013238	0.165695
50155	ITACYL	1	B	300	300	1.13934	0.13204	4.69036	1.022517	31.0083	33.0339	35.9578	2.0408	0.031662	0.161455
50156	ITACYL	1	B	1433	300	1.38744	0.093988	6.82293	1.017756	28.3765	9.7755	61.848	0	0.031957	0.130423
50157	ITACYL	1	A	1500	300	1.3707	0.086322	9.61687	0.5558	26.8181	7.9136	65.2683	0	0.078476	0.12549
50158	ITACYL	1	A	1100	300	1.64182	0.076261	23.7973	0.239272	18.14	12.728	69.132	0	0.145239	0.146734
50159	ITACYL	1	A	1219	300	1.53965	0.08025	31.2703	0.672331	18.7237	12.3506	68.9257	0	0.062562	0.145019
50160	ITACYL	1	C	1300	300	1.36978	0.110447	2.79538	0.895965	34.9883	15.005	50.0067	0	0.040498	0.137657
50161	ITACYL	1	A	300	300	1.56	0.087	17.25	2.034884	20	39.6633	40.3367	25.4633	0.004421	0.14991
50162	ITACYL	1	A	1350	300	1.39468	0.09594	14.3786	1.114273	22.9669	15.345	61.6881	0	0.026488	0.148839
50163	ITACYL	1	A	1500	300	1.36368	0.098739	10.9561	2.337808	24.1391	17.2942	58.5667	0	0.002453	0.149207
50164	ITACYL	1	A	1267	300	1.39823	0.107016	11.8968	2.264419	24.7626	19.997	55.2404	0	0.002829	0.15271
50165	ITACYL	1	B	1500	300	1.63053	0.104449	6.724	0.332763	27.5564	17.858	54.5856	0	0.121093	0.150716
50166	ITACYL	1	B	1332	300	1.4726	0.098861	7.51071	1.275895	27.1062	15.5177	57.3761	0	0.019343	0.144926
50167	ITACYL	1	A	1442	300	1.61901	0.095646	14.6294	0.65275	23.2481	16.4344	60.3175	0	0.064991	0.151964
50168	ITACYL	1	A	300	300	1.19204	0.08563	19.8021	1.322599	19.355	14.7097	65.9353	0	0.017664	0.14945
50169	ITACYL	1	A	300	300	1.05459	0.094286	17.6199	1.023145	20.6055	18.0893	61.3052	0	0.031624	0.156357
50170	ITACYL	1	A	300	300	1.19416	0.089877	19.9101	1.259163	19.0359	16.8013	64.1628	0	0.019983	0.154481
50171	ITACYL	1	A	300	300	1.15463	0.074543	37.5846	1.339052	13.6698	14.5517	71.7785	1.2987	0.017108	0.148162
50172	ITACYL	1	A	1200	300	1.91228	0.07394	74.8907	0.992047	7.34029	16.97041	75.6893	0	0.033595	0.15486
50173	ITACYL	1	A	1307	300	1.68474	0.045975	52.9508	1.734779	13.1934	12.5442	74.2624	0	0.007924	0.141142
50174	ITACYL	1	A	1260	300	1.86234	0.058847	92.7159	1.366756	6.52372	9.63598	83.8403	0	0.01621	0.109856
50175	ITACYL	1	A	1200	300	1.85635	0.067093	89.0128	0.90682	6.28856	14.17284	79.5386	0	0.039652	0.138387
50176	ITACYL	1	A	1200	300	1.74182	0.078495	46.5602	1.021977	11.8543	16.5729	71.5728	0	0.031696	0.15747
50177	ITACYL	1	A	1329	300	1.70066	0.079883	40.9363	1.035331	12.8805	16.2831	70.8364	0	0.030883	0.156743
50178	ITACYL	1	A	1200	300	1.90574	0.080904	29.7982	0.730424	15.2829	15.3379	69.3792	0	0.055879	0.15475
50179	ITACYL	1	A	1250	300	1.87245	0.07233	44.9844	0.793884	12.0921	13.3292	74.5787	0	0.049391	0.146052
50180	ITACYL	1	A	1308	300	1.87244	0.06671	90.5652	0.938308	6.03222	14.64848	79.3193	0	0.037296	0.140333
50181	ITACYL	1	A	1320	300	2.02898	0.061636	103.18	0.553963	5.14672	14.06298	80.7903	0	0.078757	0.134998

MUID	S5ID	NLAYERS	HYDGRP	SOL_ZMX	SOL_Z1	SOL_BD1	SOL_AWC1	SOL_K1	SOL_CBN1	CLAY1	SILT1	SAND1	ROCK1	SOL_ALB1	USLE_K1
50182	ITACYL	1	A	1253	300	2.10727	0.05552	136.965	0.548681	3.48515	11.19155	85.3233	0	0.07957	0.11276
50183	ITACYL	1	A	300	300	1.67633	0.063818	94.9688	0.721093	5.45606	14.11774	80.4262	0	0.056902	0.136196
50184	ITACYL	1	A	1500	300	1.96885	0.051666	128.387	0.584395	5.5188	8.3402	86.141	0	0.074231	0.101329
50185	ITACYL	1	A	1288	300	1.75339	0.094632	108.403	1.367157	1.86021	29.30129	68.8385	0	0.016198	0.185366
50186	ITACYL	1	A	1300	300	1.88707	0.081792	108.231	0.584605	3.34362	23.10468	73.5517	0	0.074201	0.173946
50187	ITACYL	1	A	1300	300	1.81627	0.070634	67.1099	0.70675	8.03014	15.68136	76.2885	0	0.058512	0.150923
50188	ITACYL	1	A	1257	300	1.87951	0.082914	119.099	1.084093	2.12726	24.56074	73.312	0	0.028089	0.176025
50189	ITACYL	1	A	300	300	1.8109	0.082128	72.5529	1.146262	6.58026	20.77114	72.6486	0	0.02489	0.167516
50190	ITACYL	1	A	300	300	1.80934	0.064449	82.1204	1.013273	6.82683	13.31297	79.8602	0	0.032237	0.134599
50191	ITACYL	1	A	300	300	1.6	0.084973	121.085	2.034884	1.81135	23.72225	74.4664	0	0.004421	0.17038
50192	ITACYL	1	A	300	300	1.90421	0.058547	125.31	0.665669	4.45079	13.64121	81.908	0	0.063378	0.131183
50193	ITACYL	1	A	300	300	1.55719	0.084193	105.189	1.241297	3.75859	23.56231	72.6791	0	0.02069	0.174081
50194	ITACYL	1	A	1500	300	1.36627	0.095561	17.7494	1.4565	22.0184	17.4897	60.4919	0	0.013614	0.152509
50195	ITACYL	1	B	300	300	1.3539	0.107129	6.69666	1.308669	26.6471	22.7662	50.5867	6.3492	0.018149	0.147303
50196	ITACYL	1	B	300	300	1.264	0.107761	4.52573	2.083552	30.9475	16.9253	52.1272	1.0638	0.004021	0.140806
50197	ITACYL	1	A	300	300	1.16794	0.089063	18.3386	1.20468	19.578	16.5965	63.8255	0	0.022217	0.153087
50198	ITACYL	1	A	1224	300	1.13945	0.094559	13.805	0.889064	22.8597	15.9289	61.2114	0	0.041045	0.150839
50199	ITACYL	1	A	1173	300	1.41349	0.073566	32.9554	0.517117	14.7345	13.106	72.1595	0	0.084608	0.147621
50200	ITACYL	1	A	300	300	1.86965	0.066616	86.2501	1.024523	5.93544	15.34636	78.7182	0	0.031539	0.143683
50201	ITACYL	1	A	300	300	1.76778	0.061129	103.579	0.914326	5.17872	12.65898	82.1623	0	0.039077	0.125948
50202	ITACYL	1	A	1131	300	1.50944	0.096479	21.9261	2.446558	21.4876	15.8053	62.7071	0	0.001985	0.148815
50203	ITACYL	1	A	1500	300	2.04533	0.069929	66.1459	0.409017	7.9557	15.2027	76.8416	0	0.104403	0.148804
50204	ITACYL	1	A	1200	300	2.00394	0.061118	80.8524	0.531305	7.56786	12.18734	80.2448	0	0.082305	0.130893
50205	ITACYL	1	A	1350	300	1.84462	0.095743	14.5471	0.351419	20.4976	20.0277	59.4747	0	0.116778	0.160739
50206	ITACYL	1	A	1105	300	1.69902	0.075962	47.16	1.526372	12.6613	13.5586	73.7801	0	0.011884	0.14534
50207	ITACYL	1	A	1071	300	1.91692	0.077306	39.9209	0.778866	13.6244	14.8639	71.5117	0	0.050855	0.153127
50208	ITACYL	1	A	1500	300	1.74693	0.076585	48.0851	0.843267	10.6427	16.8424	72.5149	0	0.044868	0.158392
50209	ITACYL	1	A	300	300	1.80354	0.09314	68.9127	0.978076	6.20541	26.28419	67.5104	0	0.034521	0.180377
50210	ITACYL	1	A	300	300	1.22331	0.101122	20.1129	4.482337	19.2177	20.4351	60.3472	0	3.79E-05	0.158501
50211	ITACYL	1	A	975	300	1.49005	0.055994	60.74789	2.61407	0.802434	30.8382	68.35937	21.85684	0.001433	0.18295
50212	ITACYL	1	A	300	300	1.45	0.055823	80.4267	2.616279	0.147508	26.41072	73.44177	14.63845	0.001427	0.176467

MUID	S5ID	NLAYERS	HYDGRP	SOL_ZMX	SOL_Z1	SOL_BD1	SOL_AWC1	SOL_K1	SOL_CBN1	CLAY1	SILT1	SAND1	ROCK1	SOL_ALB1	USLE_K1
50213	ITACYL	1	A	300	300	1	0.126155	10.4839	2.674419	27.1065	26.2324	46.6611	0	0.001274	0.157496
50214	ITACYL	1	A	300	300	1.1439	0.107752	13.5655	6.319128	23.2946	20.0364	56.669	0	1.06E-06	0.154059
50215	ITACYL	1	A	300	300	1.50195	0.107427	11.0991	1.790047	25.796	18.8199	55.3841	0	0.007117	0.150413
50216	ITACYL	1	A	300	300	1.44062	0.082689	26.6759	2.648645	16.64188	13.66009	69.69803	1.86721	0.00134	0.142592
50217	ITACYL	1	A	300	300	1.59135	0.089822	20.0716	0.984314	20.0676	15.3726	64.5598	0	0.034104	0.150258
50218	ITACYL	1	B	1134	300	1.31938	0.093759	6.39993	1.825279	29.0411	8.7954	62.1635	0	0.006645	0.124705
50219	ITACYL	1	A	1200	300	1.41258	0.095086	9.59283	1.366599	25.7367	12.5804	61.6829	0	0.016215	0.139406
50220	ITACYL	1	A	300	300	1.41718	0.117177	10.4757	2.346552	24.6971	25.8119	49.491	0	0.002411	0.159465
50221	ITACYL	1	A	300	300	1.15	0.093916	12.1009	2.906977	23.0739	15.6239	61.3022	0	0.000811	0.147077
50222	ITACYL	1	A	1500	300	1.67528	0.100543	7.944	0.235594	25.9639	17.0511	56.985	0	0.146281	0.150886
50223	ITACYL	1	A	1425	300	1.46184	0.102263	11.0174	1.420814	24.6971	18.6429	56.66	0	0.014593	0.151964
50224	ITACYL	1	A	1300	300	1.57812	0.083703	83.555	2.940576	8.44016	17.98744	73.5724	0	0.000759	0.157602
50225	ITACYL	1	B	1367	300	1.40637	0.093458	5.24041	0.239445	30.4498	8.2501	61.3001	0	0.14519	0.124579
50226	ITACYL	1	C	1500	300	1.41025	0.107329	1.19164	0.430319	37.0865	10.6136	52.2999	0	0.100166	0.127114
50227	ITACYL	1	C	1500	300	1.45829	0.101372	2.91748	0.240123	33.93	9.3338	56.7362	0	0.144999	0.125739
50228	ITACYL	1	B	1500	300	1.37343	0.100165	5.29796	0.990198	30.2026	11.4933	58.3041	0	0.033716	0.134114
50229	ITACYL	1	A	1230	300	1.81958	0.060163	101.422	1.208041	5.5444	11.1516	83.304	0	0.022072	0.116839
50230	ITACYL	1	A	300	300	1.83009	0.071216	85.6899	0.837186	6.00093	16.87897	77.1201	0	0.045402	0.152403
50231	ITACYL	1	A	1282	300	2.10272	0.043905	210.859	0.437159	1.29833	6.56117	92.1405	0	0.098843	0.088877
50232	ITACYL	1	A	300	300	1.94715	0.055163	112.736	0.78564	4.17606	10.74644	85.0775	0	0.050189	0.111321
50233	ITACYL	1	A	300	300	1.78743	0.04203	190.651	0.728331	0.858965	5.276435	93.8646	0	0.056107	0.085687
50234	ITACYL	1	A	300	300	1.85	0.080162	121.919	0.988372	1.92568	22.93452	75.1398	0	0.033836	0.170463
50235	ITACYL	1	A	300	300	1.16534	0.087496	24.1035	1.231198	16.4625	20.7074	62.8301	4	0.0211	0.158562
50236	ITACYL	1	A	300	300	1.39163	0.095714	15.0734	1.050116	21.9398	17.5442	60.516	0	0.030008	0.154111
50237	ITACYL	1	A	1500	300	1.20605	0.104146	16.2053	1.019023	22.0615	22.4645	55.474	0	0.031878	0.159169
50238	ITACYL	1	A	300	300	1.24652	0.101587	23.5434	2.885936	19.8615	17.8806	62.2579	0	0.000845	0.154
50239	ITACYL	1	A	300	300	1.47215	0.106642	13.5107	2.368785	22.6507	19.7569	57.5924	0	0.002309	0.154352
50240	ITACYL	1	A	300	300	1.39101	0.099262	15.6712	3.403087	22.1664	16.5394	61.2942	0	0.000309	0.149596
50241	ITACYL	1	A	720	300	1.14363	0.095286	22.5049	4.850669	19.8631	16.0122	64.1247	0	1.85E-05	0.150483
50242	ITACYL	1	A	300	300	1.3004	0.087415	20.5669	3.527523	19.8128	12.8718	67.3154	0	0.000243	0.142877
50243	ITACYL	1	A	780	300	1.1259	0.098713	13.7627	3.602297	22.938	15.856	61.206	0	0.00021	0.147637

MUID	S5ID	NLAYERS	HYDGRP	SOL_ZMX	SOL_Z1	SOL_BD1	SOL_AWC1	SOL_K1	SOL_CBN1	CLAY1	SILT1	SAND1	ROCK1	SOL_ALB1	USLE_K1
50244	ITACYL	1	A	300	300	1.29355	0.087267	26.6798	5.02289	17.6378	14.9894	67.3728	0	1.32E-05	0.149583
50245	ITACYL	1	A	900	300	1.13805	0.09227	18.1752	5.37475	20.7166	15.2361	64.0473	0	6.68E-06	0.148198
50246	ITACYL	1	A	300	300	1.40623	0.095456	29.8955	1.922233	16.3882	18.9352	64.6766	0	0.005503	0.158968
50247	ITACYL	1	B	1420	300	1.30512	0.106204	9.73435	2.250581	26.4513	18.5808	54.9679	0	0.002906	0.149136
50248	ITACYL	1	A	300	300	1.3436	0.10235	22.8486	1.923971	18.7742	19.9331	61.2927	0	0.005485	0.158492
50249	ITACYL	1	A	938	300	1.45881	0.09599	17.8777	2.04136	21.19	15.0979	63.7121	0	0.004365	0.147718
50250	ITACYL	1	A	950	300	1.32497	0.09059	15.276	2.354709	22.1508	12.5966	65.2526	0	0.002373	0.140861
50251	ITACYL	1	A	1278	300	1.5521	0.078787	16.4711	0.664047	21.634	9.4405	68.9255	0	0.063579	0.133797
50252	ITACYL	1	A	1350	300	1.86321	0.06792	79.9175	0.904215	6.07284	15.96116	77.966	0	0.039853	0.147663
50253	ITACYL	1	A	1391	300	2.00672	0.071388	56.6183	0.547949	9.69453	15.13657	75.1689	0	0.079684	0.151364
50254	ITACYL	1	A	1260	300	1.80205	0.065259	154.526	0.696256	0.842352	17.06205	82.0956	0	0.059718	0.138558
50255	ITACYL	1	B	1329	300	1.13394	0.117921	4.24534	3.533174	32.2645	21.8984	45.8371	0	0.00024	0.148486
50256	ITACYL	1	A	1500	300	2.07129	0.047164	178.821	0.549416	2.29564	7.81416	89.8902	0	0.079457	0.093946
50257	ITACYL	1	A	300	300	1.8825	0.058833	94.9712	0.654105	5.29601	11.03069	83.6733	0	0.06482	0.117102
50258	ITACYL	1	A	300	300	1.71541	0.06553	73.9491	0.877523	7.15139	14.20981	78.6388	0	0.041976	0.141009
50259	ITACYL	1	A	300	300	1.70146	0.058473	112.764	0.864343	3.80422	12.52248	83.6733	0	0.043066	0.120736
50260	ITACYL	1	A	300	300	1.91468	0.057606	110.078	0.497623	4.42744	12.49676	83.0758	0	0.087877	0.123098
50261	ITACYL	1	A	300	300	1.83973	0.044048	191.184	0.605756	1.25736	6.87494	91.8677	0	0.071211	0.089453
50262	ITACYL	1	A	300	300	1.78927	0.047238	161.85	1.038721	1.29377	7.19303	91.5132	0	0.03068	0.08956
50263	ITACYL	1	A	300	300	1.74436	0.044717	183.309	0.861203	1.91184	6.96806	91.1201	0	0.04333	0.089264
50264	ITACYL	1	A	300	300	1.72385	0.073647	114.829	0.705372	3.66563	19.80737	76.527	0	0.058669	0.161626
50265	ITACYL	1	A	300	300	1.92853	0.039998	242.298	0.271062	0.103033	5.066367	94.8306	0	0.136531	0.08809
50266	ITACYL	1	A	300	300	1.82306	0.043115	156.16	0.596605	2.76225	5.50515	91.7326	0	0.072489	0.083928
50267	ITACYL	1	A	300	300	2.00983	0.047355	199.852	0.330599	0.406249	8.748951	90.8448	0	0.121604	0.095842
50268	ITACYL	1	A	300	300	2.02542	0.082545	52.1555	0.575872	9.63235	20.32275	70.0449	0	0.075472	0.168737
50269	ITACYL	1	A	300	300	1.41976	0.089838	43.0559	1.086442	12.4865	20.3079	67.2056	0	0.027961	0.16637
50270	ITACYL	1	A	300	300	1.09641	0.081806	33.0815	1.119395	15.8178	13.8179	70.3643	0	0.026225	0.148941
50271	ITACYL	1	A	300	300	1.31392	0.081707	26.3496	0.95561	18.3513	12.5144	69.1343	0	0.036062	0.144989
50272	ITACYL	1	A	300	300	1.21252	0.098202	16.153	0.880529	20.8076	18.9687	60.2237	0	0.041732	0.158048
50273	ITACYL	1	A	300	300	1.82801	0.060455	101.405	0.697738	5.351	12.2564	82.3926	0	0.059546	0.124527
50274	ITACYL	1	A	300	300	1.80569	0.062829	79.8319	0.830599	6.73467	12.79473	80.4706	0	0.045987	0.131704

MUID	S5ID	NLAYERS	HYDGRP	SOL_ZMX	SOL_Z1	SOL_BD1	SOL_AWC1	SOL_K1	SOL_CBN1	CLAY1	SILT1	SAND1	ROCK1	SOL_ALB1	USLE_K1
50275	ITACYL	1	A	300	300	1.69248	0.047949	161.698	0.735628	2.35403	7.99417	89.6518	0	0.055316	0.093636
50276	ITACYL	1	A	300	300	1.84942	0.054995	93.3212	0.459265	6.29645	9.52145	84.1821	0	0.094683	0.11025
50277	ITACYL	1	A	1157	300	1.78041	0.06982	80.0228	1.266413	7.14568	15.41712	77.4372	0	0.019703	0.146141
50278	ITACYL	1	A	1380	300	1.44921	0.053	92.3877	0.46664	7.15262	9.09298	83.7544	0	0.093335	0.109919
50279	ITACYL	1	A	1260	300	1.80322	0.062436	96.2012	1.267517	6.72528	12.69102	80.5837	0	0.019661	0.129784
50280	ITACYL	1	A	300	300	1.85091	0.051609	160.382	0.599436	2.47861	9.88269	87.6387	0	0.072091	0.102913
50281	ITACYL	1	A	300	300	1.79335	0.062679	81.8404	0.764157	6.7812	12.8735	80.3453	0	0.052331	0.132452
50282	ITACYL	1	A	300	300	1.9713	0.04342	563.409	0.307655	1.9043	6.9297	91.166	0	0.127153	0.090095
50283	ITACYL	1	A	300	300	1.7821	0.057064	144.537	0.725523	2.48215	12.93925	84.5786	0	0.056414	0.119493
50284	ITACYL	1	A	1152	300	1.45859	0.067064	42.8272	0.585093	14.9497	9.1701	75.8802	0	0.07413	0.129254
50285	ITACYL	1	A	300	300	1.80241	0.055668	87.5867	0.496226	6.46027	10.21893	83.3208	0	0.088116	0.115121
50286	ITACYL	1	A	300	300	1.79406	0.05703	75.6191	0.629279	7.70768	9.50472	82.7876	0	0.068026	0.114108
50287	ITACYL	1	A	300	300	1.31938	0.064639	41.052	0.437266	13.8513	9.3891	76.7596	0	0.098822	0.128899
50288	ITACYL	1	A	300	300	1.91376	0.055515	86.7527	0.307565	6.41444	10.38736	83.1982	0	0.127175	0.116152
50289	ITACYL	1	A	300	300	1.21976	0.084874	26.9721	1.040872	17.9192	14.0392	68.0416	0	0.030552	0.149459
50290	ITACYL	1	A	300	300	1.0785	0.074361	38.7767	1.410128	8.87672	18.20568	72.9176	5.32658	0.014899	0.153858
50291	ITACYL	1	A	300	300	0.675329	0.096179	13.5277	4.438849	22.7143	17.8432	59.4425	0	4.12E-05	0.151352
50292	ITACYL	1	A	300	300	1.28002	0.070955	27.8803	0.913605	17.8783	7.2035	74.9182	0	0.039132	0.120838
50293	ITACYL	1	A	1113	300	1.73754	0.052605	132.191	0.675186	5.94455	7.71595	86.3395	0	0.062216	0.098494
50294	ITACYL	1	A	1083	300	1.79843	0.055977	125.823	0.811791	5.14046	10.56294	84.2966	0	0.047701	0.113494
50295	ITACYL	1	A	300	300	1.81303	0.066688	86.1096	0.622797	5.45904	15.79746	78.7435	0	0.068889	0.145782
50296	ITACYL	1	A	300	300	1.76556	0.051888	135.924	0.553409	4.21673	9.74067	86.0426	0	0.078842	0.105939
50297	ITACYL	1	A	300	300	1.73977	0.059888	106.787	0.914	3.7924	12.681	83.5266	0	0.039102	0.121564
50298	ITACYL	1	A	1380	300	1.13514	0.083585	23.7948	0.981407	17.8281	13.9879	68.184	0	0.034298	0.149547
50299	ITACYL	1	A	1500	300	1.33494	0.072398	32.7849	0.838047	15.5355	10.9578	73.5067	0	0.045326	0.138615
50300	ITACYL	1	A	300	300	1.1782	0.088345	17.5233	0.822744	21.1286	14.3944	64.477	0	0.046695	0.149137
50301	ITACYL	1	A	300	300	1.18447	0.112131	7.59591	0.721959	26.6464	22.1756	51.178	0	0.056806	0.157142
50302	ITACYL	1	A	300	300	1.12455	0.091756	18.7407	0.933849	19.8984	17.3654	62.7362	1.5038	0.037621	0.153725
50303	ITACYL	1	A	1275	300	1.93862	0.092994	81.9696	0.666907	3.12145	30.01905	66.8595	0	0.063226	0.188245
50304	ITACYL	1	A	1300	300	1.85455	0.066036	105.36	0.832174	4.14333	16.54927	79.3074	0	0.045847	0.145843
50305	ITACYL	1	A	300	300	1.71224	0.101981	105.691	0.728826	1.53111	34.13309	64.3358	0	0.056053	0.193428

MUID	S5ID	NLAYERS	HYDGRP	SOL_ZMX	SOL_Z1	SOL_BD1	SOL_AWC1	SOL_K1	SOL_CBN1	CLAY1	SILT1	SAND1	ROCK1	SOL_ALB1	USLE_K1
50306	ITACYL	1	A	300	300	1.57082	0.095296	108.162	1.576012	2.14322	28.70198	69.1548	0	0.010791	0.183855
50307	ITACYL	1	A	300	300	1.88621	0.061655	175.768	0.838762	0	16.2383	83.7617	0	0.045263	0.130271
50308	ITACYL	1	A	300	300	1.33437	0.075007	153.327	1.021541	0	21.708	78.292	0	0.031722	0.160644
50309	ITACYL	1	A	300	300	1.56586	0.098839	58.8897	1.324936	6.93938	28.77332	64.2873	0	0.017584	0.181375
50310	ITACYL	1	A	300	300	1.77349	0.084373	93.0885	0.98107	6.85463	22.84097	70.3044	0	0.03432	0.173735
50311	ITACYL	1	A	300	300	1.67424	0.099188	29.2512	0.979006	15.4109	22.6337	61.9554	0	0.034458	0.168213
50312	ITACYL	1	B	1433	300	1.06598	0.098613	8.55009	2.464378	26.695	14.5988	58.7062	0	0.001917	0.141911
50313	ITACYL	1	A	300	300	1.27882	0.087989	23.5542	0.691645	17.7589	15.5048	66.7363	0	0.060256	0.154287
50314	ITACYL	1	A	300	300	0.998666	0.095711	12.7032	2.932965	22.8222	16.2833	60.8945	0	0.000771	0.148555
50315	ITACYL	1	A	300	300	1.28361	0.099167	15.968	1.115459	21.4638	18.2778	60.2584	0	0.026427	0.155534
50316	ITACYL	1	A	300	300	1.15919	0.103327	12.9968	1.233733	23.5525	17.7563	58.6912	0	0.020996	0.152286
50317	ITACYL	1	A	1088	300	1.9016	0.084703	118.332	1.37968	2.03305	24.47685	73.4901	0	0.015808	0.174452
50318	ITACYL	1	A	1350	300	1.88181	0.071614	119.469	0.64589	2.7013	19.1697	78.129	0	0.065864	0.156226
50319	ITACYL	1	A	300	300	1.85047	0.083409	136.918	1.528145	0.729676	23.62462	75.6457	0	0.011843	0.169183
50320	ITACYL	1	A	300	300	1.51514	0.075977	152.088	0.763151	0	21.5952	78.4048	0	0.052433	0.160843
50321	ITACYL	1	A	300	300	1.73909	0.054565	164.031	0.800913	2.26503	11.36237	86.3726	0	0.048721	0.110303
50322	ITACYL	1	A	300	300	1.84646	0.10192	74.0319	1.71982	6.57161	30.46529	62.9631	0	0.008158	0.182162
50323	ITACYL	1	A	300	300	1.136	0.089757	17.5021	2.965116	21.0883	12.8352	66.0765	0	0.000724	0.142111
50324	ITACYL	1	A	1033	300	1.27896	0.098087	18.1305	3.558988	21.192	17.3144	61.4936	0	0.000228	0.151841
50325	ITACYL	1	A	300	300	1.26071	0.092454	17.4087	3.043244	21.0187	15.06203	63.91927	1.13807	0.000622	0.145552
50326	ITACYL	1	A	955	300	1.28058	0.085104	25.9678	4.33218	18.1419	13.394	68.4641	0	5.07E-05	0.145046
50327	ITACYL	1	A	1220	300	1.40097	0.10115	19.174	1.99936	20.7179	18.0976	61.1845	0	0.004737	0.153807
50328	ITACYL	1	A	1156	300	1.30536	0.082604	17.5189	2.043023	21.8977	9.7577	68.3446	0	0.004351	0.132023
50329	ITACYL	1	A	300	300	0.96	0.099064	24.9891	2.965116	19.1971	16.2173	64.5856	0	0.000724	0.151415
50330	ITACYL	1	A	300	300	1.2803	0.111858	18.7532	3.928151	21.2655	22.5203	56.2142	0	0.000111	0.159111
50331	ITACYL	1	A	300	300	1.13474	0.077716	37.2828	5.582762	14.6697	12.8825	72.4478	0	4.46E-06	0.14317
50332	ITACYL	1	A	300	300	1.342596	0.106172	10.261	1.956058	25.6226	18.2098	56.1676	0	0.005153	0.149484
50333	ITACYL	1	A	300	300	1.3568	0.099784	13.8666	3.548512	23.904	16.3058	59.7902	0	0.000233	0.147627
50334	ITACYL	1	A	1408	300	1.90802	0.076414	50.8407	0.813953	11.2092	16.3586	72.4322	0	0.0475	0.157134
50335	ITACYL	1	A	750	300	1.39454	0.068636	51.5016	2.334273	1.86216	29.22518	68.91266	18.24957	0.00247	0.178391
50336	ITACYL	1	A	750	300	1.65766	0.060568	137.69	2.809186	2.63863	11.93487	85.4265	0	0.000981	0.112393

MUID	S5ID	NLAYERS	HYDGRP	SOL_ZMX	SOL_Z1	SOL_BD1	SOL_AWC1	SOL_K1	SOL_CBN1	CLAY1	SILT1	SAND1	ROCK1	SOL_ALB1	USLE_K1
50337	ITACYL	1	A	1067	300	1.58409	0.091165	76.54	1.833337	7.08423	22.22557	70.6902	0	0.006542	0.169625
50338	ITACYL	1	A	1300	300	1.79224	0.071297	131.163	0.948884	2.30917	18.33573	79.3551	0	0.036537	0.150325
50339	ITACYL	1	A	300	300	1.93365	0.064082	128.54	0.826808	3.21993	15.10327	81.6768	0	0.046328	0.134829
50340	ITACYL	1	A	922	300	1.60969	0.056287	86.6157	2.314483	1.1725	56.51042	42.31708	45.88724	0.002566	0.188931
50341	ITACYL	1	A	1167	300	2.02806	0.06802	75.4059	0.408658	7.22861	14.63079	78.1406	0	0.104476	0.144204
50342	ITACYL	1	A	1200	300	2.15645	0.073061	86.96	0.347011	4.7871	20.0958	75.1171	0	0.117784	0.165043
50343	ITACYL	1	A	1500	300	1.98129	0.072966	73.3039	0.563581	6.66895	18.93625	74.3948	0	0.077298	0.162923
50000	ITACYL	1	B	300	300	1.38013	0.107845	7.89307	1.332884	27.1017	19.5217	53.3766	0	0.017314	0.151298
50001	ITACYL	1	A	300	300	1.8563	0.077623	65.2473	0.883808	9.02159	18.01111	72.9673	0	0.041466	0.161275
50344	ITACYL	1	A	1181	300	1.77952	0.071884	82.102	0.812767	5.70292	18.48148	75.8156	0	0.04761	0.159184
50345	ITACYL	1	C	300	300	1.46229	0.111849	2.77037	0.47248	32.8274	21.4352	45.7374	5.4053	0.092281	0.142959
50346	ITACYL	1	A	300	300	1.33859	0.096405	9.32927	0.808238	26.0254	15.8105	58.1641	0	0.048031	0.146907
50347	ITACYL	1	B	1425	300	1.46106	0.091259	6.93364	0.32869	27.9866	9.235	62.7784	0	0.122056	0.129928
50348	ITACYL	1	B	1074	300	1.36013	0.094741	9.90348	0.312916	25.482	15.3267	59.1913	0	0.125858	0.148104
50349	ITACYL	1	A	1350	300	1.47709	0.063699	50.0507	0.964169	11.8745	10.9887	77.1368	0	0.035467	0.133563
50350	ITACYL	1	A	1216	300	1.33862	0.074311	31.6203	0.697535	16.4735	11.9249	71.6016	0	0.05957	0.143462
50351	ITACYL	1	A	1150	300	1.51107	0.093826	19.4346	0.726628	19.6236	17.9711	62.4053	0	0.056293	0.157876
50352	ITACYL	1	A	300	300	0.986206	0.079089	33.7552	1.397977	15.5419	11.5192	72.9389	0	0.015255	0.139353
50353	ITACYL	1	A	1247	300	1.36871	0.100998	7.63323	2.287471	26.7641	16.9742	56.2617	0	0.002705	0.146293
50354	ITACYL	1	A	1500	300	1.7739	0.083136	48.1432	1.26936	10.1677	20.2778	69.5545	0	0.019591	0.166431
50355	ITACYL	1	A	1188	300	1.86432	0.069046	87.6724	0.786297	5.98296	16.55004	77.467	0	0.050125	0.150797
50356	ITACYL	1	A	300	300	1.79206	0.057535	116.076	0.720052	4.32339	11.39621	84.2804	0	0.057017	0.115922
50357	ITACYL	1	A	1200	300	1.11715	0.078461	23.9077	0.74389	17.7717	12.2346	69.9937	0	0.054435	0.144651
50358	ITACYL	1	A	1260	300	2.13536	0.071174	150.816	0.795826	0.422756	19.55324	80.024	0	0.049205	0.151219
50359	ITACYL	1	B	1136	300	1.45745	0.097502	6.94483	1.022087	27.6914	12.6025	59.7061	0	0.031689	0.13896
50360	ITACYL	1	A	1118	300	1.30325	0.089027	18.6284	0.473854	20.0267	16.0964	63.8769	0	0.092035	0.154307
50361	ITACYL	1	A	300	300	1.38923	0.106347	13.4993	2.279395	21.75	18.25	60	0	0.002748	0.154866
50362	ITACYL	1	A	300	300	1.42668	0.083064	18.2047	1.99936	17.5606	17.63239	64.80701	6.508864	0.004737	0.144127
50363	ITACYL	1	A	300	300	1.2141	0.080259	17.6002	2.079227	15.35426	24.38234	60.2634	12.10703	0.004055	0.151784
50364	ITACYL	1	A	914	300	1.45878	0.096678	21.3684	1.69286	19.1009	19.2209	61.6782	0	0.008597	0.154224
50365	ITACYL	1	A	1133	300	1.53451	0.083021	15.4969	1.014023	22.3173	9.5018	68.1809	0	0.03219	0.13307

MUID	S5ID	NLAYERS	HYDGRP	SOL_ZMX	SOL_Z1	SOL_BD1	SOL_AWC1	SOL_K1	SOL_CBN1	CLAY1	SILT1	SAND1	ROCK1	SOL_ALB1	USLE_K1
50366	ITACYL	1	B	1350	300	1.36465	0.102925	4.88418	0.462505	30.7865	14.2416	54.9719	0	0.094088	0.14108
50367	ITACYL	1	A	300	300	1.89843	0.095049	90.2328	1.010924	3.50982	28.61188	67.8783	0	0.032384	0.18512
50368	ITACYL	1	A	1100	300	1.7351	0.069894	122.341	1.519512	2.87487	16.63123	80.4939	0	0.012044	0.140483
50369	ITACYL	1	A	1300	300	1.73437	0.063155	127.505	1.483919	3.14471	13.46159	83.3937	0	0.012907	0.122842
50370	ITACYL	1	A	1100	300	1.87134	0.069135	125.572	1.431878	2.49141	16.70979	80.7988	0	0.014282	0.139891
50371	ITACYL	1	A	1200	300	1.88813	0.064251	87.2285	0.771948	6.24543	13.22627	80.5283	0	0.051544	0.132967
50372	ITACYL	1	A	1269	300	1.78169	0.065105	140.392	1.329134	2.16004	16.58136	81.2586	0	0.017441	0.138424
50373	ITACYL	1	A	1329	300	2.01489	0.060445	82.2399	0.711552	7.06836	11.67304	81.2586	0	0.057968	0.126006
50374	ITACYL	1	A	300	300	1.64358	0.072785	133.748	1.578419	1.91691	18.17959	79.9035	0	0.01074	0.146006
50375	ITACYL	1	A	1233	300	1.90363	0.068659	141.032	1.070698	1.36708	17.73702	80.8959	0	0.02883	0.143367
50376	ITACYL	1	A	300	300	1.78982	0.070357	147.841	1.129506	0.903575	18.48463	80.6118	0	0.025714	0.145882
50377	ITACYL	1	A	300	300	1.57845	0.088709	119.601	1.970128	1.72333	25.59577	72.6809	0	0.005014	0.176097
50378	ITACYL	1	A	300	300	1.91379	0.056638	122.37	0.627116	4.44694	11.81846	83.7346	0	0.068313	0.118919
50379	ITACYL	1	A	300	300	1.06002	0.089779	20.4787	1.083413	19.3333	16.5484	64.1183	0	0.028126	0.154404
50380	ITACYL	1	A	1175	300	1.71616	0.059189	59.3459	0.928971	10.41	9.0502	80.5398	0	0.03798	0.118331
50381	ITACYL	1	A	1500	300	2.06676	0.052651	122.454	0.439208	4.87829	9.39541	85.7263	0	0.098449	0.105588
50382	ITACYL	1	A	1500	300	2.08554	0.078683	49.8018	0.528646	9.82621	19.19229	70.9815	0	0.082732	0.165878
50383	ITACYL	1	A	1300	300	1.66881	0.059076	87.3515	1.099169	5.92604	11.92736	82.1466	0	0.027277	0.123168
50384	ITACYL	1	A	1200	300	1.81526	0.089567	44.3554	1.291645	11.7564	21.6284	66.6152	0	0.01876	0.16835
50385	ITACYL	1	A	300	300	1.83	0.112782	43.2781	1.860465	9.10101	33.01439	57.8846	0	0.006206	0.180715
50386	ITACYL	1	A	1069	300	1.78585	0.072214	112.382	1.607616	4.20237	16.65213	79.1455	0	0.010147	0.144421
50387	ITACYL	1	A	1167	300	2.01583	0.059945	172.317	0.785157	0.022431	14.34597	85.6316	0	0.050237	0.119737
50388	ITACYL	1	A	1009	300	1.52705	0.061804	50.3633	2.490884	5.916409	48.01823	46.06536	38.13894	0.001821	0.169272
50389	ITACYL	1	A	300	300	1.77932	0.073235	135.773	1.214849	1.90255	19.16105	78.9364	0	0.021782	0.1524
50390	ITACYL	1	A	300	300	1.435	0.094733	93.7001	2.151163	3.96642	26.96038	69.0732	0	0.003526	0.179275
50391	ITACYL	1	A	1300	300	1.4338	0.096537	18.5822	2.869244	20.9144	16.3906	62.695	0	0.000873	0.150401
50392	ITACYL	1	A	600	300	1.40568	0.09933	14.2442	3.18707	23.1928	16.493	60.3142	0	0.00047	0.148605
50393	ITACYL	1	A	1053	300	1.31885	0.097385	16.6293	2.703372	21.6813	17.1122	61.2065	0	0.001205	0.151073
50394	ITACYL	1	A	1140	300	1.49731	0.082077	21.3294	1.467715	20.6386	10.7274	68.634	0	0.01332	0.136712
50395	ITACYL	1	A	300	300	1.01312	0.092788	15.86	5.571558	22.0084	14.9888	63.0028	0	4.55E-06	0.146657
50396	ITACYL	1	A	1340	300	1.45442	0.078587	13.4742	1.1825	24.0325	5.6271	70.3404	0	0.023196	0.113578

MUID	S5ID	NLAYERS	HYDGRP	SOL_ZMX	SOL_Z1	SOL_BD1	SOL_AWC1	SOL_K1	SOL_CBN1	CLAY1	SILT1	SAND1	ROCK1	SOL_ALB1	USLE_K1
50397	ITACYL	1	A	1143	300	1.13758	0.095034	8.65149	2.273413	26.8214	11.31	61.8686	0	0.00278	0.133996
50398	ITACYL	1	A	1248	300	1.30568	0.093153	11.2789	2.035163	24.8456	12.2502	62.9042	0	0.004418	0.138142
50399	ITACYL	1	A	1250	300	1.43508	0.098365	10.3558	2.094041	25.4831	14.3192	60.1977	0	0.00394	0.142479
50400	ITACYL	1	A	1200	300	1.86255	0.078844	141.299	1.068442	0.40785	25.65715	73.935	0	0.028957	0.177595
50401	ITACYL	1	A	300	300	1.88935	0.096302	102.678	1.198703	2.76224	29.86016	67.3776	0	0.022477	0.186432
50402	ITACYL	1	A	300	300	1.76483	0.0835	95.9948	1.174174	4.86846	22.45734	72.6742	0	0.023575	0.171434
50403	ITACYL	1	A	300	300	1.50887	0.091577	14.2008	1.47361	22.0606	14.7361	63.2033	0	0.013169	0.147091
50404	ITACYL	1	A	1273	300	1.51226	0.09166	11.1563	0.738209	24.5178	12.6276	62.8546	0	0.055039	0.142351
50405	ITACYL	1	A	300	300	1.23146	10.0615	21.7141	1.789177	19.8639	18.2182	61.9179	0	0.007129	0.154555
50406	ITACYL	1	A	300	300	1.32589	9.23517	27.8516	3.287657	17.7422	15.3173	66.9405	0	0.000387	0.150342

Annex 9. Simulation details of SWAT model set-up and parameterization.

General details	
Simulation length [years]	11
Warm Up [years]	1
Hydrological response Units << HRUs >>	1000
Sub-basins	121
Precipitation method	Measured + TPM
Watershed area [km^2]	7,850.4
Hydrology (water balance percent)	
Stream flow/precipitation	15%
Base flow/total flow	74%
Surface run-off/total flow	26%
Percolation/precipitation	9%
Deep recharge/precipitation	0.45%
ET/precipitation	80%
Hydrological parameters (all units in mm)	
Average curve number	51.57
ET and transpiration	358.1
Precipitation	447.5
Surface run-off	17.66
Lateral flow	28.81
Return flow	22.35
Percolation to shallow aquifer	39.97
Recharge to deep aquifer	2
Revaporation from shallow aquifer	24.96

Annex 10. Yearly average water associated processes to the land use.

LULC: Land Use Land Change, CN: Curve number, AWC: Available water content, USLE_LS: Universal soil loss equation value as combined slope length factor (L) and slope steepness factor (S), IRR: irrigation amount, PREC: precipitation, SURQ: Surface runoff to streams, GWQ: groundwater flow and ET: evapotranspiration.

LULC	Area (Km^2)	CN	AWC (mm)	USLE_LS	IRR (mm)	PREC (mm)	SURQ (mm)	GWQ (mm)	ET (mm)
AGRC	39.12	64.07	328.55	0.34	0	391.83	3.22	8.64	350.19
AGRL	3.05	67	365.09	0.3	0	420.5	0.9	2.12	378.08
ALFA	0.47	35	365.09	0.17	0	385.62	0	0.14	395.64
BARL	1,783.49	64.56	273.19	0.65	0	437.04	3.33	53.23	348.66
BERM	647.72	96.79	275.85	0.84	0	444.74	202.26	4.1	237.06
FRSD	37.28	45	251.65	1.43	0	476.55	0.03	49.24	418.51
FRSE	2,650.97	35.35	246.29	1.2	0	445.12	0.03	56.77	368.66
HAY	11.12	35	250.98	1.48	0	482.67	0	62.36	403.6
HORT	42.57	67	258.03	0.21	1.93	437.86	1.61	19.87	398.03
POTA	5.56	67	282.08	0.2	16.63	408.04	4.15	14.37	391.14
RNGE	486.6	49.5	244.74	2.27	0	477.79	0.16	76.36	387.46
SGBT	3.57	67	328.3	0.21	6.83	372.37	2.12	0.58	365.58
SUNF	143.09	67.79	259.83	0.53	0	443.16	1.9	25.15	396.94
SWRN	1,517.10	40.26	277.17	2.05	0	455.18	0.04	48.33	390.69
WWHT	478.17	63.13	251.91	0.66	0	452.89	2.03	74.57	344.33